Effect of VRM on a polymetallic sulfide ore and the flotation response as compared to conventional wet and dry rod milling

Hebert Simbarashe Nyakunuhwa

A dissertation submitted to the Faculty of Engineering and the Built Environment, University of Cape Town in fulfilment of the requirements for the degree of Master of Science in Chemical Engineering.

June 2019

ABSTRACT

Comminution is an energy intensive, size reduction and mineral dressing process which consumes up to 50% of concentrator energy consumption. Conventional methods use mainly a combination of crushers and tumbling mills in comminution circuits. Energy consumption in these circuits has been found to be relatively high. To reduce the energy requirements, compression grinding equipment, Vertical Roller Mills (VRMs) and High-Pressure Grinding Rolls (HPGRs) have been identified as potential solutions, and they have been adopted in the cement industry. Reports from plants where these technologies have been installed in circuits indicate they are more energy efficient than the conventional comminution circuits. Studies have also suggested that the use of VRMs results in comminution products with relatively higher mineral liberation degrees. Unlike in the cement industry, comminution equipment in mineral processing circuits are also required to produce particles that can be separated and recovered in downstream processes.

Froth flotation is a selective separation process that utilises differences in surface properties to separate value minerals from unwanted gangue. The success of flotation is dependent on chemistry, operational and equipment factors. The chemistry factors consider the interaction between flotation reagents and solids particles surface. The operational factors consider the effect of particle size distribution, mineralogy, feed rate, pulp density, pulp potential (Eh), bubble size, temperature and circuit design on flotation. The use of different comminution procedures may result in flotation feeds of different particle size distributions (PSDs), mineral liberation characteristics and pulp potential. Due to these differences, the resultant flotation response may differ.

The present study was aimed at assessing the particle size distribution, mineral liberation profiles and the flotation response from material comminuted using the VRM floated under batch flotation conditions in a 3 litre Barker flotation cell. A complex polymetallic sulfide ore containing chalcopyrite (1.3 %), galena (2.4 %) and sphalerite (1.8 %) as the main value minerals and magnetite (68.0 %) and quartz (15.7 %) as dominant gangue minerals was used for the study. The ore was milled to target grinds of 55 %, 60 %, 65 %, 70 % and 75 % passing 75 μm respectively, at a grinding pressure of 600 kPa, air temperature of 300 K. For the benchmarking grind of 65 % passing 75 μm, the ore was also milled using heated air of temperature of 373 K and at elevated grinding pressures of 800 kPa and 1000 kPa. Further work was performed to evaluate if the VRM results are comparable to conventional dry and wet rod milling products floated under the same batch flotation conditions.

An increase in grinding pressure was observed to result in an increase in throughput and a general decrease in specific energy consumption without a change in product particle size distribution nor the recovery of chalcopyrite, galena and sphalerite. Using heated air (373 K) resulted in the production of slightly less fines in the comminution products. The recovery of chalcopyrite, galena and sphalerite were not affected by the change in operating temperature. However, concentrate grade (selectivity) was compromised at elevated temperatures of comminution probably due to surface oxidation. The results indicated that the grind range to achieve the best flotation performance when using the VRM as a comminution device is between 60 % and 70 % passing 75 μm. The results also indicated that at the benchmarking grind of 65 % passing 75 μm, the specific energy consumption for comminution using the VRM was 54.3 % lower than that of the conventional tumbling mill circuit. The grind of 55 % passing 75 μm resulted in lower flotation efficiencies as the minerals were unlikely liberated enough whereas the grind of 75 % passing 75 μm resulted in poor performances due to low water recovery.

Comparing VRM with wet and rod milling, the different comminution procedures resulted in flotation feed of similar PSDs for all grinds compared. The wet and dry rod milling products of grinds 55 % and 75 % passing 75 μm achieved better recoveries of chalcopyrite, galena and sphalerite as compared to the VRM performance mainly due to high water recoveries achieved. While mineral recoveries were above 90 % for the grinds of 60 % and 70 % passing 75 μm, the rod milling products had statistically better flotation recoveries at 95 % confidence compared to the VRM products. The mineral recoveries after dry rod milling were marginally better than after wet rod milling due to the minimisation of galvanic interactions during dry rod milling.

For the benchmarking grind of 65 % passing 75 μm, VRM grinding resulted in 84 %, 84 % and 90 % liberated chalcopyrite, galena and sphalerite respectively. The liberation of chalcopyrite, galena and sphalerite after wet and dry rod milling were 80 %, 78 % and 90 % respectively. Chalcopyrite recovery was 96.7 %, 96.3 % and 96.7 % for the VRM, dry rod mill (RD) and wet rod mill (RW) products respectively. Galena recovery was 94.3 %, 94.3 % and 92.9 % for the VRM, RD and RW products respectively. Sphalerite recovery was 96.6 %, 97.4 % and 97.4 % for the VRM, RD and RW products respectively. The differences in recovery were statistically insignificant at 95 % confidence. Liberation differences did not translate to differences in recoveries as the ore was coarse grained. The recovery kinetics were very fast and independent of comminution procedure. Reference to the benchmarking grind therefore, the VRM can be retrofitted into existing plant installations as it is more energy efficient and the flotation performance was similar when using the flotation procedure tailored for tumbling mill-flotation systems.

PLAGIARISM DECLARATION

I, Hebert Simbarashe Nyakunuhwa declare that:

1. This dissertation, submitted for the degree of Master of Science in Chemical Engineering at the University of Cape Town is my own work, and has not been submitted prior to this for any degree at this university or any other institution. Guidance was, however, provided by my supervisors. The conclusions and recommendations are based on my understanding of literature and interpretation of results.
2. I know the meaning of plagiarism and declare that all the work in the document, save for that which is properly acknowledged, is my own.

Signed: Signed by candidate

Date: 12 October 2019

TABLE OF CONTENTS

ACKNOWLEDGEMENTS

I would like to thank my primary supervisor, Professor Aubrey Njema Mainza and the co-supervisors, Associate Professor Kirsten Clare Corin and Associate Professor Megan Becker for their supervision, motivation and critics in the areas of expertise during the project.

The management and staff in the Centre of Minerals Research laboratories: Shireen Govender, Refilwe Moalosi, Lorraine Nkemba for preparing blocks for mineralogical analysis and Gaynor Yorath for running the samples through the QEMSCAN are sincerely acknowledged for their assistance. I also express sincere gratitude to Loesche GmbH for sponsoring the project and Markus Stapelmann for conducting the comminution tests using the vertical roller mill, the CMR for allowing me to use their laboratory equipment, Black Mountain Mine for providing the ore used during the study, Mintek for blending the ore and Scientific Services for the timeous chemical analysis of samples.

To my friends: Takunda Mashayamombe, Maloba Tshehla, Mathew Dzingai, Herbert Hill, Lucia Dzinza, Andrea Molifie and Conchita Kamanzi, thank you for your friendship and unwavering support.

To my four parents: Justin and Priscilla Nyakunuhwa, Louis and Virginia Mabiza, thank you for your unconditional and unwavering support. To my siblings: Kuda, Masimba, Rufaro, Noreen, Takudzwa, Tererai and Natalie, thank you for being the best siblings I could ever ask for.

To Shingai Mutasa, thanks for being great motivation and to July Ndlovu, I am always inspired.

I dedicate the thesis to my family: Audrey, my life long best friend and wife.

To God be the Glory. Everything was possible because of Him.

Joshua 1:9

LIST OF FIGURES

LIST OF TABLES

LIST OF ABBREVIATIONS

μm	Micrometers
HPGR	High Pressure Grinding Roll
ICP-OES	Induction Coupled Plasma - Optical Emission Spectroscopy
kV	kilo Volts
nA	nano Amperes
PGM	Platinum Group Minerals
PSD	Particle Size Distribution
QEMSCAN	Quantitative Evaluation of Minerals by Scanning Electron Microscopy
RD	Dry Rod Mill Grinding
RW	Wet Rod Mill Grinding
SABC	Semi-autogenous ball milling-crusher
SAG/RoM	Semi-Autogenous Grinding/Run of Mine
SHE	Standard Hydrogen Electrode
TDS	Total Dissolved Solids
UCT	University of Cape Town
VRM	Vertical Roller Mill
XRF	X-ray Fluorescence spectrometry

SYMBOLS AND NOMENCLATURE

(v/v) %	Percent by volume
Cu	Copper
d50	The 50th percentile of a particle/grain size distribution
Mass pull	The mass of solids that reports to concentrates as a ratio of the feed solids mass
P_{80}	The 80th percentile of a particle size distribution
Pb	Lead
wt. %	weight percent
wt.	weight
Zn	Zinc

1. INTRODUCTION

The purpose of this research is to assess the flotation response of a complex ore comminuted using the vertical roller mill (VRM) and compare it to the flotation response from conventional laboratory scale wet rod milling as well as laboratory scale dry rod milling. The section begins with providing a background to the investigation carried out in this work. The later parts discuss the problem statement, research objectives and the scope and the limitations of the research.

1.1. Background of the research

Comminution is an energy intensive, size reduction and mineral dressing process which consumes up to 50% of concentrator energy consumption (Cohen, 1983; Tromans, 2008; Ballantyne and Powell, 2014). The role of comminution is to prepare minerals for downstream concentration processes like flotation and leaching.

In the past, comminution was easier due to the availability of simple to process, high grade ores. Present day, ores are becoming increasingly difficult to process due to complex, fine grained mineralisation (Powell and Mainza, 2012). The fine grained and heterogeneous mineralisation means the ores need to be ground finer to liberate the valuable minerals for efficient downstream concentrating and recovery processes (Reichert et al., 2015).

The increasing complexity of ore has resulted in the increase in energy requirements for comminution (Norgate and Jahanshahi, 2011). With the dwindling of fossil fuels, increasing complexity of mineral ores and the call for increased energy savings, research has intensified to identify feasible and energy efficient grinding technologies whilst maintaining final product expectations. This has seen the increased quest for the adoption of more energy efficient comminution equipment in the minerals processing sector.

To reduce the energy requirements, compression grinding equipment, Vertical Roller Mills (VRMs) and High-Pressure Grinding Rolls (HPGRs) have been identified as potential solutions, and they have been adopted in the cement and coal industry (Schaefer, 2001). Reports from plants where these technologies have been installed in circuits indicate they are more energy efficient than the conventional comminution circuits (Aydogan and Benzer, 2011; Benzer et al., 2018). Studies have also suggested that the use of the VRMs results in comminution products with relatively higher mineral liberation degrees (von Michaelis, 2005). Unlike in the cement industry, comminution equipment in mineral processing circuits are also required to produce particles that can be recovered in downstream processes.

While research has informed of the comminution energy savings realisable from using compression grinding, the VRM utilises dry grinding whereas the traditional mineral processing circuit has widely adopted wet grinding prior to the flotation process. In the conventional comminution circuit, wet grinding has been preferred over dry grinding because it has been reported to be more energy efficient and also that dry grinding would require dust control mechanisms (Farrokhpay and Manouchehri, 2012).

During wet grinding, galvanic interactions occur in the presence of water, oxygen, steel medium and sulfide minerals resulting in the precipitation of sulphur-oxy and metal hydroxide species on sulfide mineral surfaces (Ye et al., 2010; Palm et al., 2011). These oxy-hydroxide species impact negatively on the recovery of the sulfide minerals. The effect of galvanic coupling is minimised in VRM operations as it is a dry and mostly autogenous process, hence steel-ore interactions are minimised (Drunick et al., 2010; Erkan et al., 2012). Progeny particles from dry grinding have rough surfaces with microstructural defects, which tends to accelerate collector adsorption during flotation due to the increased surface area and improve recoveries at the expense of selectivity. On the other hand, wet grinding products are smoother and cleaner, which improves selectivity (Feng and Aldrich, 2000). In studies where the particle size distribution was the only reference and the particle size distributions were similar for wet and dry grinding, dry grinding resulted in superior flotation performance in terms of mineral recoveries (Feng and Aldrich, 2000; Bruckard et al., 2011; Palm et al., 2011; Koleini et al., 2012).

High compression grinding has been reported to result in preferential breakage along grain boundaries resulting in higher liberation of value minerals (Apling and Bwalya, 1997; Celik and Oner, 2006; Loesche GmbH, 2016). If sulfide minerals surfaces exposure is high due to the preferential fracturing, collector attachment probabilities are increased. It follows that with the higher degree of liberation, better flotation response in terms of recovery is expected should the liberated particles fall inside the optimum particle size range for flotation. The operation of the VRM can be manipulated using online parameters, such as operating grinding pressure, classifier rotor speed and dam ring height. These influence the resultant progeny characteristics and hence will affect flotation response.

While they have a proven energy saving record in the cement industry, high compression grinding equipment have had minimal mineral processing adoption in Southern Africa. Pilot tests have been conducted that validated applicability, downstream processes responses and energy savings of VRMs in the mineral processing industry (von Michaelis, 2005; Drunick, Gerold & Palm, 2010; Erkan et al., 2012; Altun et al., 2015; Benzer et al., 2018).

As studies have indicated that VRM operations have dust control systems and are potentially more energy efficient (Aydogan and Benzer, 2011; Loesche GmbH, 2016; Benzer et al., 2018; Stapelmann, 2018), it is important to understand whether efficiencies can be maintained in the downstream flotation unit operations Should the flotation performance of the VRM be competitive, it becomes a potential substitute for wet milling operations in arid regions and allows for better control and conservation of water within industrial operations.

1.2. Problem Statement

The economic and efficient extraction of minerals from complex ores will require increased energy input for size reduction and mineral liberation due to their fine-grained mineralisation. The adoption of high compression grinding equipment such as the VRM has potential to contribute towards reduced energy consumptions at similar or improved mineral recoveries by flotation.

1.3. Research objectives

The main objectives of this project are to:

- Investigate and understand the effects of varying VRM online operational parameters on valuable mineral recoveries after flotation
- Compare the energy consumption, mineral liberation and achieved flotation mineral recoveries of the VRM product with the laboratory scale dry and wet rod milling

1.4. Scope and limitations of the research

This research was focused on and was limited to the use of a 20-ton Swartberg blend ore sample sourced from Black Mountain Mine in South Africa to assess the flotation response with the varying comminution procedures. The comminution procedures included the pilot VRM at different operating conditions and the laboratory scale rod mill. The nominal capacity of the pilot VRM used was 700 kg/hr.

The sample was homogenised at Mintek. This was to ensure that the subsamples used in the planned testwork were representative of the bulk ore collected. The homogenised sample was split into two: 2 tons taken to Cape Town in South Africa and 18 tons shipped to Dusseldorf in Germany.

Grinding tests were done on the sample both in Germany and South Africa while flotation was done in South Africa. Flotation tests were conducted after laboratory scale rod milling and after comminuting with the VRM under different conditions. As Swartberg ore mainly contains galena, sphalerite and chalcopyrite as the value minerals, flotation tests were conducted for and analysis

focused on the flotation performance in recovering these minerals. Flotation tests were done using typical Swartberg ore reagents. The QEMSCAN was used to quantify the mineralogical characteristics of the comminution products from using the three comminution procedures at the benchmarking grind of 65 % passing 75 μm.

1.5. Thesis Structure

This thesis is structured into six chapters followed by references and appendices. An overview of each chapter is presented in this section.

Chapter 1: Introduction

The section begins with providing a background to the investigation carried out in this work: comminution research, the depletion of simple to process ore, increase in complexity of ores and the need to identify sustainable processing technologies. The later parts discuss the problem statement, research objectives and the scope and the limitations of the research

Chapter 2: Literature Review

This section critically reviews the literature relevant to this study, including previous work done in the mineral processing sector. Key findings are then synthesized and presented, and the proposed hypothesis stated.

Chapter 3: Experimental Methods

The materials and methods used to test the proposed hypothesis is given in this chapter in detail. The operating procedures for each critical step are outlined.

Chapter 4: Results

The chapter presents results from the experimental work done. The bulk mineralogical analysis and the grain size distribution of the ore are presented first. The characteristics of the VRM products comminuted under different operating conditions are presented. The outcomes of the comminution tests conducted in terms of progeny PSDs for the different target grinds from the three comminution procedures under study are presented. The flotation response of copper, lead and zinc minerals constituting the Swartberg blend ore are presented. For the benchmarking grind, mineral liberation characteristics of flotation feed and flotation tailings as well as grain size distribution are presented after flotation response results. To conclude the results section, the specialised flotation tests are presented, which were an assessment of the aging characteristics of the ore and recovery by size characteristics.

Chapter 5: Discussion

This section focusses on the discussion of results presented in Chapter 4. It mainly focusses on the interpretation of the data presented and how they compared with published work.

Chapter 6: Conclusions and Recommendations

This section concludes the work done based on the scope as answers to the key questions and the outcomes of the hypotheses tested. It summarises the key findings of the research. Various recommendations based on the results of the research are outlined and these may include opinions which might aid future studies.

1.6. Sustainable Development Goals

The following sustainable development goals (SDG) are addressed in this investigation:

- SDG 12. Ensuring sustainable consumption and production patterns. This study aimed to investigate the options of introducing energy efficient comminution and better process efficiencies in mining operations.
- SDG 9. Industry, innovation and infrastructure. The adoption of VRMs is novel to the mining industry and potentially results in better process efficiencies.
- SDG 6. Clean water and sanitation. The VRM technology is a dry grinding process. This results in better control of water resources.

This is a mining industry project and as such, other SDGs will be indirectly addressed (UNDP et al., 2016)

2. LITERATURE REVIEW

This section critically reviews the literature relevant to this study, including previous work done in the mineral processing sector. The fundamentals of particle breakage are reviewed. The VRM is introduced and reviewed on its operating parameters. The flotation process is reviewed, with reference to the differences in product characteristics that can rise from comminution using the VRM and conventional rod milling. The mineralisation of the Swartberg ore as well as the typical process flow for the concentration of chalcopyrite, galena and sphalerite contained in the Swartberg ore are reviewed. A summary of the key findings from literature is presented and the proposed hypothesis is also presented.

2.1. Comminution research review

Comminution is the process of breaking down large particles and in the process liberating valuable minerals from gangue minerals. Valuable minerals are found naturally finely disseminated in an ore body and can only be separated from the unwanted gangue using comminution (Napier-Munn and Wills, 2005). Comminution is therefore an essential step for downstream valuable mineral recovery processes to be efficient. The process of comminution starts from the mine, where fragmentation occurs through blasting and is usually followed by a series of crushing steps and then grinding. Comminution is a mineral dressing process which makes the ore more amenable to concentration processes like flotation (Napier-Munn and Wills, 2005).

Industrial comminution processes have been found to be both energy intensive and energy inefficient (Tromans, 2008; Ballantyne and Powell, 2014). Most energy supplied for comminution is dissipated in driving the comminution equipment and only 0.1-5 % is used for actual particle breakage (Cleary, 1998; Tavares and King, 1998). Comminution at mining operations takes up to 70% of total operating costs due to high energy consumptions and consumables costs (Curry et al., 2014).

The energy requirements for comminution have increased as the ores being processed have become complex, fine grained and heterogenous. The ores have to be ground finer to liberate the valuable minerals (Norgate and Jahanshahi, 2011; Powell and Mainza, 2012; Reichert et al., 2015). As a result, research has intensified to identify feasible and energy efficient grinding technologies to counter the increased energy demand whilst maintaining final product expectations. One of the potential comminution technologies is high compression grinding in the Vertical Roller Mill (VRM), which is reviewed in section 2.1.3.

2.1.1. Particle Breakage

A rock can be defined as a solid aggregate formed from the consolidation of minerals. Rock breakage is the disintegration of bonds that keep the rock as a solid aggregate to form two or more progeny fragments using applied stress (force per unit area) (King, 2001). According to its definition, particle breakage is thus the primary process governing comminution, as rocks are broken to specific particle sizes to liberate valuable minerals from host rocks and/or expose the valuable minerals surfaces for downstream concentrating processes like leaching and flotation (Tavares and King, 1998; Napier-Munn and Wills, 2005).

Particle breakage is influenced by the size and orientation of parent particle, the material characteristics, the way in which the stress conditions are applied (direction and magnitude) as well as the environment which the particle finds itself in (moisture, chemicals) (Tavares, 2007; Umucu et al., 2013). The stress conditions applied for particle breakage can be divided into two broad categories: compressive stresses and tensile stresses (Napier-Munn and Wills, 2005).

The material characteristics and environment determine the stressing conditions required to break the particles. When stress is applied on a particle, it undergoes plastic deformation. Plastic deformation is the ability of particle to sustain stressing forces without being permanently deformed. Beyond a certain stress, the particle loses its plastic deformation, becomes brittle and disintegrates (Umucu et al., 2013; Chikochi, 2017). The ideal behaviour of a particle under compressive loading is presented in Figure 2-1.

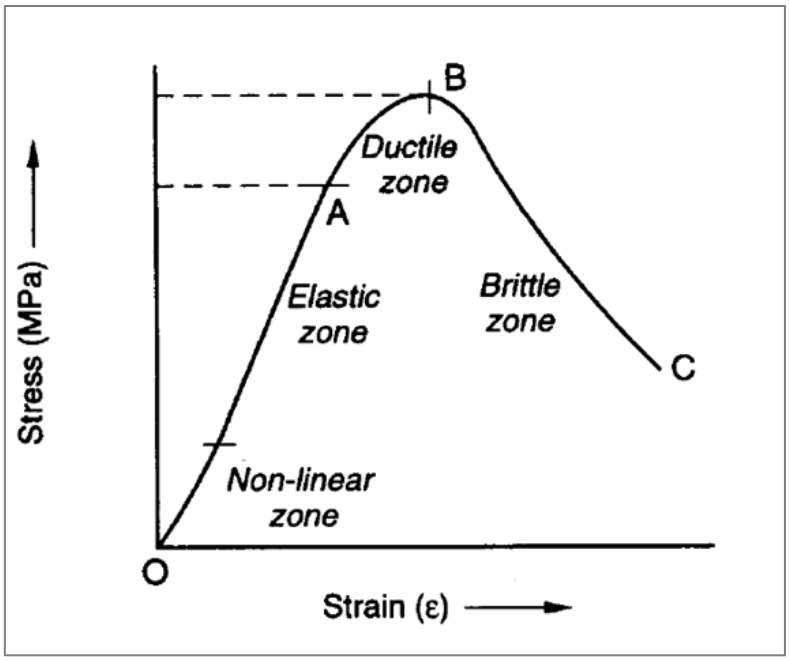

Figure 2-1: Idealised stress-strain response of a cylindrical sample of rock under uniaxial compression (Napier-Munn et al., 2005)

Region OA is the elastic zone, where a rock particle elastically deforms without losing its original characteristics. In the ductile zone (between A and B), the rock continues to deform without losing its ability to resist load. Between B and C, the rock becomes brittle and sudden failure occurs (Napier-Munn et al., 2005).

2.1.2. Particle breakage mechanisms

The mechanism of breakage mostly determines the characteristics of the progeny particles. Compression, impact (rapid compression) and shear are the main mechanisms of breakage. In multiple particle breakage, ore fracture occurs through more than one mechanism. Depending on the type of equipment used for comminution, one mechanism can be more dominant compared to the other.

Crushers and roller mills, including the vertical roller mill (VRM) and High Pressure Grinding Rolls (HPGR) have compression as dominant breakage mechanism while impact or shear are dominant in tumbling mills depending on their function in the mineral processing circuit (Ye et al., 2010). Figure 2-2 illustrates the different particle breakage mechanisms.

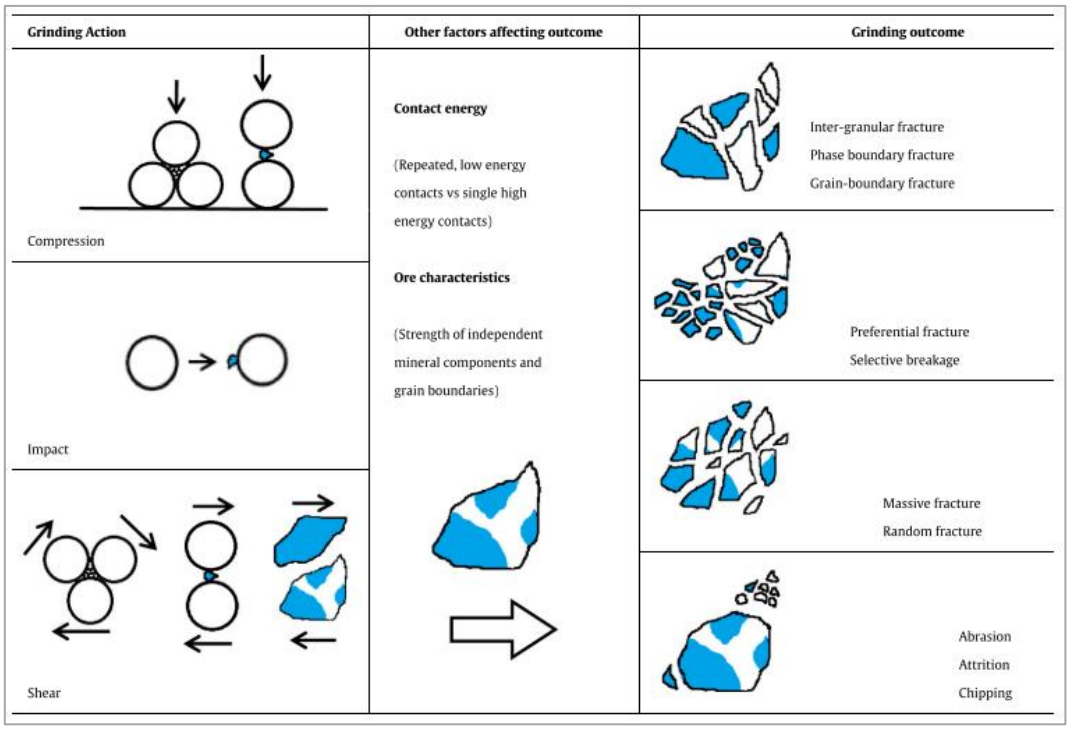

Figure 2-2: Different breakage mechanisms and their comminution associated outcomes. Grinding media is represented by circles, arrows represent the direction of applied stress and irregular, shaded shapes represent the different mineral phases (Little et al., 2016)

2.1.2.1. *Particle breakage in compression grinding equipment*

Compression breakage occurs when particles experience stress in opposing directions. The contact forces can be from other particles, grinding rollers or grinding table. The energy is therefore applied directly for size reduction (Viljoen et al., 2001). This makes compression breakage more energy efficient compared to impact/shear at low reduction ratios (Fuerstenau et al., 1996; Daniel, 2007).

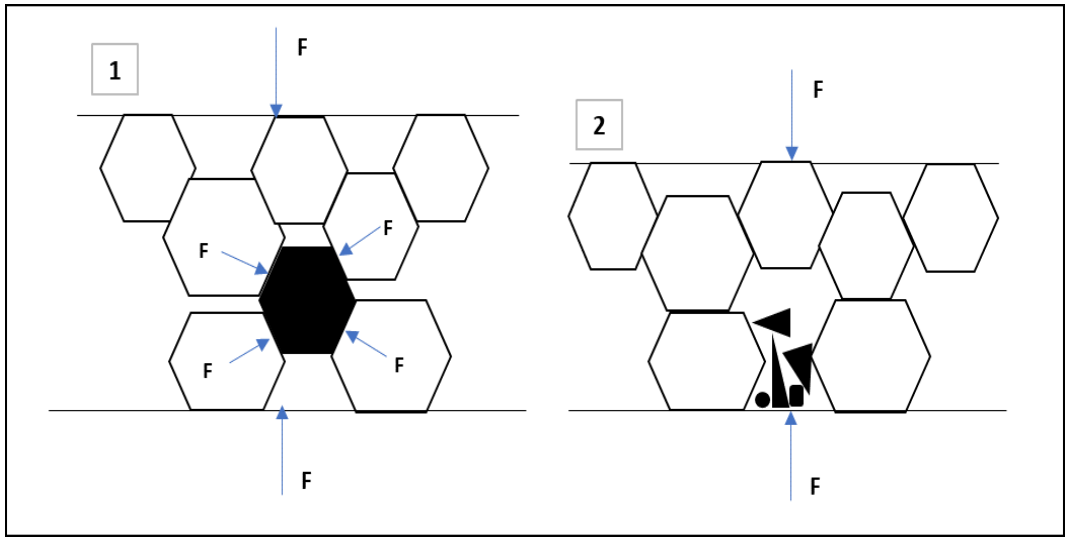

Figure 2-3: Compression driven inter-particle breakage schematic (Viljoen et al., 2001)

Inter-particle breakage is common in compression breakage. A particle to be comminuted is in contact with various particles in the bed. When the bed is compressed, the particle is subjected to multiple stress forces resulting in breakage (Viljoen et al., 2001). In-bed breakage results in secondary fracturing, increasing the probability of generating fine products. Secondary fracturing may therefore needs some control in order to minimise overgrinding (Viljoen et al., 2001). Compression breakage and inter-particle breakage is affected by bed depth, bed porosity, magnitude of compressive force, the residence time of particles in the particle bed, feed particle size and feed moisture (Viljoen et al., 2001).

2.1.2.2. *Particle breakage in tumbling mills*

In the traditional comminution circuits with tumbling mills, particle breakage occurs typically through three mechanisms: impact, abrasion and attrition. Impact breakage occurs when a particle is subjected to a sudden compressive force from a bigger particle (source of impact force) (King, 2001). The force is applied normally to the particle and results in disintegrative fracture (Tavares, 2007). Abrasion and attrition occur when a particle is subjected to forces parallel to the surfaces (Napier-Munn and Wills, 2005). Particles suffer gradual wearing of surfaces making the progeny

particles more rounded (King, 2001). The breakage mechanisms in a tumbling mill are presented in Figure 2-4.

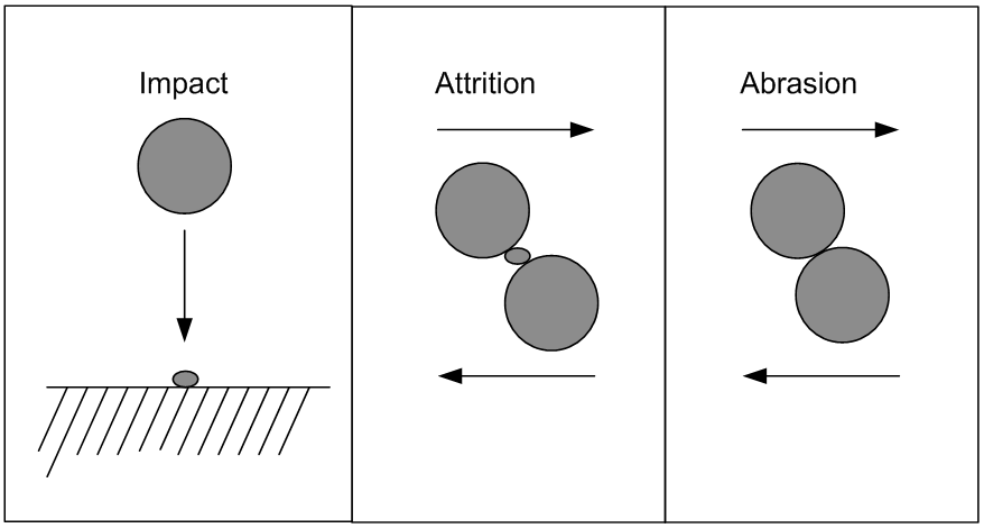

Figure 2-4: Principal breakage mechanisms (Napier-Munn et al., 2005)

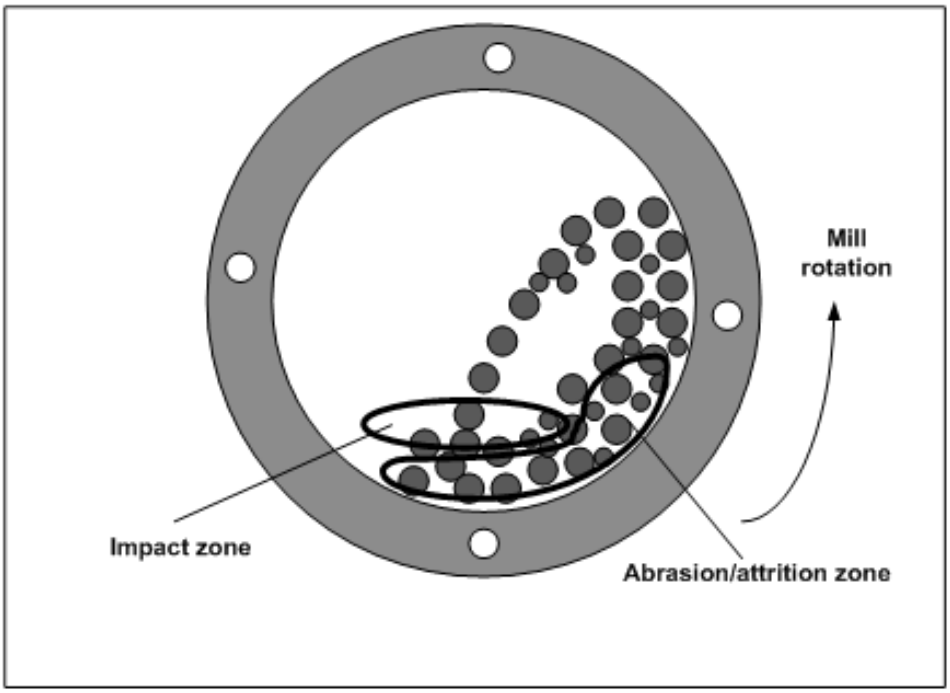

Figure 2-5: Charge motion and its association with breakage mechanism (Napier-Munn et al., 2005)

The charge motion and the associated breakage mechanism inside a tumbling mill are presented in Figure 2-5. In the impact zone or toe region, impact breakage occurs. As the charge of ore is lifted by the mill rotation, layers of rock slip over one another resulting in abrasion and attrition breakage (Kapur et al., 1997; Napier-Munn et al., 2005). To illustrate the typical process flow of material through a typical tumbling mill, Figure 2-6 shows a SAG/RoM ball mill with grate discharge.

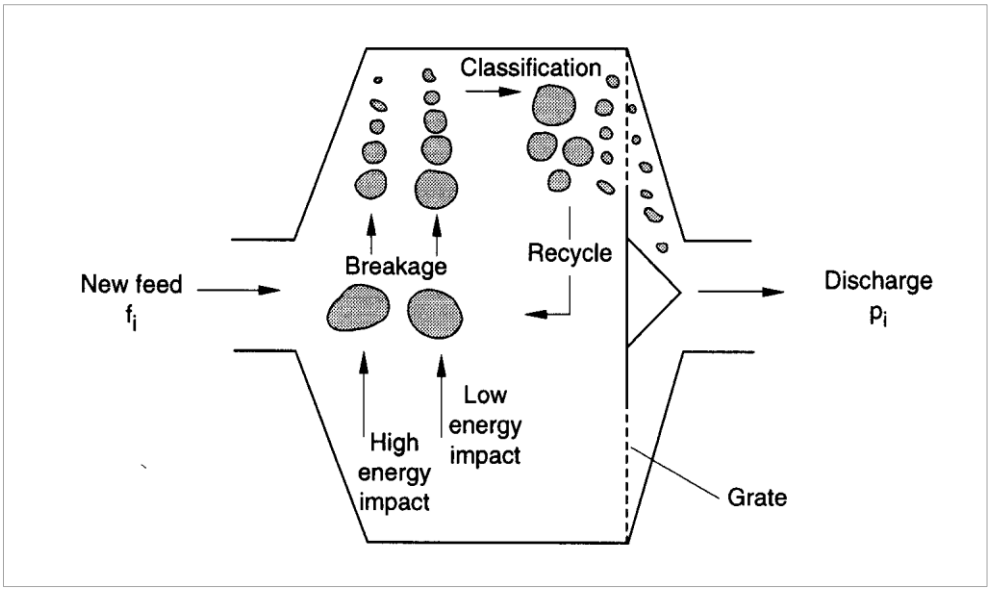

Figure 2-6: Schematic diagram of AG/SAG mill process mechanisms (Morrell, 1992)

Feed enters the mill and is subjected to breakage due to interaction with the charge or with the mill shell. According to Napier-Munn et al. (2005), the particles are subjected to mostly high energy impact breakage, followed by low energy impact breakage before classification at the discharge end of the mill. During the high energy impact, particle breakage is mainly due to brittle fracturing (King, 2001). The low energy impacts are responsible for progressive weakening of particles, which are eventually comminuted (Kapur et al., 1997). In the case of a grate discharge mill shown in Figure 2-6, the products from comminution exit the mill if they are smaller than the grate aperture and are circulated for further breakage if they are larger in size than the grate apertures (Napier-Munn et al., 2005).

As ores are inherently heterogenous, the breakage characteristics of the ore vary continuously. The variability of material breakage characteristics due to variation in composition, texture and grain size affects the performance of the AG/SAG or ball mill comminution circuit (Morrell, 1992; Napier-Munn et al., 2005). Hard to break ores limit the capacity of the mill due to the reduced breakage rates from the ore hardness. On the other hand, soft ores likely generate fine products due to the ease of breakage.

2.1.3. The Vertical Roller Mill (VRM)

Vertical Roller Mills (VRMs) and High-Pressure Grinding Rolls (HPGR) are dominantly compression grinding equipment. The mechanisms of breakage within the VRM are compression and a bit of shear. Shear can however be minimised with modification of roller geometry (Knoflicek and Wentzel, 1995; Reichert et al., 2015). Grinding occurs mostly in a dry environment (Schaefer, 2001; van Drunick et al., 2010; Reichert et al., 2015; Altun et al., 2017). The VRM incorporates both grinding and classification in a single unit operation.

The VRMs have been used in the cement industry and in the production of pulverised coal (Schaefer, 2001; Altun et al., 2015, 2017; Reichert et al., 2015). Their perceived better energy consumption and better product quality control compared to tumbling mills resulted in an increase in installations in the mineral processing industry (Schaefer, 2001; Altun et al., 2017; Stapelmann, 2018). According to Erkan et al (2012), the VRMs can take up feed as coarse as 150 mm and mill to as fine as 20 μm. VRMs have therefore the ability to substitute at least 2 comminution stages in the conventional circuit, eliminating tertiary crushing and SAG/ball milling. As studies have shown the potential benefits of adopting high compression grinding equipment in the mineral processing circuit, there has been increased research in their adoption.

2.1.3.1. Loesche VRM Operating Principles

The grinding components of a Loesche VRM as presented in Figure 2-7 are the circular rotating grinding table (1), conical grinding rollers (2) and dynamic separator (3). Grinding occurs at the lower section of the mill using the grinding table and the conical grinding rollers. Classification is performed using the dynamic separator situated at the upper section of the mill.

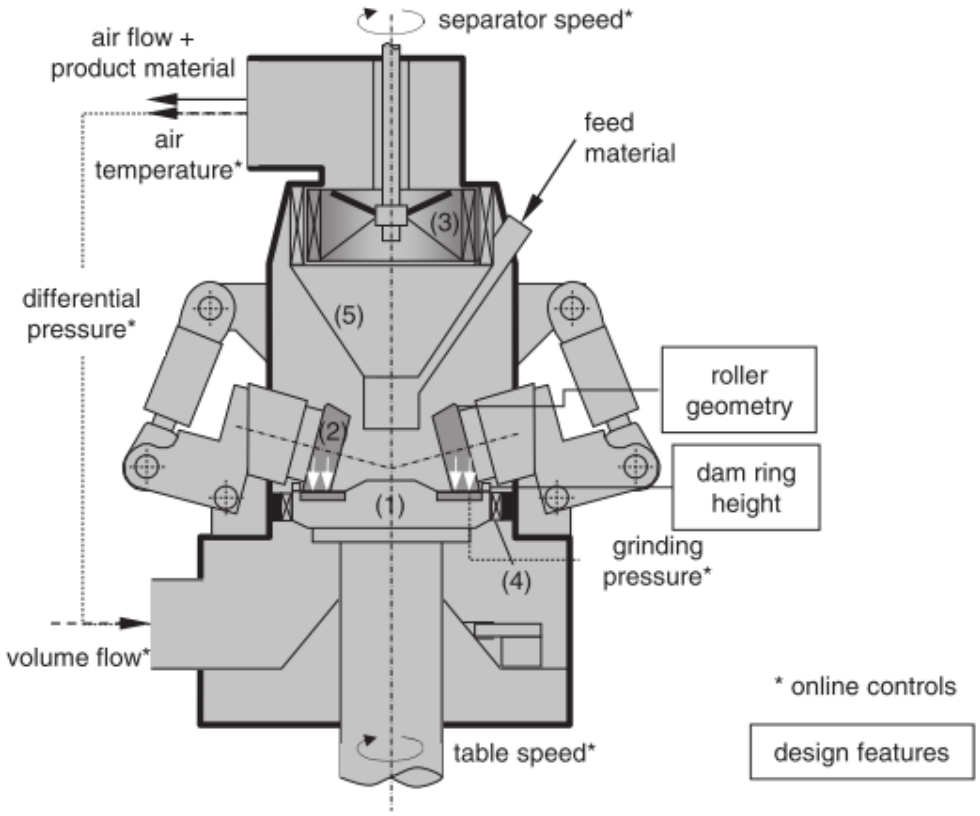

Figure 2-7: Vertical Roller Mill operating principles (Reichert et al., 2015)

The raw materials (feed) are added at a controlled rate to the centre of the grinding table. The particles are subjected to centrifugal forces from the rotating grinding table and are pushed towards the edge of the table. As particles move towards the edge of the table, they pass through the working surfaces of the grinding table and rollers where comminution takes place (Reichert et al., 2015). Using a hydro-pneumatic spring system, the conical rollers introduce compressive grinding pressure onto the particle bed resulting in compressive interparticle breakage (Schaefer, 2001; Altun et al., 2015; Reichert et al., 2015).

When ground material reaches the edge of the table, it can be subjected to three different classification options. These are air-swept internal, air-swept external and external screening mode. In the air-swept external mode, product is pneumatically transported to an external classifier. For the external screening mode, product falls off the grinding table and is conveyed to a separate classifying unit which is normally a classification screen. In both cases, the coarse product is fed back to the mill through the grit cone (5).

In the air-swept internal classification mode, the product is transported pneumatically to the dynamic classifier located at the upper section of the mill. The rotor and blade of the dynamic classifier generates a centrifugal force opposite the direction of airflow. Particles experience radial

and centrifugal forces and are separated based on size, density and shape (Plitt, 1976). Particles whose size is less than the cut point as collected as overflow, while the rejects are sent back to the mill for further grinding via the grit cone (Reichert et al., 2015). The overflow product is collected in a filter and stored in silos before being conditioned for downstream processes (Schaefer, 2001).

The mode of classification employed has a significant influence on the total energy consumption for the VRM. The fan operation can consume up to 50% of total comminution energy (Drunick et al., 2010). In work done by Altun et al. (2015), the total classification energy was 40 % of the total comminution energy. VRM in external classification mode, allows for the installation of a smaller fan which requires about 50% less energy than that for the air swept mode (Drunick et al., 2010).

2.1.3.2. Operational Parameters affecting VRM performance

The product specifications from the comminution process in the Vertical Roller Mill can be manipulated by changing design or online variables. The design variables are roller geometry, dam ring height, number of rollers in operation and method of classification. Dam ring height is the distance between the rotating grinding table and the conical grinding roller. The online variables to manipulate product specifications are grinding pressure, table speed, classifier rotor speed and pressure drop across the unit (Reichert et al., 2015; Altun et al., 2017).

Roller geometry and dam ring height can be adapted for the mill to meet the required grinding specifications (Reichert et al., 2015). The roller geometry can also be changed to alter the dominance of compression over shear breakage, thereby controlling fines generation and controlling product particle size distribution (Reichert et al., 2015).

The volume of material in the grinding space is controlled by changing dam ring height. When the dam ring height is larger, the retention time of particles in the grinding space is higher (Tamashige et al., 1991). Given dam ring height has an influence on residence time of particles, it follows that throughput and grind are influenced by changes in dam ring height. Reichert et al (2015) observed that an increase in dam ring height resulted in a slight increase in throughput, a marked increase in energy consumption and marginal changes in grind. Conversely, Tamashige et al (1991) observed that an increase in dam height resulted in a decrease in throughput and decrease in energy efficiencies. The decrease in energy efficiencies with increased dam ring height was attributed to friction losses between particles, generating heat as a result. High dam ring heights were also observed to result in increased generation of fines and flatter particle size distributions (Roy, 2002; Jørgensen, 2005).

Grinding pressure, adjustable using the hydro-pneumatic spring system controls, is an online parameter used to control product quality. An increase in grinding pressure was observed to result in an decrease in specific energy consumption, increase in production rate, increase in ratio of liberation and a gradual decrease in P_{80} (Tamashige et al, 1991; Reichert et al., 2015). It was however reported that the increase in grinding pressure resulted in an increase in mineral liberation up to a certain point beyond which it resulted in overgrinding and fines generation, which is detrimental for downstream process performance (Altun et al., 2017). With the increased grinding pressure, particles are ground finer in the grinding gap and this results in more particles reporting to the product stream in the classifier. A reduction in circulating load allows for higher feed rates.

Literature reported that an increase in grinding table speed results in an increase in product size (P_{80}) and product rate (Altun et al., 2015, 2017). An increase in table speed at constant classifier speed results in ore reaching the grinding gap in less time hence more ore can be ground per unit time. There is decreased residence time of ore particles on the grinding table due to the increased centrifugal forces acting on them. Product becomes coarser as a result. Specific energy consumption decreases primarily due to the increase in throughput and increase in product coarseness (Altun et al., 2017).

Classifier rotor speed is presented in literature as having a key influence on product quality and energy efficiencies (Tamashige et al., 1991; Altun et al., 2015, 2017). For work done on iron ore (Reichert et al., 2015) and work done on gold ore (Altun et al., 2017), it was observed that the increase in classifier rotor speed resulted in a reduction in fresh feed rate, an increase in specific energy consumption and a decrease in P_{80} (product became finer). The higher the classifier rotor speed, the finer the products from the comminution process and the lower the throughput. This is because as the rotor speed increases, the rejection rate of particles back to the grinding table increases and therefore recirculating load to the grinding table increases. All other parameters kept constant, an increase in recirculating load yields an expected reduction in fresh feed to the mill. According to the work done on magnetite iron ore (Reichert et al., 2015), degree of liberation increased with increasing classifier rotor speed up to a maxima and then started decreasing. This was likely due to an increased generation of fines and overgrinding.

Air flow is the driving force for comminuted particles movement from the lower section to the classifiers. The higher the air flowrate, the smaller the proportion of particles dropping back to the table and the lower the fines generation (Tamashige et al., 1991). The proportion of coarse product is dependent on the combination of air flowrate and classifier rotor speed. These two parameters directly influence cut size (Tamashige et al., 1991).

2.1.3.3. VRM Case Studies

A summary of the studies done on the VRM relevant to this study reported in literature are presented in Table 2-1.

Table 2-1: Summary of VRM-tumbling mills comparative studies in literature

Ore Type	Authors	Aspect	Comparison with tumbling mills
Zinc ore	van Drunick et al., 2010	Specific energy consumption	Specific energy consumption for VRM circuit 29-32 % lower.
Gold ore	Erkan et al., 2012	Specific energy consumption, grinding media wear rates, leach recovery	Finer product using VRM at same specific energy consumption. Grinding media wear rates 50 % lower for VRM circuit. Leach recoveries comparable.
Copper ore	Altun et al., 2015	Specific energy consumption, wear rates	Specific energy consumption for VRM circuit 18 % lower. Wear rates reduced by 58.7 %.
Iron ore	Reichert et al., 2015	Liberation ratio	Ratio of liberation of product was 97.5 % from tumbling mill circuit and 98.5 % from the VRM
Copper-gold ore	Benzer et al., 2018	Specific energy consumption, grinding media wear rates	Specific energy consumption for VRM circuit 9-15,7 % lower. Grinding media wear rates 94 % lower for VRM circuit.

All previous studies indicated that there is a reduction in energy consumption and reduction in media wear rates when using the VRM instead of the conventional tumbling mills (Erkan et al., 2012; Altun et al., 2015; Reichert et al., 2015; Benzer, Gerold & Schmitz, 2018; Stapelmann, 2018). With regards to liberation, there is marginal difference realised based on the work done on the iron ore by Reichert et al (2015). The use of either the conventional comminution circuit and the VRM resulted in high liberation ratios of iron minerals, and the ratios are both very close to each other. From a statistical point of view, if propagation of error were to be done on the two results, they would be no difference. Reviewing the work done on a gold ore by Erkan et al. (2012), the leach performance of the VRM products and the tumbling mill products were similar.

Based on the previous work done, there is a clear indication that the VRM has an energy efficiency and low operating cost advantage, and that the other parameters (leach performance, mineral liberation characteristics) are comparable to those from the conventional tumbling mill circuits.

2.2. Flotation Review

2.2.1. Flotation principles

Froth flotation is a selective separation process that utilises differences in surface properties to separate value minerals from unwanted gangue (Napier-Munn and Wills, 2005).

There are two types of flotation, namely normal flotation and reverse flotation. In normal flotation, valuable minerals are made hydrophobic and are recovered in the froth phase while the unwanted gangue minerals are made hydrophilic, stay in the pulp phase and are recovered as tailings. The opposite is true for reverse flotation. With regards to this study, flotation refers to normal flotation. The typical flotation process is presented in Figure 2-8.

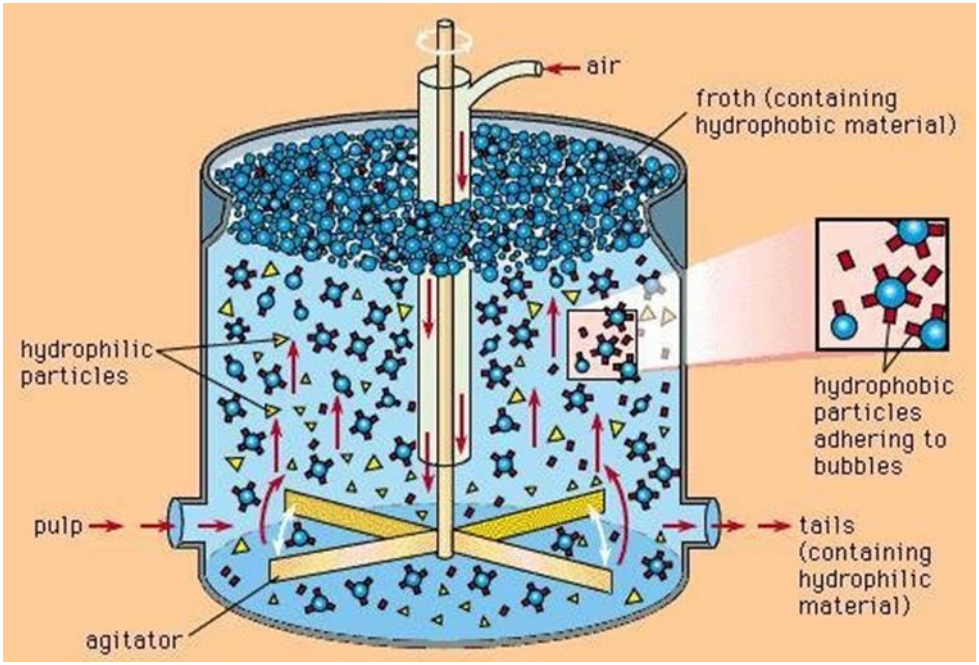

Figure 2-8: The froth flotation process (Encyclopedia Britannica, 2019)

The flotation process occurs sequentially as follows: Air bubbles are introduced at the bottom of an agitated flotation cell. The flotation cell is agitated for air dispersion and to keep solids in suspension. Valuable minerals are made hydrophobic and unwanted gangue minerals more hydrophilic using chemical reagents (Bradshaw et al., 1998). As the air bubbles rise through the pulp phase, the hydrophobic valuable minerals attach to the rising air bubbles and are recovered in the froth phase. This is termed true flotation.

Recovery of valuable minerals also occurs in two other sub-processes: entrainment of particles recovered in the froth phase and physical entrapment of particles between bubbles (Napier-Munn and Wills, 2005). As entrainment is defined as the mechanical carryover of particles unselectively

due to the movement of water from the pulp to the froth phase, fine particles (< 10 μm) are more likely to be recovered through this subprocess because of slow drainage back to the pulp (Neethling and Cilliers, 2002; Yianatos and Contreras, 2010).

The success of flotation is dependent on chemistry, operational and equipment factors. During normal operation, flotation efficiencies are dependent on chemistry and operational factors as equipment factors will be fixed. The chemistry factors consider the interaction between flotation reagents and solids particles surface. The operational factors consider the effect of particle size distribution, mineralogy, feed rate, pulp density, bubble size, temperature and circuit design on flotation (Klimpel, 1995).

2.2.2. Review of Chemistry Factors

Flotation reagents used in base metal sulfide flotation can be classified under the following groups: collectors, frothers and modifiers.

2.2.2.1. Collectors

Collectors are organic compounds added to the pulp to make minerals hydrophobic, which allows the value minerals to attach to air bubbles and float. Collectors mostly consist of a polar head and non-polar tail. As a factor of physio-chemical interactions, the polar head adsorbs onto the mineral surface and the non-polar tail towards the bulk of the solution thus rendering the particle hydrophobic as shown in Figure 2-9 (Bulatovic, 2007, 2014). The hydrophobic particle then attaches itself to the rising air bubble and is recovered in the froth phase. The most widely used anionic collectors for sulfide minerals flotation are xanthates (Napier-Munn and Wills, 2005).

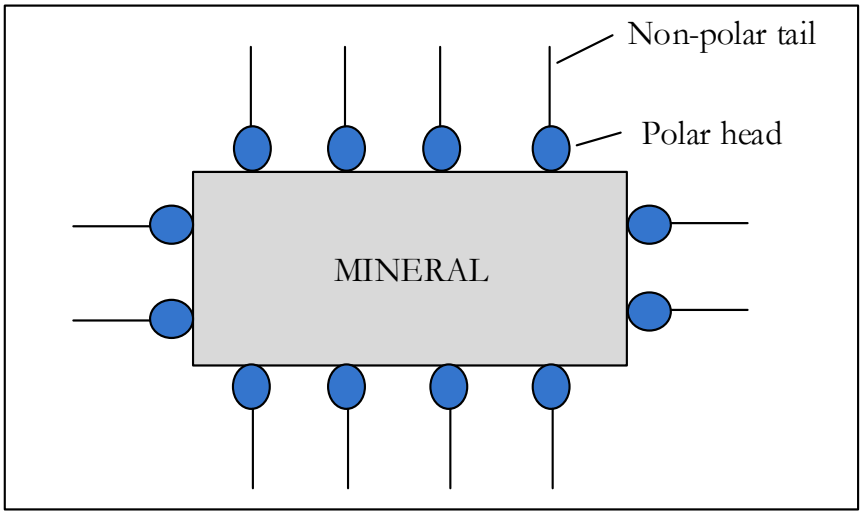

Figure 2-9: Collector adsorption on mineral surface (Napier-Munn and Wills, 2005)

The condition in the pulp (pulp potential) affects the action of sulfide collectors. Oxidising pulp environments result in sulphur rich, non-polar mineral surfaces. This increases the value mineral hydrophobicity and improves xanthate adsorption (Hintikka and Leppinen, 1995; King, 2001). The opposite is true for very reducing pulp environments, where hydroxide precipitation occurs on the mineral surfaces hindering the action of collectors (Koleini et al., 2012).

2.2.2.2. Frothers

Frothers are used to stabilise the froth as well as controlling bubble size by reducing bubble coalescence (Laskowski, 2004). Frothers are non-ionic, heteropolar, surface-active organic reagents which adsorb on the air-water interface, thereby providing bubble stability and minimising bubble coalescence (Napier-Munn and Wills, 2005). The action and orientation of the polar and non-polar end of a frother in action is presented in Figure 2-10.

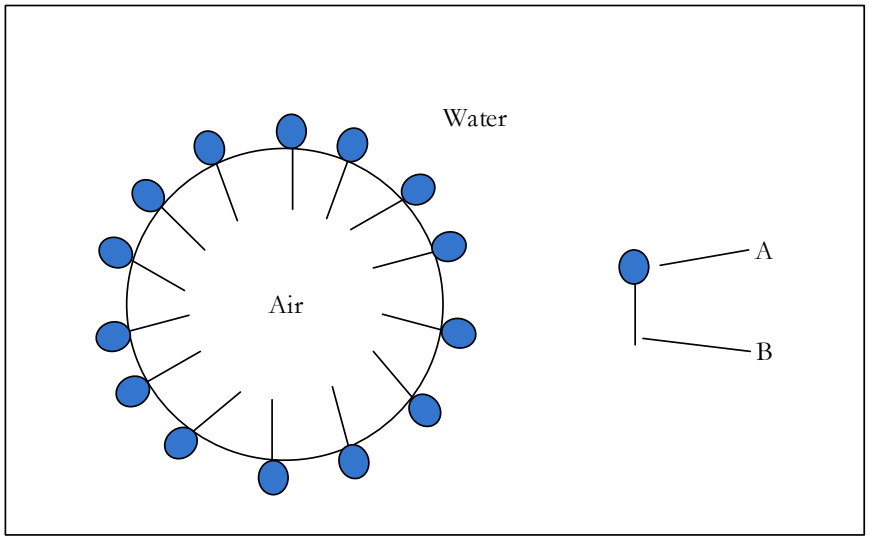

Figure 2-10: Frother action A – polar head; B–non-polar tail (Napier-Munn and Wills, 2005).

The stability of the froth allows for selective drainage of entrained gangue from the froth phase (Napier-Munn and Wills, 2005; Bulatovic, 2007). If the froth is too stable because of excess frother, water recovery increases and this results in low selectivity and in the process gangue minerals are recovered in the froth phase. An unstable froth results in bursting of bubbles, and the recovered valuable minerals have increased probability of draining back into the pulp phase and eventually be lost as tailings (Napier-Munn and Wills, 2005; Fuerstenau et al., 2007; Yianatos and Contreras, 2010).

2.2.2.3. Modifiers

Modifiers are added to either manipulate the surface properties of minerals in the pulp or alter the conditions of the pulp in order to optimise value mineral recovery (Bulatovic, 2007). Modifiers are classified into three main categories: activators, depressants and pH modifiers (Napier-Munn and Wills, 2005; Bulatovic, 2014).

pH modifiers are used to alter the redox chemistry within the pulp, therefore enabling the selective recovery of minerals. pH is related to the pulp potential (Eh). Eh is the potential difference of a mineral-solution interface and has been shown to be related to floatability of sulfide minerals (Göktepe, 2002). It can be measured by inserting noble metal electrodes into the pulp phase. Literature reports that sulfide mineral flotation can be controlled by changing the oxidising and reducing conditions in the pulp (Janetski et al., 1977; Gardner and Woods, 1979; Göktepe, 2002; Fuerstenau et al., 2009).

Depressants render gangue minerals hydrophilic. As recovery through flotation mainly targets hydrophobic minerals, the recovery potential of gangue is subsequently lowered by the action of depressants (Napier-Munn and Wills, 2005). Activators chemically alter the surface properties of valuable minerals, rendering the surfaces more hydrophobic and more amenable to sulfide collector action (Napier-Munn and Wills, 2005).

2.2.3. Review of Operational Factors

It has already been stated that the role of comminution is to prepare ores and ore surfaces for downstream recovery processes (Napier-Munn and Wills, 2005). With respect to flotation, particle size distribution, mineral liberation and association and surface properties are important outcomes from comminution as they influence efficiencies.

Particle size is critical as it affects particle-bubble interactions, influences froth stability and level of entrapment (Feng and Aldrich, 1999; King, 2001; Rao, 2004; Napier-Munn and Wills, 2005; Jameson, 2012). The mineral surface properties are affected by the comminution procedure employed. This will affect the action of collectors and resultant floatability (Farrokhpay and Manouchehri, 2012; Koleini et al., 2012; Corin et al, 2013). Higher degrees of valuable mineral liberation at the optimum mean particle size results in higher recoveries as more minerals can be recovered through true flotation (Jameson, 2012). Compression grinding is reported to result in preferential fractures along grain boundaries and result in higher liberation of value minerals (Reichert et al., 2015; Loesche GmbH, 2016). The more liberated the valuable minerals are, the higher the probability of recovering them in the downstream concentration processes.

A review of factors affecting flotation response pertinent to this study was conducted and the findings presented.

2.2.3.1. The effect of particle size distribution

Pease et al (2006) conducted a study on the influence of different particle size fractions on flotation (Figure 2-11). Gaudin et al (1931) also studied the influence of particle size on the flotation of copper, lead and zinc (Figure 2-12).

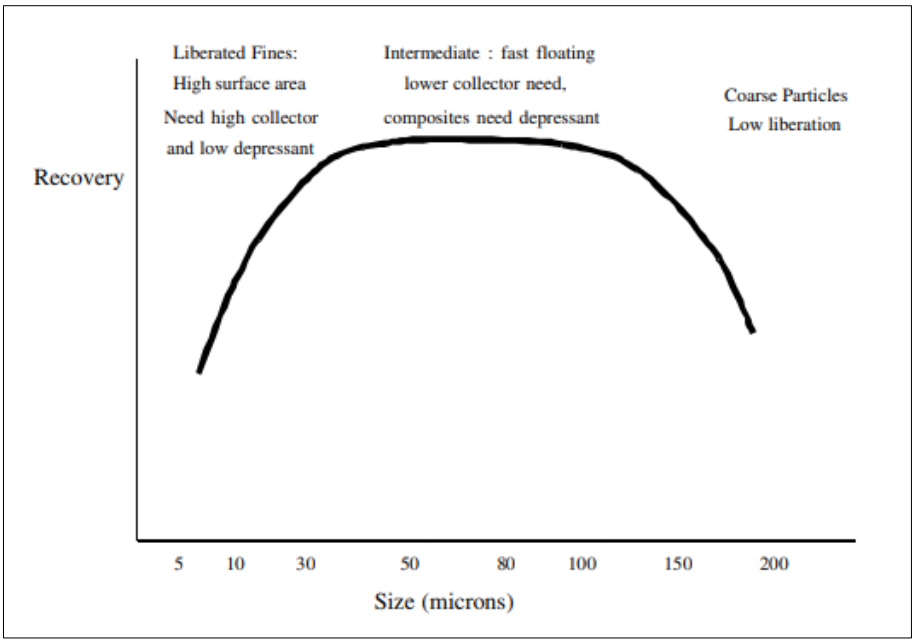

Figure 2-11: Typical view of the flotation of different size fractions (Pease et al., 2006)

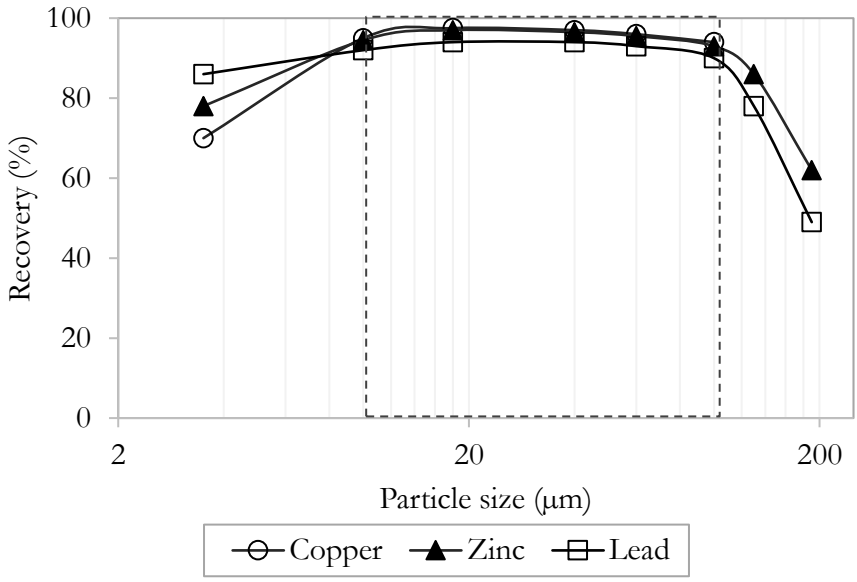

Figure 2-12: Flotation recovery against particle size for copper, zinc and lead (Gaudin et al., 1931).

Pease et al (2006) generalised the flotation behaviour of particles of different particle sizes. Very fine particles can only be recovered by entrainment as they do not have enough momentum to attach to the rising bubble (Pease et al., 2006). The recovery of fine particles through entrainment is not selective and stabilises the froth phase. Due to no-selective nature of recovery by entrainment, both recovery and grade are compromised. Very fine particles tend to require excessive collector dosages, complicate the pulp rheology and in most cases require a change in equipment design to be recover the particles. On the other hand, coarse particles are poorly liberated and are too heavy to be recovered through bubble attachment to the froth phase. Some are entrapped but fall back to the pulp phase. This also results in low recoveries.

Figure 2-12 indicates that highest recovery of copper, lead and zinc minerals was achieved for particle sizes greater than 10 μm but less than 100 μm. Other authors also confirmed that the optimal particle size range to maximise flotation efficiencies is between 10 μm and 90 μm (Feng and Aldrich, 1999; Napier-Munn and Wills, 2005; Jameson, 2012).

Gamsberg zinc ore was used by van Drunick et al (2010) while Merensky and UG2 platinum ore was used by Solomon et al (2011) to test compression grinding and its effect on downstream processes. Their work indicated that compression grinding produced a slightly finer grind in terms of cut size (d50). van Drunick et al (2010) went on to state that while the finer grind could be optimal for PGM flotation, it was potentially detrimental to base metal flotation. Solomon et al (2011) observed that the 6 mm feed comminuted using the ball mill was steeper as compared to the HPGR product and a larger proportion of the ball mill product was in the optimum size range for flotation for PGMs (Figure 2-13).

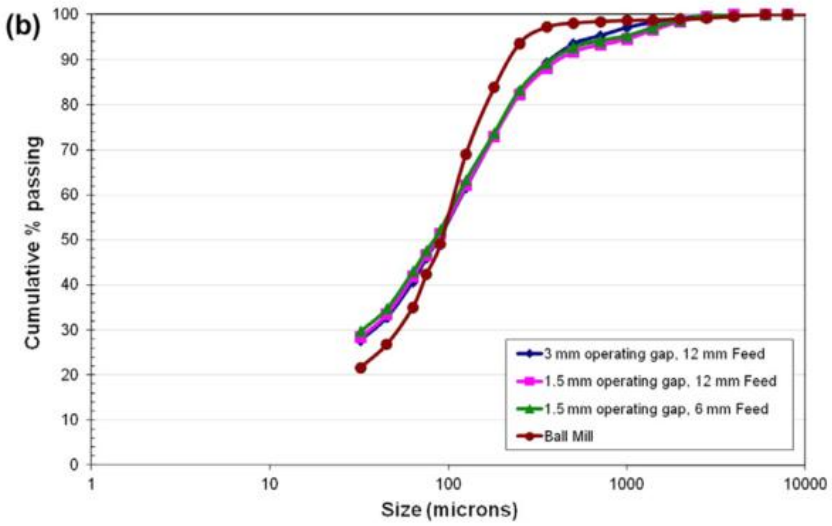

Figure 2-13: Particle size distribution of the flotation feed for the UG2 platinum ore (Solomon et al., 2011)

The differences in shape of the PSD curves for similar feed (6 mm feed) comminuted using the ball mill and the HPGR was attributed to the differences in breakage mechanisms. Solomon et al (2011) postulated that interparticle breakage caused by compression breakage from the HPGR resulted in higher fines generation and hence a flatter PSD curve, while impact and abrasion grinding resulted in lower fines generation hence the steeper PSD curve. This had a direct impact on flotation as the ball mill product had the lower fine to coarse particles ratio and more particles in the optimal flotation size range, resulting in better selectivity and better PGM recovery.

Reference to compression grinding, several studies have been conducted and showed that grinding roller pressure can be manipulated to produce the optimum particle size distribution for flotation (Schaefer, 2001; von Michaelis, 2005). This means that product particle size distribution from compression grinding equipment can be manipulated to tailor the downstream requirements.

2.2.3.2. The effect of wet vs. dry grinding

In the study by Palm et al (2011) on a base metal sulfide ore, secondary dry grinding resulted in better flotation performance compared to secondary wet grinding irrespective of the primary grinding process (crushing or HPGR). In these tests, secondary grinding was done using stainless steel balls (for wet) and mild steel balls (for dry). The improved recoveries from dry grinding were attributed to surface chemistry differences between secondary dry grinding and secondary wet grinding.

Galvanic Interactions

As steel is relatively anodic in comparison to most sulphidic ores, the flow of electrons to the mineral surface results in the formation of metal hydroxides (Ye et al., 2010; Palm et al., 2011). The reactions are presented in Figure 2-14.

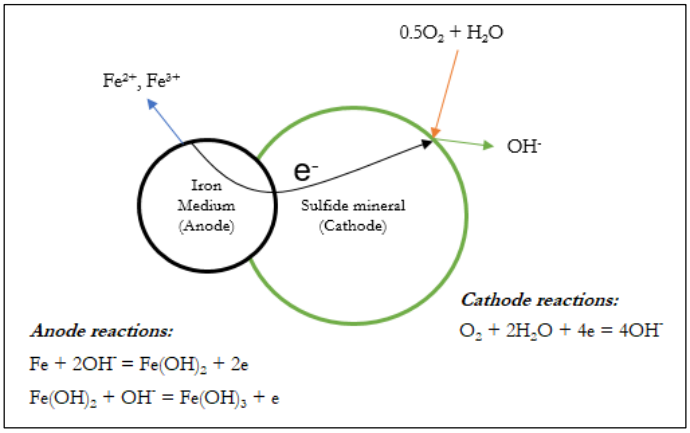

Figure 2-14: Galvanic interactions occurring between sulfide minerals and the iron medium (Adopted from Koleini et al (2012))

The formation of the metal hydroxides on the mineral surface renders the surface less amenable to collection by the sulfide collector resulting in poor recoveries. This phenomenon was said to be more dominant in wet grinding using steel balls than dry grinding. Dry grinding product will only be exposed to water before flotation which minimises these galvanic interactions. This was also concluded by van Drunick et al (2010) and Erkan et al (2012), who stated that the use of HPGR/VRM is mostly autogenous and hence steel-ore interactions are minimised.

Microstructural defects and kinetics

Using scanning electronic microscopy (SEM) on Merensky ore, Feng and Aldrich (2000) found that dry ground particles had rough surfaces with microstructural defects while wet ground particles were smoother. The present of microstructural defects means an increase in surface area on the particle for collector adsorption to take place. The dry ground particles thus exhibited better collector adsorption kinetics as shown in Figure 2-16.

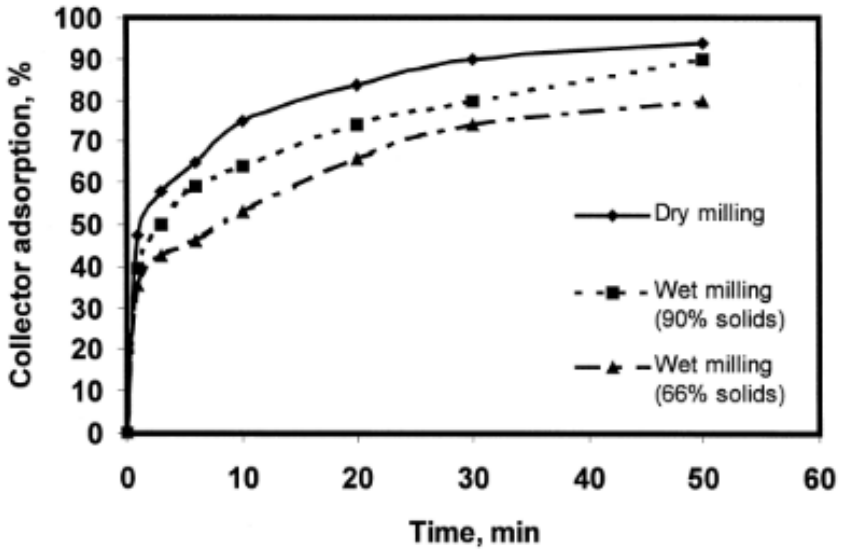

Figure 2-15: Collector adsorption kinetics on sulfide particles (Feng and Aldrich, 2000)

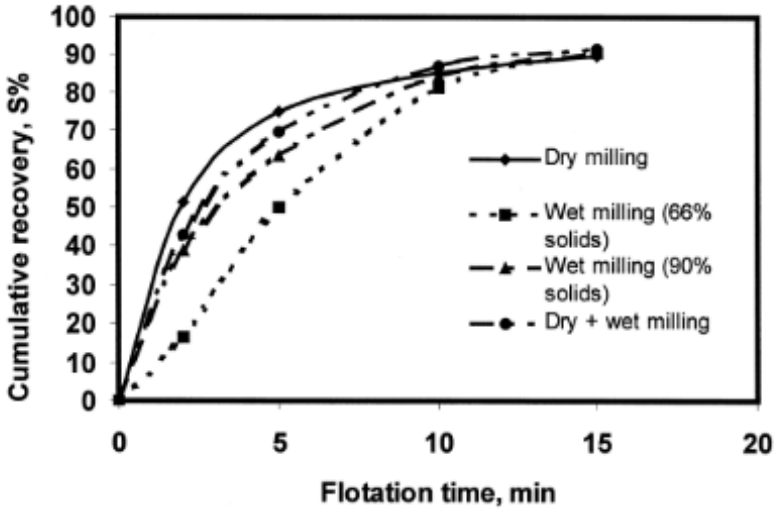

Figure 2-16: Sulfide recovery vs. time at varying % solids in the mill (Feng and Aldrich, 2000)

The recovery attained using either dry or wet milling prior to flotation were similar as shown in Figure 2-16. The only difference was selectivity, where floating dry ground products resulted in lower selectivity. In order to improve flotation selectivity after dry grinding, high intensity conditioning was found to be effective (Feng and Aldrich, 2000; Bruckard et al., 2011). High intensity conditioning is subjecting the flotation pulp to high shear forces (agitation) before flotation, thereby making the particles smoother and cleaner of fines. Reviewing the effects of grinding environment on the flotation of copper sulfides, Bruckard et al (2011) found that selectivity was improved by using high intensity conditioning after dry grinding, thereby improving grades and recovery. The increase in selectivity observed as a result of high intensity conditioning in the study of Merensky ore by Feng and Aldrich (2000) is presented in Figure 2-17.

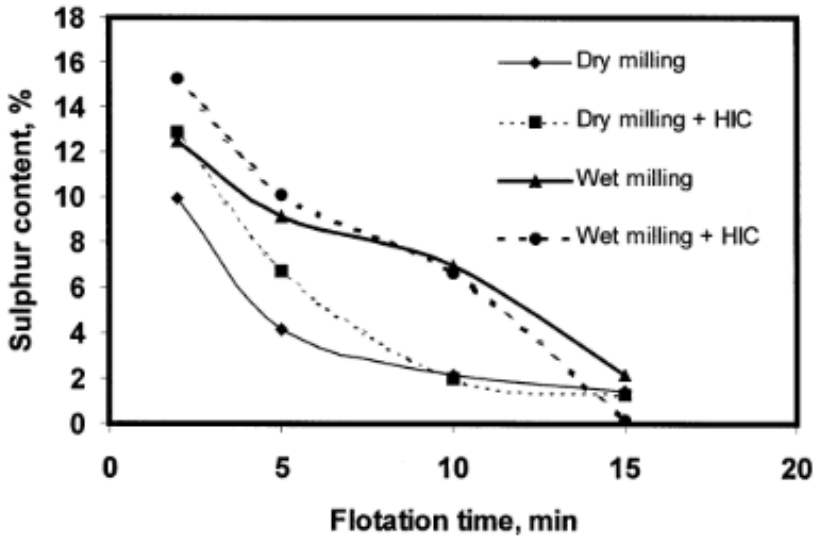

Figure 2-17: Variation of concentrate sulphur content vs. flotation time before and after high intensity conditioning (HIC) (Feng and Aldrich, 2000)

Pulp potential (Eh)

Another parameter that is influenced by whether dry or wet grinding is employed prior to flotation is pulp/redox potential. Literature indicates that dry grinding results in higher pulp potential of product (van Drunick et al., 2010; Chapman et al., 2011; Farrokhpay and Manouchehri, 2012; Koleini et al., 2012). In the study of complex Cu-Zn sulfide ore by Koleini et al (2012), the lower pulp potential in the wet product was explained to be an indication of the presence and action of oxygen consumers like iron in the wet milled pulp and the influence of water in galvanic coupling (Grano, 2009). It also follows that more positive pulp potential is a result of higher amounts of dissolved oxygen at constant pH. Koleini et al (2012) stated the more positive pulp potential from dry grinding as the main contributor of the observed higher recoveries for dry ground ore, though the dry ground product had a coarser particle size distribution.

In the flotation studies done on a copper sulfide ore, Gonçalves et al (2003) stated the more positive pulp potential promoted xanthate oxidation to dixanthogen as well as the moderate oxidation of the surface of sulfides present in the slurry. This favoured the adsorption of dixanthogen on sulfide deficient metal surfaces, thereby enhancing self-induced floatability and hydrophobicity (Gonçalves et al., 2003). There is a limit to which the pulp potential can be more oxidising, beyond which major oxidation of sulfide surfaces will occur and the deficiency of oxygen in the pulp minimises xanthate oxidation or adsorption. Self-floatability and recoveries are compromised as a result (Heyes and Trahar, 1979; Gonçalves et al., 2003).

Separate studies that reported on redox potential postulated that the more positive redox potential from dry grinding may result in a greater degree of oxidation of the mineral surface which in turn may be detrimental to flotation (Chapman et al., 2011; Palm et al., 2011; Solomon et al., 2011). In their argument, pulping the dry ground product prior to flotation was accompanied by a significant layer of passivating ions attaching to the surfaces with the microstructural defects thereby negatively affecting collector adsorption. This postulated phenomena was found to be true and detrimental for the flotation of a PGM ore after dry grinding (Chapman et al., 2011; Solomon et al., 2011). However, using the same procedures on a zinc ore, zinc recovery was highest for dry milling (Palm et al., 2011). This may then mean that the postulated phenomena of passivating ions attachment of high energy sites and the effect on flotation performance may be ore-dependent and may need verification.

Heat generation factor

Dry grinding has been reported to have its limitations if not done in a controlled environment (Farrokhpay and Manouchehri, 2012). Dry grinding generates heat, and this may alter surface properties through the oxidation of sulfides. If milling times in laboratory mill are also different for dry and wet grinding, differences in morphology may arise and could influence flotation performance (Gonçalves et al., 2003; Bruckard et al., 2011). As the subsequent flotation procedure will be focusing on sulfide mineral recovery, the oxidation of mineral surfaces lowers collection efficiencies (using conventional sulfide collectors). The poor collection efficiencies will inevitably result in compromised flotation efficiencies. If these highlighted limitations are addressed, dry grinding can possibly compete or better wet grinding when it comes to downstream process performance.

Traditional preference

Lastly, wet grinding has often been traditionally preferred as most downstream processes (e.g. flotation and leaching) are performed wet and that wet grinding does not require dust control systems (Farrokhpay and Manouchehri, 2012). Studies on the VRM and other compression grinding devices have demonstrated that the use of these equipment have energy saving benefits without compromising downstream requirements. The VRM design has dust control systems and hence the challenge of dust is not a factor.

2.2.3.3. The effect of mineral liberation

To recover valuable minerals from unwanted gangue, the valuable minerals need to be liberated before the concentration steps. This is done by comminution, breaking down the ore to expose the mineral grains. Mineral liberation is defined as the cross-sectional area of the valuable mineral that is exposed and is available for the subsequent separation process in comparison to the whole particle (Lastra, 2002). It has been proposed that the different grinding mechanisms would result in products of different levels of liberation.

The comparison of the liberation profiles reported in literature has been variable. Compression and impact have been associated with higher percent liberation while abrasion/attrition to lower liberation (Apling and Bwalya, 1997; Hoşten and Özbay, 1998; Celik and Oner, 2006; Loesche GmbH, 2016). Using a copper ore, the VRM product had more liberated copper and nickel containing minerals as compared to the ball mill product (Viljoen et al., 2001). The flotation recovery of copper and nickel in this particular study were consequently higher for the VRM product (Viljoen et al., 2001), and this was attributed to the differences in mineral liberation characteristics.

In a study to quantify the liberation of minerals from using different comminution devices, Daniel (2007) concluded that the results were ore dependent more than equipment dependent. Bauxite and Pb-Zn ore did not show any differences, but chromite minerals were better liberated in the coarse fractions after using compression grinding. Wightman et al (2008) compared the degree of liberation from comminution using the rod mill, hammer mill, stirred mill and piston and die. The MLA was used to measure the degree of liberation obtained. The study also showed that degree of liberation was independent of comminution procedure used. In a comparative study of liberation profiles between a similar feed comminuted using the HPGR and the ball mill by Solomon et al (2011), there was no difference in the amount of liberated PGMs.

The study by van Drunick et al (2010) focussed on the differences between mineralogical results from using a combination of HPGR-VRM at different grinding pressures. The results indicated that degree of liberation reduced with increased grinding pressure potentially because of overgrinding. While this study informs of the different outputs from HPGR-VRM combinations, there is no conventional milling benchmark to compare the outcome with. The findings in literature to some degree agree that the differences in mineral liberation profiles are more dependent on the ore than the comminution procedure employed.

2.2.4. Summary of literature on flotation response

Research that has been carried out on VRMs in minerals processing has mostly validated the energy savings realisable and assessing the effect of the operational parameters on grinding performance and throughput. Within this body of research, some tests have been carried out to assess the response of downstream flotation processes from using the dry compression grinding in comminution. Some of the key studies aligned to this work are summarised in Table 2-2.

Table 2-2: Knowledge contributed by authors regarding PSD, mineralogy, wet vs. dry grinding effect on flotation performance

Author	Factor	Contribution to knowledge
Palm et al., 2011 - sphalerite Chapman et al., 2011 – PGM ore	Mineralogical characteristics of zinc and PGM ore	No preferential liberation irrespective of comminution procedure in a primary-secondary mill setup
Chapman et al., 2011 – PGM ore Palm et al., 2011 - sphalerite, Solomon et al., 2011 – PGM ore, van Drunick et al., 2010 – Gamsberg Chelgani et al., 2019 - review	Wet vs. Dry Grinding	Ball mill dry grinding = ↑ pulp oxidation potential ↑ pulp oxidation potential = ↑ mineral surface oxidation ↑ mineral surface oxidation = ↓flotation performance
Solomon et al., 2011 – PGM ore	PSD	HPGR less steep PSD compared to ball mill. Steeper PSD in optimum flotation range = better flotation response

A systematic study of the flotation response of the VRM product on a complex ore and a comparison with rod mill product flotation response will provide the required insight on the applicability of VRMs in mineral processing. This would give important input into whether they can be retrofitted into the existing mineral processing circuits. The study will also provide options for new installations in the mineral processing industries should the flotation response be similar or better than the conventional approach.

2.3. Process Mineralogy

Process mineralogy is the application of mineralogical information to understand and solve problems encountered during the processing of ores and other related materials in an extraction circuit (Petruk, 2000; Becker et al., 2016). In order to efficiently recover valuable minerals from these complex ore bodies, process mineralogy has been adopted to identify minerals (abundance, associations, liberation), provide essential plant design input and inform extraction processes of the required grind and operating philosophy (Evans et al., 2011; Lotter, 2011; Schouwstra and Smit, 2011; Ntlhabane et al., 2018). The understanding of process mineralogy is pivotal in providing valuable information for optimisation of metallurgical flowsheets (Henley, 1983). Henley (1983) provided detailed application of process mineralogy in mineral processing and is presented in Figure 2-18.

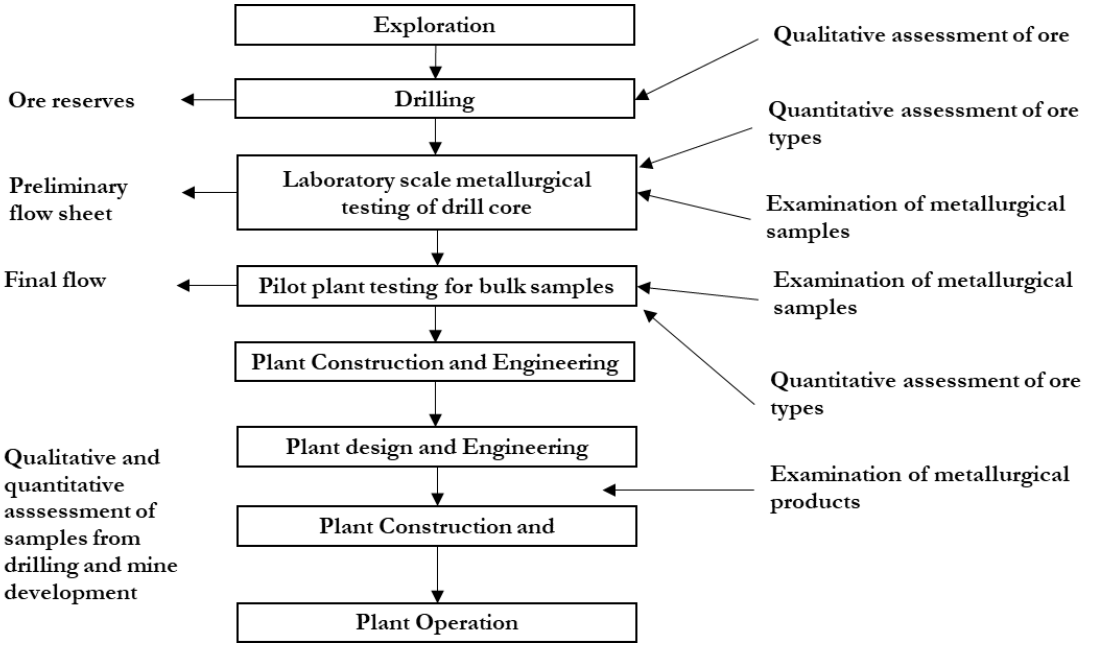

Figure 2-18: Linking process mineralogy to metallurgy (Henley, 1983)

As presented in Figure 2-18, exploration occurs first to quantify the ore body and provide information on the design of comminution and concentration processes. During the day to day running of operations, process mineralogy can be used to detect any changes in the ore body and determine any metallurgical changes necessary to maintain efficiencies. Flowsheet development has been optimised through process mineralogy, and success in case studies in platinum ore operations has been realised (Humphries et al., 2006; Rule and Schouwstra, 2012). Studies by Solomon et al (2011), Ntlhabane et al (2018) and Lotter (2011) showed the application of process mineralogy in mineral process circuit optimisation.

2.3.1. Ore texture and characteristics of ore bodies

Ore texture refers to the relationship between the mineral grains making up a rock. It refers to shape, size, distribution, association and arrangement of grains of one or more minerals which make up the rock (Schwartz, 1951). The texture of the ore defines the behaviour of the ore during plant operations and thus has a major influence throughout the full mining cycle: from mining strategy on blast and fragmentation management to process strategy with regards to comminution and concentration processes, recovery potential as well as tailings management. In processing operations, ore texture informs of the grain sizes and distribution which informs the required target grind to liberate the target minerals. Ore texture also determines the amount of energy required for comminution.

Ore characteristics can be determined from mineralogical studies and can be explained by ore texture. These characteristics include mineral identities, grain sizes, mineral associations, degree of liberation and distribution of minerals in the ore body. Understanding the ore characteristics can be used to predict the response of various treatment processes and can be used as an optimisation tool in existing circuits by metallurgists (Schouwstra and Smit, 2011).

2.3.2. Common measurement techniques applied in process mineralogy

To quantify characteristics of ores, many quantification techniques have been developed. The common measurement techniques are summarised according to Becker et al (2016) as:

- Optical microscopy: Uses visible light and a system of lenses to magnify the particles. The magnification allows for identification of mineral type and ore textures. Point counting is used to quantify mineral compositions.
- Quantitative X-ray diffractometer (QXRD): Uses X-ray diffraction and Bragg's law to obtain the mineral identities. The mineral identities are based on the unique crystallographic properties of minerals. Measurement is limited to crystalline material.
- Quantitative Evaluation of Minerals and Scanning Electron Microscopy (QEMSCAN): Ore specimen surfaces are scanned by high-energy accelerated electron beams to produce low-count energy dispersive X-ray spectra. The elemental composition information gathered from the low-count energy dispersive X-ray spectra is combined with back-scattered electron (BSE) and X-ray count to produce information on mineral phases (in the form of differently coloured mineral maps). The outputs from the QEMSCAN include bulk mineralogy, mineral grain size and distribution and mineral liberation. This measurement technique is subject to stereological error. The Mineral Liberation Analyser (MLA) is an automated mineral analysis system that can identify minerals and quantify mineral characteristics such as mineral abundance, grain size and liberation.

2.3.3. Mineralisation of the Swartberg Ore

The Aggeneys-Gamsberg ore district of the Northern Cape, South Africa consists of five major sulfide deposits (Swartberg, Gamsberg, Broken Hill Deeps, Broken Hill and Big Syncline) (McClung et al., 2007). The deposits are sedimentary and are regarded as examples of Broken Hill-type. McClung et al (2007) summarised the characteristics of the five sulfide deposits as presented in Table 2-3.

Table 2-3: Summary of characteristics of the Aggeneys-Gamsberg district deposits (McClung et al., 2007)

	West Aggeneys				East Gamsberg
	Swartberg	Broken-Hill	Broken Hill Deeps	Big Syncline	
Tonnage Grade	83.2Mt 2.52% Pb 0.69% Zn 0.63% Cu 45g/t Ag	37.9Mt 6.35% Pb 2.87% Zn 0.45% Cu 82g/t Ag	18.8Mt 3.98% Pb 3.94% Zn 0.74% Cu 56g/t Ag	100.0Mt 1.01% Pb 2.45% Zn 0.09% Cu 13g/t Ag	199.3Mt 5.51% Zn 6Mt barite
Host rock Lithology	Oxide-/Silicate-facies	Iron formation and aluminous pelitic schist		Oxide-/Silicate-facies, Iron formation and calc-silicate-rich pelitic schist	Calc-silicate-rich pelitic schist
Ore Horizons	Two discrete ore horizons	Two discrete ore horizons	One discrete ore horizon	Sulfides disseminated in schist	Sulfides disseminated in schist
Barite morphology and relation to sulfides	Thin lateral equivalent	Thin lateral equivalent	Not observed	Massive body that underlies the sulfides	Massive body that overlies stratigraphically equivalent sulfide horizons
Mineralogy	Py-Po-Mag-Marc-Sph-Bar ± Gn-Cpy	Mag-Bar-Gn-Sph-Cpy-Py-Po	Mag-Sph-Gn-Cpy-Py-Po	Mag-Sph-Gn-Cpy-Py-Po ±Ba	Py-Po-Marc-Mag-Sph-Bar ±Gn-Cpy
Metal Assemblage	Pb–Cu–Zn–Ag ±Ba	Pb–Zn–Cu–Ag ±Ba	Zn–Pb–Cu–Ag	Zn–Pb–Cu–Ag–Ba	Zn–Pb–Ba

Py-pyrite, Po-pyrrhotite, Mag-magnetite, Marc-marcasite, Sph-sphalerite, Bar-barite, Gn-galena, Cpy-chalcopyrite

The Swartberg ore body, found at the westernmost part of the Aggeneys-Gamsberg district, has metal distribution that follows the decreasing order of lead>zinc>copper>silver (Stedman, 1980).The Swartberg deposits comprise the Upper Ore Body (UOB) and Lower Ore Body (LOB) which are distinctly stacked, and the garnet quartzite zone which encompasses the UOB and LOB (Rudnick, 2016).

The lithological end-members in the Swartberg ore are magnetite quartzite (QM), amphibole magnetite quartzite (AM), garnet quartzite (GQ), mineralised quartzite schist (MC) and sulfidic quartzite (Gordon et al., 2018). The overall texture of the end-members is presented in Figure 2-19. The bulk mineralogy characteristics of the five end members are presented in Table 2-4.

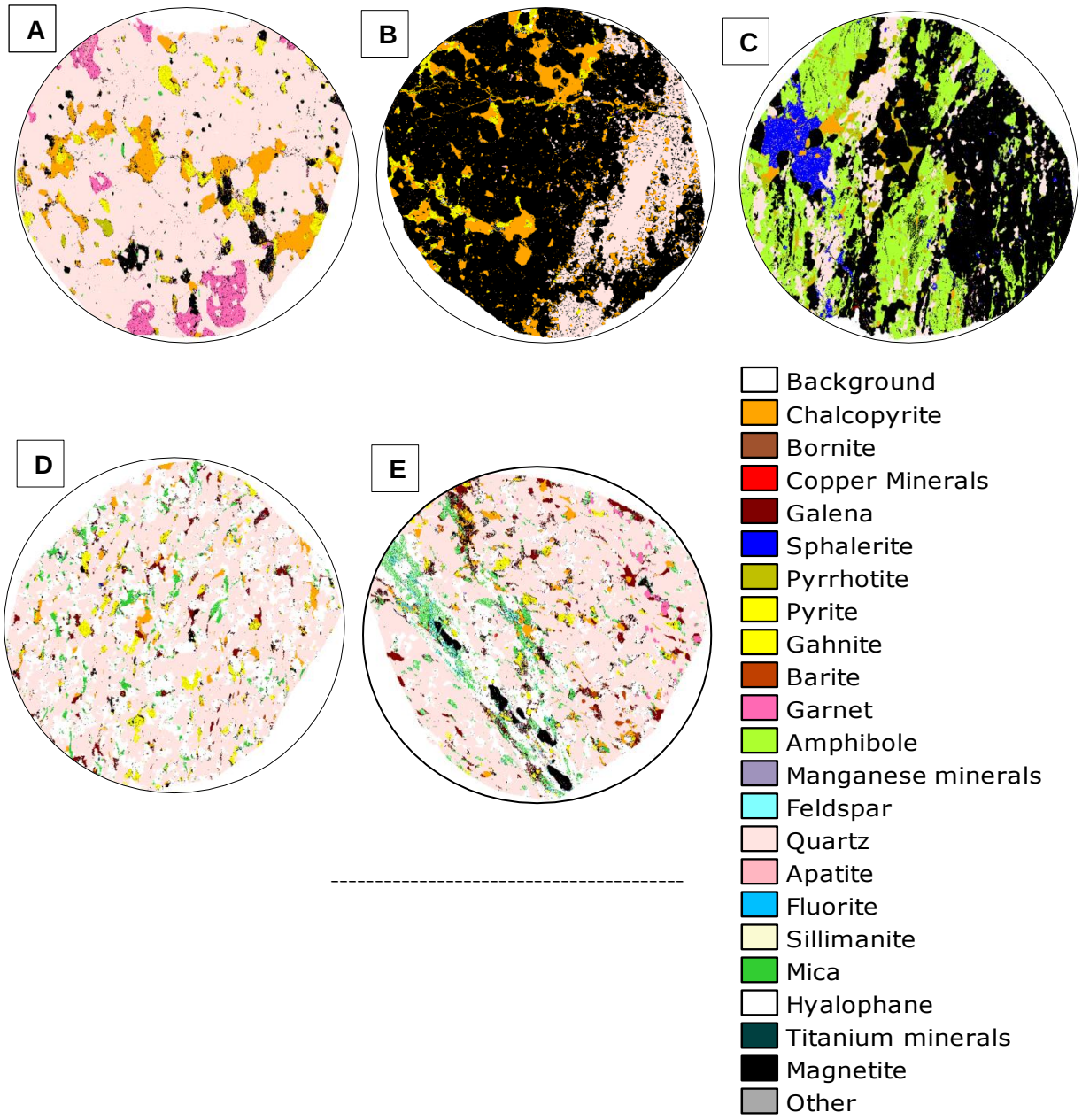

Figure 2-19: QEMSCAN false-colour images generated for the five main geological end-members. A-Garnet quartzite, B-magnetite quartzite, C-amphibole magnetite quartzite, D-mineralised schist, E-sulfidic quartzite (Gordon et al., 2018)

Table 2-4: Bulk mineralogical comparison of Swartberg geological end-members (wt. %) (Gordon et al., 2018)

Geological Ore Types					
Minerals	GQ	QM	AM	SQ	MC
Chalcopyrite	12.6	7.2	2.9	3.7	1.1
Bornite	<0.1	0.2	<0.1	<0.1	<0.1
Galena	0.6	4.6	4.8	8.1	17.3
Sphalerite	0.3	0.6	4.0	0.1	0.2
Pyrrhotite	2.9	0.3	5.9	0.7	4.4
Pyrite	0.8	1.9	0.9	2.9	2.0
Gahnite	0.1	<0.1	<0.1	<0.1	3.5
Barite	<0.1	1.0	<0.1	0.8	1.4
Garnet	5.5	0.6	<0.1	2.0	1.2
Amphibole	<0.1	0.7	12.1	0.1	0.1
Manganese minerals	<0.1	0.4	2.7	<0.1	<0.1
Feldspar	0.2	0.1	<0.1	1.0	0.6
Quartz	59.1	27.0	9.7	44.9	44.6
Apatite	0.3	0.3	0.5	0.1	0.1
Fluorite	<0.1	<0.1	<0.1	0.1	<0.1
Sillimanite	2.3	0.2	<0.1	1.0	1.2
Mica	4.5	1.5	<0.1	5.0	6.3
Hyalophane	<0.1	<0.1	<0.1	19.0	13.4
Ti-minerals	0.2	0.1	<0.1	1.4	1.0
Magnetite	10.6	53.3	56.3	9.2	1.5
Other	0.1	0.1	<0.1	0.1	0.2
Minerals	100	100	100	100	100

The economic sulfides from the ore are mainly chalcopyrite. galena and sphalerite. According to the classification by Gordon et al (2018), GQ has chalcopyrite, pyrrhotite and pyrite as dominant sulfides. QM has chalcopyrite, galena and pyrite as dominant sulfides. AM has galena, sphalerite and pyrrhotite as dominant sulfides. SQ has chalcopyrite, galena and pyrite as main sulfides while MC has pyrrhotite, galena and pyrite as main sulfides.

Using available data, the grain size distribution of sulfide minerals in the Swartberg blend ore from drill core QEMSCAN analysis is presented in Table 2-5.

Table 2-5: Mineral grain size from Swartberg geological end-members constituting the Swartberg blend ore (Gordon et al., 2018)

Ore Type	Copper minerals		Lead minerals		Zinc minerals	
	d50 (µm)	max (µm)	d50 (µm)	max (µm)	d50 (µm)	max (µm)
GQ	617	1075	108	375	36	300
QM	436	2000	1880	2375	261	1350
AM	732	1100	203	1675	850	1550
MC	139	375	660	1525	20	425
SQ	207	350	128	550	49	150

The information presented in Table 2-5 showed that the sulfide minerals in the ore are quite coarse. If ground to a small enough particle size, that is within the optimum flotation particle size range of < 100 μm (Gaudin et al., 1931), the copper mineral grains will be liberated from the associated gangue minerals and can be recovered through flotation. The grain size distribution information gathered for zinc and lead minerals also indicated that the grains were quite coarse, and if ground to the minus 100 μm size fraction, the value minerals would be well liberated from gangue and be recovered through flotation.

2.4. The Cu-Pb-Zn concentrating process

Figure 2-20 shows the Cu-Pb-Zn sulfide concentrator flowsheet of where the ore was sourced.

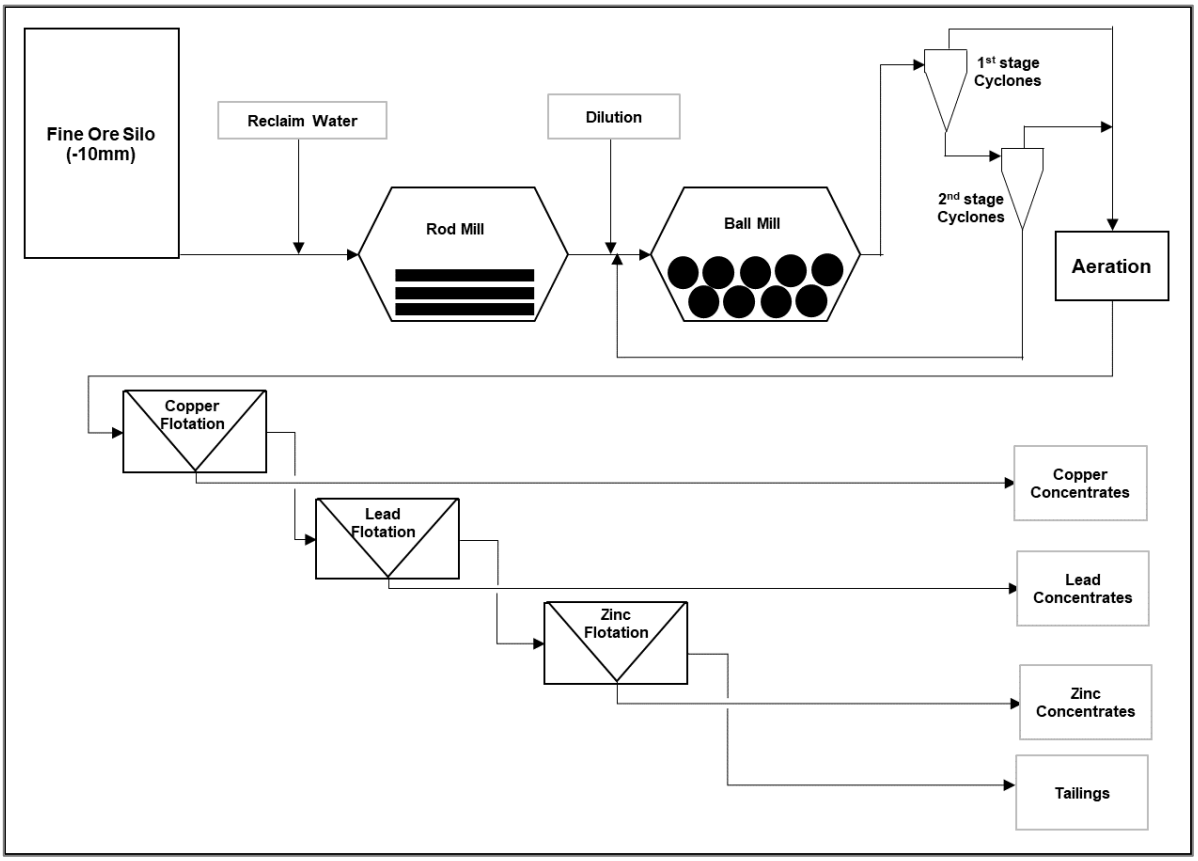

Figure 2-20: Flowsheet for Cu-Pb-Zn sulfide ore comminution and flotation

Crushed ore (10 mm top size) enters the milling circuit for size reduction. The first stage is an open circuit rod mill, followed by a ball mill in closed circuit with two hydrocyclone clusters. Hydrocyclone overflow product, which is the flotation feed, is aerated and fed to flotation. Flotation can occur in one of the two options: sequential (as shown in Figure 2-20) or bulk followed by segregation.

In the sequential flotation flowsheet shown in Figure 2-20, the slurry passes through three flotation stages: firstly, copper flotation followed by lead flotation and finally zinc flotation. Each stage of flotation consists of rougher and cleaner flotation to separate the valuable mineral from the bulk stream. The cleaning stage is for upgrading the concentrate grade of the target mineral.

In bulk flotation, all the three valuable minerals are recovered first, and segregation follows to separate the individual minerals. The choice of bulk vs. sequential flotation is mainly guided by ore characteristics, reagent choices and consumptions as well as the flowsheet options available during design or operation (Bulatovic, 2014).

The advantages of bulk flotation are that maximum recovery can be achieved, requires less capital expenditure (less flotation cells required to achieve the same recovery) and lower operating expenditure (reagent consumption can decrease). Reagent consumptions can decrease as there will be one bulk flotation stage to produce a bulk concentrate, at normally less than 10 wt. % mass pull. Only the bulk concentrates will be subjected to segregation, unlike sequential flotation where reagents will be added to the bulk stream. Tests conducted in the development of the flowsheet for treating Broken Hill type ore indicated that the sequential flotation was preferable for Gamsberg ore (Twidle and Englebrecht, 1984). With the changes in mineralisation, these findings may or may no longer be applicable to the treatment of Swartberg ore.

The recovery performance data from a plant that processes the Cu-Pb-Zn sulfide ore, where the Swartberg ore used for this study was sourced is presented in Table 2-6. The results presented are for an ore mixture of Deeps and Swartberg ore bodies. Mineral recoveries obtained from sequential flotation work done on Swartberg blend at the plant are presented in Table 2-7.

Table 2-6: Sequential flotation historical recovery performance data

	Mass pull (%)	Cu (%)	Pb (%)	Zn (%)
Cu concentrate	1.8	72.4	2.9	1.7
Pb concentrate	3.5	8.8	83.7	4.2
Zn concentrate	4.1	5.6	3.2	77.0
Total	**9.4**	**86.8**	**89.8**	**82.9**

Table 2-7: Sequential batch flotation recoveries for past flotation tests done on Swartberg blend

	Cu (%)	Pb (%)	Zn (%)
Cu concentrate	66.7	59.2	40.3
Pb concentrate	29.2	37.5	10.7
Zn concentrate	2.3	1.2	38.4
Total	**98.2**	**97.9**	**89.4**

Looking at copper, the historical plant performance data presented in Table 2-6 shows that the historical copper circuit recovery performance is low. However, doing a mass balance around the whole circuit indicates that the cumulative recovery of copper is 86.8 %. Another sequential flotation study conducted on Swartberg blend ore (Table 2-7) also indicated that the recovery of copper in the copper circuit was low, though the recovery potential (total recovery over the three flotation circuits) was 98.2 %. The misplacement of copper in the lead and zinc circuits is therefore most likely a flotation circuit design and optimisation problem that can be addressed by process engineers.

2.5. Hypothesis

2.5.1. Hypotheses

The following hypotheses were proposed for the study:

1. Dry rod milling results in better recovery of chalcopyrite, galena and sphalerite compared to wet rod milling. This is because dry grinding results in a more positive pulp potential of the flotation pulp as galvanic interactions are reduced in the absence of water and less precipitation of metal hydroxides on the valuable minerals sulfide surfaces occurs. Sulfide mineral and collector interactions are not compromised, and hence better flotation performance results.
2. Increase in compressive force during comminution using the VRM results in an improvement in flotation response of the products. This is because an increase in compressive force means more energy is applied for particle breakage, resulting in higher breakage rates and increased liberation of particles.
3. The VRM can be used to prepare ore for flotation at a reduced specific energy input compared to rod milling. This is because compression and in-bed breakage are more energy efficient than impact and shear breakage.

2.5.2. Key Questions

The following key questions have been developed to test each hypothesis:

1. What are the differences in pulp potential between the VRM, dry rod milling and wet rod milling products? Can the differences be correlated to the resultant flotation performance?
2. What is the effect of varying compressive forces on elemental recoveries? Variation in compressive force is achieved by changing grinding pressure.
3. For the same grinding time, what are the characteristics of the products from dry milling and wet milling in a rod mill? What are the subsequent differences in the recovery of chalcopyrite, sphalerite and galena?
4. Are there any differences in the mineral liberation profiles between the VRM, dry rod milling and wet rod milling products? Can the differences be correlated to the resultant flotation performance?
5. What are the differences in specific energy consumption from using the VRM and the conventional comminution circuit for the ore under study?

3. EXPERIMENTAL PROGRAM

The materials and methods used to test the proposed hypothesis is given in this chapter in detail. The operating procedures for each critical step are outlined.

3.1. Ore Sampling and Preparation

Swartberg ore, a polymetallic sulfide ore containing galena, chalcopyrite and sphalerite, was used for this study. As per the test protocol designed and agreed on by Loesche and the University of Cape Town, 20 tons of the Swartberg ore blend was sourced from silo feeding the primary mill at Black Mountain Mine in Northern Cape, South Africa. The 20-ton sample was homogenised at Mintek, South Africa. The chevron staking system was used to blend the bulk sample and ensure homogeneity. Three subsamples of 1 kg each were generated to assess if blending produced a homogenous sample. The particle size distributions of the blended products sub-samples ratified homogeneity as shown by the overlaying of the three curves in Figure 3-1.

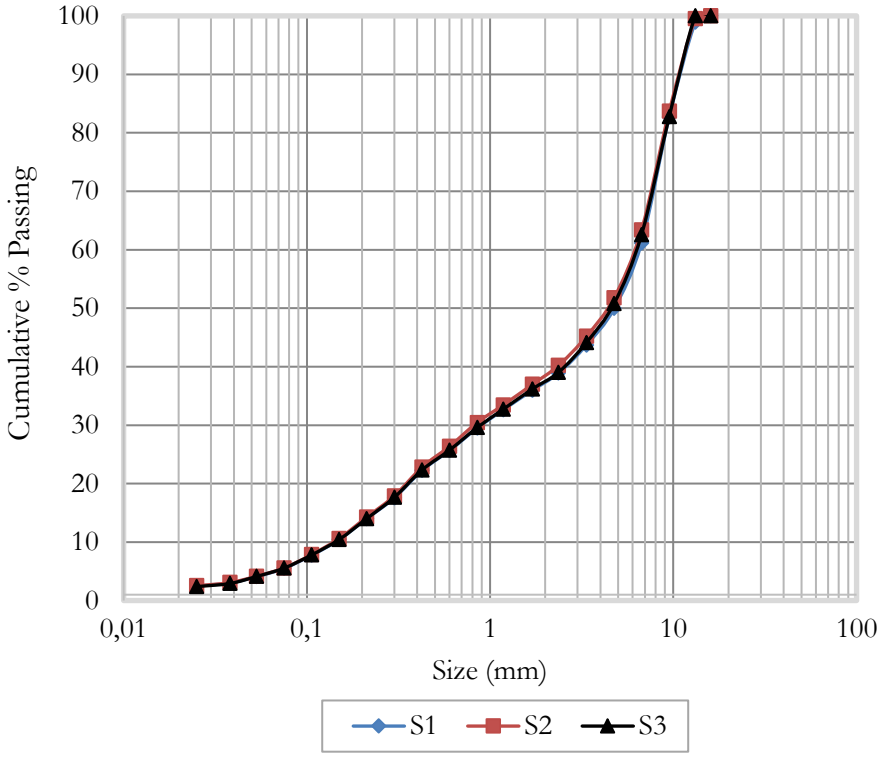

Figure 3-1: PSDs of 3 subsamples of blended Swartberg ore.

The homogenised product was packaged into drums. Of the homogenised and packaged samples, 2 tons was transported to the Centre of Minerals Research (CMR) at the University of Cape Town and 18 tons transported to the Loesche Test Centre facilities in Germany.

The Loesche mill (LM3.6/2) was used for the grinding tests at the Loesche Test Centre in Germany. For the study, the LM3.6/2 was operated in conjunction with the high efficiency dynamic air classifier. For each set-point tested, the VRM product was purged in argon and sealed, then couriered by air to Cape Town for flotation tests.

The homogenised sample transported to Cape Town was crushed to -2 mm using the laboratory scale jaw crusher. The -2 mm crushed ore was split using the riffle splitter and the rotary splitter to generate homogenous 1.3 kg samples for rod milling and flotation. The splitting to 1.3 kg was done in order to float at 33 wt.% solids, which is the standard flotation density at the plant operations.

3.2. Project test matrix

The test matrix for the experimental plan is presented in Table 3-1.The comminution, flotation and mineralogy tests procedures are detailed later in this section.

Table 3-1: Project test matrix

Comminution Method	Product Size (% passing 75µm)	Grinding pressure (kPa)	Dam Ring height (mm)
			7
VRM	55	600	
	60	600	
	65	600	
		800	
		1000	
	70	600	
	75	600	
Rod Mill - Dry	55		
	60		
	65		
	70		
	75		
Rod Mill - Wet	55		
	60		
	65		
	70		
	75		

PSD, mineralogical analysis, flotation tests
PSD, flotation tests

3.3. VRM Milling

The Loesche mill (LM3.6/2) was used for the grinding tests at the Loesche Test Centre in Germany. The LM3.6/2 is the pilot plant VRM with a table diameter of 0.36 m and two installed grinding rollers (Figure 3-2). For this study, the mill was used in conjunction with a dynamic air classifier which is mounted above the grinding section. For each test conducted using the VRM, the target grind was the independent variable, the grinding pressure and classifier rotor speed were the manipulated variables, while dam ring height was maintained constant at 7 mm. Load factor (ratio of measured throughput to nominal throughput) and specific grinding energy (Ecs) were output variables. The products from each of the runs were split representatively for particle size analysis, flotation and mineralogical analysis in line with test protocol.

Figure 3-2: LM3.6/2 Grinding Rollers with Shear

3.4. Laboratory Scale Rod Milling

The Eriez Magnetics MASCLAB stainless steel laboratory scale rod mill was used for comminution of the -2 mm crushed ore. Using the rod mill, both dry and wet comminution was done. The rod mill had an internal diameter of 200 mm and a belly length of 297 mm. The mill charge was composed of 20 rods whose specifications are presented in Table 3-2.

Table 3-2: Mill charge specifications

Rod diameter (mm)	Number of rods
25	6
20	8
16	6
Total	**20**

The baseline target grind for comminution was 65 % passing 75 µm, benchmarked from Black Mountain Mines operations. To determine the required grind time, grind curves were done.

3.4.1. Grind Curves

For wet grinding curves, 1.3 kg samples of ore were milled for different durations at 67 wt.% solids in the rod mill. This was done to determine the time required to produce a grind of 65 % passing 75 µm, matching the benchmarking target grind for Black Mountain. For dry grind curves, only 1.3 kg of sample was added to the mill and was ground at different durations to also determine the time required to produce a grind of 65 % passing 75 µm. The milling times required to achieve the desired grind were 15.8 minutes for wet grinding and 16.2 minutes for dry grinding, as presented in Figure 3-3 and Figure 3-4. The milling times to achieve the different target grinds for wet and dry rod milling are presented in Table 3-3.

Table 3-3: Grind time required to achieve specific target grind

Grind (% passing 75 µm)	RW (min)	RD (min)
55	12	12.6
60	14	14.4
65	15.8	16.2
70	17.7	18.0
75	19.5	19.8

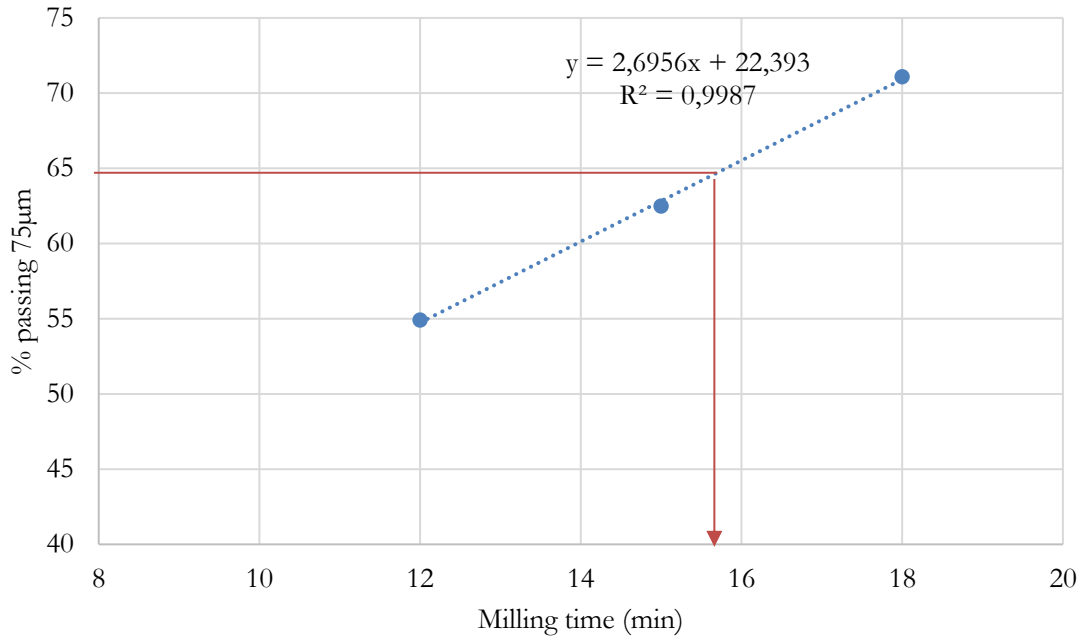

Figure 3-3: Wet Milling Curve for Swartberg ore.

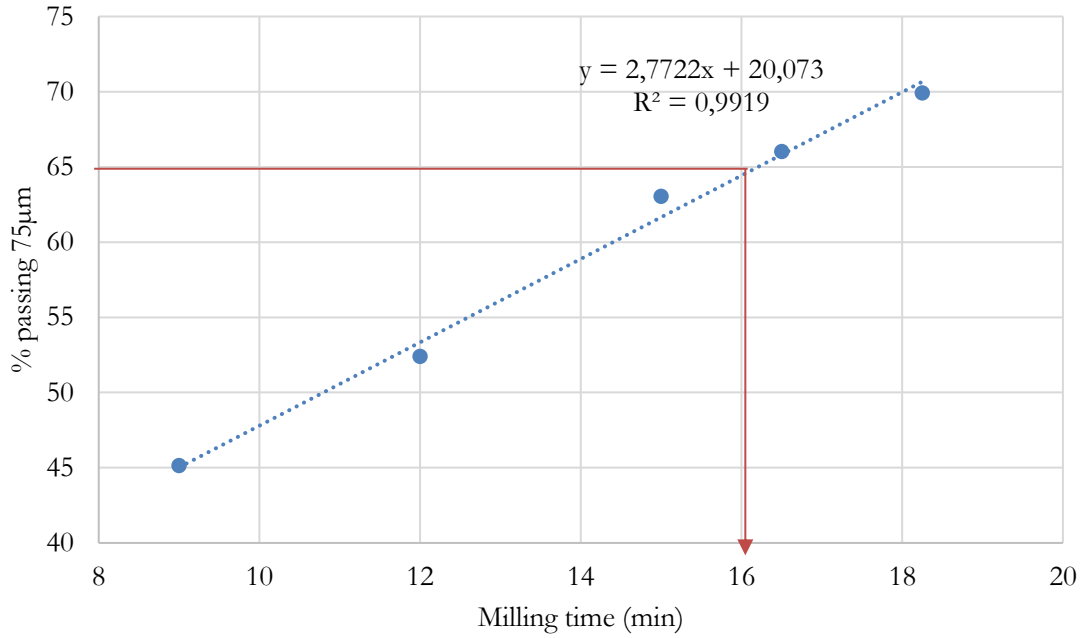

Figure 3-4: Dry Milling Curve for Swartberg ore.

3.4.2. Wet Grinding for Flotation

For wet milling and the subsequent flotation tests, only prepared standard synthetic plant water (SPW) was added to the rod mill to make up the 67% solids required for comminution. 650 ml of the synthetic plant water were added to 1.3 kg of Swartberg ore. Prepared standard synthetic water was used to maintain water quality consistency for all the flotation tests.

The SPW synthetic water for these tests was prepared according to the standard CMR procedure in 40 litre batches (Wiese et al., 2005). The inorganic salts added, and their quantities are presented in Table 3-4. The composition of ions in the prepared synthetic water is summarised in Table 3-5.

Table 3-4: UCT-CMR standard recipe for SPW-40L batch

Inorganic Salt	Chemical formula	Mass per SPW batch (g)
Magnesium sulphate	$MgSO_4.7H_2O$	24.60
Magnesium Nitrate	$Mg(NO_3)_2.6H_2O$	4.28
Calcium Nitrate	$Ca(NO_3)_2.4H_2O$	9.44
Calcium Chloride	$CaCl_2.2H_2O$	5.88
Sodium Chloride	NaCl	14.24
Sodium Carbonate	Na_2CO_3	1.20

Table 3-5: Total ions present in SPW

Ions Present	Ca^{2+}	Mg^{2+}	Na^{+}	Cl^{-}	SO_4^{2-}	NO_3^{2-}	CO_3^{2-}	TDS
Concentration (ppm)	80	70	153	287	240	176	17	1023

3.5. Size Analysis

Products from the comminution tests were screened for size analysis. Wet grinding products were oven dried before sieving.

3.5.1. Wet Sieving

Wet screening was used first to avoid misplacement of fine particles into larger size classes because of agglomeration. The sample was first wet sieved using the 25 µm sieve to remove slimes and minimise misplacement of the sub 25 µm particles. The particles retained on the 25 µm sieve was then sieved on the 106 µm sieve. Particles less than 106 µm were progressively screened on the 75, 53, 38 and 25 µm sieves. The sub 25 µm particles were collected and filtered. Particles retained on the 106 µm sieve were oven dried.

3.5.2. Dry Sieving

Material retained on the 106 µm sieve was dry sieved mechanically using a vibrating screen shaker for 20 minutes. The typical root 2 series of top size 1000 µm and bottom sieve size of 106 µm was used.

Mass of solids retained on each size class was weighed and reconciled to produce particle size distribution curves.

3.6. Flotation Procedure

3.6.1. Test Equipment

All the batch flotation tests were carried out using the 3 L Barker flotation cell at the University of Cape Town. The 3 L Barker flotation cell is shown in Figure 3-5.

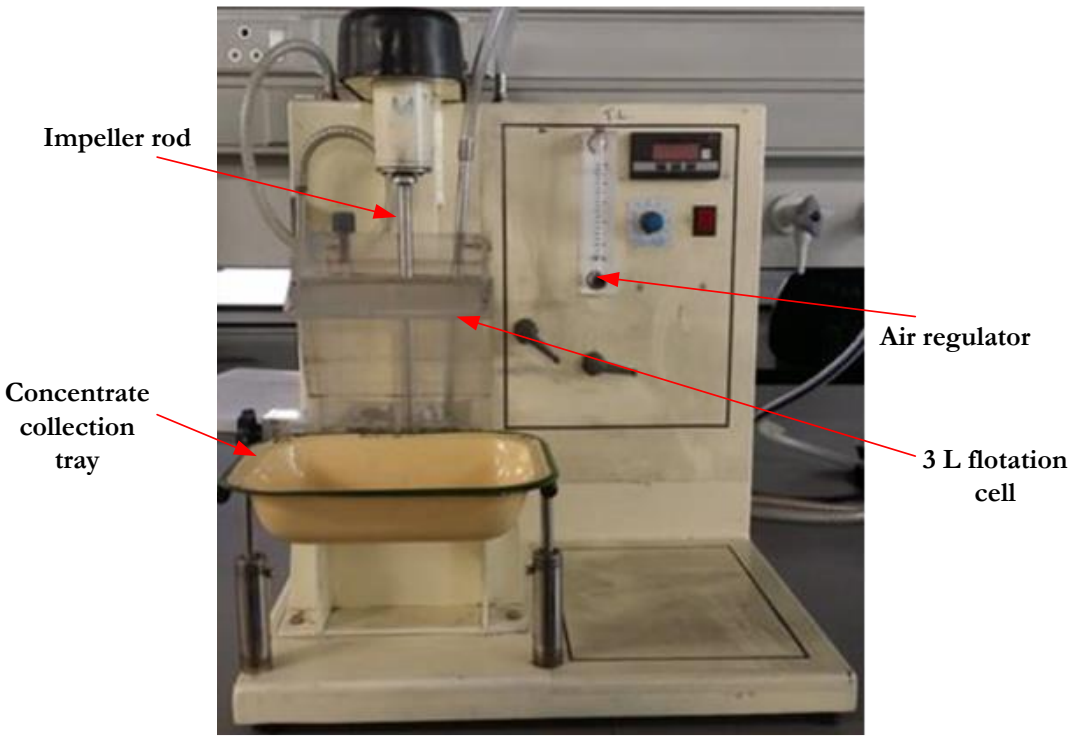

Figure 3-5: The UCT 3L Barker flotation cell

The cell was made of clear Perspex, which made it easier to maintain the operational froth height of 2 cm and visually observe the hydrodynamics within the cell. The impeller speed was maintained at 1250 rpm. Air flowrate was maintained at 7.5 L/min. Pulp potential (Eh) was measured using the HANNA meter, supplied by HANNA instruments. The meter was calibrated for Eh before any measurements were done.

3.6.2. Flotation Procedure

Bulk flotation was done to determine the maximum recovery potential for the ore from the different comminution routes. Milled slurry or dry solids (from dry rod milling and VRM) was transferred to the 3 L Barker flotation cell and SPW water added to the 2 cm froth height mark, thereby achieving 33 wt.% solids of the pulp. The slurry was kept in suspension using an impeller. The impeller speed was 1250 rpm. The pulp potential was measured using the HANNA probe. Pulp potential measurements were done immediately after making up the flotation cell with water.

Before adding any reagents, a 50 ml feed sample was collected from the flotation cell using a syringe. An activator, copper sulphate, was added at 160 g/t and allowed to condition for 1 minute. This was followed by a mixed collector addition, SEX at 80 g/t and Senkol 700 at 10 g/t, with 2 minutes conditioning time. A frother, MIBC, was added at 25 g/t and conditioned for 1 minute. Air was then introduced at a regulated and constant rate of 7.5 L/min for all the tests.

Froth was scraped every 15 seconds from the cell and was collected into pre-weighed concentrate trays. Pre-weighed wash bottles were used to clean the scraper and the cell launders after each scrapping. C1, C2, C3 and C4 were the concentrates collected after 2, 4, 6 and 8 minutes of scrapping respectively. Froth height was maintained at 2 cm using SPW water.

Each flotation test was done in duplicate to measure repeatability and level of confidence in the observations. Figure 3-6 summarises the bulk flotation recipe used for floating the different comminution products.

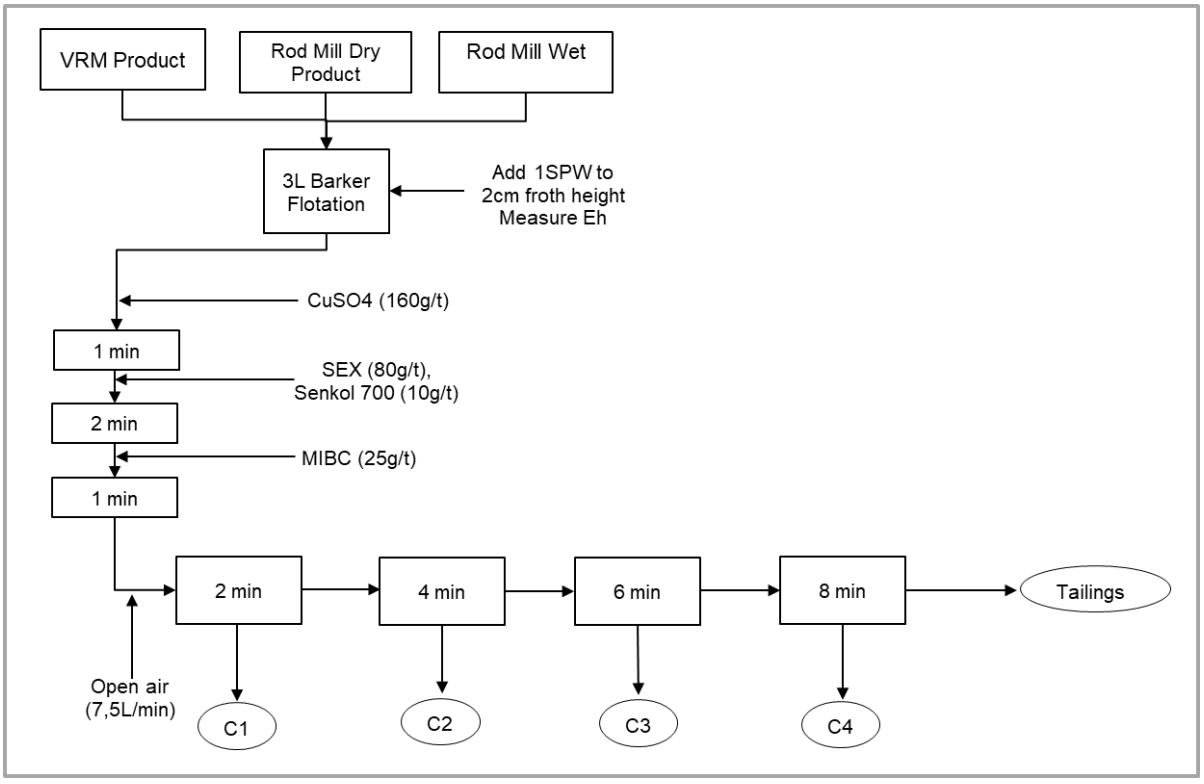

Figure 3-6: Summary of batch flotation program

After C4 was collected, two 50 ml tailings samples namely Tailings 1 (T1) and Tailings 2 (T2) were collected for analysis. Air was switched off. The masses of the trays with concentrates and the used wash bottles were recorded for water recovery calculations.

The concentrates, feed and 50 ml tailings are then filtered using pre-weighed filter paper for dry solids recovery and mass pull calculations. The bulk tailings sample was collected in a bucket and filtered. All solids were oven dried at a controlled temperature of 80°C to prevent sulfide oxidation. The dried samples were weighed for mass recovery and flotation efficiency calculations.

3.6.3. Sample preparation of flotation samples for Cu, Zn and Pb assays

Table 3-6 shows the number of samples generated from each test run. The duplicate tests were done to assess reproducibility.

Table 3-6: Samples collected for each test run

Sample Name	Duplicate 1	Duplicate 2
Feed	F	F
Concentrate 1	C1	C1
Concentrate 2	C2	C2
Concentrate 3	C3	C3
Concentrate 4	C4	C4
Tailings 1	T1	T1
Tailings 2	T2	T2
Bulk Tailings	T	T

The dried concentrates, feed and tailings were de-lumped. Splitting was done to some of the samples to generate sub-samples for the necessary analyses. A split-portion of the dried feeds, concentrates and tailings (Tailings 1 and Tailings 2) was packaged and sent for Cu, Pb, Zn and Fe analysis using the Spectro Arcos ICP-OES at Scientific Services Laboratory in Cape Town (see section 3.7). The assay results are presented in Chapter 4.

3.6.4. Specialised flotation tests

As a way of characterising the ore being investigated, additional specialised tests were conducted by modifying the flotation procedure. The first set of tests sort to assess the behaviour of the ore without adding an activator. The second set of tests sort to investigate whether the ore's flotation performance is affected by aging. Aging is the oxidation of sulfide mineral surfaces produced from milling and is due to prolonged exposure to the atmosphere and has potential to negatively affect flotation response.

3.7. ICP-OES Metal Analysis

Induction Coupled Plasma – Optical Emission Spectroscopy was the technique used to determine the composition of value elements (Cu, Pb, Zn) and gangue (Fe). A Spectro Arcos ICP-OES was used for the analysis at Scientific Services in Cape Town. The operating conditions of the Spectro Arcos are presented in Table 3-7.

Table 3-7: The Spectro Arcos ICP-OES operating conditions

Parameter	**Condition/ Type**
Plasma power	1400 W
Pump speed	30 rpm
Coolant flow	14.00 L/min
Auxiliary flow	2.10 L/min
Nebuliser flow	0.80 L/min
Nebuliser	Crossflow
Sample Injection	Continuous nebulisation

The aqueous standards solutions were prepared by dilution from stock individual standards of 1000 mg/L. A 7-point calibration curve on all the elements was plotted. The calibration standard was 10 (v/v) % HNO_3. The calibrated curves were used to determine the unknown element composition.

3.7.1. Sample Preparation for ICP-OES

A sample of mass between 0.25 g and 1.0 g sample digested sequentially in hydrochloric acid (HCl), nitric acid (HNO_3) and perchloric acid ($HClO_4$). The digested samples were topped up to 250 ml in the same matrix as the calibration standards.

3.8. Mineralogical Analysis

Mineralogical analysis was done to obtain the bulk mineralogical composition of the ore as well as the sulfide liberation and association profiles of the selected VRM, dry rod milling and wet rod milling flotation feeds. The liberation profiles of the flotation tailings of the selected VRM, dry rod milling, and wet rod milling were also characterised to understand where the mineral value losses occurred.

The Quantitative Evaluation of Minerals by Scanning Electron Microscopy (QEMSCAN) machine was used to obtain bulk mineralogical data and sulfide mineral liberation data. The samples analysed using the QEMSCAN are summarised in Table 3-8.

Table 3-8: Samples analysed using the QEMSCAN

VRM Feed	VRM Tails
RD Feed	RD Tails
RW Feed	RW Tails

About 150 g of each sample was screened to produce the size fractions: -300+75 μm, -75+38 μm, -38+10 μm and -10+0 μm. The samples from each size class were split using the rotary splitter to produce 4 g subsamples. The 4 g subsamples were further split using the Quantachrome microrifler to produce 1 g aliquots for the preparation of QEMSCAN blocks. Each block for QEMSCAN analysis was then prepared by mixing the 1 g aliquot with graphite and resin and allowed to cure. The cured block was polished and dried in the oven. Quality checks were done on the block using an optical microscope. The dried block was then carbon-coated using an Emitech carbon evaporator before being run through the FEI QEMSCAN 650F. Carbon coating is done so that carbon can diffuse electrons off the surface of the sample block during analysis by the QEMSCAN. 2 blocks per each size fraction were prepared and run through the FEI QEMSCAN 650F.

3.8.1. QEMSCAN Analysis

The QEMSCAN uses the Species Identification Protocol (SIP), which is a mineral library system. The SIP consists of a list of user-specified entries and matching criteria for X-ray spectra and back scattered electron (BSE) data. Information gathered from the scanning electron microscope is synchronised with the SIP to classify mineral composition or mineral species. As each point on a sample is scanned, its spectrum is converted to element information. The element information is matched to the entries in the SIP list to determine the mineral or species. The scanning parameters and QEMSCAN characteristics and analysis routines are presented in Table 3-9, Table 3-10 and Table 3-11.

Table 3-9: The QEMSCAN Operating Parameters

Parameter	**Type/Condition**
Type	FEG QEMSCAN 650F
Voltage (kV)	25
Beam Current (nA)	10

Table 3-10: The QEMSCAN Operating Conditions

	Size Fraction (µm)	Field size (µm)	Pixel size (µm)	SMS Particle Count		
				VRM	RD	RW
SMS Sulfide Mineral Search (Feed)	-10	300	1	57931	63124	57655
	+10/-38	750	2	15658	23883	14043
	+38/-75	1000	3	3737	1998	4901
	+75/-300	1500	4	3927	2160	2278
SMS Sulfide Mineral Search (Tails)	-10	300	1	8411	5577	10149
	+10/-38	750	2	2476	3233	10806
	+38/-75	1000	3	2271	2354	3764
	+75/-300	1500	4	2229	2113	2807

Table 3-11: The QEMSCAN Analysis Routines

Measurement	Description	Samples Processed
BMA (Bulk Mineral Analysis)	Line scan analysis that gives bulk mineralogy	+10/-38, +38/-75, +75/-300 (Feed, Tails)
PMA (Particle Mineral Analysis)	Particle by particle analysis that produces false colour images of the particle and particle mineralogical information	-10 (Feed, Tails)
SMS (Specific Mineral Search – Galena, Chalcopyrite, Sphalerite, Pyrrhotite)	Particle by particle analysis that produces false colour images of the sulfide particle and gives sulfide particle mineralogical information	-10, +10/-38, +38/-75, +75/-300 (Feed, Tails)

Bulk mineralogical analysis (BMA) for particles size greater than 10 µm and particle mineralogical analysis (PMA) for particles less than 10 µm were used to obtain the quantitative description of the minerals present in the polymetallic sulfide ore blend ore used for this study.

3.8.2. Data Validation

Data from the QEMSCAN analysis was validated by comparing with chemical assay data and XRF data. XRF was done to validate mineral abundance. A parity close to 1 between the chemical assays and the QEMSCAN assays validated the data obtained from the QEMSCAN. The parity chart is presented in Figure 3-7.

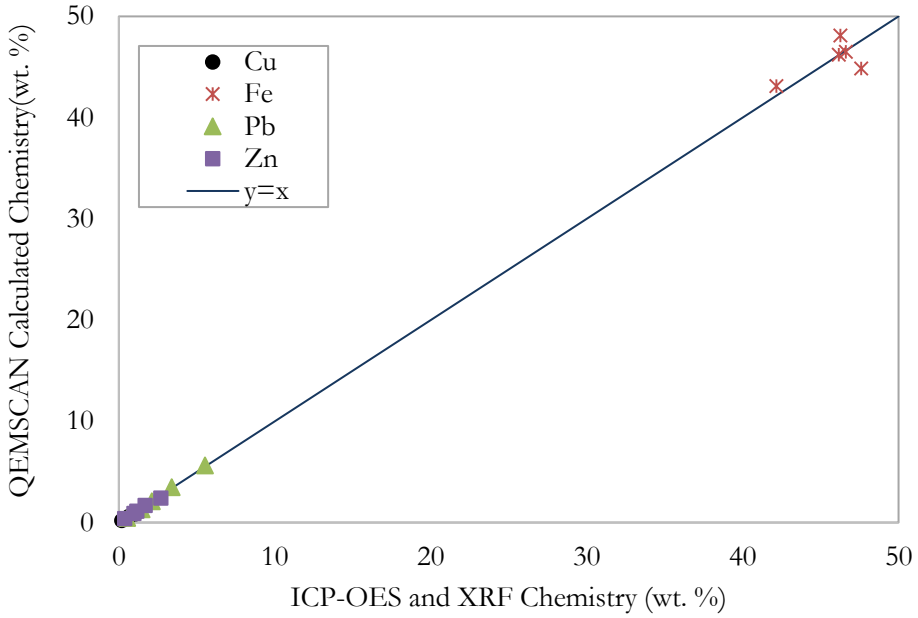

Figure 3-7: Data reconciliation for QEMSCAN calculated chemistry with ICP-OES and XRF chemistry

3.9. Reproducibility of Results

All flotation experiments were conducted in duplicate. This was done to assess reproducibility of the results. Duplicate results of the same parameter/measurement were used to calculate the arithmetic mean, standard deviation and standard error. The arithmetic mean, $\bar{x}$, was calculated using equation 3-1:

$$\bar{x} = \frac{1}{N}\sum_{i=1}^{N} x_i \quad \text{..... Equation 3-1}$$

where N is the sample size and *i* is the measurement number.

The sample standard deviation of the data, σ_s, was calculated using equation 3-2.

$$\sigma_s = \sqrt{\frac{\sum_{i=1}^{N}(x_i - \bar{x})^2}{N-1}} \quad \text{..... Equation 3-2}$$

The standard error, represented as error bars on graphs, was calculated using equation 3-3.

$$Standard\ Error = \frac{\sigma_s}{\sqrt{N}} \quad \text{..... Equation 3-3}$$

Results from all the test runs were reproducible. For example, Table 3-12 shows mass of solids recovered in the concentrates for the individual runs during the flotation of the dry rod milling product, the mean and standard deviation. Figure 3-8 shows the mean cumulative solids recovery to concentrate curve and the associated error bars.

Table 3-12: Solids mass recovered to concentrates during the flotation of dry rod milling product

Sample	Mass recovered to concentrates (duplicate 1)	Mass recovered to concentrates (duplicate 2)	Mean	Standard Deviation
C1	118.1	122.0	120.0	2.8
C2	35.4	31.9	33.6	2.5
C3	13.1	16.6	14.9	2.5
C4	13.0	9.5	11.2	2.5

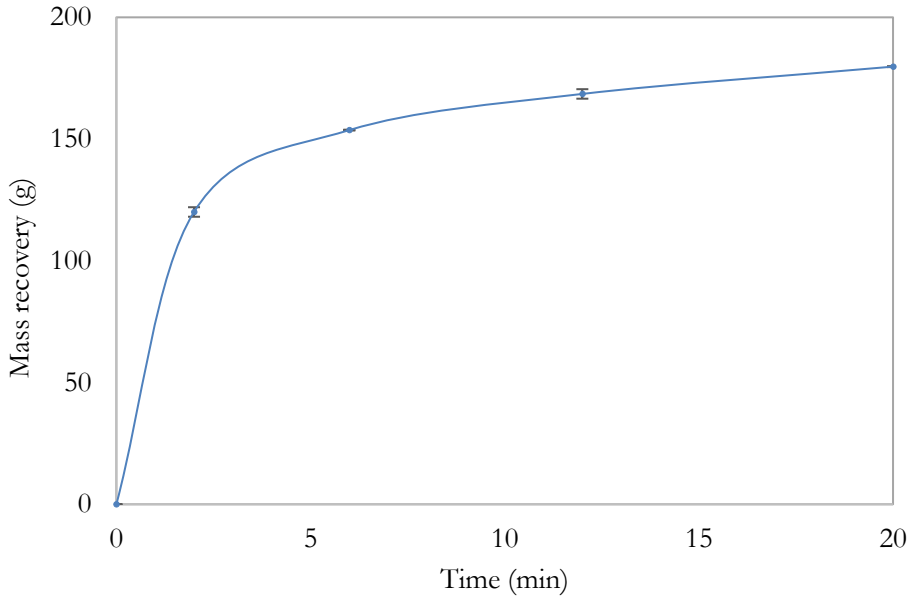

Figure 3-8: Cumulative solids recovery to concentrates over time from the flotation of dry rod milling product

4. RESULTS

The chapter presents results from the experimental work done. The bulk mineralogical analysis and the grain size distribution of the ore are presented first. The characteristics of the VRM products comminuted under different operating conditions are presented. The outcomes of the comminution tests conducted in terms of progeny PSDs for the different target grinds from the three comminution procedures under study are presented. The flotation response of copper, lead and zinc minerals constituting the Swartberg blend ore are presented. For the benchmarking grind, mineral liberation characteristics of flotation feed and flotation tailings as well as grain size distribution are presented after flotation response results. To conclude the results section, the specialised flotation tests are presented, which were an assessment of the aging characteristics of the ore and recovery by size characteristics.

4.1. Bulk Mineralogy and Ore Grain Size Distribution

The bulk mineralogy of the polymetallic sulfide ore is presented in Table 4-1.

Table 4-1: Bulk mineral abundance from QEMSCAN (wt. %)

Mineral	Swartberg Blend (wt. %)
Sphalerite	1.8
Chalcopyrite	1.3
Galena	2.4
Pyrrhotite	0.2
Pyrite	2.3
Other sulphides	<0.1
Magnetite	68.0
Quartz	15.7
Manganogrunerite	0.9
Pyroxmangite	5.5
Apatite	0.5
Others	1.0
Total	100.0

The analysis presented in Table 4-1 shows that the sulfide ore is mainly composed of magnetite (68.0 %), quartz (15.7 %), pyroxmangite (5.5 %) and pyrite (2.3 %). The value bearing minerals: chalcopyrite, galena and sphalerite have composition of 1.3 %, 1.8 % and 2.4 % respectively.

4.2. VRM on comminution performance

4.2.1. Effect of changing target grind

The effect of changing target grind on progeny PSD, specific energy consumption and throughput is presented in Figure 4-1 and Figure 4-2.

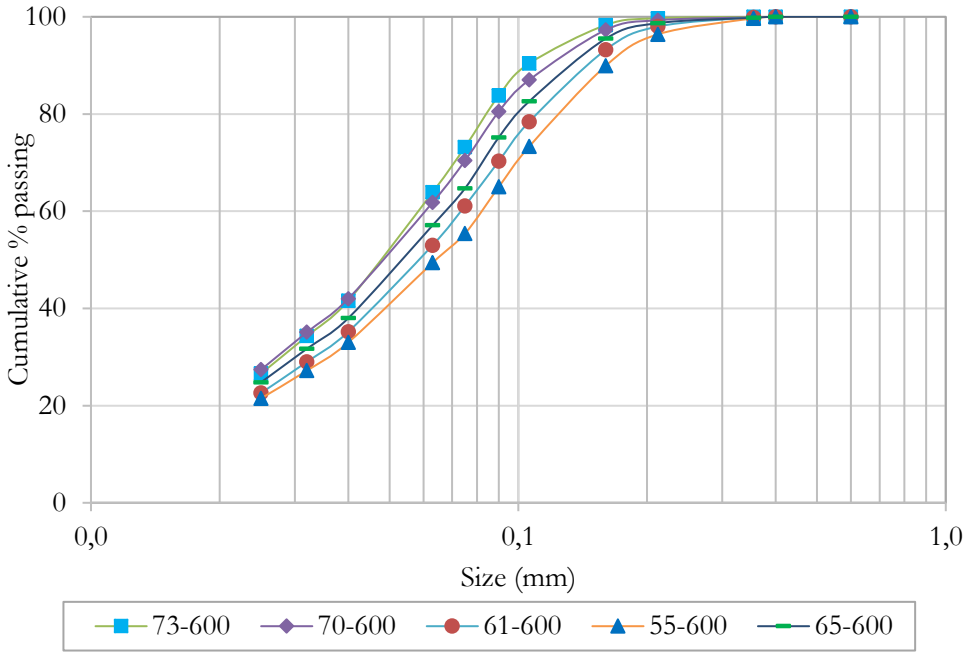

Figure 4-1: The progeny PSDs from changing target grind. For the legend, the first number represents the grind (% passing 75 µm) and the second number is the grinding pressure (kPa)

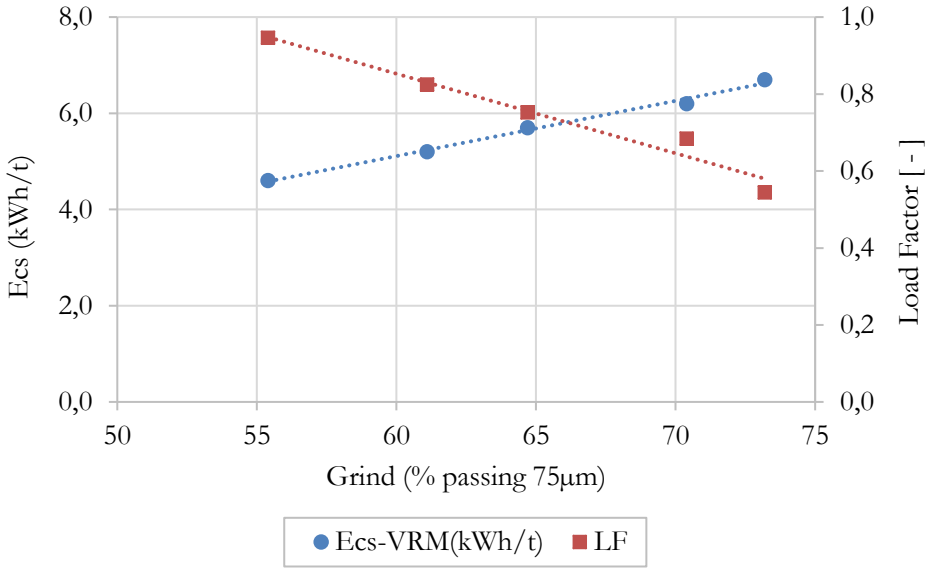

Figure 4-2: The effect of changing target grind on specific energy consumption and load factor (ratio of measured throughput to nominal throughput)

Based on the results shown in Figure 4-1 and Figure 4-2, the specific energy consumption increases as the product becomes finer. This is because more energy will be required for comminution to break the particles to the finer sizes. The load factor (throughput/nominal throughput) decreases with increasing product fineness. As the dynamic classifier cuts finer, there will be higher recirculation to the grinding table and hence the fresh feed capacity will be reduced. These results are in agreement with Altun et al. (2017) who found on a gold ore that for the same grinding pressure, specific grinding energy increases and throughput decreases with increasing fineness of product.

4.2.2. Effect of changing grinding pressure

The effects of changing grinding pressure on particle size distribution, classifier rotor speed, load factor and specific energy consumptions (Ecs) is presented in Figure 4-3, Figure 4-4 and Figure 5-7. Load factor is the ratio of observed throughput through the mill to the design capacity.

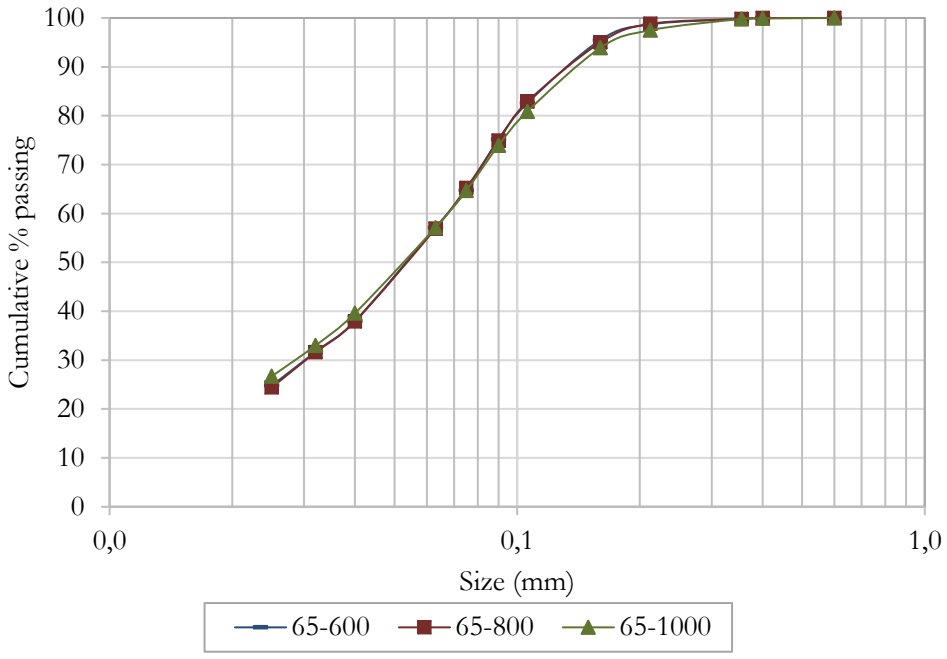

Figure 4-3: Progeny PSDs with varying grinding pressure. 65 on the legend represents the grind (65 % passing 75 µm) and the second number is the varying grinding pressure (kPa)

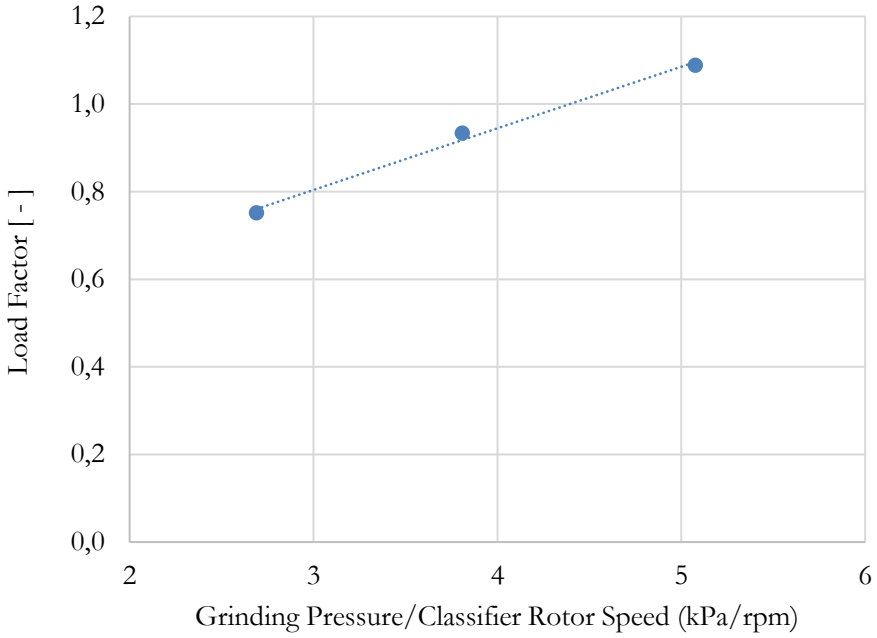

Figure 4-4: The effect of changing grinding pressure/classifier rotor speed on load factor

Figure 4-3 shows that grinding roller pressure does not have a noticeable effect on the progeny particle size distributions. Figure 4-4 shows that for the same target grind, an increase in grinding pressure/classifier rotor speed results in an increase in the load factor (throughput/nominal capacity) to the VRM. The increase in grinding pressure means more energy is applied for compression and in-bed breakage per unit area, resulting in faster breakage kinetics. This reduces the residence time required for particles to reach the target grind specifications, resulting in lower circulating loads in the VRM. Fresh feed capacity as inferred from load factor (fresh feed throughput/ nominal design throughput) increases because of the reduced circulating load. These results are also congruent to the findings of Reichert et al. (2015) for work done on iron ore and Altun et al. (2017) for work done on a fold ore, where the increase in grinding pressure resulted in an increase in production rate.

4.2.3. Effect of changing air temperature

The effect of changing temperature of the volumetric air flowing through the VRM is presented in Figure 4-5. The tests conducted were for feeding the VRM with air at atmospheric temperature (65-600-300 K) and air heated to 363 K (65-600-363 K).

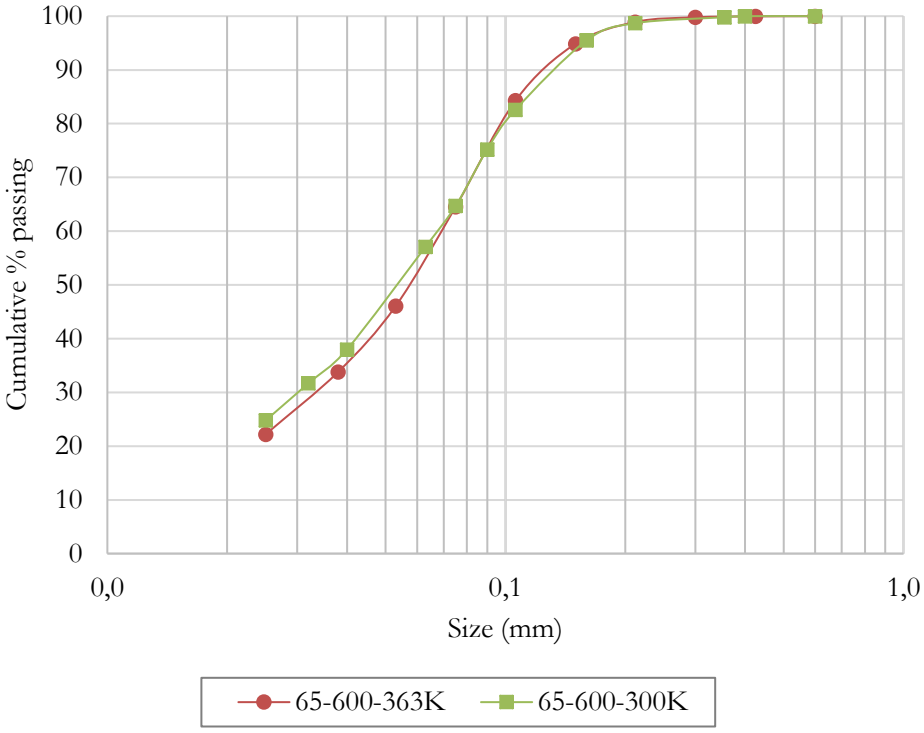

Figure 4-5: The effect of changing air temperature on progeny PSDs

The results presented in Figure 4-5 indicate that the progeny PSDs are similar, with very minor differences in the percentage of fines generated. When heated air was used (65-600-363 K), The product had slightly less fines than when atmospheric air (65-600-300 K) was used. It would be expected that the heated air would reduce agglomeration of particles after comminution hence facilitating representative separation in the classifier. The reduced agglomeration and classification based on individual particles (not agglomerated particles) will reduce the rate of fines generation, hence the observed difference in particle size distribution between using heated air and atmospheric air.

4.3. Comparison of VRM and rod milling

4.3.1. Benchmarking Grind Progeny PSDs

The progeny PSDs from comminution using the wet rod milling, dry rod milling, and the standard VRM milling for a target grind of 65% passing 75 µm as feed to flotation are as presented in Figure 4-6. The standard VRM operating conditions are a grinding pressure of 600 kN/m^2 and a dam ring height of 7 mm. A comparison of the 3 PSDs is presented in Table 4-2.

Table 4-2: Summary table of the comparison of the three progeny PSDs from wet rod milling (RW), dry rod milling (RD) and the VRM

	% passing 75 µm	% passing 38 µm	% passing 10 µm
VRM	64.7	33.9	11.6
RD	65.8	36.7	12.9
RW	65.3	36.5	12.3

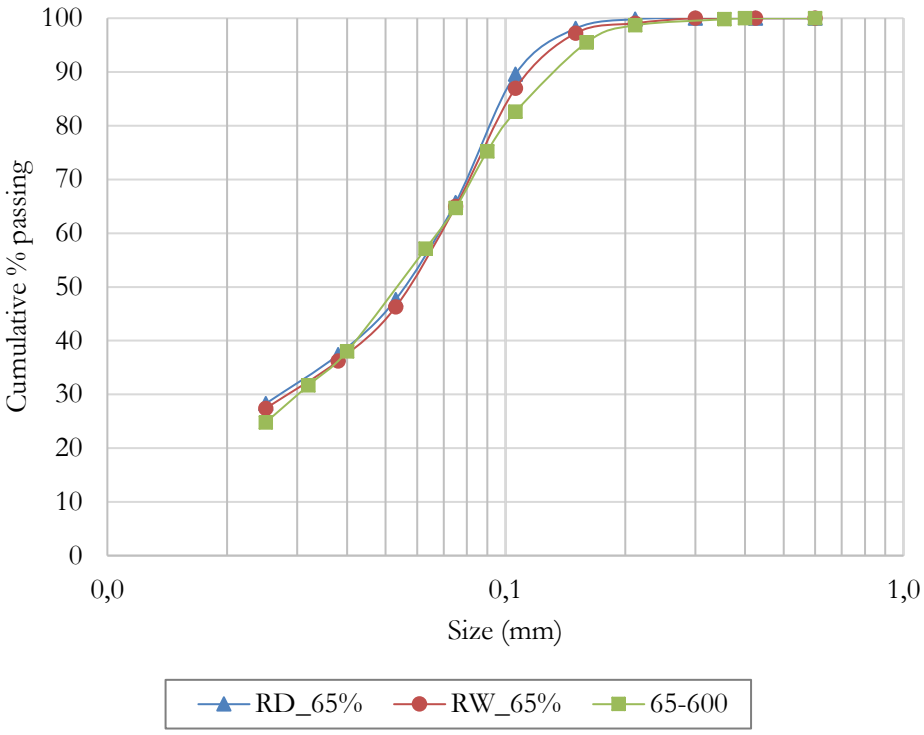

Figure 4-6: Progeny PSDs at benchmark grind (65 % passing 75 µm). RD_65%, RW_65% and 65-600 is dry grinding, wet grinding and VRM milling at 600 kPa to produce the grind of 65 % passing 75 µm

Both Table 4-2 and Figure 4-6 show that the progeny PSDs from the different comminution routes are similar. The shapes of the PSDs are also similar. While the target grind was 65% passing 75 µm, the screened PSDs showed minor deviations from the target. These deviations can be used to explain the differences in the percent passing the 10 µm sieve. The VRM, which had a slightly lower than target grind had the least sub 10 µm particles (11.6% passing 10 µm) while dry rod

milling's grind was above the expected grind, hence the highest percent passing 10 µm (12.9%). The similarity in PSDs contradicts some reported literature (Loesche GmbH, 2016), which stated that using the VRM grinding results in steep PSDs for the same target grind.

4.3.2. Progeny PSDs from VRM and rod milling at varying target grinds

The study on the benchmarking grind indicated no difference in progeny particle size distribution from comminuting using the VRM as compared to either wet or dry rod milling. More experiments were conducted to test whether this outcome would be true for a range of grinds. A total of 4 other grinds were chosen: 55 %, 60 %, 70 % and 75 % passing 75 µm. The particle size distributions from each target grind using the 3 comminution methods are presented in Figure 4-7, Figure 4-8, Figure 4-9 and Figure 4-10.

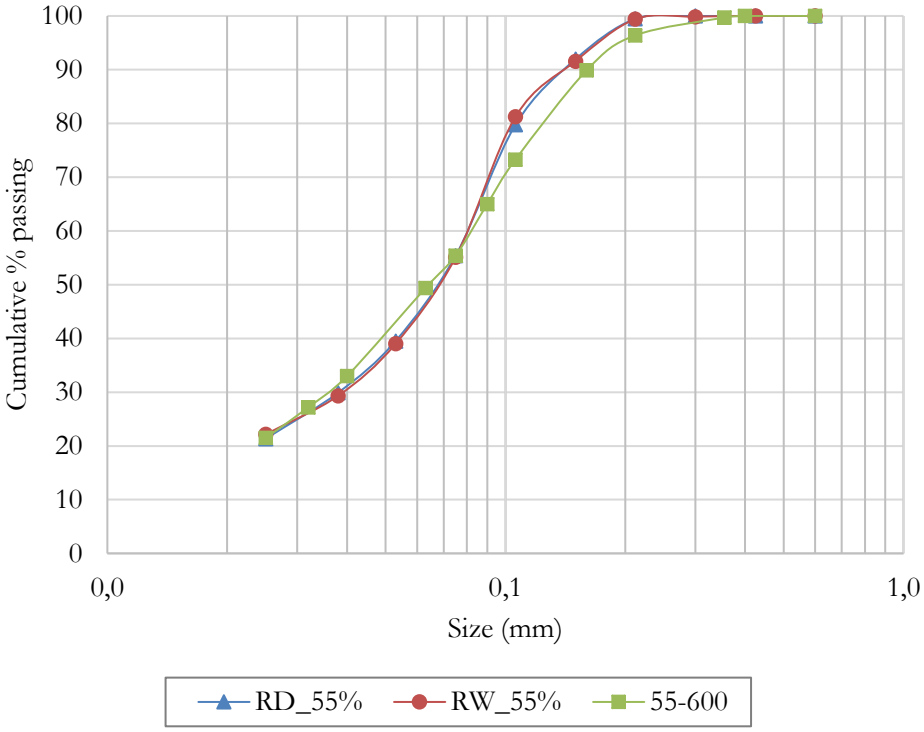

Figure 4-7: Progeny PSDs (55 % passing 75 µm). RD_55%, RW_55% and 55-600 is dry grinding, wet grinding and VRM milling at 600 kPa to produce the grind of 55 % passing 75 µm

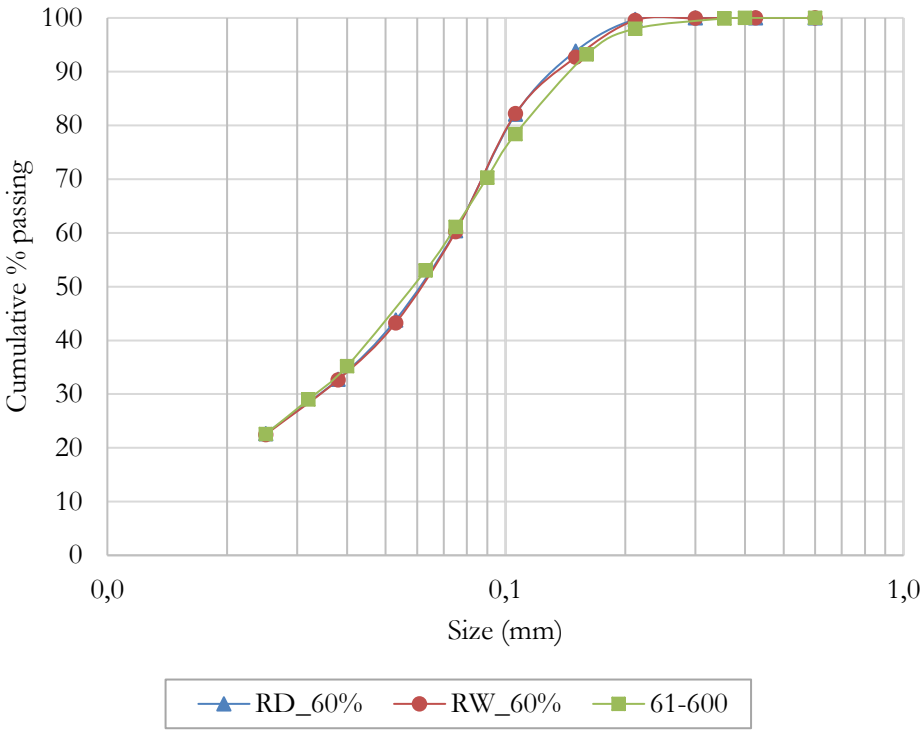

Figure 4-8: Progeny PSDs (60 % passing 75 µm). RD_60%, RW_60% and 61-600 is dry grinding, wet grinding and VRM milling at 600 kPa to produce the grind of 60 % passing 75 µm

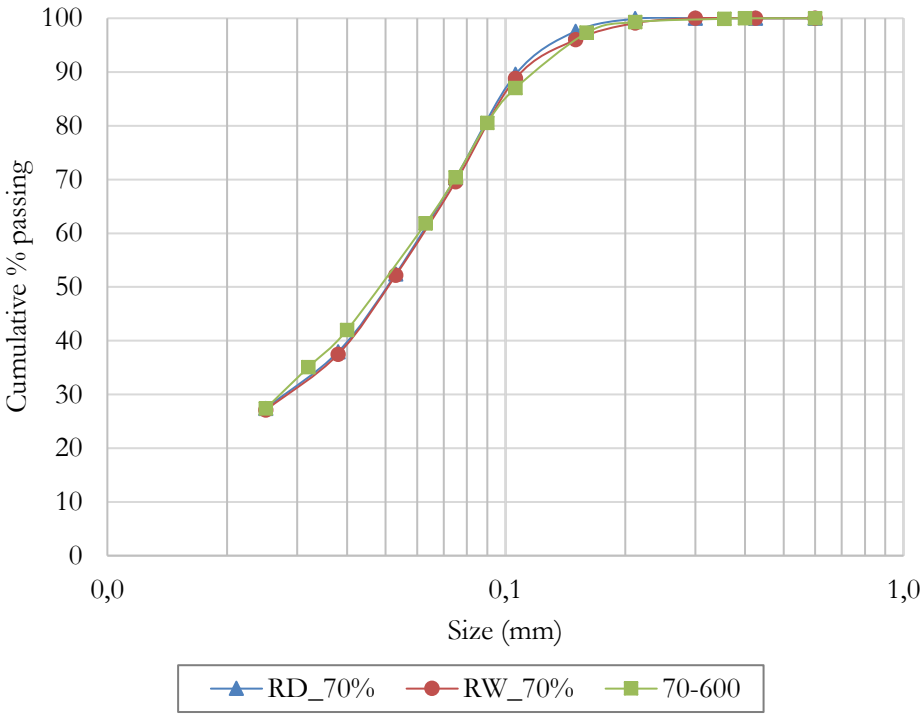

Figure 4-9: Progeny PSDs (70 % passing 75 µm). RD_70%, RW_70% and 70-600 is dry grinding, wet grinding and VRM milling at 600 kPa to produce the grind of 70 % passing 75 µm

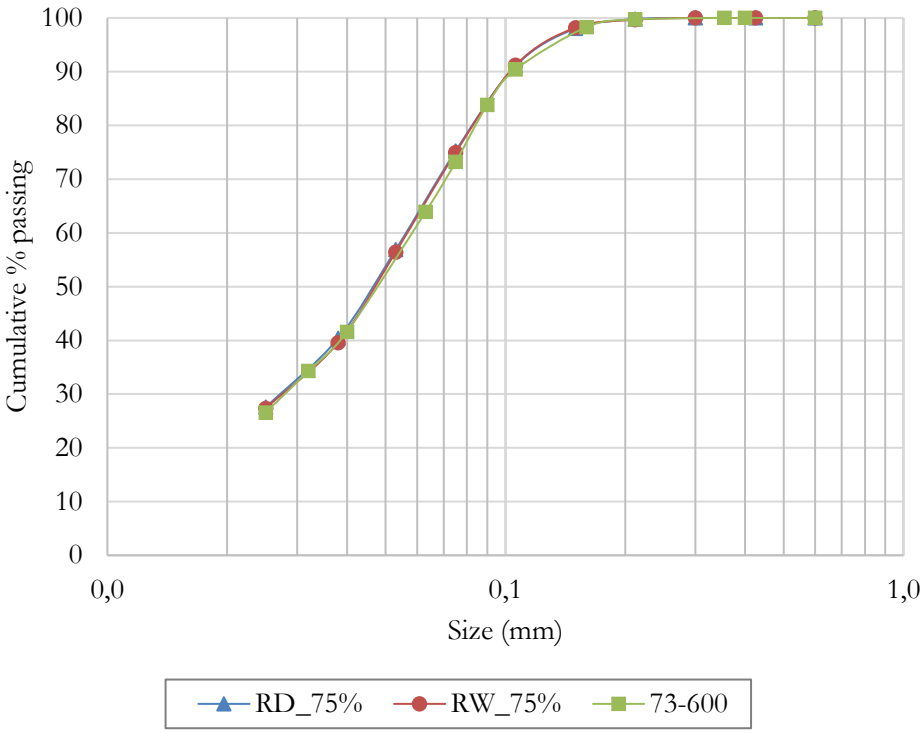

Figure 4-10: Progeny PSDs (75 % passing 75 µm). RD_75%, RW_75% and 73-600 is dry grinding, wet grinding and VRM milling at 600 kPa to produce the grind of 75 % passing 75 µm

Evident from the graphs is that the particle size distribution curves have a similar shape and can be classified as similar. This was expected as the outcome from the standard benchmarking tests had also shown that the PSDs from using the VRM and rod mill (dry/wet) would be similar.

4.4. VRM on flotation response

Tests were also conducted to understand the factors that affect the operation of the VRM and their consequences on downstream flotation performance. These were done by varying the grinding pressure, varying gas temperature and target grind for the operation of the VRM. The tests on varying target grind were conducted to assess the optimal grind for the flotation of the polymetallic ore. The results would assist in further optimising energy usage without affecting mineral recoveries during flotation.

4.4.1. Effect of changing target grind on flotation response

With regards to flotation response of the VRM products with varying grinds, the flotation performance summary for the different VRM grinds is summarised in Table 4-3.

Table 4-3: Recovery and grade for copper, lead and zinc at different grinds

Grind (% passing 75um)	Mass Pull (%)	Cu		Pb		Zn	
		Rec (%)	Grade (%)	Rec (%)	Grade (%)	Rec (%)	Grade (%)
55	10.2	84.9	4.7	89.2	22.0	90.0	12.6
61	10.1	95.1	4.9	90.7	19.7	96.0	12.1
65	11.2	96.7	4.2	94.3	18.7	96.6	10.9
70	10.2	95.9	4.7	89.6	19.8	95.3	12.1
73	8.2	87.1	5.4	87.1	24.5	83.7	13.3

The solids vs. water recovery relationships after floating VRM products of varying grinds are presented Figure 4-11. The grade-recovery curves for copper, lead and zinc are presented in Figure 4-12, Figure 4-13 and Figure 4-14.

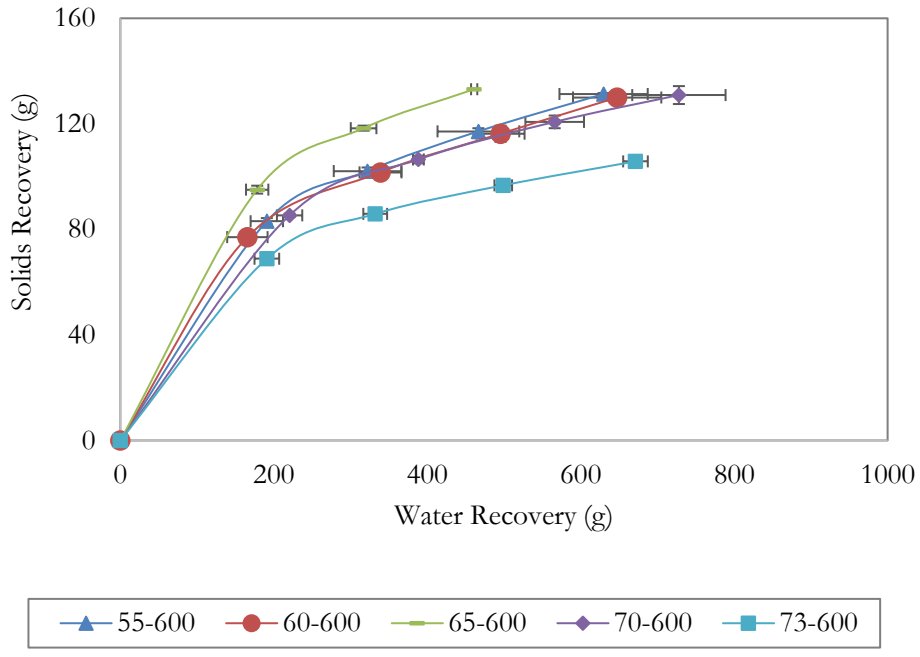

Figure 4-11: Solids vs. water recovery for the flotation of VRM product produced at varying target grind

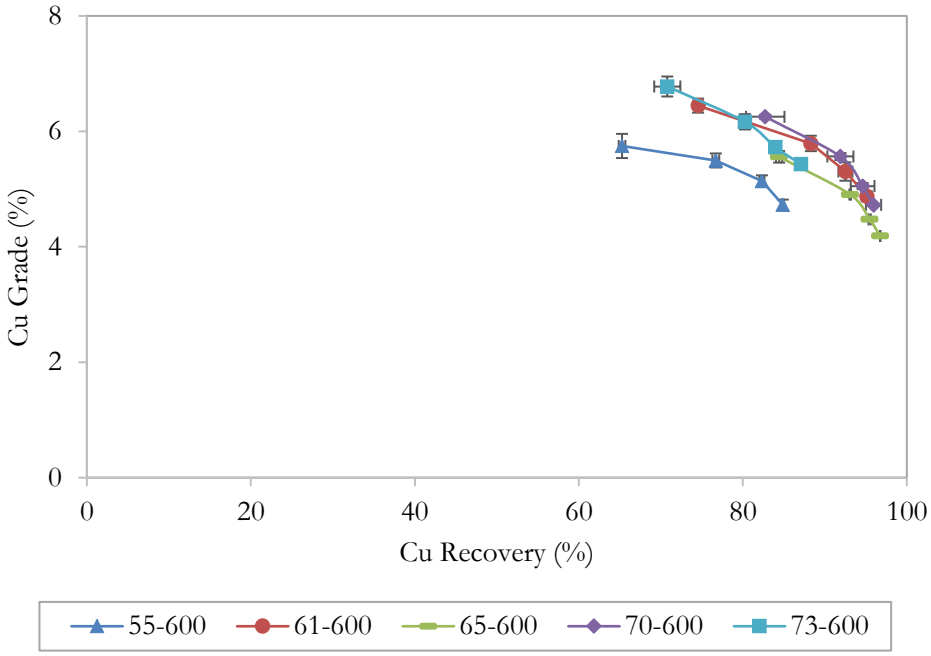

Figure 4-12: Copper concentrate grade vs. recovery relationship for the flotation of varying grind VRM product

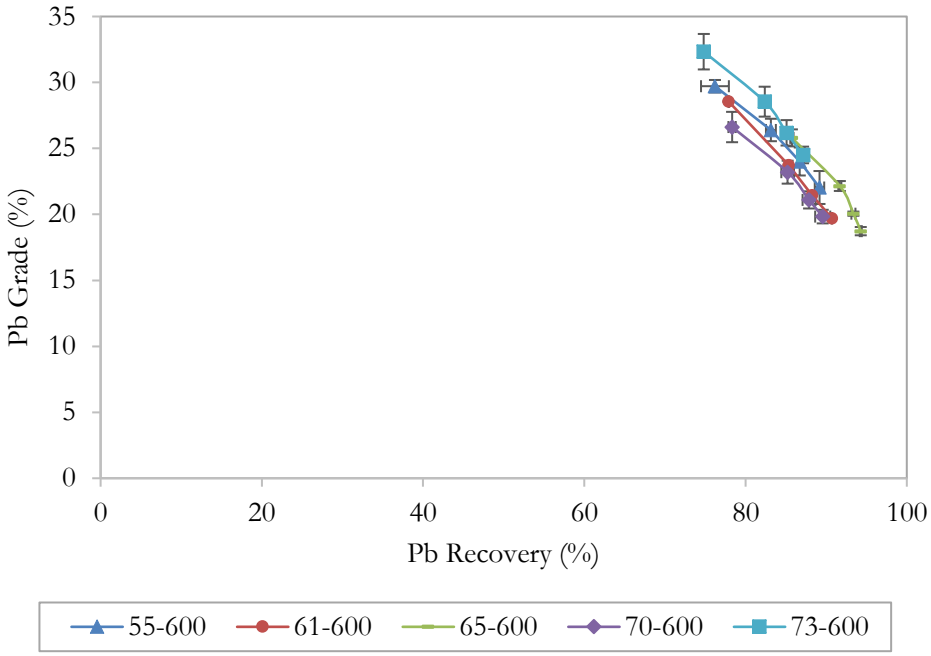

Figure 4-13: Lead concentrate grade vs. recovery relationship for the flotation of varying grind VRM product

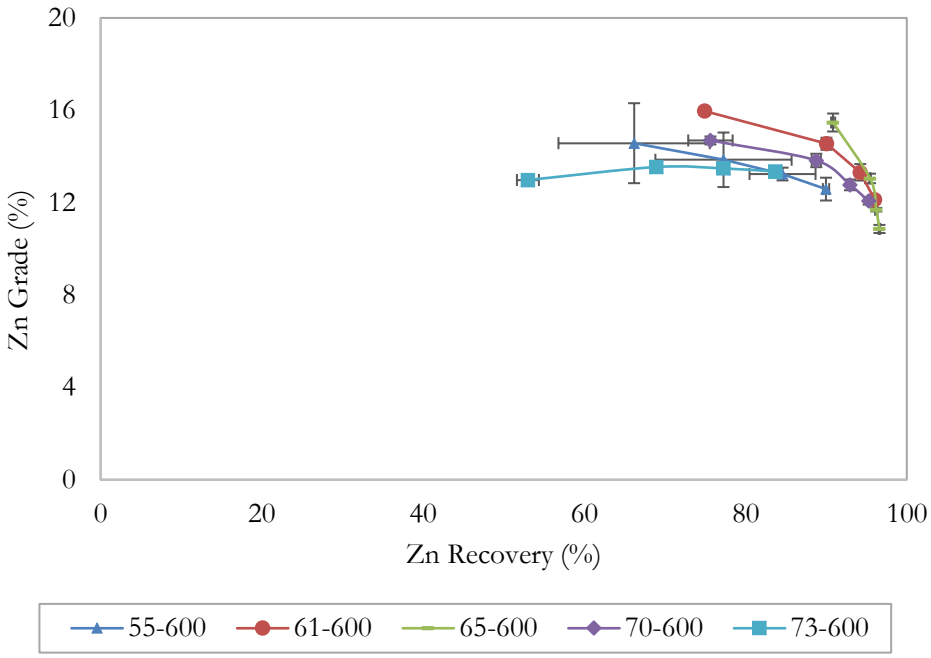

Figure 4-14: Zinc concentrate grade vs. recovery relationship for the flotation of varying grind VRM product

It can be observed from the results that the optimum grind for the polymetallic Swartberg ore is 65 % passing 75 µm. The grind range for optimum flotation performance is between 60 % and 70 % passing 75 µm. Table 4-3 shows that the recovery is low for 55% passing as well as 75 % passing 75 µm. For the 55% passing 75 µm flotation feed, value mineral liberation is likely to be incomplete, which compromises their recovery. Mineral recoveries were also low after floating the 75 % passing 75 µm VRM product. Grinds greater than 70 % passing 75 µm may have resulted in high fines generation, which needed another tailored flotation recipe to cater for the increased fines (change in reagents suite, change in bubble size generation to produce smaller ones). Grinding to above 70 % passing 75 µm also implies that energy is wasted during comminution as the results indicate that there is no need to grind that fine.

4.4.2. Effect of changing grinding pressure on flotation response

The flotation response of ore comminuted using the VRM at varying grinding pressures are presented in this section. The target grind was 65 % passing 75 µm and the grind pressures used were 600 kN/m^2, 800 kN/m^2 and 1000 kN/m^2.The flotation response, in terms of solids-water recovery and elemental recoveries is presented in Figure 4-15, Figure 4-16, Figure 4-17, Figure 4-18 and Figure 4-19. On the graphs, 65-600 represents a grind of 65 % passing 75 µm achieved at 600 kN/m^2, 65-800 for the same grind achieved at 800 kN/m^2 and 65-1000 for the same grind achieved using grinding roller pressure of 1000 kN/m^2.

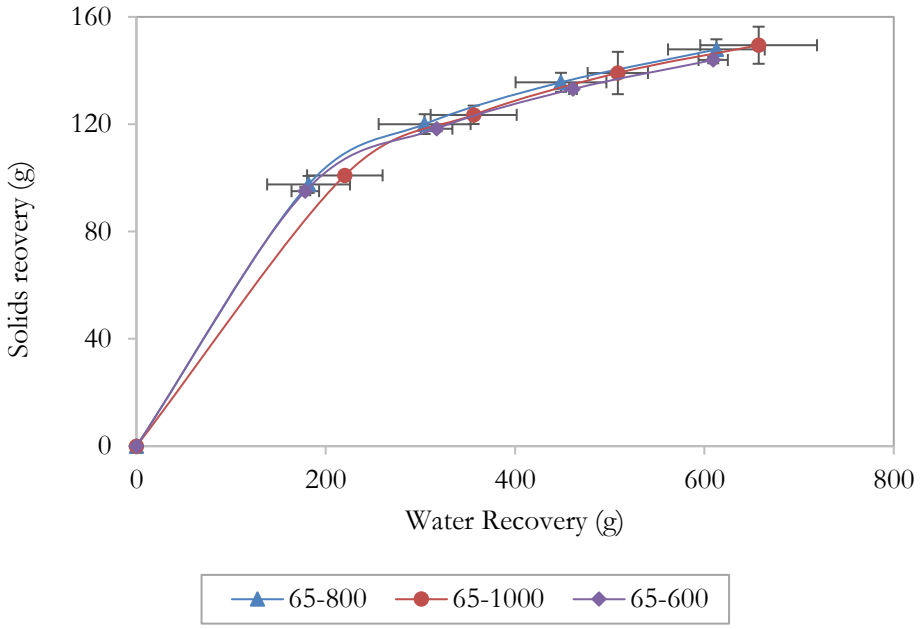

Figure 4-15: Solids vs. water recovery for the flotation of VRM product produced at varying grinding pressures

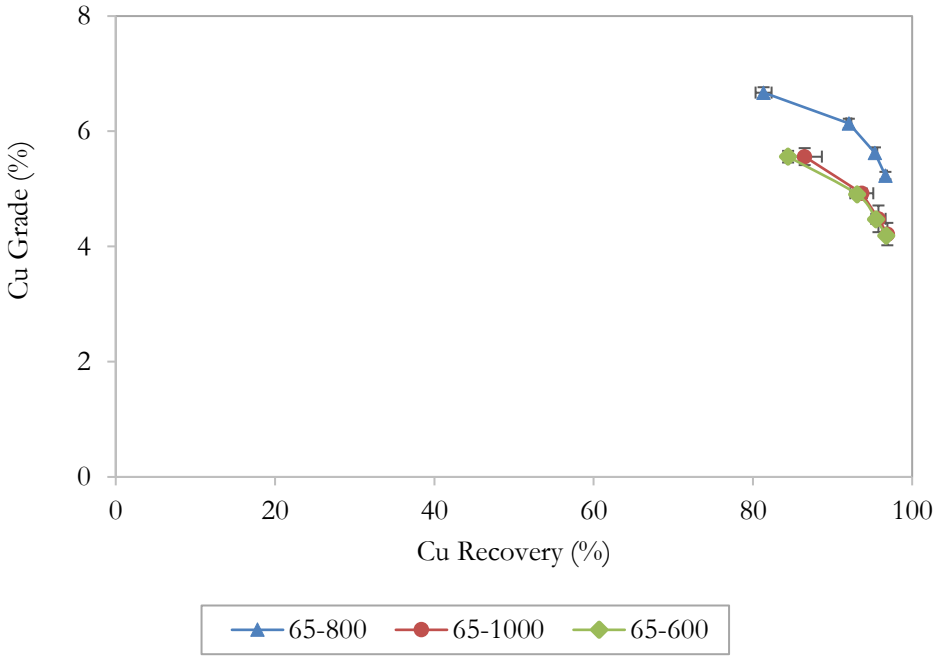

Figure 4-16: Copper concentrate grade vs. recovery relationship for the flotation of VRM product from varying grinding pressure

The concentrate grade for 65-800 is magnified because of the higher feed grade in the feed (0.60% Cu vs. 0.48% Cu). To correct the feed grade effect on selectivity, the upgrade ratio vs. recovery is presented in Figure 4-17.

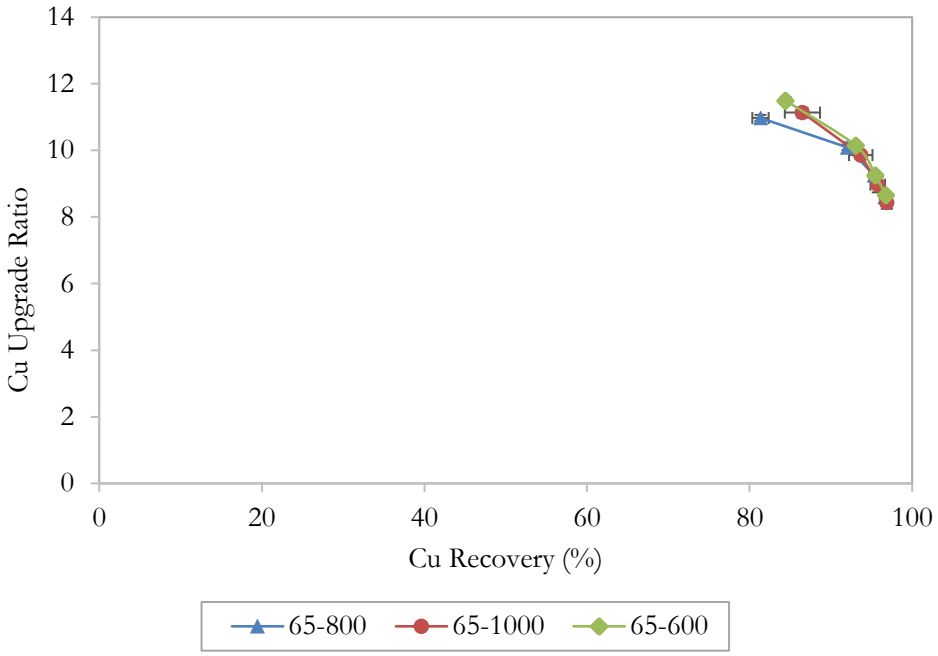

Figure 4-17: Copper upgrade ratio vs. recovery relationship for the flotation of VRM product from varying grinding pressure

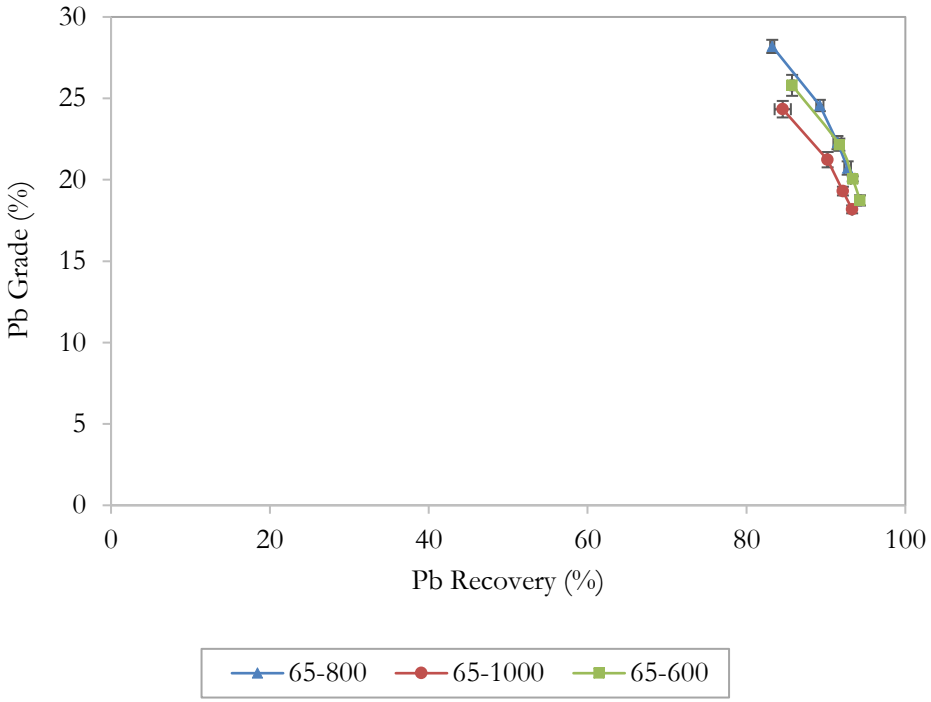

Figure 4-18: Lead concentrate grade vs. recovery relationship for the flotation of VRM product from varying grinding pressure

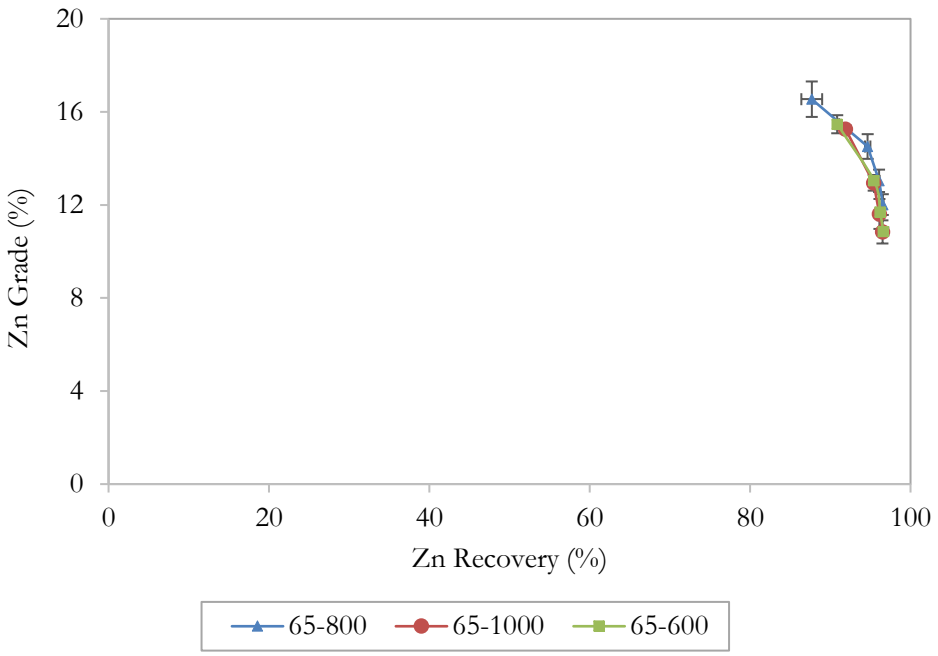

Figure 4-19: Zinc concentrate grade vs. recovery relationship for the flotation of VRM product from varying grinding pressure

The total solids and water recoveries obtained (Figure 4-15) show that there is marginal increase in solids and water recovery during flotation as grinding pressure is increased from 600 kN/m^2 to 1000 kN/m^2. However, the confidence limits show that the solids and water recoveries are similar. The recovery of copper, lead and zinc are similar for the three grinding pressures under study as shown by the low statistical confidence that differences exit (minimum accepted confidence: 95 %) (Table 4-4).

Table 4-4: Cumulative recovery and the ANOVA statistical confidence level of differences in recovery

	65-600	65-800	65-1000	Confidence level (%)
Cu	96.9	96.6	96.9	12.6
Pb	93.3	92.7	93.3	10.9
Zn	96.5	96.5	96.5	2.5

Coupling the outputs from comminution and flotation, the results indicate that grinding pressure/classifier rotor speed increases capacity (throughput) without compromising recovery and grade in the case of the polymetallic sulfide ore under study.

4.4.3. Effect of changing gas temperature on flotation response

The gas flow through the VRM had temperature control. In one test, atmospheric air temperature (300 K) and in the second test, the air was heated to 373 K. The benchmarking grind of 65 % passing 75 µm was used. The effect of the variation in gas temperature on the flotation response is presented in Figure 4-20, Figure 4-21, Figure 4-22 and Figure 4-23. 65_300K represents the use of air at 300 K and 65_363K represents the use of air at 363 K during comminution to achieve the grind of 65 % passing 75 µm.

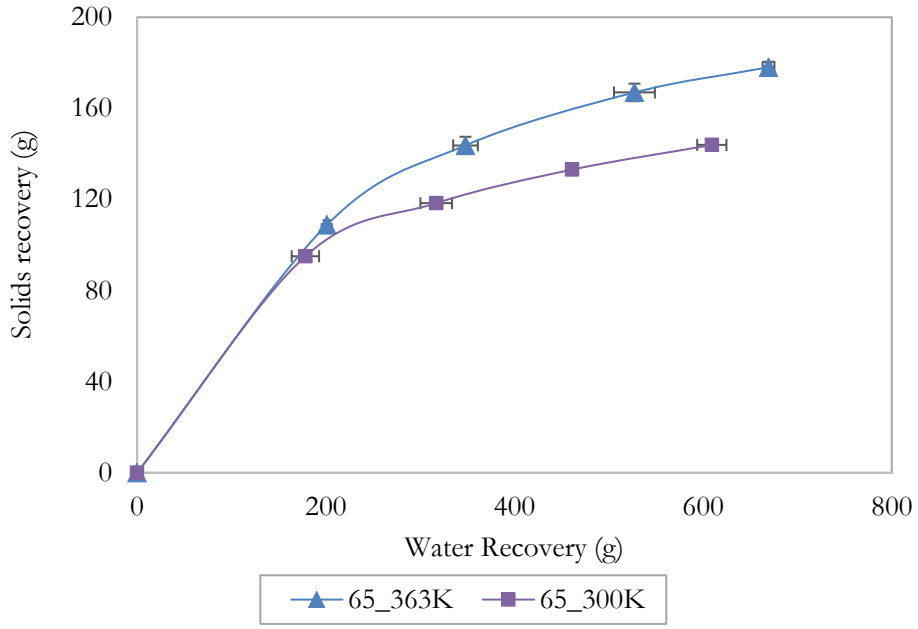

Figure 4-20: Solids vs. water recovery for the flotation of VRM product produced at varying gas temperature

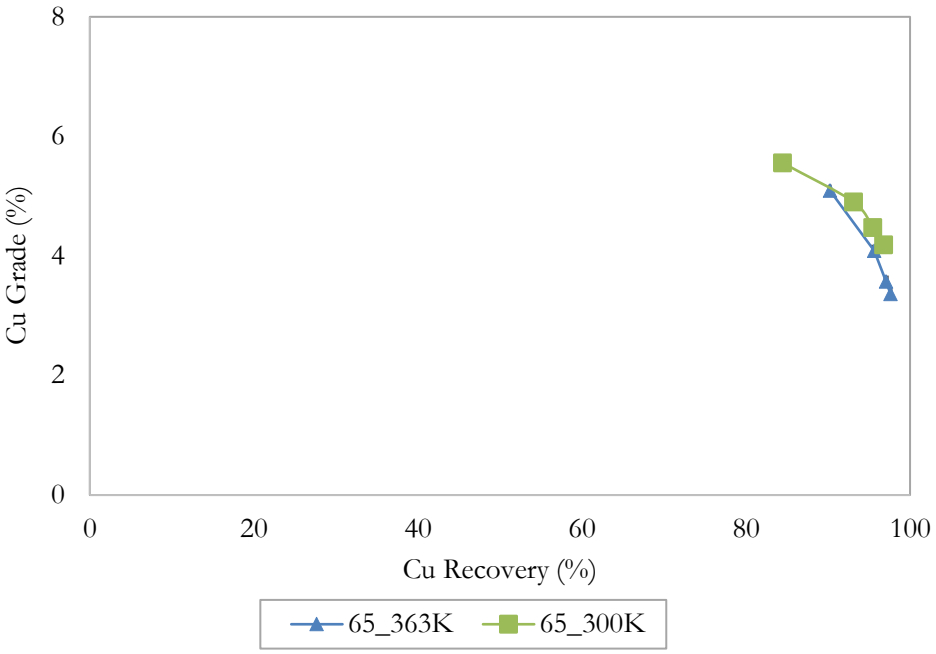

Figure 4-21: Effect of gas temperature on copper concentrate grade vs. recovery relationship

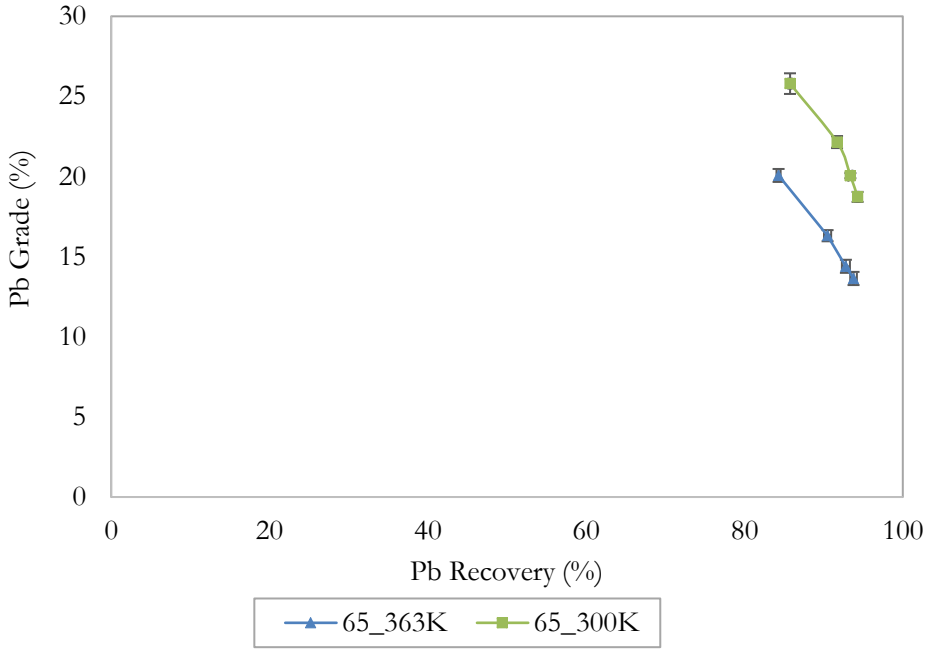

Figure 4-22: Effect of gas temperature on lead concentrate grade vs. recovery relationship

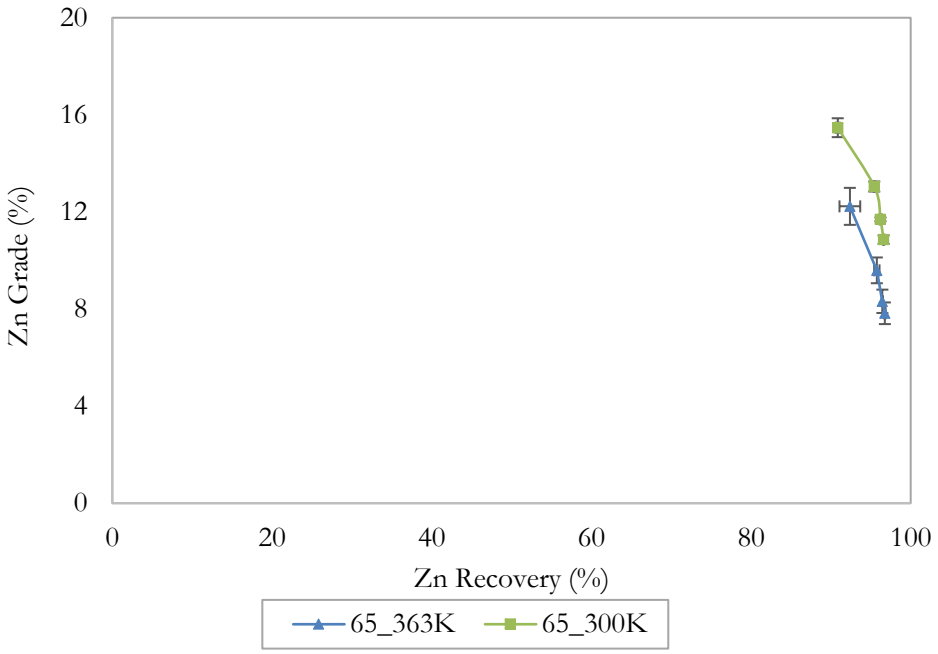

Figure 4-23: Effect of gas temperature on zinc concentrate grade vs. recovery relationship

Figure 4-20 shows that the total water and solids recovery was higher after floating VRM product produced using heated air. The recoveries of copper, lead and zinc minerals were similar. Statistical analysis using ANOVA indicated that there was 76 %, 29 % and 69 % confidence of a difference in the recovery of copper, lead and zinc respectively. The concentrate grades from the heated product were significantly lower. This could be because heated air may have caused some oxidation on the sulfide minerals surfaces, thereby affecting surface chemistry and selectivity during flotation.

4.5. Comparison of rod milling and VRM flotation response

4.5.1. Benchmarking flotation tests

The flotation response of the ore comminuted to the benchmarking grind of 65 % passing 75 µm using the three mechanisms: wet rod milling (RW), dry rod milling (RD), and the standard VRM (grinding pressure of 600 kPa) are presented in this section. The results are presented in sequence: redox chemistry measurements of the pulp prior to flotation, water recovery and solids recovery, flotation kinetics and kinetics modelling followed and then the recovery-grade relationships.

4.5.1.1. Redox chemistry

The pulp potential prior to adding reagents was measured using the HANNA meter and is presented in Table 4-5.

Table 4-5: Pulp potential (SHE) and its standard error (S.E) after making up with SPW to the 3-L mark of the Barker flotation cell

Milling method	Average Eh (mV)	S.E Eh (mV)
Dry Rod Milling (RD)	324.8	5.5
Wet Rod Milling (RW)	252.6	2.8
VRM Standard (VRM)	272.5	2.9

The measurements taken indicate the most positive pulp potential was observed for dry grinding using mild steel rods while wet rod milling had the lowest pulp potential. The standard VRM had a pulp potential higher than that for wet grinding, but almost half that observed with dry rod milling. These findings agree with findings from Gonçalves et al (2003) who found that dry grinding results in more positive pulp potential. This, coupled with the findings of Feng and Aldrich (2000) that dry grinding results in rougher particles with microcracks (Feng and Aldrich, 2000), can be used to infer that collector adsorption rates would be highest for RD, followed by VRM and then RW.

4.5.1.2. Solids and Water Recovery

The solids and water recovery for the flotation of dry rod mill product, wet rod mill product and the standard VRM product is presented in Figure 4-24, Figure 4-25, Figure 4-26 and Figure 4-27.

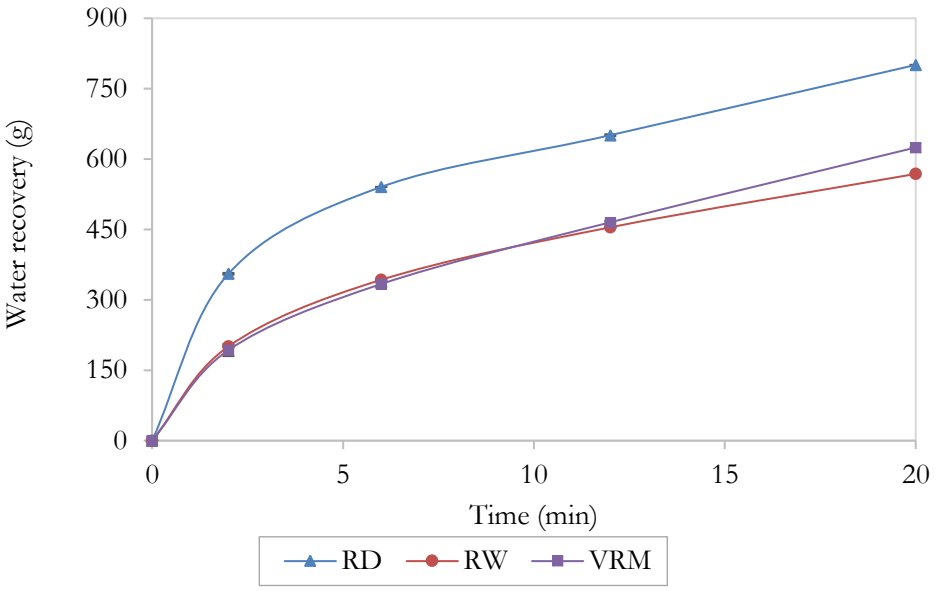

Figure 4-24: Water recovery over time for the flotation of products from wet rod milling (RW), dry rod milling (RD) and the VRM

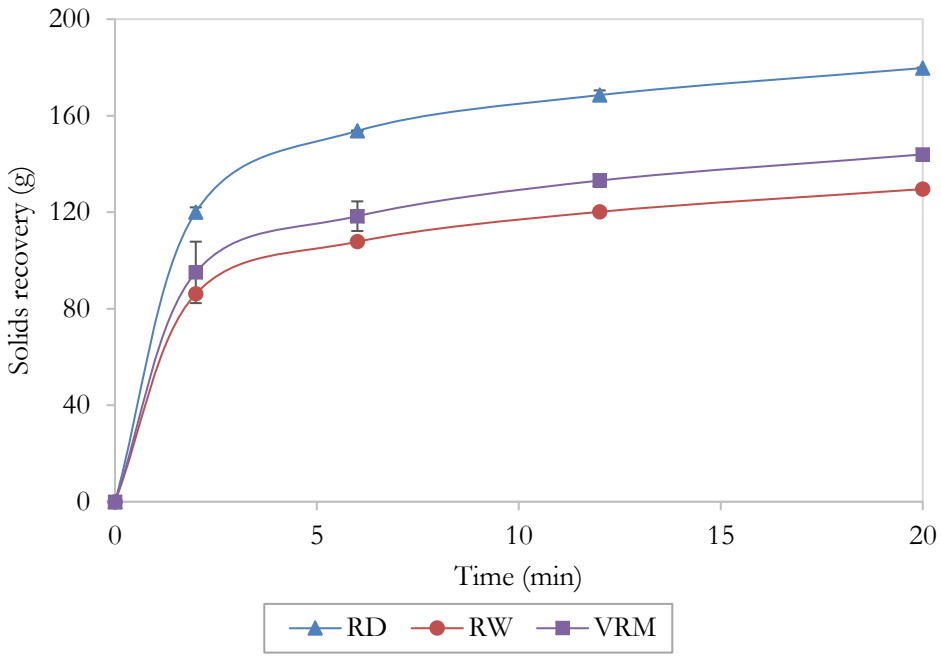

Figure 4-25: Solids recovery over time for the flotation of products from wet rod milling (RW), dry rod milling (RD) and the VRM

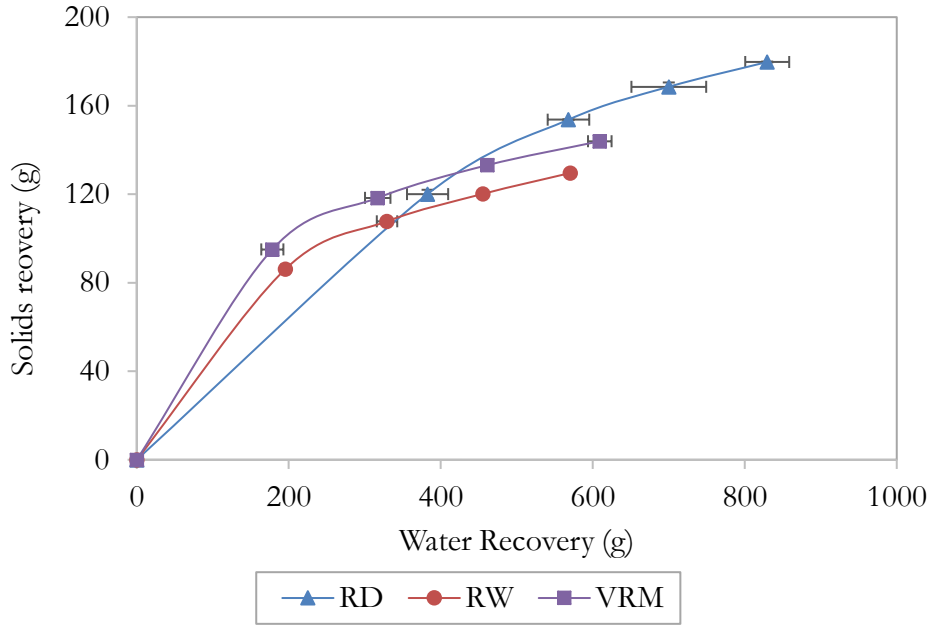

Figure 4-26: Solids vs. water recovery for the flotation of products from wet rod milling (RW), dry rod milling (RD) and the VRM

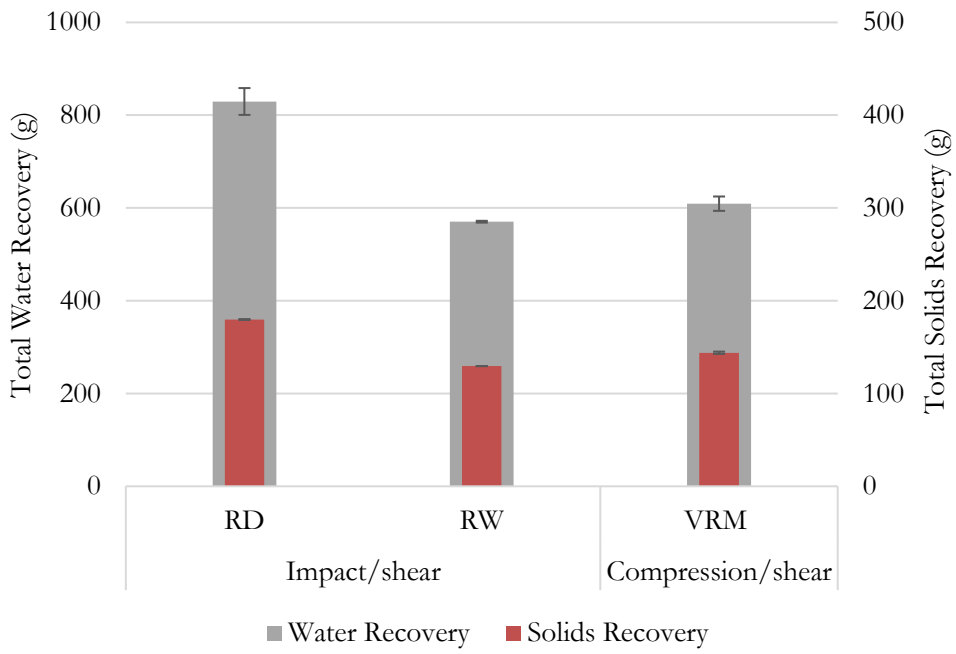

Figure 4-27: Total solids recovery and total water recovery for the flotation of products from wet rod milling (RW), dry rod milling (RD) and the VRM

The results show that dry rod milling had the highest total and solids recovery while wet rod milling grinding had the lowest solids/water recovery. The solids and water recovery for the VRM were slightly higher, but comparable to wet rod grinding. The water recovery could be correlated to pulp potential, as the higher the pulp potential from the comminution procedure, the higher the resultant water recovery.

4.5.1.3. Recovery-Grade Relationship

The recovery-grade relationships of copper, lead and zinc from the flotation of products from the three comminution mechanisms are presented in Figure 4-28, Figure 4-29 and Figure 4-30 respectively.

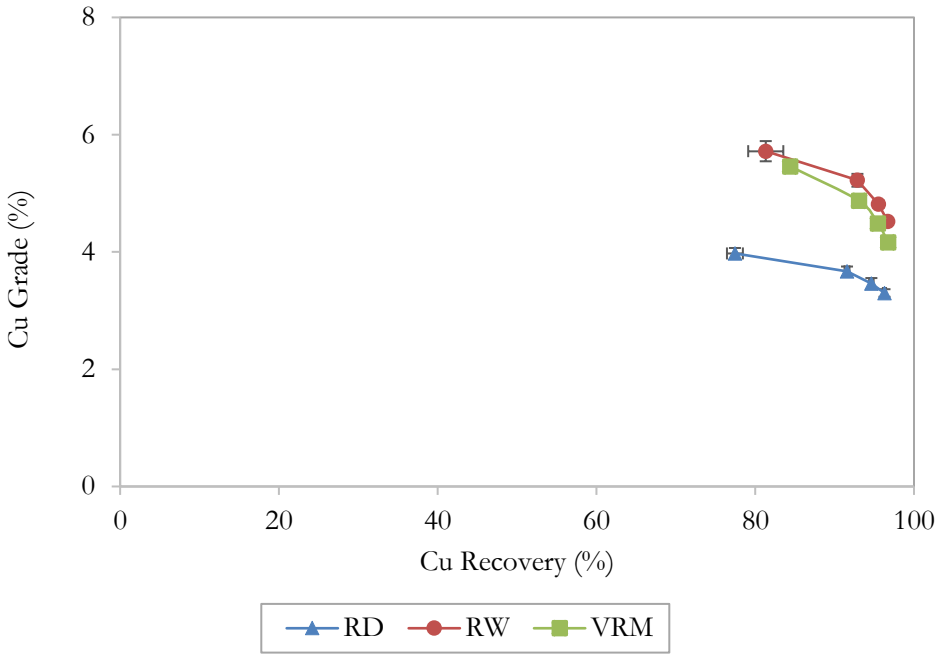

Figure 4-28: Copper concentrate grade vs. recovery relationship for the flotation of products from wet rod milling (RW), dry rod milling (RD) and the VRM

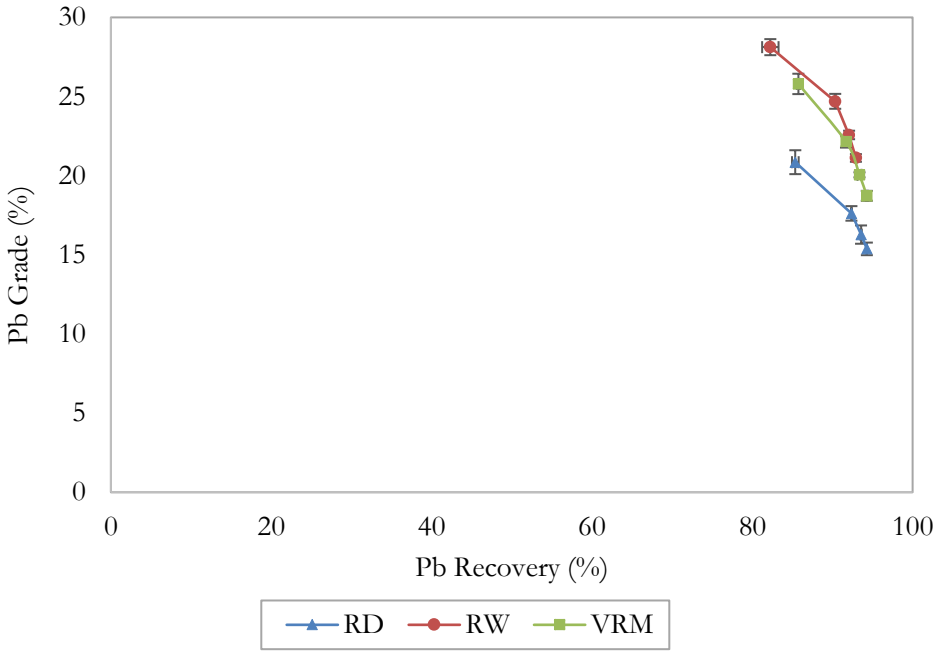

Figure 4-29: Lead concentrate grade vs. recovery relationship for the flotation of products from wet rod milling (RW), dry rod milling (RD) and the VRM

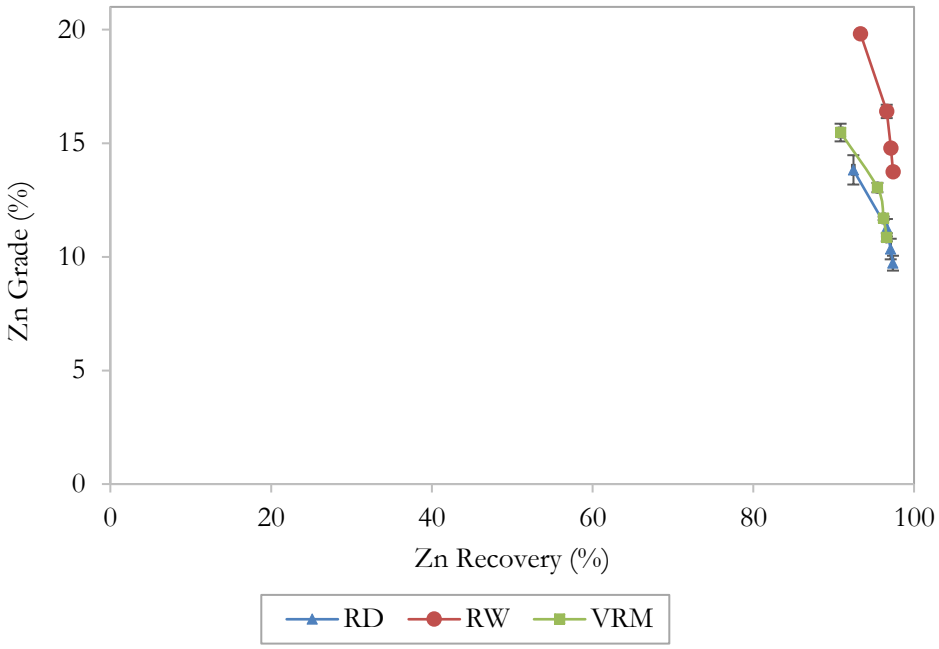

Figure 4-30: Zinc concentrate grade vs. recovery relationship for the flotation of products from wet rod milling (RW), dry rod milling (RD) and the VRM

The cumulative concentrate grade and total recovery for the copper, lead and zinc are presented in Table 4-6.

Table 4-6: Recovery and grade for copper, lead and zinc for RD, RW and VRM

Grinding Mechanism	**Cu**		**Pb**		**Zn**	
	Rec (%)	Grade (%)	Rec (%)	Grade (%)	Rec (%)	Grade (%)
VRM	96.7	4.2	94.3	18.7	96.6	10.9
RD	96.3	3.3	94.3	15.4	97.4	9.7
RW	96.7	4.5	92.9	21.1	97.4	13.7

The recovery of the minerals after being comminuted by either comminution procedure is high, and very close to the maximum achievable recovery of 100 %. This similarity in final recoveries for copper, zinc and lead means that the flotation performance of the Swartberg ore is mostly independent of grinding mechanism used prior to flotation. While final recoveries for the elements are similar, the concentrate grades for the elements (Cu, Zn, Pb) showed significant differences. Wet milling product (RW) flotation had the highest selectivity, followed by the VRM product and dry rod milling (RD) had the lowest selectivity.

Given that the final elemental recoveries for copper and lead were similar irrespective of comminution mechanism, the concentrate grades can be closely correlated to the mass and solids recovery. This is in line with the accepted correlation that water recovery is a measure of recovery by entrainment (Wiese et al., 2006; Liu et al., 2018), and hence higher water recoveries often result in lower concentrate grades. Wet rod milling (RW) had the lowest mass pull and lowest water recovery, translating to higher selectivity of chalcopyrite, galena and sphalerite. Dry rod milling (RD) had the highest mass pull and water recovery, and this translated in the lowest selectivity of the target minerals.

4.5.1.4. Recovery kinetics

The recovery kinetics were modelled using the first order Klimpel Flotation Model (Klimpel, 1980). The model equation is presented in equation 4 1.

$$R(t) = R_{max}\left[1 - \frac{1}{kt}(1 - e^{-kt})\right] \quad \text{Equation 4-1}$$

where R is the model recovery at time t (min), R_{max} is the theoretical maximum recovery (%) and k is the first order kinetic rate constant (min^{-1}).

The Excel tool called Solver was used to minimise root mean sum of squares for the modelling. The derived flotation constants from the Klimpel Flotation Model are presented in Table 4-7.

Table 4-7: Rmax and k for kinetics modelling for the 3 comminution mechanisms

	Model	RD	RW	VRM
Cu (for chalcopyrite)	R_max (%)	98.4	98.5	97.8
	k (min^{-1})	2.3	2.9	3.7
Pb (for galena)	R_max (%)	95.4	94.1	95.0
	k (min^{-1})	4.8	4.0	5.1
Zn (for sphalerite)	R_max (%)	98.1	97.9	97.4
	k (min^{-1})	8.8	10.8	7.6

The recovery kinetics for the elements (Cu, Pb, Zn) are presented in Figure 4-31, Figure 4-32 and Figure 4-33.

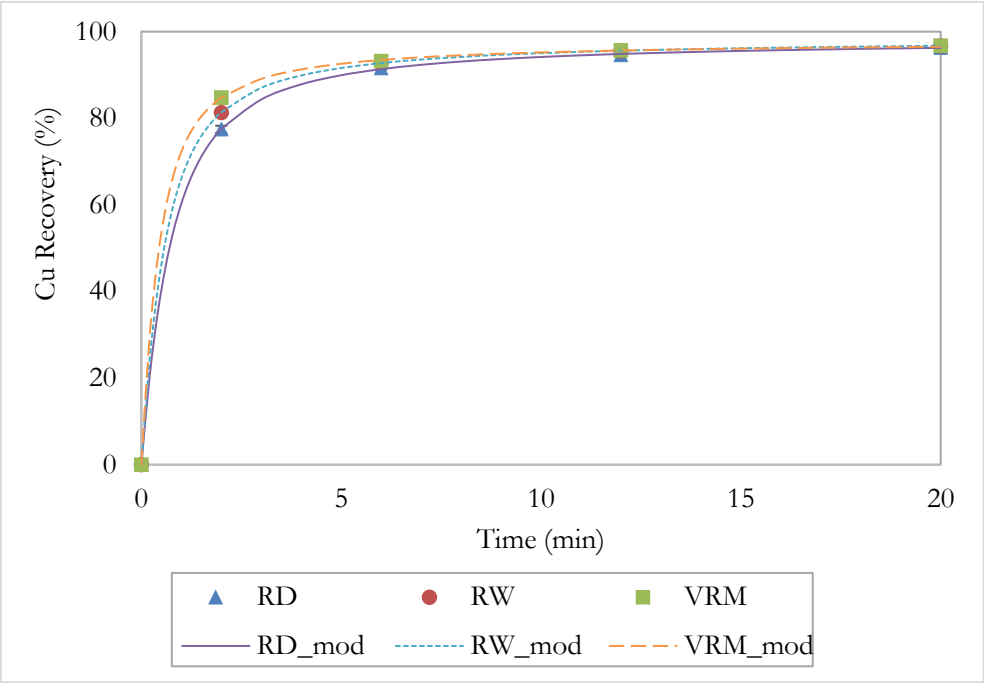

Figure 4-31: Copper recovery vs. time for the flotation of products from wet rod milling (RW), dry rod milling (RD) and the VRM

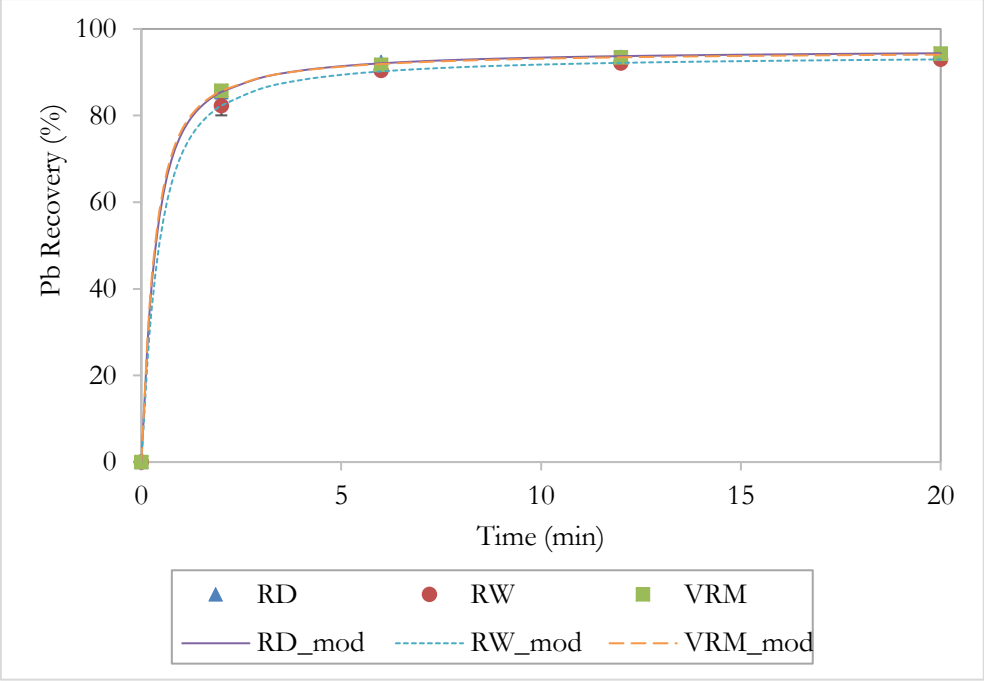

Figure 4-32: Lead recovery vs. time for the flotation of products from wet rod milling (RW), dry rod milling (RD) and the VRM

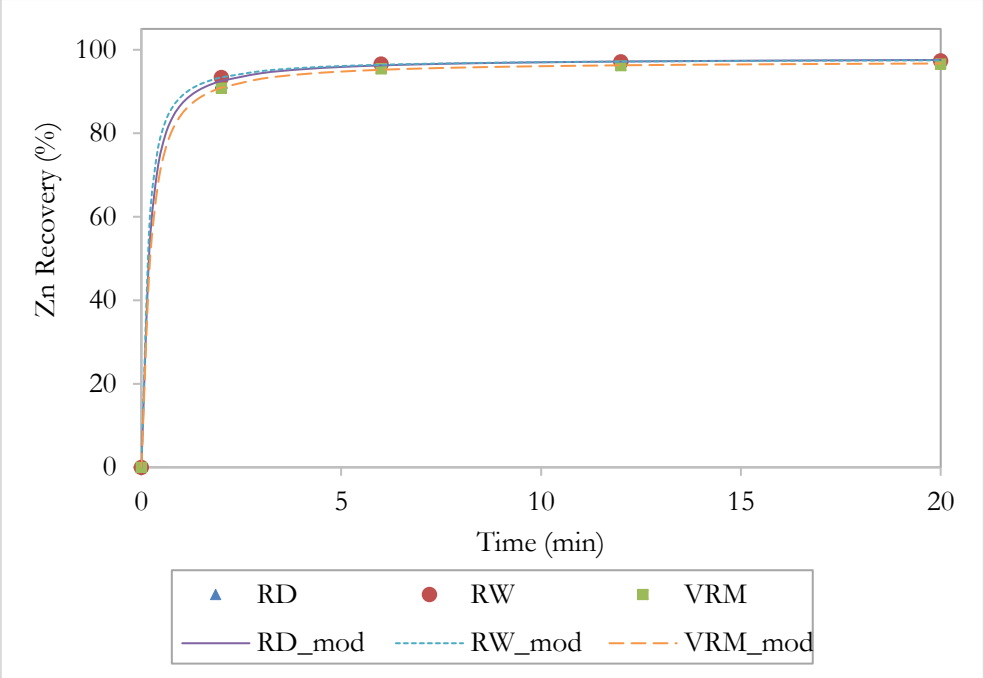

Figure 4-33: Zinc recovery vs. time for the flotation of products from wet rod milling (RW), dry rod milling (RD) and the VRM

From the graphical information, recoveries of copper, lead and zinc minerals are high irrespective of the mechanism used for comminution. The kinetics are similar (Figure 4-31, Figure 4-32 and Figure 4-33), and show that within two minutes of flotation; copper, lead and zinc mineral recoveries were above 80% with the exception of copper recovery after dry rod milling.

Table 4-7 shows that the theoretical maximum recovery (Rmax) is independent of comminution procedure as the value are very similar. The first order rate constants vary inconsistently, as dry rod mill (RD) has lowest rate constant for copper, wet rod milling (RW) has the lowest for galena and VRM has the lowest flotation rate constant for sphalerite.

The flotation kinetics within the first two minutes for the VRM product are marginally better for copper and lead as the recoveries are slightly higher (within the two minutes of concentrates collection) than the other two mechanisms used.

4.5.2. Effect of changing target grind on flotation response

The flotation performance of the VRM products at the different grinds is presented in Table 4-8.

Table 4-8: Recovery performance of the different comminution products at different target grinds

Grind (% passing 75 µm)	Cu Rec (%)			Pb Rec (%)			Zn Rec (%)		
	RD	RW	VRM	RD	RW	VRM	RD	RW	VRM
55	97.7	97.6	84.9	95.2	94.3	89.2	96.8	96.9	90.0
60	97.9	97.8	95.1	95.6	94.7	90.7	97.3	97.0	96.0
65	96.3	96.7	96.7	94.3	92.9	94.3	97.4	97.4	96.6
70	97.6	97.9	95.9	94.9	94.7	89.6	97.0	97.1	95.3
75	98.0	97.6	87.1	95.7	94.3	87.1	97.0	96.9	83.7

It can be observed from the results that the recovery of copper, lead and zinc was compromised dry milling using the VRM for the very coarse grind of 55 % passing 75 µm. This could be because at that grind (55 % passing 75 µm), the valuable minerals were not sufficiently liberated to be recovered through flotation. Between grinds of 60 % and 70 % passing 75 µm, elemental recoveries were highest. Beyond 70 % passing 75 µm, the VRM recovery performance dropped. This could be an anomaly as it would be expected that as more energy is used for comminution, the particles become finer and valuable minerals become more and more liberated, thus becoming more accessible to flotation. In the same light however, there is a limit of product fineness in relation to flotation. As particles become finer, recovery by entrainment (which is unselective) starts becoming dominant and valuable mineral recoveries (hence efficiencies) drop.

Statistical analysis through the application of analysis of variance (ANOVA) was conducted to compare the flotation performance of the products from the VRM and the products from wet rod milling. Wet rod milling products were chosen as they are representative of the current mineral processing flowsheet. A confidence level above 95 % meant that there was a statistically significant difference between the performances, with the percent difference also quoted as RW-VRM (Table 4-9). In the table, the numbers in bold indicate scenarios where confidence levels are less than 95 %.

Table 4-9: ANOVA analysis used to determine differences in recovery performance between VRM and RW

Grind (% passing 75 µm)	Cu		Pb		Zn	
	Conf. level (%)	(RW - VRM)	Conf. level (%)	(RW - VRM)	Conf. level (%)	(RW - VRM)
55	100.0	12.8	98.7	5.1	99.6	6.9
60	98.5	2.7	99.8	4.0	97.2	1.0
65	**25.3**	**-0.2**	**23.1**	**-0.4**	95.6	0.9
70	99.6	2.0	96.9	5.2	99.2	1.9
75	99.2	10.6	99.6	7.2	100.0	13.2

The statistical analysis informed that the flotation performance from wet rod milling was better than the flotation performance from the VRM. In the cases where the VRM mean performance was better for the recovery of copper and lead at a grind of 65 % passing 75 µm, the confidence levels were too low to ratify the difference.

Statistical analysis using ANOVA was also conducted to compare the flotation performance of the products from the VRM and the products from dry rod milling. Both comminution procedures occur in a dry environment, and thus, the statistical analysis sort to quantify differences recovery performance if any. The summary ANOVA statistics are presented in Table 4-10, with RD-VRM being the recovery of dry milling products less recovery of VRM products.

Table 4-10: ANOVA analysis used to determine differences in recovery performance between VRM and RD

Grind (% passing 75 µm)	Cu		Pb		Zn	
	Conf. level (%)	(RD - VRM)	Conf. level (%)	(RD - VRM)	Conf. level (%)	(RD - VRM)
55	100.0	12.8	99.0	6.0	99.7	6.8
60	98.5	2.7	98.7	4.9	**94.7**	**1.3**
65	**69.9**	**-0.6**	**53.2**	**1.0**	95.6	0.9
70	99.2	1.6	96.8	5.3	97.8	1.7
75	99.3	10.9	99.4	8.6	100.0	13.4

The results from Table 4-10 also indicate that the flotation performance from dry rod milling was better than the flotation performance from the VRM. At a grind of 65 % passing 75 µm, the VRM copper recovery performance was better than RD. However, the confidence levels were too low to ratify the difference. The statistical comparison of recovery from wet and dry rod milling is presented in Table 4-11. RD-RW is the difference in recovery between the achieved recovery from dry rod milling (RD) and wet rod milling (RW).

Table 4-11: ANOVA analysis used to determine differences in recovery performance between RD and RW

Grind (% passing 75 μm)	Cu		Pb		Zn	
	Conf. level (%)	(RD - RW)	Conf. level (%)	(RD - RW)	Conf. level (%)	(RD - RW)
55	74.9	0.1	**95.8**	**0.9**	32.2	-0.1
60	21.6	0.1	75.8	0.9	59.2	0.3
65	74.2	-0.4	**99.9**	**1.4**	12.0	0.0
70	**97.9**	**-0.4**	43.2	0.2	43.5	-0.1
75	83.6	0.3	89.6	1.4	71.4	0.1

The results from Table 4-11 indicate that for most of the recovery performance comparisons, dry rod milled products performed better than wet milled products at however low statistical confidence levels. From Table 4-9 and Table 4-10, it can be generalised that while flotation recoveries were very high irrespective of comminution procedure employed, flotation after rod milling statistically resulted in superior recovery performance to flotation after milling using the VRM.

4.6. Sulfide mineralogical characterisation: a comparison

The percent liberation of a value mineral plays a role in determining the fate of the mineral during selective flotation separation. In this regard, liberation is defined as the area of the mineral exposed to the pulp and rising air bubbles. Using probability theory, the higher the liberation of the value sulfide minerals, the larger the surface area available for collector adsorption and bubble attachment, and consequently the higher the minerals chances of being recovered through true flotation (adsorption onto collector and recovered in the froth). Sulfide minerals with greater than 90 % of the total mineral area are termed liberated, ones with area between 60 % and 90 % defined as high grade middlings (HG Middlings), ones with area between 30 % and 60 % termed low grade middlings (MG Middlings) and sulfide minerals that occupy less than 30 % of the total particles area defined as locked.

Sulfide mineralogical characterisation was done using the QEMSCAN on the flotation feed and tailings of products from the VRM at a grinding roller pressure of 600 kN/m^2, wet rod milling (RW) and dry rod milling (RD). The products from comminuting using the three procedures had a product specification of 65% passing 75 μm. The sulfide count for the sulfide mineralogical characterisation is presented in 3.8 in Table 3-10. The sulfide particle counts were greater than 1000 to improve confidence in the data.

4.6.1. Feed liberation profiles and grain sizes

The flotation feed liberation profiles are presented in Figure 4-34. The grain size distribution for chalcopyrite, galena and sphalerite in the products of comminution using VRM, wet rod milling, and dry rod milling are presented in Figure 4-35, Figure 4-36 and Figure 4-37.

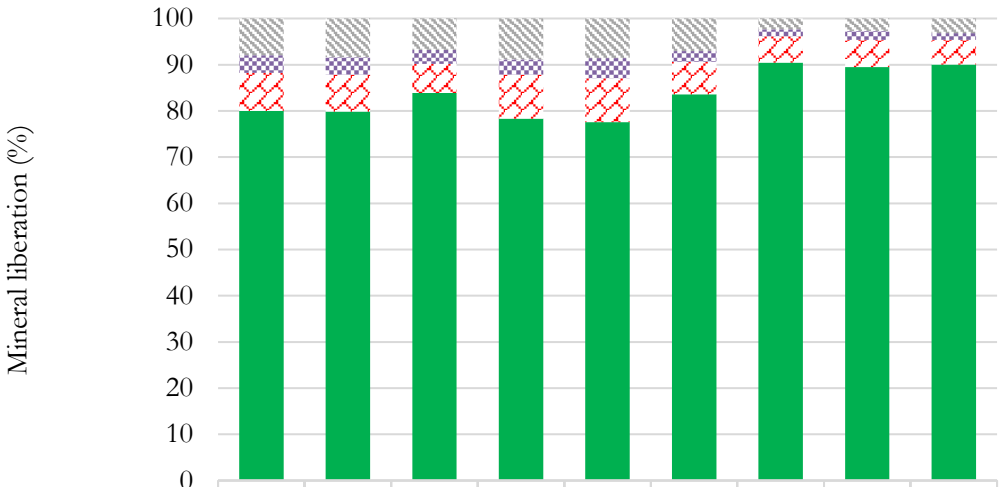

	RD	RW	VRM	RD	RW	VRM	RD	RW	VRM
	Chalcopyrite			Galena			Sphalerite		
Locked	8	8	7	9	9	7	2	3	3
MG Middlings	4	4	3	3	4	2	2	2	1
HG Middlings	8	8	6	9	9	7	6	6	5
Liberated	80	80	84	78	78	84	90	90	90

Figure 4-34: Liberation profiles of chalcopyrite, galena and sphalerite after comminution to the benchmarking grind of 65 % passing 75 µm using the VRM, wet rod mill and dry rod mill

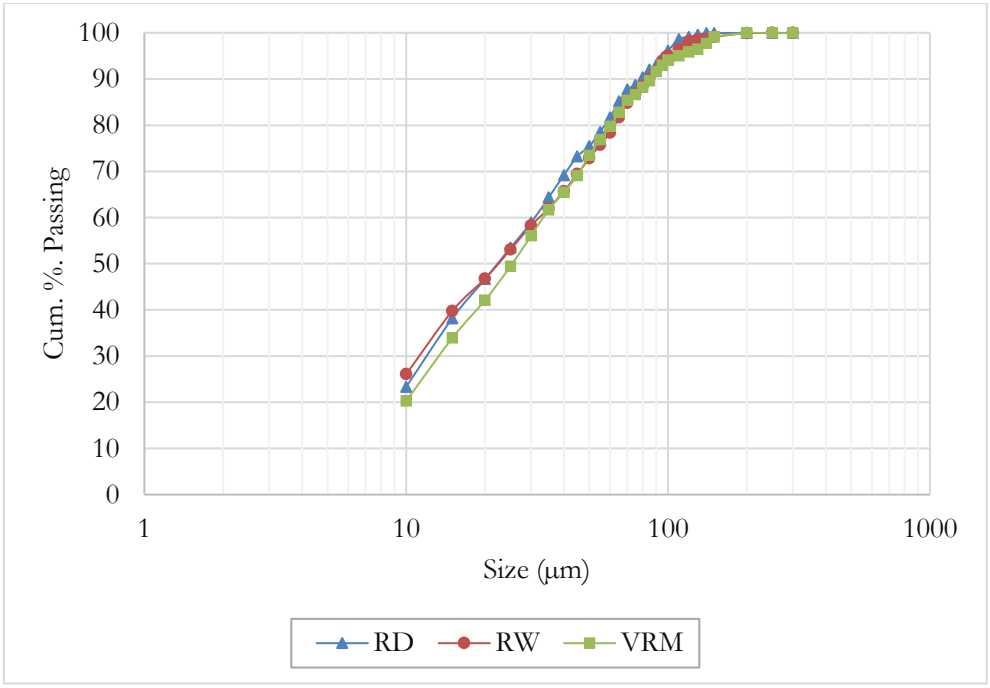

Figure 4-35: Chalcopyrite grain size distribution

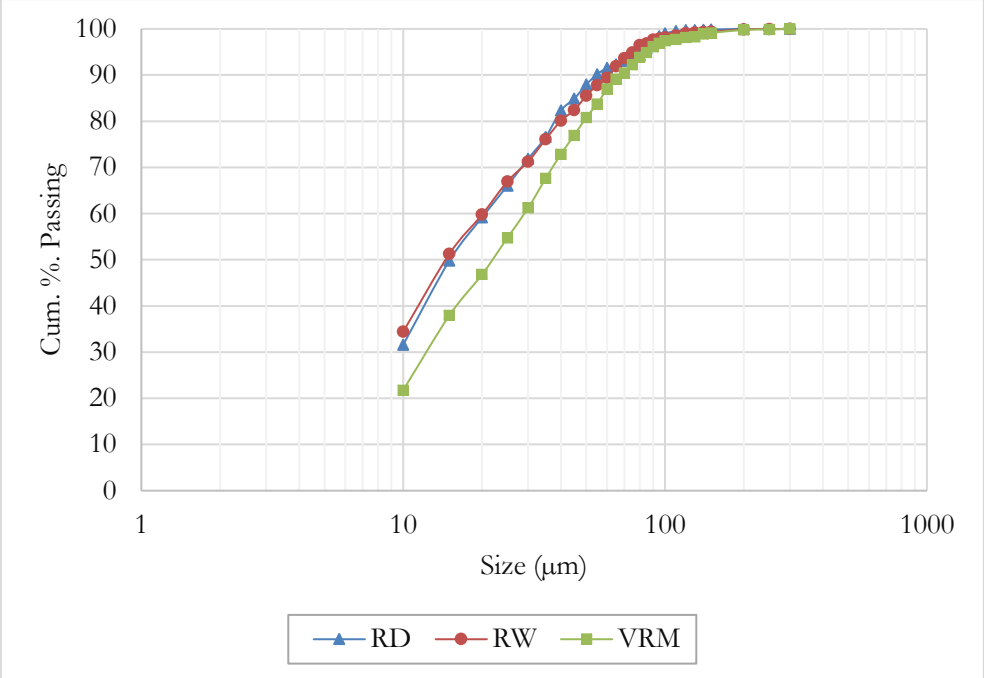

Figure 4-36: Galena grain size distribution

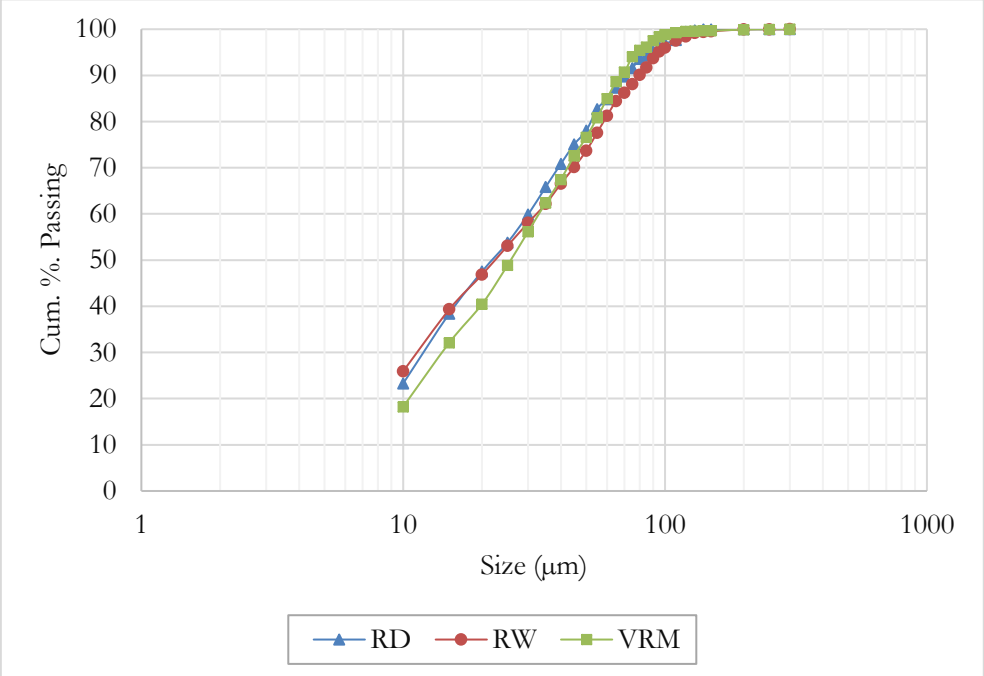

Figure 4-37: Sphalerite grain size distribution

Of the three comminution procedures under study, liberated chalcopyrite was highest with the VRM (84 %) and the same for dry rod milling and wet rod milling (80 %). Liberated galena was highest with the VRM (84 %) and the same for RD and RW (80 %). Liberated sphalerite was the same for all comminution procedures under study.

The d50 grain sizes of the minerals from the three comminution procedures are presented in Table 4-12.

Table 4-12: d50 grain size for chalcopyrite, galena and sphalerite

	Chalcopyrite d50 (µm)	Galena d50 (µm)	Sphalerite d50 (µm)
RD	24	14	23
RW	24	14	23
VRM	26	21	25

Figure 4-35 and Figure 4-37 show that the grain size distribution profiles are identical and almost overlay over each. Figure 4-36 shows that the galena grains are coarser for the VRM product as compared to wet and dry rod milling. This is evident from the d50 data presented in Table 4-12, showing that the d50 for galena from the VRM is 21 µm while it is 14 µm for the wet and dry milling product.

4.6.2. Tailings liberation profiles

Flotation tailings mineralogical characterisation was done to characterise the losses from the flotation process. The flotation tailings liberation profiles are presented in Figure 4-38 and the flotation tailings per size class are presented in Table 4-13.

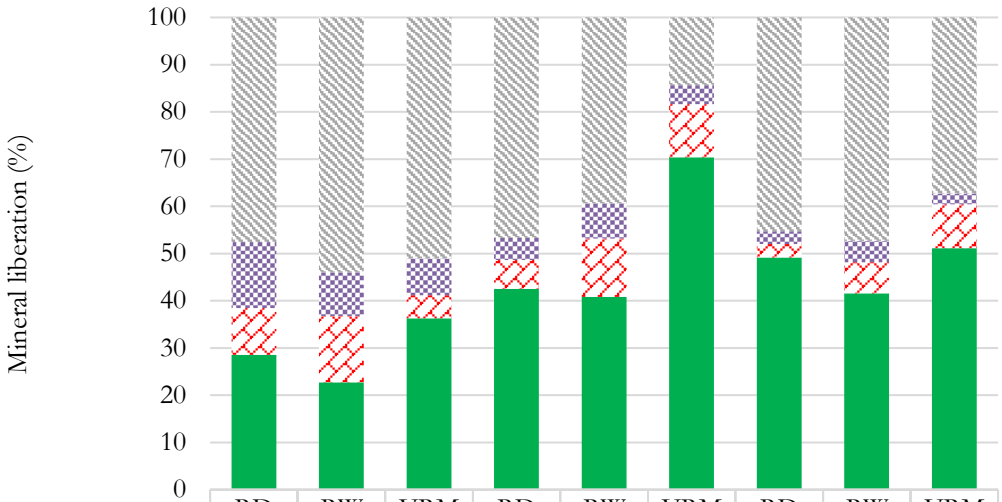

	RD	RW	VRM	RD	RW	VRM	RD	RW	VRM
	Chalcopyrite			Galena			Sphalerite		
Locked	48	54	51	47	39	14	45	47	37
MG Middlings	14	9	8	5	7	4	3	5	2
HG Middlings	10	14	5	6	12	11	3	7	9
Liberated	29	23	36	43	41	70	49	42	51

Figure 4-38: Flotation tailings liberation profiles of chalcopyrite, galena and sphalerite

Table 4-13: Flotation losses in tailings per size class.

		-300/+75 (%)	-75/+38 (%)	-38/+10 (%)	-10 (%)
Chalcopyrite	RD	42	23	11	25
	RW	51	19	14	15
	VRM	49	21	12	18
Galena	RD	28	29	22	21
	RW	28	21	25	26
	VRM	25	25	30	20
Sphalerite	RD	36	25	19	19
	RW	38	21	21	20
	VRM	39	26	19	16

The losses from flotation in relation to grinding equipment used during comminution were predominantly either locked or liberated. Reference to Table 4-13, 42 % of the copper lost in the tailings stream after the flotation of dry rod mill product was in the -300/+75 μm size class. For chalcopyrite and sphalerite, most losses were in the coarser fractions while losses from galena were evenly distributed across the size classes. From the information, it can be postulated that there is potential to recover liberated minerals falling in floatable size classes.

4.7. Specialised flotation characterisation tests of the ore

4.7.1. Aging tests

After ore is mined, it typically undergoes various crushing stages and is stored in silos before being introduced to the mineral processing circuit. In the mineral processing circuit under study, wet comminution using the rod and ball mill creates new surfaces while liberating the sulfide value minerals. The liberated sulfides are then floated. With the dry VRM operations, this set up will change as the comminuted products can be stored before water addition, density correction and flotation. It is important to therefore understand the characteristics of the comminuted products and know whether the flotation response will be negatively affected by storage time before flotation, a consequence known as "aging". Aging is described as the surface oxidation of sulfide minerals to form hydroxide and sulphur-oxy compounds, which reduces the collection efficiencies of the sulfide collectors leading to poor recoveries.

The aging tests were conducted to determine whether the recovery profile of copper, lead and zinc contained in the polymetallic sulfide ore would be affected if the newly created surfaces from comminution were exposed to surface oxidation. Dry rod milling was used. The first test, conducted in duplicate for reproducibility, comprised milling to a grind of 65 % passing 75 µm and floating the fresh sample immediately after milling. The aging test, also done in duplicates, was milling to a grind of 65 % passing 75 µm, storage of milled sample for 25 days and then flotation. The flotation procedure used was a modification of the standard procedure outlined in Chapter 3, where copper sulphate activator was not added.

The results from the aging tests are presented in Figure 4-39, Figure 4-40, Figure 4-41 and Figure 4-42. RD_NoA is flotation of a dry milled sample with no activator added during flotation, while RD_NoA_Aged is flotation of a dry milled sample with no activator added during flotation 25 days after milling was done. The final elemental recoveries and grades are presented in Table 4-14.

Table 4-14: Summary of elemental recovery and grades for the aging tests

	Cu Rec (%)	Cu Grade (%)	Pb Rec (%)	Pb Grade (%)	Zn Rec (%)	Zn Grade (%)
RD_NoA	97.0	3.0	95.2	12.2	96.0	7.2
RD_NoA_Aged	34.7	2.6	56.6	17.6	29.4	5.4

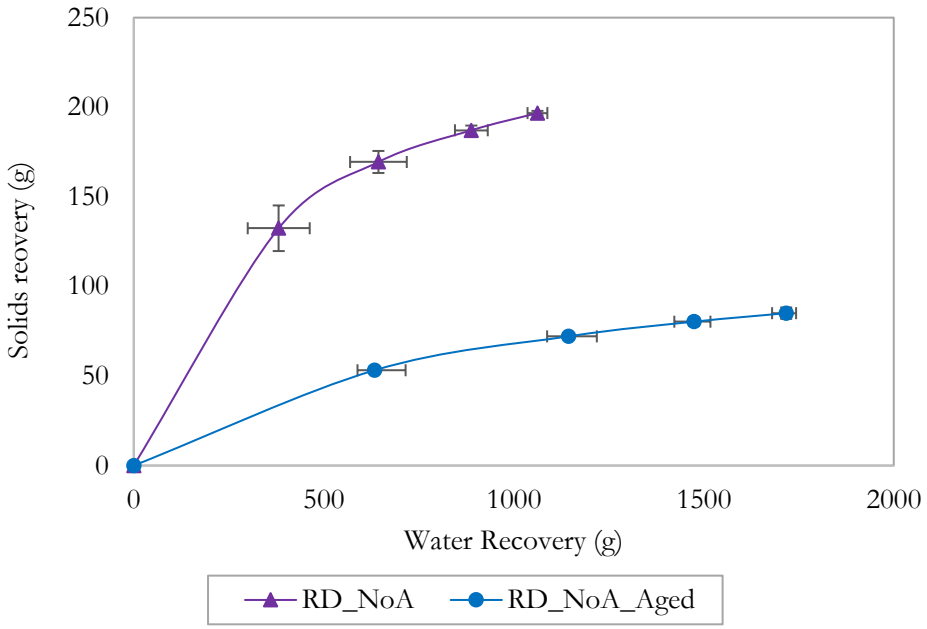

Figure 4-39: Solids vs. water recovery for aging tests

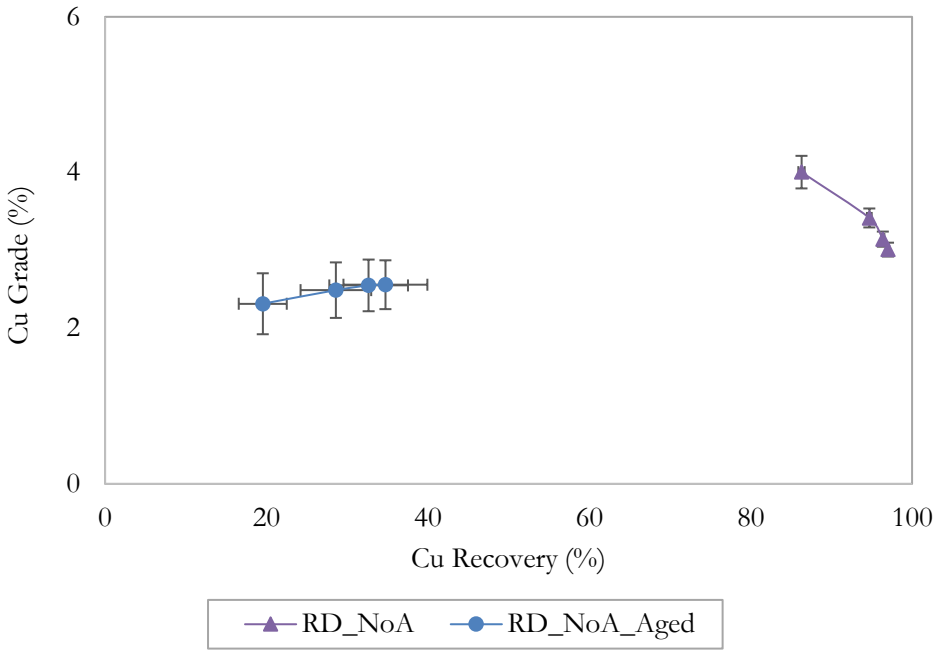

Figure 4-40: Copper concentrate grade vs. recovery relationship for aging tests

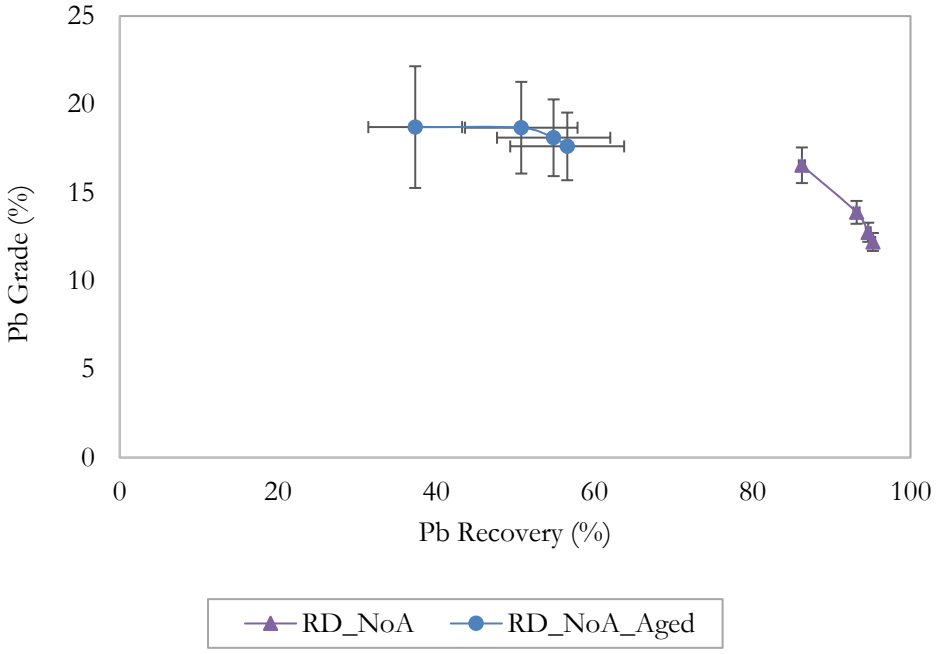

Figure 4-41: Lead concentrate grade vs. recovery relationship for aging tests

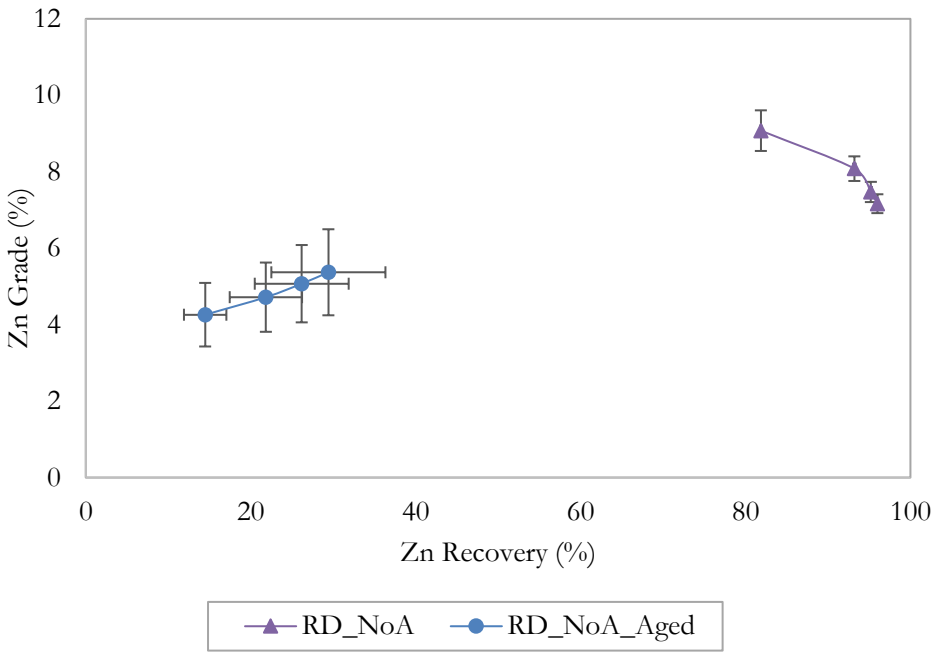

Figure 4-42: Zinc concentrate grade vs. recovery relationship for aging tests

The results indicate that the recovery of copper, lead and zinc is negatively affected by aging. Table 4-14 summarises the performance, with recovery of copper dropping to less than 35% and that of zinc to less than 30%. Water recovery of the aged sample was higher than the fresh sample, as shown in Figure 4-39, meaning that the recovery of the minerals was driven mostly by entrainment.

These observations confirm that the sulfide ore surfaces oxidise if the newly ground surfaces are exposed to air, which compromises their flotation performance. Surface oxidation results in the formation of metal hydroxides and sulphur-oxy compounds. Surface oxidation will thus reduce value mineral hydrophobicity and render sulfide collector adsorption less selective (Guy and Trahar, 1985; Shannon and Trahar, 1986; Clarke et al., 1995). The lower collector selectivity, coupled with high water recoveries results in lower sulfide mineral flotation efficiencies hence the lower elemental recoveries of copper, lead and zinc for the aged sample.

4.7.2. Recovery by size tests

The recovery by size tests were done to understand the flotation response of each size class. For the tests, dry rod milling was used to achieve 65% passing 75 µm. The concentrates were collected for 6 minutes. The decision to collect for 6 minutes was based on the preliminary tests, were flotation recoveries greater than 90% for all the elements (Cu, Pb, Zn) were reached within 6 minutes of concentrate collection.

The recovery by size profiles for copper (Cu), lead (Pb) and zinc (Zn) is presented in Figure 4-43. The screen sizes used, the percent retained on each size class for the flotation feed and the elemental recoveries are also presented in Table 4-15.

Table 4-15: Recovery by size for copper, lead and zinc. The screen sizes have the corresponding percentage retained on the sieve.

Screen size (µm)	% retained on sieve (feed)	Cu Rec (%)	Pb Rec (%)	Zn Rec (%)
106	10.1	39.2	41.7	69.2
75	21.6	77.7	83.3	93.1
53	18.4	87.7	85.8	93.8
38	10.9	96.5	92.8	97.2
25	8.4	95.6	90.4	95.7
10	15.2	97.2	93.3	96.9
0	12.8	89.6	93.4	96.0

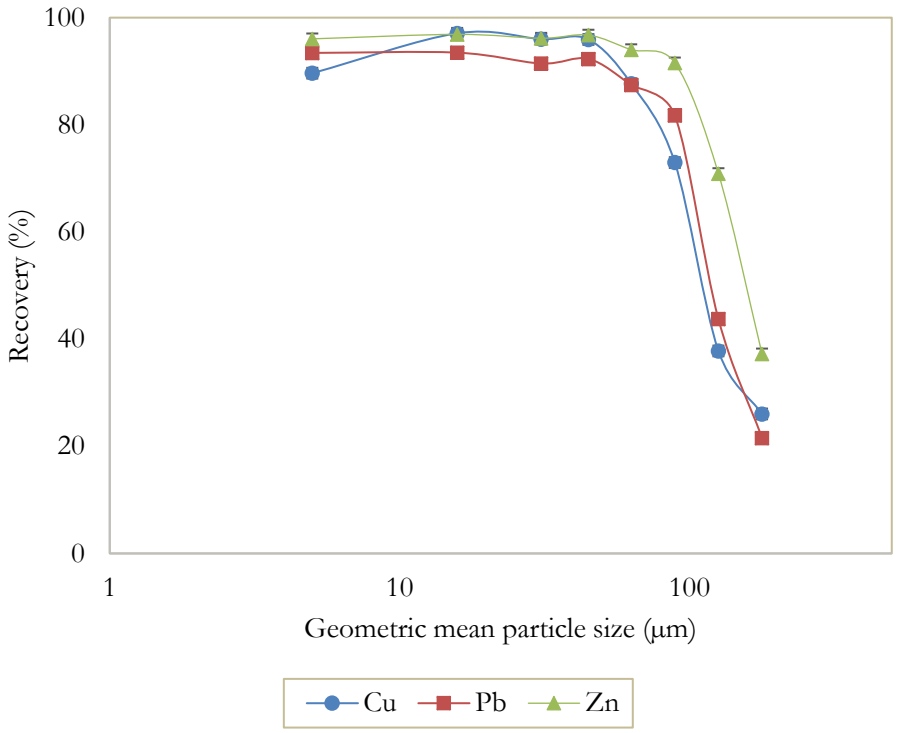

Figure 4-43: Recovery by size profile for copper, lead and zinc after batch floating the sulfide ore comminuted to 65 % passing 75 µm

The results indicate that the recovery of each of the elements is above 90 % for particle sizes less than 53 μm. The recoveries start decreasing significantly as the particles became coarser than 106 μm. This observation is in line with expected behaviours reported in literature (Gaudin et al., 1931), where the recoveries dropped significantly for particle size greater than 100 μm. As particles sizes increase beyond the optimum flotation range, the particles become too heavy, fail to attach to rising air bubbles and fall back into the pulp and are recovered as tailings. As well, large particles are poorly liberated resulting in reduced probability of recovery through true flotation. In the study of concentrator performance of the polymetallic sulfide ores at Broken Hill South Limited, Cameron et al (1970) observed the recovery maximising flotation size range for galena as 7-70 μm and that for sphalerite as 15-100 μm. This complements the observations from the recovery by size tests conducted.

5. DISCUSSION

The effect of using the VRM to comminute the polymetallic Swartberg ore on throughput, particle size distributions, energy consumption, flotation performance, grain size distribution and liberation have been discussed in this chapter.

5.1. Throughput

One focus of the work done in this project was to determine the effect of changing target grind and grinding pressure on throughput. The effect of changing target grind is shown in Figure 4-2 and Figure 5-1. Figure 5-1 shows the actual throughput in kg/hr while Figure 4-2 shows the load factor, which is a quotient of actual throughput to nominal throughput. To be able to explain the cause for the observed trend, the relationship between classifier rotor speed and target grind is also presented in Figure 5-2.

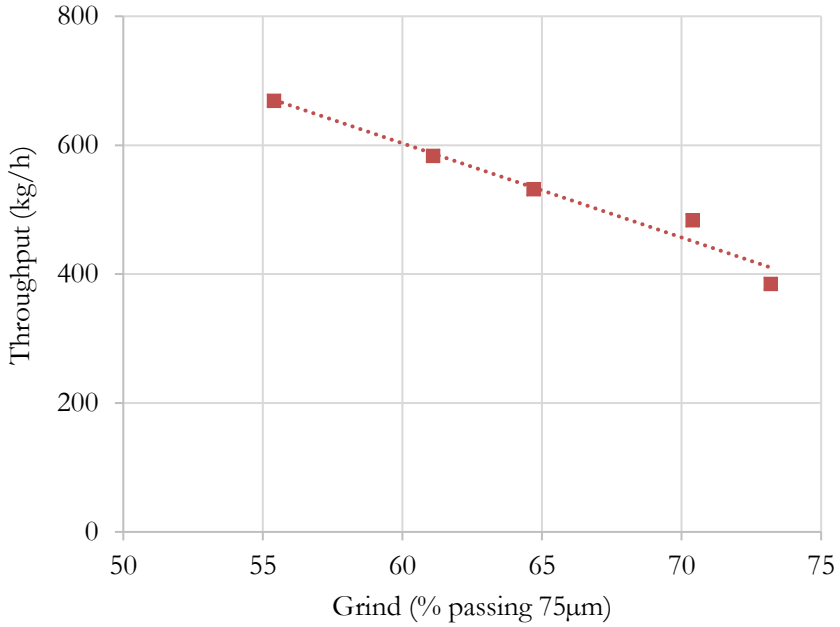

Figure 5-1: The effect of changing target grind on throughput

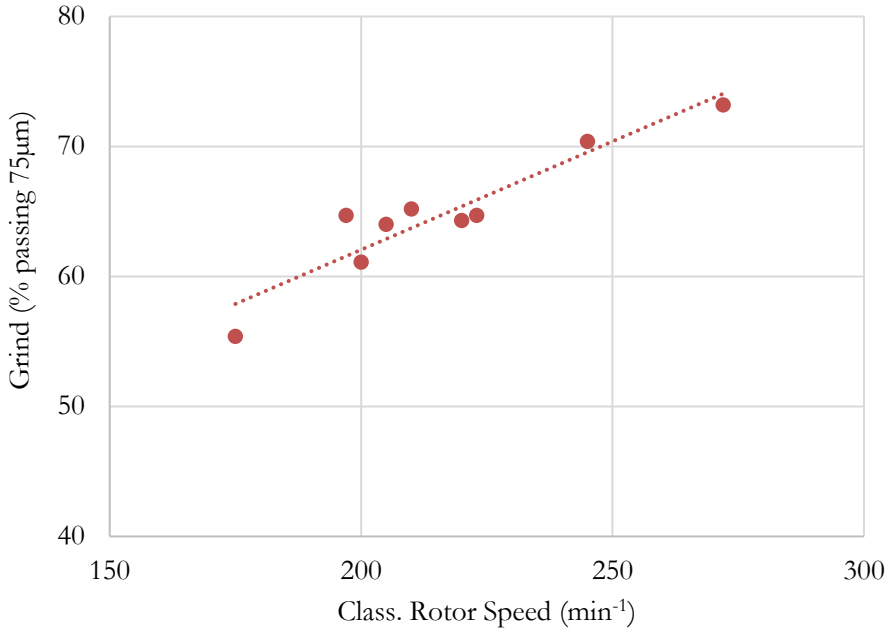

Figure 5-2: The relationship between classifier rotor speed and product grind

Throughput was seen to decrease as the product became finer. To be able to cut finer, the classifier rotor speed increases. As the classifier rotor speed increases, it rejects more particles and are returned to the grinding table for further grinding which increases the circulating load. The increase in circulating load limits the fresh feed to the VRM, and hence the fresh feed capacity is reduced. These results are in agreement with Altun et al. (2015, 2017) who also observed that for the same grinding pressure, throughput decreases with increasing fineness of product.

The increase in grinding pressure was seen to result in an increase in throughput while maintaining the same product grind (Figure 5-3).

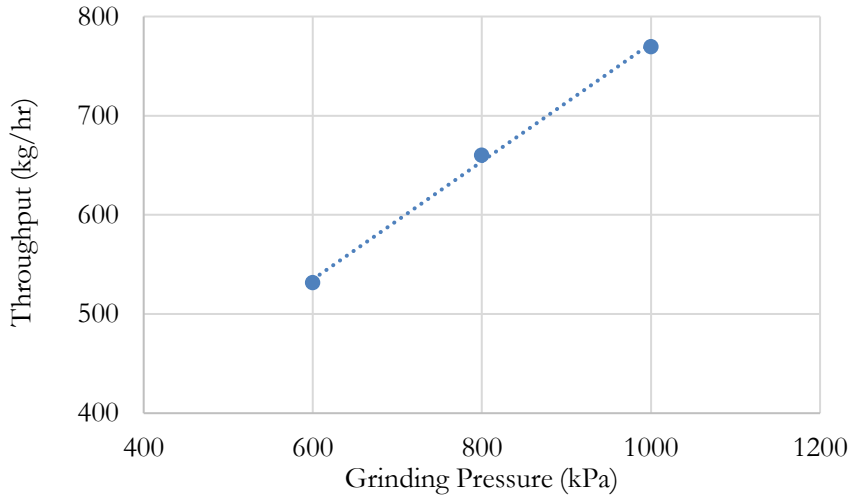

Figure 5-3: The relationship between grinding pressure and throughput

The increase in grinding pressure resulted in an increased supply of grinding energy to material on the grinding table per unit time (Tamashige et al, 1991). The increase in grinding pressure also means more energy is applied for compression and in-bed breakage per unit area, resulting in faster breakage kinetics. Due to the increased supply of energy, more particles reach the target size for classification.

The classifier rotor speed is reduced to maintain the required cut point as more particles would have reached the required grind in a reduced number of passes. As a result, more particles report as overflow during classification and circulating load drops. Because of the reduced residence time of particles in the VRM and the reduced circulating load, the VRM can process more feed hence the observed results that the increase in grinding pressure resulted in an increase in throughput. These findings are congruent to the findings of Reichert et al. (2015) for work done on iron ore and Altun et al. (2017) for work done on a fold ore, where the increase in grinding pressure resulted in an increase in production rate.

5.2. Particle size distributions

Using atmospheric or heated air to drive particle transport to the classifier, the results presented in Figure 4-5 indicated that the progeny particle size distributions have very minor differences in the percentage of fines generated for the same target grind and keeping constant all the other operating variables. When heated air was used (65-600-363 K), the product had slightly less fines than when atmospheric air (65-600-300 K) was used. The heated air may have assisted in removing moisture from the ore, thereby reducing agglomeration of particles after comminution and facilitating representative separation in the classifier.

Without the aid of heating, two or more particles may agglomerate and present themselves to the classifier as one 'bigger than cut size' particle and be rejected back to the grinding table for further grinding. The reduced agglomeration and classification based on individual particles (not agglomerated particles) will therefore reduce the rate of fines generation as each particle will be separated based on its own characteristics, hence the observed difference in particle size distribution between using heated air and atmospheric air.

While the increase in grinding pressure resulted in an increase in throughput, it was observed that the resultant particle size distributions varied minimally with the increase in grinding pressure. The percent passing the 25 μm sieve was 24.8 %, 24.4 % and 26.7 % for grinding pressures of 600, 800 and 1000 kPa respectively.

The marginal increase in the sub-25 μm when grinding pressure was increased to 1000 kPa could have been an indication of an increase rate of fines generation, a phenomena which has been reported to be closely correlated to an increase in grinding pressure (Tamashige et al., 1991; Altun et al., 2017). The marginal change in particle size distribution may also be attributed to the fact that the VRM is a closed-circuit comminution and classification system. The increase in grinding pressure reduces residence time of particles in the comminution section, and the classifier rotor speed reduces to handle the change in product output. If optimised and based on the outputs of this study, it would mean the increase in grinding pressure would result in an increase in throughput while product particle distribution remains almost unchanged.

5.2.1. Comparison to rod milling

A comparison of the product particle size distribution after wet rod milling, dry rod milling and VRM milling is presented in Figure 4-6, Figure 4-7, Figure 4-8, Figure 4-9 and Figure 4-10. It is evident from the graphs that the particle size distribution curves have a similar shape and can be classified as similar. The possible shapes of the PSDs that can be produced from grinding roller mills in comparison to the ball mill product from the work on cement are presented in Figure 5-4.

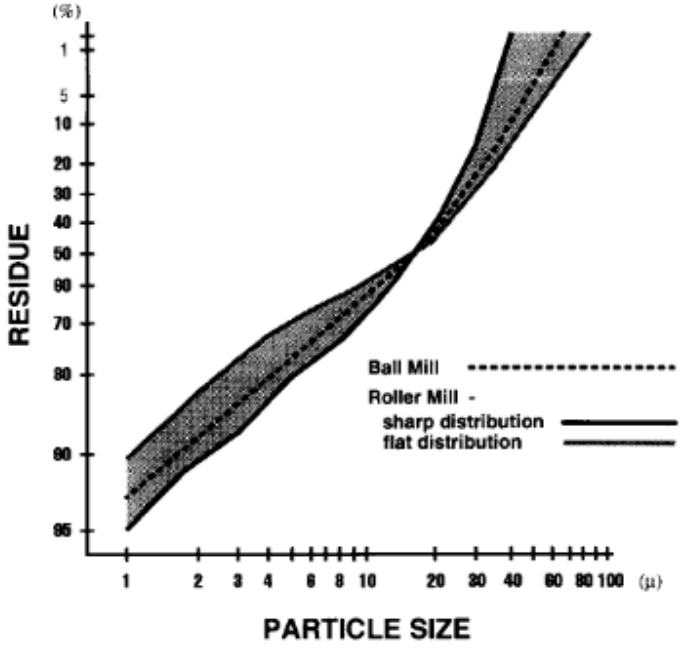

Figure 5-4: Particle size distributions of cement (Knoflicek and Wentzel, 1995)

Figure 5-4 indicates that there are many possibilities with regards to the shape of the particle size distribution from compression grinding using the VRM in comparison to the particle size distribution from impact/shear breakage, one of which is that the particle size distributions can be identical. The shape of particle size distribution of the VRM product has also been reported to be

manipulated using grinding pressure, mill air flow, dam ring height and classifier rotor speed (Reichert et al., 2015). This means that the manipulated variable control the shape of the particle size distribution. Knoflicek and Wentzel (1995) reported that flatter size distributions are produced from reducing mill air flow, reducing classifier rotor speed and increasing dam ring height. From this knowledge of the ability to influence the product particle size distribution from a VRM, the similarity of the PSDs could be because of the operating conditions (mill air flow and dam ring height – 7 mm and grinding pressure – 600 kN/m^2) that matched the requirements of the VRM to produce products with the same PSDs as rod milling products.

Solomon et al (2011) observed differences in PSD curves and postulated that the differences for similar feed (6 mm feed) comminuted using the ball mill and the HPGR (a compression grinding mill) were due to the differences in breakage mechanisms (Figure 5-5).

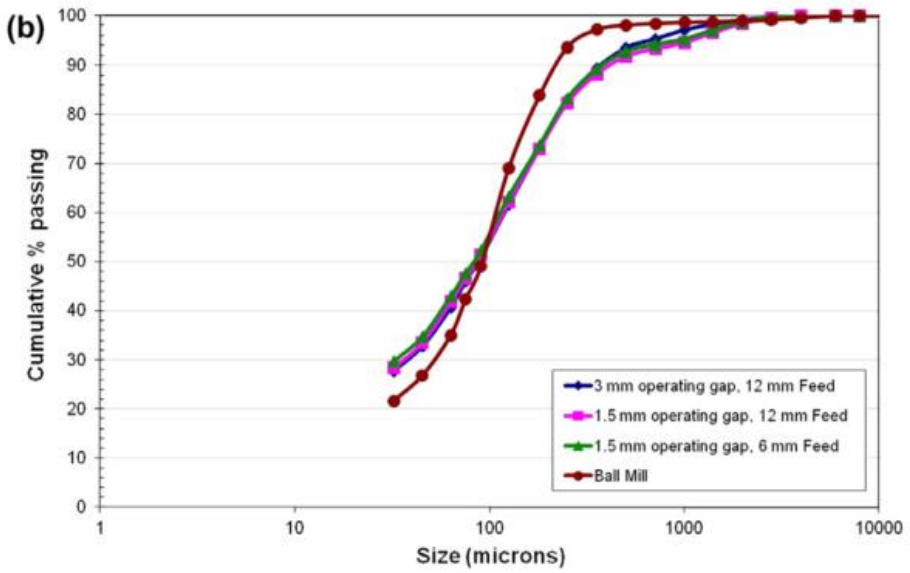

Figure 5-5: Particle size distribution of the flotation feed for the UG2 platinum ore (Solomon et al., 2011)

They argued that interparticle breakage caused by compression breakage from the HPGR resulted in higher fines generation and hence a flatter PSD curve for the same target grind required, while impact and abrasion grinding resulted in lower fines generation hence the steeper PSD curve as shown in Figure 5-5. However, based on the findings of Knoflicek and Wentzel (1995), the difference may have been rather due to the interaction of the manipulating variables used in the operation of the HPGR.

5.3. Specific energy consumption (Ecs)

The effect of change in grind on the specific comminution energy consumption was carried out as part of the study. The relationship between specific grinding energy and target grind is presented in Figure 5-6.

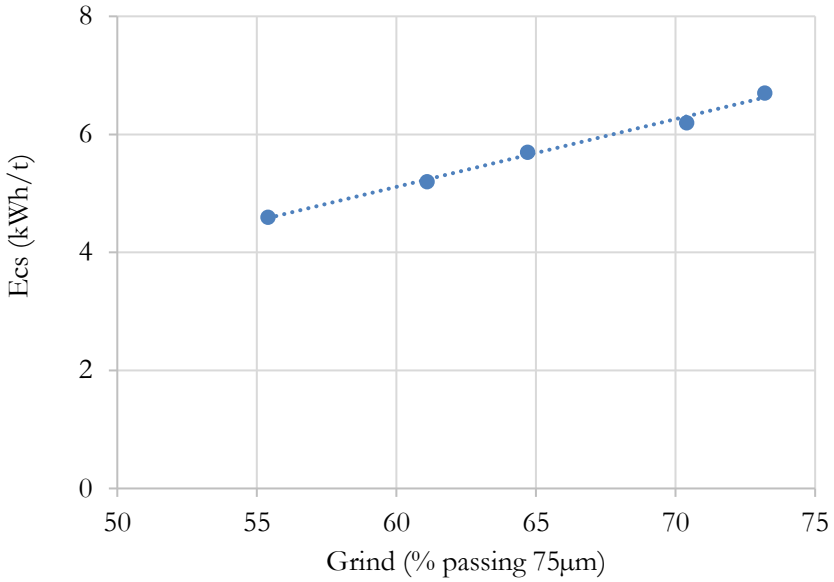

Figure 5-6: The effect of changing target grind on specific grinding energy consumption (Ecs)

The observation that the increase in product fineness results in an increase in the energy requirement is as expected. To grind finer, more energy must be applied for particle breakage to achieve the required grind. The effect of grinding pressure on energy consumption is also presented (Figure 5-7).

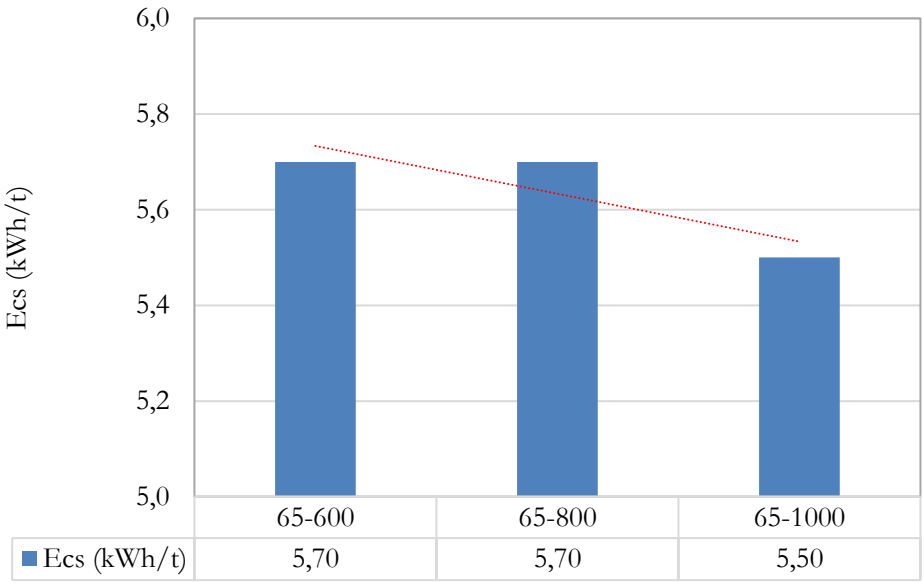

Figure 5-7: The effect of changing grinding pressure on specific grinding energy

There was a general decrease in specific energy consumption observed with the increase in grinding pressure. As the grinding pressure increases, there is increased confinement of particles and more energy is applied for particle breakage. This results in increased breakage rates. Depending also on response of the particles being broken to the increase energy input, the resultant relationship between energy input and the change in throughput determines whether the specific energy consumption increases or decreases with the increase in grinding pressure.

On the work done on iron ore (Reichert et al., 2015), specific energy consumption increased with energy consumption. Studies conducted on cement (Knoflicek and Wentzel, 1995) observed that the relationship between specific energy consumption and grinding pressure was dependent on dam ring height as dam ring height had a dominant effect throughput. Increasing grinding pressure at low and medium dam ring height resulted in an increase in throughput and an increase in specific energy consumption. Conversely, increasing grinding pressure at high dam ring height resulted in a decrease in production rate and a decrease in specific energy consumption.

The specific grinding energies of the two comminution systems are compared. The dry and wet impact/shear grinding are considered as one comminution system due to the similarity in grinding time required to achieve the required grind. The average specific grinding energy of the traditional comminution circuit study was calculated from comminution data from the plant where the ore was sourced. The comminution circuit where ore was sourced comprises a rod mill (RM) followed by a ball mill (BM). The specific grinding energy from the standard VRM (grinding pressure of 600 kN/m^2, dam ring height of 7 mm) was obtained online from the pilot plant at the test centre in Germany. The specific grinding energies are presented in Figure 5-8.

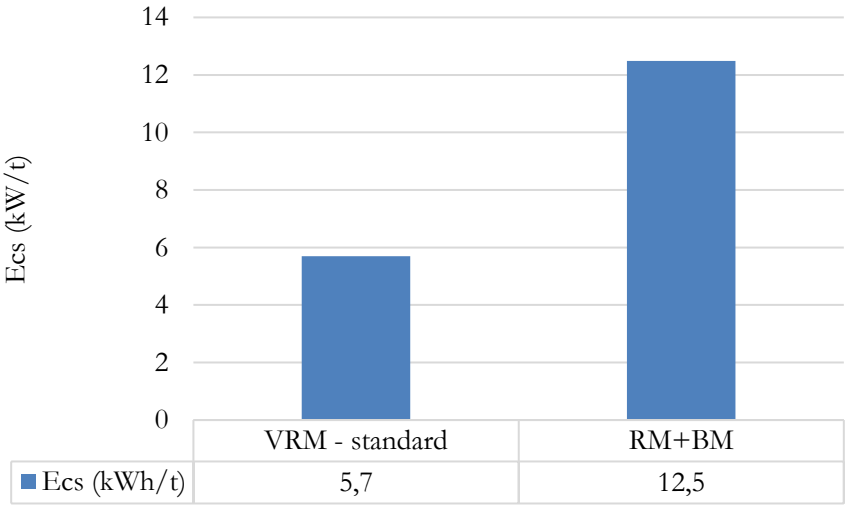

Figure 5-8: Specific grinding energy from VRM milling and conventional tumbling mill comminution circuit

Figure 5-8 shows that the VRM specific grinding energy is 54.3% lower than that from using the typical processing route of rod milling followed by ball milling. It is important to note that as the VRM is in closed circuit with classification, the quoted energy saving can considerably decrease depending on the classification mode used. This comparison shows that the VRM is more energy efficient compared to conventional impact/shear grinding. Compression/shear grinding is therefore a potential replacement of impact/shear should the downstream process efficiencies of the two systems be comparable. It would be expected that compression grinding, which utilises in-bed particle breakage, would be more energy efficient as the applied energy is distributed across the bed (Viljoen et al., 2001). The observations of better energy efficiencies in comparison to impact/shear grinding is in agreement with literature findings and previous studies done (Drunick et al, 2010; Erkan et al., 2012; Loesche GmbH, 2016).

Grinding is coupled with classification in the VRM. In the air-swept mode, the fan has been reported to use a considerable amount of energy (Drunick et al., 2010). This increases the total comminution energy and would need to be considered during design of industrial mills. Even with the additional fan and dynamic classifier considerations, the VRM use is reported to have total comminution energy compared to the traditional impact/shear processing routes (Drunick et al., 2010; Erkan et al., 2012). Erkan et al (2012) reported total comminution circuit specific energy savings of between 8.34 % and 15.67 % by using the VRM instead of SABC (semi-autogenous ball mill-crusher circuit), HPGR-Ball Mill circuit or conventional crushing-ball mill circuit.

5.4. Grain size distribution and feed liberation

The grain size distribution of the ore (as obtained from the drill cores) and the grain size distribution of comminution products at the benchmarking grind of 65 % passing 75 μm are presented in Table 2-5 (for copper, lead and zinc minerals in the ore), Figure 4-35, Figure 4-36 and Figure 4-37 for copper, lead and zinc minerals in the comminution products respectively.

Copper, lead and zinc mineral grains in the ore are quite coarse considering the flotation particle size requirements. According to conducted on a Cu-Pb-Zn ore by Gaudin et al. (1931), the maximum particle size for optimum recovery of copper, lead and zinc minerals was 100 μm. Above this size, flotation efficiencies were observed to drop. On the very fine end, the study also showed that the recovery for particles less than 10 μm was compromised. As such, comminution is expected to reduce the grain size to within the optimum flotation size ranges. The recovery by size tests conducted as part of this study also agreed to the findings of Gaudin et al. (1931) and Pease et al (2006). The results (Figure 4-43) indicated that the recovery of each of the elements is above

90 % for particle sizes less than 53 μm and they start decreasing significantly as the particles became coarser than 106 μm.

The grain size distribution of the three minerals (copper, lead, and zinc) in the comminution products (Figure 4-35, Figure 4-36 and Figure 4-37) show that at least 94 % of all copper mineral grains are less than 100 μm, at least 97 % of lead mineral grains are less than 100 μm and at least 96 % of all zinc mineral grains are less than 100 μm. The d50 grain sizes are shown in Table 4-12. The d50 from the wet and dry rod milling are the same, and generally slightly finer than the grains from the VRM product. Knowing that the maximum particle size for highest achievable recoveries is 100 μm based on Gaudin et al (1931) and 106 μm based on the recovery by size tests from this project, and that almost all grains for the valuable minerals under study are less than the maximum particle size, highest achievable recoveries of the minerals are expected.

The mineral liberation profiles in Figure 4-34 show that slightly better liberation was obtained with the VRM compared to wet and dry rod milling. Liberated chalcopyrite was highest with the VRM (84 %) and the same for dry rod milling and wet rod milling (80 %). Liberated galena was highest with the VRM (84 %) and the same for RD and RW (80 %). Liberated sphalerite was the same for all comminution procedures under study. These findings agree with some of the previous studies done that associated compression breakage to higher percent liberation compared to impact/shear breakage (Apling and Bwalya, 1997; Hoşten and Özbay, 1998; Celik and Oner, 2006; Loesche GmbH, 2016). In other studies however, impact/shear breakage resulted in marginally higher percent liberation of value minerals (Solomon et al., 2011).

The effect of the differences in downstream process performance have also been variable. Using a copper ore, the VRM product had more liberated copper and nickel containing minerals as compared to the ball mill product and they associated the resulting difference in recovery with the difference in percent liberation (Viljoen et al., 2001). In a comparative study between a ball mill and an HPGR, Solomon et al. (2011) attributed the higher PGM recovery achieved after ball milling to the higher percent liberation of the PGMs and also the larger amount of grains in the optimum size range for flotation. However, Chapman et al. (2011) found that the comminution using the HPGR resulted in higher percent liberation of PGMs but this did not translate into better flotation performance.

Chapman et al (2011) concluded that liberation needed to be analysed paying close attention to grain size distribution to quantify its effect on the downstream process performance. From the results outlined, it can be concluded that comminuting the Cu-Pb-Zn ore to 65 % passing 75 μm

using the VRM resulted in slightly better liberation of chalcopyrite and galena. The grain size distributions are relatively similar, though the VRM had a slightly coarser grain size distribution.

5.5. Flotation performance

The effect of varying target grind on flotation response was studied and the results presented in Table 4-3. The achieved recoveries of copper, lead and zinc minerals were lowest for a 55 % passing 75 µm feed, reached a maximum between 60 % and 70 % passing 75 µm, and dropped at 75 % passing 75 µm. The recovery by size studies done by Gaudin et al (1931) as well as the relationship between mass/water recovery and achieved mineral recoveries (Wiese et al, 2006) presented in Figure 5-9 can be used to explain the results. It can be interpreted from Figure 5-9 that there is threshold water recovery (A) beyond which there will be marginal change in flotation recovery. Beyond point A as well, increase in water recovery increases non-selective solids recovery by entrainment, and concentrate grade will be compromised. The cumulative water and solids recovery after floating comminution products at the varying grinds are presented in Figure 5-10.

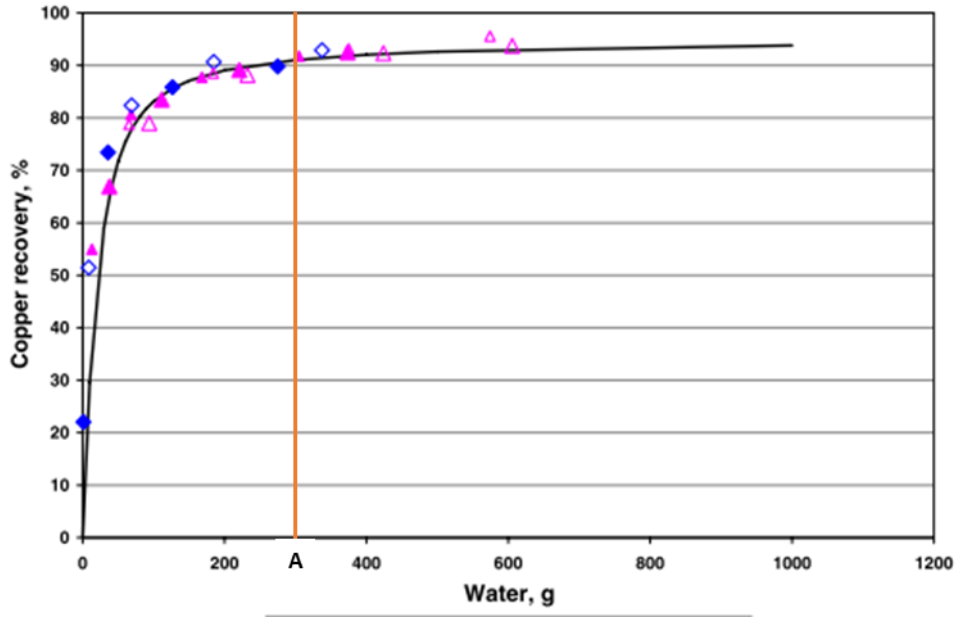

Figure 5-9: Comparison of copper recovery versus water recovered (Wiese et al., 2006)

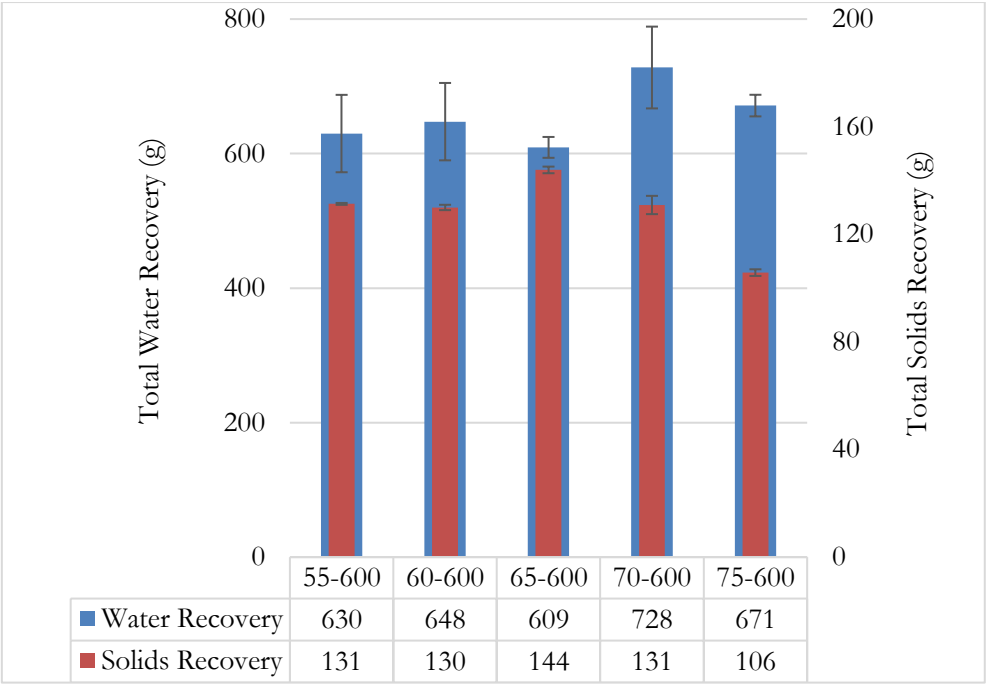

	55-600	60-600	65-600	70-600	75-600
Water Recovery	630	648	609	728	671
Solids Recovery	131	130	144	131	106

Figure 5-10: Cumulative water and solids recovery after floating VRM products of varying grinds

At 55 % passing 75 µm, the product from comminution may not have been liberated enough and will have minerals grains with particle sizes larger than the maximum of 100 µm required for optimum flotation performance (Gaudin et al., 1931). The water recovery was high and comparable to water recovery from the other grinds, and as such would have expected the recovery of the chalcopyrite, galena and sphalerite to be high according to the relationship between water and mineral recovery observed by Wiese et al (2006). However, as some the grain sizes may have been outside the expected size range for optimum flotation, the valuable mineral recoveries observed for that grind were low.

The mass and water recoveries from the flotation of comminution products with grinds 60 %, 65 % and 70 % were within error to each other. The observed recoveries of chalcopyrite, galena and sphalerite were also similar which agrees to the proposed relationship between water recovery and mineral recovery (Wiese et al, 2006). It also follows that for the three grinds, the minerals were liberated enough, and the grains were within the expected optimum size range to achieve maximum recoveries through flotation. For the flotation of the VRM product of grind 75 % passing 75 µm, the achieved recoveries dropped. As the comminution products became finer, it may have resulted in the production of fines and grains less than 10 µm. The high amount of fines may have been the reason for the drop in recovery as past studies also indicated that the minus 10 µm particles are poorly recovered through flotation (Gaudin et al., 1931; Chapman et al., 2011).

The variation in grinding pressure resulted in products of similar particle size distributions (Figure 4-3). The water and solids recovery from flotation was similar, as summarised in Figure 5-11.

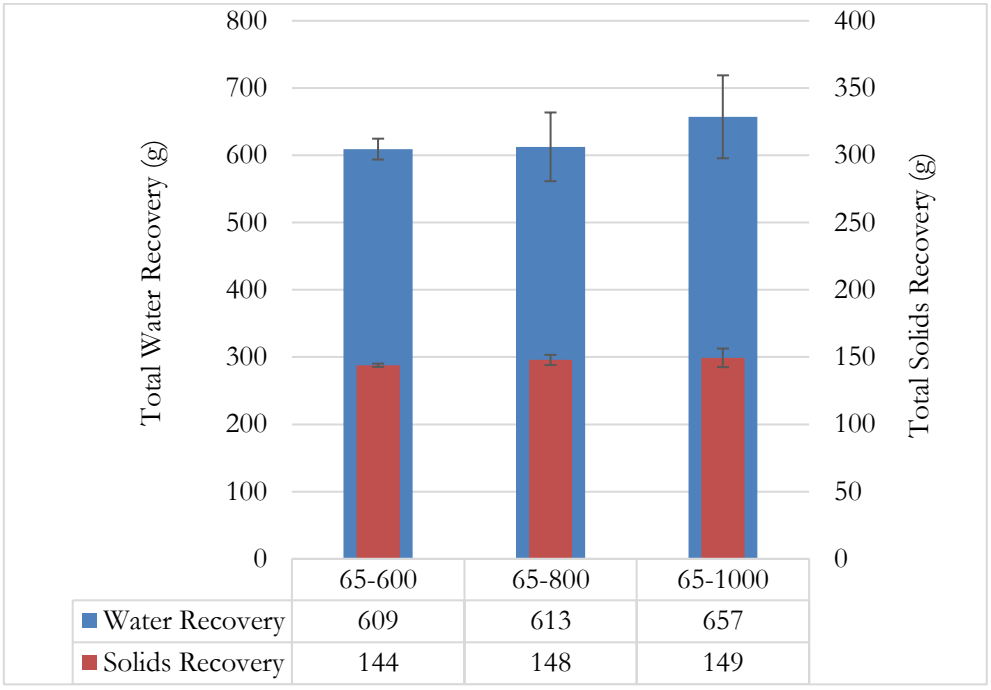

Figure 5-11: Cumulative water and solids recovery after floating VRM products produced from variation in grinding pressure

In a study of iron ore, Reichert et al. (2015) observed that the increase in grinding pressure resulted in marginal to no observable change in the ration of mineral liberation. Considering this observation, water and solids recovery data presented in Figure 5-11 and the similarity in PSDs (Figure 4-3), it was expected that the mineral recoveries be similar. This was the outcome from the flotation tests as shown in Table 4-4. The low confidence levels from ANOVA statistically proved that there was no difference in flotation performance with the variation of grinding pressure during comminution.

The results from the study of the effect of air temperature during comminution using the VRM on the flotation showed similarities in achieved recovery and differences in concentrate grade (Figure 4-21,Figure 4-22 and Figure 4-23). Mass and water recovery were higher for the flotation of VRM float feed of a grind of 65 % passing 75 µm produced using heated air (Figure 4-20). The heated air may have caused some surface activation of the sulfide surfaces. However, the copper sulfate used during flotation may have managed to reactivate the mineral surfaces thus recovery was not compromised. The more mass recovered in the concentrates resulted in the reduction in concentrate grade.

5.5.1. Comparison to rod milling

The recovery of copper minerals was similar and statistically independent of the comminution procedure used to produce the flotation feed of the benchmarking grind of 65 % passing 75 µm (Figure 4-28). The non-existence of a correlation between comminution procedure used and recovery was also observed for zinc minerals and lead minerals for the grind of 65 % passing 75 µm (Figure 4-29 and Figure 4-30). As there was no difference in particle distribution and the observed mineral recoveries, the total water and mass recovery can be used to interpret the differences in grade (Wiese et al., 2006).The total mass and water recovery are presented in Figure 5-12.

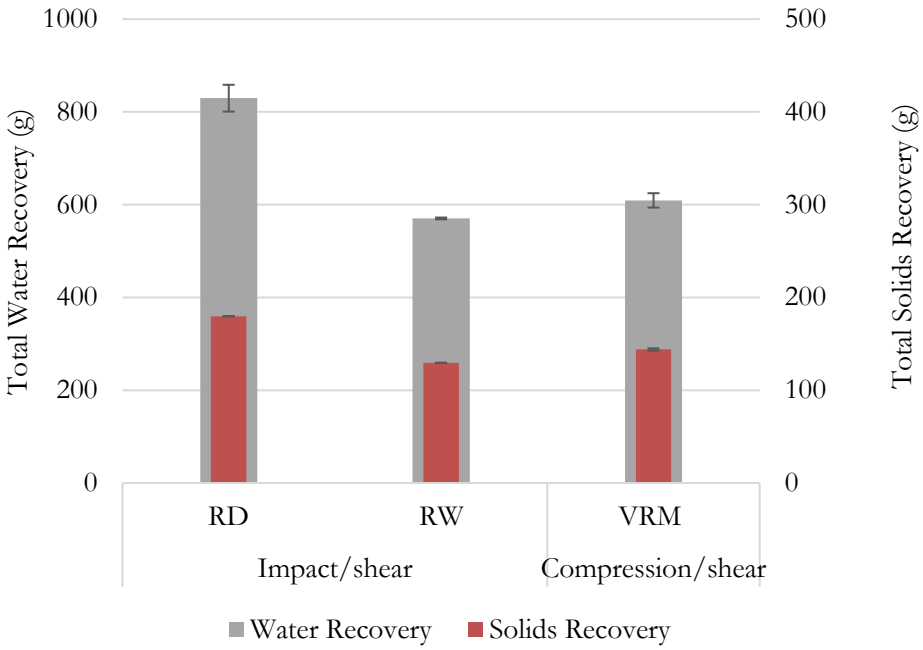

Figure 5-12: Total solids recovery and total water recovery for the flotation of products from wet rod milling (RW), dry rod milling (RD) and the VRM

As the recoveries achieved were similar, it can be hypothesised that the total water recovered from each flotation test exceeded the amount related to point A in Figure 5-9. The excess water collected therefore resulted in non-selective recovery of solids resulting in the variation in concentrate grade. This explains why the highest concentrate grade was achieved with wet rod milling. The water and mass recovery from floating the product from the VRM was slightly higher than that from wet rod milling, and this also explains why the concentrate grade was slightly lower than that from floating wet rod milled products. The copper concentrates grade as well as the lead concentrate grade and zinc concentrate grade after floating dry rod milling products were lowest because of the highest water and mass recovered.

The redox chemistry of the pulp prior to flotation showed that when standard plant water was added to make up to the 3-litre mark in the flotation cell, the dry rod milling product had the most positive pulp potential, followed by the VRM product and the wet rod milling product had the least positive pulp potential. These findings agreed with findings from Gonçalves et al (2003) who found that dry grinding resulted in more positive pulp potential. This, coupled with the findings of Feng and Aldrich (2000) that dry grinding results in rougher particles with microcracks (Feng and Aldrich, 2000), can be used to infer that collector adsorption rates may have be highest for RD, followed by VRM and then RW. The differences in collector adsorption rate did not however result in any differences in kinetics (Figure 4-31, Figure 4-32and Figure 4-33).The recovery-time or recovery kinetics were very similar and thus the differences in measured pulp potentials did not result in any observed differences in kinetics. As well, redox potential studies done in the past indicated that there is a range of potentials optimum for flotation. Chalcopyrite recoveries were observed to be high for pulp potentials between 137 mV and 476 mV (Long et al., 2012; Dzinza, 2018). The pulp potentials measured for each of the comminution procedures were within the redox potential range for optimum flotation performance.

These findings differed from literature studies, which reported that the more positive redox potential from dry grinding may result in a greater degree of oxidation of the mineral surface which in turn may be detrimental to flotation (Chapman et al., 2011; Palm et al., 2011; Solomon et al., 2011). In their argument, pulping the dry ground product prior to flotation was accompanied by a significant layer of passivating ions attaching to the surfaces with the microstructural defects thereby negatively affecting collector adsorption. This postulated phenomena was found to be true and detrimental for the flotation of a PGM ore after dry grinding (Chapman et al., 2011; Solomon et al., 2011). However, using the same procedures on a zinc ore, zinc recovery was highest for dry milling (Palm et al., 2011). This postulation does not hold for the current study as the differences in pulp potential did not affect the flotation response. This may then mean that the postulated phenomena of passivating ions attachment of high energy sites and the effect on flotation performance may be ore-dependent.

The tailings liberation data (Figure 4-38) showed that the losses from flotation in relation to grinding equipment used during comminution were predominantly either locked or liberated. For chalcopyrite and sphalerite, most losses were in the coarser fractions while losses from galena were evenly distributed across the size classes. It can therefore be argued that there is potential to recover more liberated minerals falling in floatable size classes from the tailings.

The statistical comparisons indicated that the observed flotation recoveries of products from wet rod milling and dry rod milling were similar (Table 4-11). The only difference was in selectivity where concentrate grades after wet rod milling were higher and this was because of the lower water/mass recoveries as compared to dry rod milling. The liberation characteristics and grain size distribution for the benchmarking grind were the same. This was expected as the mechanism of breakage is the same, with the only difference being in one case, comminution occurs in a dry environment and wet environment for the other.

Apart from the benchmarking grind, it was observed from the results that rod milling generally resulted in better flotation performances as compared to the VRM. This is because for the flotation of rod milling products outside of the benchmarking grind, high mass and water recoveries, which resulted in observed high recoveries through entrainment.

As shown from the aging tests (Table 4-14), the flotation performance became compromised in the absence of an activator when the ore aged. These observations confirmed that the exposed sulfide surfaces oxidise in the presence of air, which compromises collector action and the flotation performance. Surface oxidation results in the formation of metal hydroxides and sulphur-oxy compounds. Surface oxidation will thus reduce value mineral hydrophobicity and render sulfide collector adsorption less selective (Guy and Trahar, 1985; Shannon and Trahar, 1986; Clarke et al., 1995). The lower collector selectivity, coupled with high water recoveries results in lower sulfide mineral flotation efficiencies hence the lower elemental recoveries of copper, lead and zinc for the aged sample.

6. CONCLUSIONS AND RECOMMENDATIONS

This section concludes the work done based on the scope as answers to the key questions and the outcomes of the hypotheses tested. It summarises the key findings of the research. Various recommendations based on the results of the research are outlined and these may include opinions which might aid future studies.

6.1. Conclusions

Mineral recoveries were similar after floating the coarse-grained, polymetallic Swartberg sulfide blend ore comminuted using the VRM, dry and wet rod milling. Specific grinding energy consumption for the VRM was 54.3 % lower for the benchmarking grind of 65 % passing 75 μm. The PSDs were similar. The flotation feed liberation profiles and valuable minerals grain sizes were similar from the mineralogical results. The differences in pulp potential after comminution did not correlate to recovery of galena, chalcopyrite and sphalerite as the recoveries were similar. Solids recovery (mass pull) and water recovery were closely related to the measured pulp potential. The most positive pulp potential (recorded for RD) resulted in the highest mass recovery and lowest concentrate grade, while the opposite was true for RW where the least positive pulp potential was recorded.

6.1.1. Key Questions

1. **What are the differences in pulp potential between the dry rod milling and wet rod milling products? Can the differences be correlated to the resultant flotation performance?**

For the benchmarking grind tested (65% passing 75 μm), the dry rod milling products had more positive pulp potential as compared to wet rod milling. The lower pulp potential measured after wet rod milling was an indication of the presence of oxygen consumers and galvanic interactions during comminution, meaning more hydroxides precipitated on the sulfide surfaces. However, these differences in pulp potential did not affect the flotation performance as the mineral recoveries of galena, chalcopyrite and sphalerite were statistically similar. Comparing the average recoveries for copper and zinc minerals, the differences were very small (<0.5 %) and depended more on grind where with some grinds, dry rod milled products performed better than wet products and other grinds where wet rod milled products were recovered better than wet ground products. For lead, dry rod milling resulted in better flotation performance compared to wet rod milling.

2. **What is the effect of varying compressive forces on elemental recoveries? Variance in compressive force is achieved by changing grinding pressure.**

An increase in grinding pressure does not result in any statistically significant change in progeny particle size distribution and value mineral recovery. The total mass and water recovery from the flotation of VRM products produced at different grinding pressures were within standard error of each other, and flotation response was expected to the similar. The low confidence levels from ANOVA statistically proved that there was no difference in flotation performance with the variation of grinding pressure during comminution. It can thus be concluded from the results that the increase in grinding pressure results in an increase in capacity of the VRM (higher throughput) without compromising recovery of chalcopyrite, galena or sphalerite for the polymetallic sulfide ore operating at a target grind of 65 % passing 75 μm.

3. **For the same grinding time, what are the characteristics of the products from dry milling and wet milling in a rod mill? What are the subsequent differences in the recovery of chalcopyrite, sphalerite and galena?**

Grinding curves indicated that milling time required to achieve the target grind for either wet milling or dry milling was the same. The progeny PSDs were similar. While the pulp potentials were different, they were both within the range for optimum flotation. For the benchmarking grind, the liberation profiles were the same: percent liberated chalcopyrite (80 %), liberated galena (78 %) and liberated sphalerite (90 %). The grain size distributions were also similar with d50s of as chalcopyrite (24 μm), galena (14 μm) and sphalerite (23 μm). The total mass and water recovery from dry grinding were higher than from wet grinding. As the mineral recoveries were similar, the difference in mass and water recovery resulted in the differences in concentrate grade of chalcopyrite, galena and sphalerite. The recovery kinetics of products from either wet or dry milling were the same.

4. **Are there any differences in the mineral liberation profiles between the VRM, dry rod milling and wet rod milling products? Can the differences be correlated to the resultant flotation performance?**

Mineralogical examination was done on the benchmarking grind (65% passing 75 μm). The liberation profiles were similar or slightly higher for the VRM products. Liberated chalcopyrite was 84 % for the VRM (80 % for rod milling), liberated galena 84 % for the VRM (78 % for rod milling) and liberated sphalerite 90 % (90 % for rod milling). The grain size d50s were comparable: chalcopyrite (24 μm-rod milling, 26 μm-VRM), galena (14 μm-rod milling, 21 μm-VRM) and sphalerite (23 μm-rod milling, 25 μm-VRM). The ore grain size distribution was coarse for copper (maximum grain size of 2000 μm), lead (maximum grain size of 2375 μm) and zinc (maximum grain size of 1550 μm) minerals. This meant that for the grind under investigation, the value minerals would be mostly liberated irrespective of the comminution procedure. The subsequent flotation performance cannot be linked with liberation profiles and is thus independent of whether the VRM, dry rod milling, or wet rod milling was used for comminution to liberate the chalcopyrite, galena or sphalerite.

6.1.2. Hypotheses

1. **Dry rod milling results in better recovery of chalcopyrite, galena and sphalerite compared to wet rod milling. This is because dry grinding results in a more positive pulp potential of the flotation pulp as galvanic interactions are reduced in the absence of water and less precipitation of metal hydroxides on the valuable minerals sulfide surfaces occurs. Sulfide mineral and collector interactions are not compromised, and hence better flotation performance results.**

Dry rod grinding resulted in more positive pulp potential than wet rod milling. This was an indication that galvanic interactions were present during wet milling, resulting in the precipitation of hydroxides. Further, the pulp potentials measured were within reported range for optimum collector action. The flotation performance of the dry rod milled product was on average marginally better than the flotation performance of the wet milled product. However, the differences were very small and the statistical confidence levels were too low to conclude there was a difference in performance. These conclusions are similar to those reported literature (Palm et al., 2011).

2. **Increase in compressive force during comminution using the VRM results in an improvement in flotation response of the products. This is because an increase in compressive force means more energy is applied for particle breakage, resulting in higher breakage rates and increased liberation of particles.**

Based on the results, increasing the compressive force during comminution using the VRM does not affect the flotation responses of the comminution products. The total solids and water recoveries obtained showed that there were marginal differences in solids and water recovery during flotation when grinding pressure was increased from 600 kPa to 1000 kPa. However, the confidence limits show that the solids and water recoveries are similar, and as such, the recovery and concentrate grade of chalcopyrite, galena and sphalerite were expectedly similar.

3. **The VRM can be used to prepare ore for flotation at a reduced specific energy input compared to rod milling. This is because compression and in-bed breakage are more energy efficient than impact and shear breakage.**

The results indicated that the recovery of copper, lead and zinc minerals after using the VRM as comminution equipment was comparable to flotation recoveries achieved after dry and wet rod milling at the benchmarking grind of 65 % passing 75 μm. The specific grinding energy consumption for VRM comminution was 54.3 % lower than the conventional comminution circuit specific energy consumption. Accounting for fan energy using the reported scale up factor of 40 %, the specific energy consumption for comminution and classification for the VRM was 36 % lower than specific energy consumption for the conventional tumbling comminution and classification circuit.

6.2. Recommendations

Based on the results and conclusions as well as observations made during the study, the following recommendations have been proposed:

- More comparative studies should be done using various ore types. The current studies used ore with coarse grained minerals and the performance was mostly independent of comminution procedure used. If the mineral grain sizes are fine, the differences in flotation performance can then be more easily attributed to differences in comminution mechanisms.
- An investigation should be conducted whether high intensity conditioning will improve selectivity during flotation of the VRM products. This study aimed at comparing performance using the same procedure. Literature reports potential advantages of high intensity mixing of dry ground products on selectivity, hence the recommendation to test and assess if high intensity mixing can improve concentrate grades.
- Flowsheet development work could be done to assess whether it will not be more cost effective to conduct bulk flotation followed by segregation for this specific polymetallic sulfide ore. The current flowsheet and the results do not indicate recovery as a bottleneck but points more to optimisation of the circuit to minimise misplacement of mineral fractions during segregation. Bulk flotation followed by segregation is a possible optimisation route and it has potential to free up plant capacity and reduce chemicals dosage.

REFERENCES

Altun, D., Gerold, C., Benzer, H., Altun, O. & Aydogan, N. 2015. Copper ore grinding in a mobile vertical roller mill pilot plant. *International Journal of Mineral Processing*. 136:32–36. DOI: 10.1016/j.minpro.2014.10.002.

Altun, D., Benzer, H., Aydogan, N. & Gerold, C. 2017. Operational parameters affecting the vertical roller mill performance. *Minerals Engineering*. 103–104:67–71. DOI: 10.1016/j.mineng.2016.08.015.

Apling, A. & Bwalya, M. 1997. Evaluating high pressure milling for liberation enhancement and energy saving. *Minerals Engineering*. 10(9):1013–1022. DOI: 10.1016/S0892-6875(97)00080-0.

Aydogan, N.A. & Benzer, H. 2011. Comparison of the overall circuit performance in the cement industry: High compression milling vs. ball milling technology. *Minerals Engineering*. 24(3–4):211–215. DOI: 10.1016/j.mineng.2010.08.005.

Ballantyne, G.R. & Powell, M.S. 2014. Benchmarking comminution energy consumption for the processing of copper and gold ores. *Minerals Engineering*. 65:109–114. DOI: 10.1016/j.mineng.2014.05.017.

Becker, M., Wightman, E.. & Evans, C.. 2016. *Process Mineralogy: JKMRC Monograph Series in Mining and Mineral Processing: No. 6*. Brisbane: Julius Kruttschnitt Mineral Research Centre.

Benzer, H., Gerold, C. & Schmitz, C. 2018. First application of a Vertical-Roller-Mill in a sulphide Copper-Gold ore project. In *Comminution 18*. Cape Town. 1–14.

Bradshaw, D.J., Harris, P.J. & Connor, C.T.O. 1998. Synergistic interactions between reagents in sulphide flotation. *The Journal of The South African Institute of Mining and Metallurgy*.

Bruckard, W.J., Sparrow, G.J. & Woodcock, J.T. 2011. A review of the effects of the grinding environment on the flotation of copper sulphides. *International Journal of Mineral Processing*. 100(1–2):1–13. DOI: 10.1016/j.minpro.2011.04.001.

Bulatovic, S.M. 2007. *Handbook of Flotation Reagents*. DOI: 10.1016/B978-044453029-5/50010-1.

Bulatovic, S.M. 2014. *Handbook of Flotation Reagents: Chemistry, Theory and Practice*. DOI: 10.1016/C2009-0-17332-4.

Cameron, A.., Kelsall, D.., Restarick, C.. & Stewart, P.S.. 1970. A detailed assessment of concentrator performance at Broken Hill South Limited. *Australian Mining*. 63(4):53–67.

Celik, I.B. & Oner, M. 2006. The influence of grinding mechanism on the liberation characteristics of clinker minerals. *Cement and Concrete Research*. 36(3):422–427. DOI: 10.1016/J.CEMCONRES.2005.09.011.

Chapman, N.A., Shackleton, N.J., Malysiak, V. & O'Connor, C.T. 2011. The effect of using different comminution procedures on the flotation of Platinum-Group Minerals. *Minerals Engineering*. DOI: 10.1016/j.mineng.2011.01.001.

Chelgani, S.C., Parian, M., Parapari, P.S., Ghorbani, Y. & Rosenkranz, J. 2019. A comparative study on the effects of dry and wet grinding on mineral flotation separation–a review. *Journal of Materials Research and Technology*. 8(5):5004–5011. DOI: 10.1016/J.JMRT.2019.07.053.

Chikochi, C. 2017. Ore breakage characterisation of UG2 deposits using the JK RBT. University of Cape Town.

Clarke, P., Fornasiero, D., Ralston, J. & Smart, R.S.C. 1995. A study of the removal of oxidation products from sulfide mineral surfaces. *Minerals Engineering*. 8(11):1347–1357. DOI: 10.1016/0892-6875(95)00101-U.

Cleary, P.W. 1998. Predicting charge motion, power draw, segregation and wear in ball mills using discrete element methods. *Minerals Engineering*. 11(11):1061–1080. DOI: 10.1016/S0892-6875(98)00093-4.

Cohen, H.E. 1983. Energy usage in mineral processing. *Institution of Mining and Metallurgy Transactions*. (92):C160-164.

Corin, K.C., Mishra, J. & O'Connor, C.T. 2013. Investigating the role of pulp chemistry on the floatability of a Cu-Ni sulfide ore. *International Journal of Mineral Processing*. 120:8–14. DOI: 10.1016/j.minpro.2013.02.001.

Curry, J.A., Ismay, M.J.L. & Jameson, G.J. 2014. Mine operating costs and the potential impacts of energy and grinding. *Minerals Engineering*. 56:70–80. DOI: 10.1016/j.mineng.2013.10.020.

Daniel, M.. 2007. Energy efficient mineral liberation using HPGR technology. University of Queensland.

van Drunick, W., Gerold, C. & Palm, N. 2010. Implementation of an energy efficient dry grinding technology into an Anglo American zinc beneficiation process. *International Mineral Processing Congress*. (September):1333–1341.

Dzinza, L. 2018. An investigation into the effect of potential modifiers on the flotation of a copper sulphide ore. University of Cape Town.

Encyclopedia Britannica. 2019. Flotation: Ore Dressing. In *Encyclopedia Britannica*. Available: https://www.britannica.com/technology/flotation-ore-dressing/media/210944/1524.

Erkan, E., Umurhan, S., Sayiner, B., Cankurtaran, M., Benzer, H., Aydogan, N., Demir, H.K., Langel, J., et al. 2012. Comparison of the Vertical Roller Mill and Rod-Ball Mill Circuit on the Gold Extraction. In *XIII International Mineral Processing Symposium*.

Evans, C.L., Wightman, E.M., Manlapig, E. V. & Coulter, B.L. 2011. Application of process mineralogy as a tool in sustainable processing. In *Minerals Engineering*. V. 24. 1242–1248. DOI: 10.1016/j.mineng.2011.03.017.

Farrokhpay, S. & Manouchehri, H.R. 2012. Flotation characteristics of a complex copper ore: A comparison between wet and dry grinding. *XXVI International Mineral Processing Congress (IMPC)*. 1370–1377. DOI: 10.13140/2.1.4695.6485.

Feng, D. & Aldrich, C. 1999. Effect of particle size on flotation performance of complex sulphide ores. *Minerals Engineering*. 12(7):721–731. DOI: 10.1016/S0892-6875(99)00059-X.

Feng, D. & Aldrich, C. 2000. A comparison of the flotation of ore from the Merensky Reef after wet and dry grinding. *International Journal of Mineral Processing*. 60(2):115–129. DOI: 10.1016/S0301-7516(00)00010-7.

Fuerstenau, D.W., Gutsche, O. & Kapur, P.C. 1996. Confined particle bed comminution under compressive loads. *Comminution 1994*. (January, 1):521–537. DOI: 10.1016/B978-0-444-82440-0.50047-X.

Fuerstenau, M.C., Jameson, G. & Yoon, R.H. 2007. *Froth Flotation: A Century of Innovation*. Colorado: Society for Mining, Metallurgy, and Exploration. DOI: 10.1002/9780470822746.app3.

Fuerstenau, M.C., Chander, S. & Woods, R. 2009. Sulfide Mineral Flotation. In *Froth flotation : a century of innovation*. DOI: 10.1049/ic:19960393.

Gardner, J.R. & Woods, R. 1979. An electrochemical investigation of the natural flotability of chalcopyrite. *International Journal of Mineral Processing*. DOI: 10.1016/0301-7516(79)90028-0.

Gaudin, A.., Groh, J.. & Henderson, H.. 1931. Effect of particle size on flotation. *American Institute of Mining and Metallurgical Engineering*. 414:3–23.

Göktepe, F. 2002. Effect of pH on pulp potential and sulphide mineral flotation. *Turkish Journal of Engineering and Environmental Sciences*.

Gonçalves, K.L.C., Andrade, V.L.L. & Peres, A.E.C. 2003. The effect of grinding conditions on the flotation of a sulphide copper ore. *Minerals Engineering*. 16(11):1213–1216. DOI: 10.1016/j.mineng.2003.05.006.

Gordon, H.J.., Miller, J.. & Becker, M. 2018. Using mineralogy for early stage Geometallurgical domain definition: a case study of the Swartberg polymetallic sulphide deposit. In *Geometallurgy Conference 2018*. Cape Town. 121–132.

Grano, S. 2009. The critical importance of the grinding environment on fine particle recovery in flotation. *Minerals Engineering*. 22(4):386–394. DOI: 10.1016/j.mineng.2008.10.008.

Guy, P.J. & Trahar, W.J. 1985. The effects of oxidation and mineral interaction on sulphide flotation. In *Flotation of Sulphide Minerals*. K.S.E. Editor, Ed. Lulea, Sweden: Elsevier. 91–110.

Henley, K.J. 1983. Ore Dressing Mineralogy - A Review of Techniques, Applications and Recent Developments. In *Proceedings of the First International Congress on Applied Mineralogy : ICAM 81*.

Heyes, G.W. & Trahar, W.J. 1979. Oxidation-Reduction effects in the flotation of chalcocite and cuprite. *International Journal of Mineral Processing*. 6(3):229–252. DOI: 10.1016/0301-7516(79)90039-5.

Hintikka, V. V. & Leppinen, J.O. 1995. Potential control in the flotation of sulphide minerals and precious metals. *Minerals Engineering*. DOI: 10.1016/0892-6875(95)00080-A.

Hoşten, Ç. & Özbay, C. 1998. A comparison of particle bed breakage and rod mill grinding with regard to mineral liberation and particle shape effects. *Minerals Engineering*. 11(9):871–874. DOI: 10.1016/S0892-6875(98)00074-0.

Humphries, G., Rule, C.M. & Wolmarans, E. 2006. The development of a process flowsheet for the new Anglo Platinum, PPRust north concentrator, incorporating HPGR technology. In *Second International Platinum Conference*. Sun City.

Jameson, G.J. 2012. The effect of surface liberation and particle size on flotation rate constants. *Minerals Engineering*. 36–38:132–137. DOI: 10.1016/j.mineng.2012.03.011.

Janetski, N.D., Woodburn, S.I. & Woods, R. 1977. An electrochemical investigation of pyrite flotation and depression. *International Journal of Mineral Processing*. DOI: 10.1016/0301-

7516(77)90004-7.

Jørgensen, S.W. 2005. Cement grinding - a comparison between vertical roller mill and ball mill. *Cement International*. (2).

Kapur, P.C., Pande, D. & Fuerstenau, D.W. 1997. Analysis of single-particle breakage by impact grinding. *International Journal of Mineral Processing*. 49(3–4):223–236. DOI: 10.1016/S0301-7516(96)00008-7.

King, R.P. 2001. Modeling and Simulation of Mineral Processing Systems. *Modeling and Simulation of Mineral Processing Systems*. 403. DOI: 10.1016/B978-0-08-051184-9.50004-3.

Klimpel, R. 1980. Selection of Chemical Reagents for flotation Process.pdf. In *Mineral Processing Plant Design*. 907–934. DOI: 10.1016/j.ajo.2004.04.012.

Klimpel, R.R. 1995. The influence of frother structure on industrial coal flotation. In *High Efficiency Coal Preparation: An International Symposium*. 141. Available: http://scholar.google.com/scholar?hl=en&btnG=Search&q=intitle:The+Influence+of+Frother+Structure+on+Industrial+Coal+Flotation#8.

Knoflicek, M.J. & Wentzel, W.C. 1995. Experiences with Clinker Grinding in Roller Mills. *IEEE Transactions on Industry Applications*. 31(2):413–418. DOI: 10.1109/28.370293.

Koleini, S.M.J., Abdollahy, M. & Soltani, F. 2012. Wet and dry grinding methods effect on the flotation of Taknar Cu-Zn sulphide ore using a mixed collector. *XXVI International Mineral Processing Congress (IMPC)*. (603):5113–5119. DOI: 10.13140/2.1.3508.9606.

Laskowski, J.. 2004. Testing Flotation Frothers. *Physicochemical Problems of Mineral Processing*. (38):13–22.

Lastra, R. 2002. Comparison of liberation determinations by particle area percentage and exposed particle perimeter percentage in a flotation concentrator. *Mining, Metallurgy & Exploration*. 19(4):203–208.

Little, L., Mainza, A.N., Becker, M. & Wiese, J.G. 2016. Using mineralogical and particle shape analysis to investigate enhanced mineral liberation through phase boundary fracture. *Powder Technology*. 301:794–804. DOI: 10.1016/j.powtec.2016.06.052.

Liu, J., Long, H., Corin, K.C. & O'Connor, C.T. 2018. A study of the effect of grinding environment on the flotation of two copper sulphide ores. *Minerals Engineering*. 122(May):339–345.

DOI: 10.1016/j.mineng.2018.03.031.

Loesche GmbH. 2016. *LOESCHE Mills for ores and Minerals*. Available: https://www.loesche.com/sites/default/files/list-content/brochure/2017-08/164-LOESCHE-Mills-for-ores-and-Minerals-E-2016.pdf.

Long, G., Peng, Y. & Bradshaw, D. 2012. A review of copper-arsenic mineral removal from copper concentrates. *Minerals Engineering*. 36–38:179–186. DOI: 10.1016/j.mineng.2012.03.032.

Lotter, N.O. 2011. Modern Process Mineralogy: An integrated multi-disciplined approach to flowsheeting. In *Minerals Engineering*. V. 24. 1229–1237. DOI: 10.1016/j.mineng.2011.03.004.

McClung, C.R., Gutzmer, J., Beukes, N.J., Mezger, K., Strauss, H. & Gertloff, E. 2007. Geochemistry of bedded barite of the Mesoproterozoic Aggeneys-Gamsberg Broken Hill-type district, South Africa. *Mineralium Deposita*. 42(5):537–549. DOI: 10.1007/s00126-007-0128-4.

von Michaelis, H. 2005. Real and potential metallurgical benefits of HPGR in hard rock ore processing. *Proceedings of the Randol Innovative Metallurgy Forum Held in Perth, WA, Australia, 21–24 August*. 31–39.

Morrell, S. 1992. The simulation of autogenous and semi-autogenous milling circuits. In *Comminution: Theory and Practice*. S.. Kawatra, Ed. AIME. 369–380.

Napier-Munn, T. & Wills, B.A. 2005. *Wills' Mineral Processing Technology*. DOI: 10.1016/B978-0-7506-4450-1.X5000-0.

Napier-Munn, T.J., Morell, S., Morrison, R.D. & Kojovic, T. 2005. *Minerals Comminution Circuits: Their operation and optimization*. Brisbane: JKMRC.

Neethling, S.J. & Cilliers, J.J. 2002. The entrainment of gangue into a flotation froth. *International Journal of Mineral Processing*. 64(2–3):123–134. DOI: 10.1016/S0301-7516(01)00067-9.

Norgate, T. & Jahanshahi, S. 2011. Reducing the greenhouse gas footprint of primary metal production: Where should the focus be? *Minerals Engineering*. 24(14):1563–1570. DOI: 10.1016/j.mineng.2011.08.007.

Ntlhabane, S., Becker, M., Charikinya, E., Voigt, M., Schouwstra, R. & Bradshaw, D. 2018. Towards the development of an integrated modelling framework underpinned by mineralogy. *Minerals Engineering*. 116(September 2017):123–131. DOI: 10.1016/j.mineng.2017.09.013.

Palm, N.A., Shackleton, N.J., Malysiak, V. & O'Connor, C.T. 2011. The effect of using different comminution procedures on the flotation of sphalerite. *Minerals Engineering*. 24(8):731–736. DOI: 10.1016/j.mineng.2011.01.001.

Pease, J.D., Curry, D.C. & Young, M.F. 2006. Designing flotation circuits for high fines recovery. In *Minerals Engineering*. V. 19. 831–840. DOI: 10.1016/j.mineng.2005.09.056.

Petruk, W. 2000. *Applied Mineralogy in the Mining Industry*. V. 1. DOI: 10.1017/CBO9781107415324.004.

Plitt, L.R.R. 1976. A mathematical model of the hydrocyclone classifier. *CIM Bulletin*. 69(779):114–123.

Powell, M.S. & Mainza, A.N. 2012. Step Change – a Staircase Rather Than a Giant Leap. *XXVI International Mineral Processing Congress (IMPC)*. (1127):4259–4268.

Rao, S.. 2004. *Surface Chemistry of Froth Flotation*. 2nd ed. L. Jan, Ed. New York: Kluwer Academic/Plenum Publishers.

Reichert, M., Gerold, C., Fredriksson, A., Adolfsson, G. & Lieberwirth, H. 2015. Research of iron ore grinding in a vertical-roller-mill. *Minerals Engineering*. 73:109–115. DOI: 10.1016/j.mineng.2014.07.021.

Roy, G.R. 2002. Increasing cement grinding capacity with vertical roller mill technology. *IEEE Cement Industry Technical Conference (Paper)*. 205–211. DOI: 10.1109/CITCON.2002.1006507.

Rudnick, T.. 2016. The genesis of the Swartberg base-metal sulphide deposit, South Africa. University of Stellenbosch.

Rule, C. & Schouwstra, R.P. 2012. Process Mineralogy Delivering Significant Value at Anglo Platinum Concentrator Operations. In *roceedings of the 10th International Congress for Applied Mineralogy (ICAM)*. M. Broekmans, Ed. Trondheim. 613–618.

Schaefer, H.U. 2001. LOESCHE vertical roller mills for the comminution of ores and minerals. *Minerals Engineering*. 14(10):1155–1160. DOI: 10.1016/S0892-6875(01)00133-9.

Schouwstra, R.P. & Smit, A.J. 2011. Developments in mineralogical techniques - What about mineralogists? In *Minerals Engineering*. V. 24. 1224–1228. DOI: 10.1016/j.mineng.2011.02.002.

Schwartz, G.. 1951. Classification and definitions of textures and mineral structures in ores. *Society*

of Economic Geologists. 46:578–591.

Shannon, L.K. & Trahar, W.J. 1986. The role of collector in sulphide ore flotation. In *oc. Symp. Advances in Minerals Processing. Soc.* P. Somasundaran, Ed. Denver: Mining Engineers. 408–426.

Solomon, N., Becker, M., Mainza, A., Petersen, J. & Franzidis, J.P. 2011. Understanding the influence of HPGR on PGM flotation behavior using mineralogy. *Minerals Engineering*. 24(12):1370–1377. DOI: 10.1016/j.mineng.2011.07.015.

Stapelmann, M. 2018. Vertical-Roller-Mill for hard rock phosphate application. In *Comminution 18*.

Stedman, D.. 1980. The structural geology and metamorphic petrology of Black Mountain, Namaqualand. University of Witwatersrand.

Tamashige, T., Obana, H. & Hamaguchi, M. 1991. Operational Results of Ok Series Roller Mill. *IEEE Transactions on Industry Applications*. 27(3):416–424. DOI: 10.1109/28.81821.

Tavares, L.M. 2007. *Chapter 1 Breakage of Single Particles: Quasi-Static*. V. 12. DOI: 10.1016/S0167-3785(07)12004-2.

Tavares, L.. & King, R.. 1998. Single-particle fracture under impact loading. *International Journal of Mineral Processing*. 54(1):1–28. DOI: 10.1016/S0301-7516(98)00005-2.

Tromans, D. 2008. Mineral comminution: Energy efficiency considerations. *Minerals Engineering*. 21(8):613–620. DOI: 10.1016/j.mineng.2007.12.003.

Twidle, T.R. & Englebrecht, P.C. 1984. Developments in the flotation of copper at Black Mountain. *Journal of the Southern African Institute of Mining and Metallurgy*. 84(6):164–178.

Umucu, Y., Deniz, V. & Unal, N. 2013. An evaluation of a modified product size distribution model based on t-family curves for three different crushers. *Physicochemical Problems of Mineral Processing*. DOI: 10.5277/ppmp130209.

UNDP, CCSI, UNSSN & WEF. 2016. *Mapping Mining to the Sustainable Development Goals: An Atlas*. Available: http://unsdsn.org/wp-content/uploads/2016/11/Mapping_Mining_SDGs_An_Atlas.pdf [2019, March 03].

Viljoen, R.M., Smit, J.T., Du Plessis, I. & Ser, V. 2001. The development and application of in-bed compression breakage principles. *Minerals Engineering*. 14(5):465–471. DOI: 10.1016/S0892-6875(01)00034-6.

Wiese, J., Harris, P. & Bradshaw, D. 2005. The influence of the reagent suite on the flotation of ores from the Merensky reef. *Minerals Engineering*. 18(2):189–198. DOI: 10.1016/J.MINENG.2004.09.013.

Wiese, J., Harris, P. & Bradshaw, D. 2006. The role of the reagent suite in optimising pentlandite recoveries from the Merensky reef. *Minerals Engineering*. 19(12):1290–1300. DOI: 10.1016/J.MINENG.2006.04.003.

Wightman, E.., Evans, C.L., Vizcarra, T. & Sandoval, G. 2008. Process mineralogy as a tool in modelling mineral processing operations. In *Ninth International Congress for Applied Mineralogy*. Brisbane. 475–481.

Ye, X., Gredelj, S., Skinner, W. & Grano, S.R. 2010. Regrinding sulphide minerals - Breakage mechanisms in milling and their influence on surface properties and flotation behaviour. *Powder Technology*. 203(2):133–147. DOI: 10.1016/j.powtec.2010.05.002.

Yianatos, J. & Contreras, F. 2010. Particle entrainment model for industrial flotation cells. *Powder Technology*. 197(3):260–267. DOI: 10.1016/J.POWTEC.2009.10.001.

A. APPENDIX A: BATCH FLOTATION DATA

A-1: 65 % passing 75µm (RD and RW)

Table A-1: 65 % passing 75 µm (RD and RW)

Run no.	Reagents	Label	Sample	Time, min	Mass Pull, g	Water Rec, g	Cum Mass, g	Cum Water, g	Ave cum Mass, g	Ave cum w Rec, g	Copper %	Copper Grade %	Copper Rec %	Ave Cu Grade	Ave Copper rec %	Lead %	Lead Grade %	Lead Rec %	Ave Lead Grade	Ave Lead rec %	Zinc %	Zinc Grade %	Zinc Recovery %	Average Zinc Grade	Average Zinc recovery %
				0				0,00	0,00	0,00					0,00					0,00					0,00
1	SEX - 80g/t	RD	C1	2	118,09	355,56	118,09	355,56	120,05	382,64	4,07	4,07	76,62	3,97	77,44	21,61	21,61	84,96	20,85	85,37	14,47	14,47	92,27	13,83	92,44
	MIBC - 25g/t	65% Passing 75µm	C2	6	35,41	185,14	153,50	540,70	153,68	568,04	2,70	3,75	91,85	3,67	91,56	6,30	18,08	92,38	17,62	92,37	2,30	11,66	96,67	11,28	96,62
	Senkol 700 - 10g/t		C3	12	13,08	110,18	166,58	650,88	168,54	700,06	1,25	3,55	94,45	3,46	94,63	2,53	16,86	93,49	16,28	93,57	0,60	10,80	97,09	10,34	97,10
	Copper sulfate - 160g/t		C4	20	12,97	149,76	179,55	800,64	179,75	829,56	0,92	3,36	96,36	3,30	96,28	1,88	15,77	94,30	15,38	94,30	0,44	10,05	97,40	9,72	97,38
			F		1297,34						0,48					2,31					1,18				
			T		1081,16																				
			T2		21,85						0,02					0,17					0,05				
			T3		14,78						0,02					0,14					0,04				
			Cc+Tt																						
			Accountability																						
			Mass Pull		13,84%																				
2	SEX - 80g/t	RD	C1	2	122,00	409,72	122,00	409,72			3,88	3,88	78,26			20,10	20,10	85,79			13,18	13,18	92,61		
	MIBC - 25g/t	65% Passing 75µm	C2	6	31,86	185,65	153,86	595,37			2,47	3,59	91,28			5,89	17,16	92,36			2,16	10,90	96,57		
	Senkol 700 - 10g/t		C3	12	16,63	153,87	170,49	749,24			1,28	3,36	94,81			2,23	15,70	93,66			0,55	9,89	97,10		
	Copper sulfate - 160g/t		C4	20	9,45	109,24	179,94	858,48			0,90	3,23	96,21			1,94	14,98	94,30			0,46	9,39	97,35		
			F		1292,01						0,49					2,33					1,19				
			T		1071,74																				
			T2		19,81						0,02					0,15					0,04				
			T3		20,52						0,02					0,14					0,04				
			Cc+Tt																						
			Accountability																						
			Mass Pull		13,93%																				
				0				0,00	0,00	0,00					0,00					0,00					0,00
3	SEX - 80g/t	RW	C1	2	85,69	200,80	85,69	200,80	86,16	195,58	5,55	5,55	79,11	5,72	81,33	27,61	27,61	81,23	28,12	82,26	19,67	19,67	93,06	19,81	93,34
	MIBC - 25g/t	65% Passing 75µm	C2	6	23,02	141,94	108,71	342,74	107,76	329,29	3,50	5,11	92,53	5,22	92,87	11,62	24,23	90,42	24,70	90,35	2,83	16,11	96,66	16,40	96,60
	Senkol 700 - 10g/t		C3	12	11,47	111,86	120,18	454,60	120,15	455,45	1,39	4,76	95,19	4,82	95,53	4,08	22,31	92,03	22,57	92,08	0,79	14,64	97,16	14,79	97,13
	Copper sulfate - 160g/t		C4	20	9,41	113,80	129,59	568,40	129,58	570,35	0,80	4,47	96,45	4,52	96,70	2,67	20,88	92,89	21,12	92,93	0,50	13,62	97,42	13,75	97,38
			F		1289,23						0,48					2,28					1,18				
			T		1122,58																				
			T2		18,66						0,02					0,18					0,04				
			T3		18,40						0,02					0,18					0,04				
			Cc+Tt																						
			Accountability																						
			Mass Pull		10,05%																				
				0					0,00	0,00															
4	SEX - 80g/t	RW	C1	2	86,62	190,35	86,62	190,35			5,89	5,89	83,54			28,63	28,63	83,28			19,96	19,96	93,62		
	MIBC - 25g/t	65% Passing 75µm	C2	6	20,18	125,49	106,80	315,84			2,93	5,33	93,22			10,33	25,17	90,28			2,67	16,69	96,54		
	Senkol 700 - 10g/t		C3	12	13,31	140,45	120,11	456,29			1,22	4,88	95,88			4,16	22,84	92,14			0,79	14,93	97,11		
	Copper sulfate - 160g/t		C4	20	9,46	116,01	129,57	572,30			0,69	4,57	96,95			2,61	21,37	92,97			0,46	13,87	97,35		
			F		1288,74						0,48					2,32					1,20				
			T		1129,52																				
			T2		14,77						0,02					0,18					0,04				
			T3		14,88						0,02					0,18					0,04				
			Cc+Tt																						
			Accountability																						
			Mass Pull		10,05%																				

A-2: 65 % passing 75µm (RD: No Activator)

Table A-2: 65 % passing 75 µm (RD: No Activator)

Run no.	Reagents	Label	Sample	Time, min	Mass Pull, g	Water Rec, g	Cum Mass, g	Cum Water, g	Ave cum Mass, g	Ave cum w Rec, g	Copper %	Copper Grade %	Copper Rec %	Ave Cu Grade	Ave Copper rec %	Lead %	Lead Grade %	Lead Rec %	Ave Lead Grade	Ave Lead rec %	Zinc %	Zinc Grade %	Zinc Recovery %	Average Zinc Grade	Average Zinc recovery %
				0					0,00	0,00					0,00					0,00					0,00
5	SEX - 80g/t	RD5	C1	2	135,59	450,96	135,59	450,96	130,92	397,99	3,89	3,89	88,61	4,10	89,00	15,63	15,63	86,63	16,64	87,01	9,66	9,66	91,72	10,20	91,79
	MIBC - 25g/t	Aging test 2	C2	6	26,04	228,66	161,63	679,62	158,53	621,39	1,47	3,50	95,04	3,62	95,33	5,25	13,96	92,22	14,60	92,60	2,07	8,44	95,50	8,76	95,65
	Senkol 700 - 10g/t	Floated 24 days after	C3	12	15,08	215,34	176,71	894,96	173,91	811,65	0,47	3,24	96,22	3,34	96,41	2,30	12,96	93,64	13,50	93,95	0,56	7,77	96,09	8,03	96,20
	Copper sulfate - 160g/t	milling	C4	20	9,68	177,76	186,39	1072,72	183,52	958,61	0,34	3,09	96,77	3,18	96,90	1,78	12,38	94,34	12,89	94,63	0,39	7,39	96,35	7,63	96,45
			F		1295,99						0,44					1,87					1,04				
			T		1076,50																				
			T2		18,08						0,02					0,12					0,05				
			T3		15,02						0,02					0,13					0,05				
			Cc+Tt																						
			Accountability																						
			Mass Pull		14,38%																				
				0					0,00	0,00															
6	SEX - 80g/t	RD6	C1	2	126,25	345,02	126,25	345,02			4,31	4,31	89,39			17,65	17,65	87,40			10,73	10,73	91,87		
	MIBC - 25g/t	Aging test 1	C2	6	29,18	218,13	155,43	563,15			1,30	3,74	95,62			4,89	15,25	92,99			1,98	9,09	95,80		
	Senkol 700 - 10g/t	Floated 24 days after	C3	12	15,68	165,19	171,11	728,34			0,38	3,44	96,60			2,07	14,04	94,27			0,49	8,30	96,32		
	Copper sulfate - 160g/t	milling	C4	20	9,53	116,15	180,64	844,49			0,27	3,27	97,03			1,77	13,40	94,93			0,36	7,88	96,56		
			F		1282,54						0,47					1,90					1,09				
			T		1068,08																				
			T2		14,97						0,02					0,12					0,05				
			T3		18,85						0,02					0,12					0,05				
			Cc+Tt																						
			Accountability																						
			Mass Pull		14,08%																				

A-3: 65 % passing 75 µm (Aging Tests)

Table A-3: 65 % passing 75 µm (Aging Tests)

Run no.	Reagents	Label	Sample	Time, min	Mass Pull, g	Water Rec, g	Cum Mass, g	Cum Water, g	Ave cum Mass, g	Ave cum w Rec, g	Copper %	Copper Grade %	Copper Rec %	Ave Cu Grade	Ave Copper rec %	Lead %	Lead Grade %	Lead Rec %	Ave Lead Grade	Ave Lead rec %	Zinc %	Zinc Grade %	Zinc Recovery %	Average Zinc Grade	Average Zinc recovery %
				0					0,00	0,00															
7	SEX - 80g/t	RD7	C1	2	145,19	462,99	145,19	462,99	132,46	381,41	3,68	3,68	89,10	4,01	86,30	15,19	15,19	87,93	16,55	86,26	9,05	9,05	89,69	9,08	81,86
	MIBC - 25g/t		C2	6	30,40	255,44	175,59	718,43	169,45	643,86	1,20	3,25	95,19	3,42	94,70	4,61	13,36	93,51	13,88	93,17	2,65	7,94	95,20	8,08	93,20
	Senkol 700 - 10g/t		C3	12	14,18	213,13	189,77	931,56	187,13	888,39	0,54	3,05	96,46	3,14	96,37	2,29	12,53	94,81	12,76	94,65	0,78	7,40	95,95	7,47	95,20
			C4	20	8,18	156,82	197,95	1088,38	196,74	1062,33	0,40	2,94	97,01	3,01	97,02	1,63	12,08	95,34	12,21	95,24	0,58	7,12	96,27	7,16	95,99
			F		1305,32						0,42					1,74					1,00					
			T		1072,86																				
			T2		16,30						0,02					0,10					0,05					
			T3		18,21						0,02					0,11					0,05					
			Cc+Tt																						
			Accountability																						
			Mass Pull		15,16%																				
8	SEX - 80g/t	RD8	C1	2	119,73	299,83	119,73	299,83			4,33	4,33	83,50			17,91	17,91	84,60			9,10	9,10	74,03		
	MIBC - 25g/t		C2	6	43,58	269,46	163,31	569,29			1,53	3,58	94,22			4,79	14,41	92,83			5,80	8,22	91,20		
	Senkol 700 - 10g/t		C3	12	21,18	275,92	184,49	845,21			0,61	3,24	96,29			2,00	12,99	94,50			2,26	7,54	94,45		
			C4	20	11,04	191,06	195,53	1036,27			0,42	3,08	97,03			1,47	12,34	95,14			1,68	7,21	95,71		
			F		1312,17						0,46					1,83					1,07					
			T		1085,46																				
			T2		13,80						0,02					0,11					0,06					
			T3		17,38						0,02					0,11					0,06					
			Cc+Tt																						
			Accountability																						
			Mass Pull		14,90%																				
				0					0,00	0,00															
9	SEX - 80g/t	RD9	C1	2	53,62	678,79	53,62	678,79	53,21	633,81	1,92	1,92	16,57	2,31	19,54	15,27	15,27	31,43	18,71	37,36	3,43	3,43	11,90	4,26	14,47
	MIBC - 25g/t	Aging Test 3	C2	6	17,09	521,53	70,71	1200,32	72,12	1144,04	2,79	2,13	24,23	2,49	28,60	18,64	16,08	43,66	18,68	50,78	5,02	3,81	17,45	4,72	21,84
	Senkol 700 - 10g/t	Floated 25 days after	C3	12	7,25	326,01	77,96	1526,33	80,31	1474,43	3,06	2,22	27,79	2,55	32,66	14,53	15,94	47,71	18,11	54,87	6,47	4,06	20,49	5,07	26,18
		milling	C4	20	3,93	227,77	81,89	1754,10	85,06	1716,98	2,78	2,25	29,54	2,56	34,74	11,07	15,70	49,38	17,62	56,58	7,91	4,24	22,50	5,37	29,42
			F		1308,15						0,49					2,06					1,27					
			T		1186,66																				
			T2		20,27						0,35					1,07					0,98					
			T3		19,33						0,36					1,08					0,97					
			Cc+Tt																						
			Accountability																						
			Mass Pull		6,26%																				
10	SEX - 80g/t	RD10	C1	2	52,80	588,83	52,80	588,83			2,71	2,71	22,52			22,16	22,16	43,29			5,09	5,09	17,05		
	MIBC - 25g/t	Aging Test 4	C2	6	20,73	498,93	73,53	1087,76			3,20	2,85	32,98			19,03	21,27	57,89			6,98	5,62	26,22		
	Senkol 700 - 10g/t	Floated 25 days after	C3	12	9,12	334,76	82,65	1422,52			3,17	2,88	37,54			12,27	20,28	62,03			9,78	6,08	31,88		
		milling	C4	20	5,58	257,34	88,23	1679,86			2,73	2,87	39,94			8,49	19,54	63,78			12,60	6,50	36,34		
			F		1308,56						0,46					2,08					1,17					
			T		1173,13																				
			T2		22,83						0,31					0,78					0,83					
			T3		24,37						0,31					0,82					0,82					
			Cc+Tt																						
			Accountability																						
			Mass Pull		6,74%																				

A-4: 55 % passing 75 µm (RD and RW)

Table A-4: 55 % passing 75 µm (RD and RW)

Run no.	Reagents	Label	Sample	Time, min	Mass Pull, g	Water Rec, g	Cum Mass, g	Cum m. pull (%)	Ave cum Mass, g	Ave cum w Rec, g	Copper %	Copper Mass	Copper Grade %	Copper Rec %	Ave Cu Grade	Ave Copper rec %	Lead %	Lead Mass	Lead Grade %	Lead Rec %	Ave Lead Grade	Ave Lead rec %	Zinc %	Zinc Mass	Zinc Grade %	Zinc Recovery %	Average Zinc Grade	Average Zinc recovery %
				0				0,00	0,00	0,00						0,00						0,00						0,00
11	SEX - 80g/t	55 % Passing WM	C1	2	76,23	128,59	76,23	5,91	77,14	141,65	6,05	461,01	6,05	76,40	5,81	77,27	25,13	1915,64	25,13	77,92	24,00	78,30	18,80	1433,35	18,80	87,97	17,54	88,12
	MIBC - 25g/t		C2	6	36,41	268,18	112,64	8,64	112,81	400,42	2,67	97,24	4,96	92,52	4,75	92,44	7,99	291,00	19,59	89,75	18,78	89,64	3,29	119,97	13,79	95,33	12,94	95,14
	Senkol 700 - 10g/t		C3	12	26,97	243,68	139,61	10,69	139,58	662,67	0,86	23,31	4,17	96,38	4,00	96,35	2,92	78,87	16,37	92,96	15,73	92,87	0,75	20,14	11,27	96,56	10,60	96,41
	Copper sulfate - 160g/t		C4	20	20,45	318,45	160,06	12,24	159,85	972,82	0,38	7,74	3,68	97,66	3,54	97,65	1,71	34,95	14,50	94,38	13,94	94,29	0,37	7,52	9,88	97,03	9,30	96,88
			F		1301,02						0,45	584,51					1,77	2302,87					1,14	1479,08				
			T		1103,38																							
			T2		19,03						0,01	0,23					0,12	2,24					0,04	0,81				
			T3		18,55						0,01	0,23					0,12	2,31					0,04	0,79				
			Cc+Tt									0,464						1,890						1,252				
			Accountability																									
			Mass Pull		12,30%																							
12	SEX - 80g/t	55 % Passing WM	C1	2	78,05	154,70	78,05				5,57	434,70	5,57	78,14			22,87	1784,92	22,87	78,69			16,27	1269,74	16,27	88,27		
	MIBC - 25g/t		C2	6	34,93	249,37	112,98				2,27	79,18	4,55	92,37			7,03	245,58	17,97	89,52			2,75	95,96	12,09	94,95		
	Senkol 700 - 10g/t		C3	12	26,56	280,82	139,54				0,83	21,93	3,84	96,31			2,79	74,08	15,08	92,78			0,71	18,73	9,92	96,25		
	Copper sulfate - 160g/t		C4	20	20,10	301,84	159,64				0,37	7,36	3,40	97,64			1,60	32,06	13,38	94,20			0,35	6,94	8,72	96,73		
			F		1311,04						0,47	611,11					1,85	2425,69					1,17	1529,55				
			T		1108,99																							
			T2		20,62						0,01	0,23					0,12	2,39					0,04	0,84				
			T3		21,79						0,01	0,26					0,11	2,45					0,04	0,89				
			Cc+Tt									0,424						1,730						1,097				
			Accountability																									
			Mass Pull		12,18%																							
				0				0,00	0,00	0,00						0,00						0,00						0,00
19	SEX - 80g/t	55 % Passing DM	C1	2	117,32	292,91	117,32	8,85	116,42	278,13	3,82	447,63	3,82	89,84	3,80	90,42	15,30	1794,52	15,30	86,13	15,43	86,67	10,09	1184,03	10,09	91,64	10,20	91,89
	MIBC - 25g/t		C2	6	40,46	281,31	157,78	11,87	156,06	554,19	0,81	32,94	3,05	96,45	3,02	96,51	3,39	136,98	12,24	92,70	12,33	92,89	1,37	55,44	7,86	95,93	7,94	95,95
	Senkol 700 - 10g/t		C3	12	23,23	227,95	181,01	13,67	179,79	789,01	0,18	4,22	2,68	97,30	2,65	97,32	1,34	31,17	10,84	94,20	10,87	94,35	0,31	7,16	6,89	96,49	6,93	96,50
	Copper sulfate - 160g/t		C4	20	18,18	280,32	199,19	15,00	197,27	1056,27	0,11	1,92	2,44	97,68	2,42	97,73	0,95	17,36	9,94	95,03	10,00	95,20	0,22	3,95	6,28	96,79	6,34	96,81
			F		1310,74						0,46	597,34					1,84	2412,61					1,13	1487,53				
			T		1074,48																							
			T2		19,52						0,01	0,20					0,09	1,81					0,04	0,74				
			T3		17,55						0,01	0,18					0,09	1,64					0,04	0,65				
			Cc+Tt									0,380						1,590						0,986				
			Accountability																									
			Mass Pull		15,20%																							
20	SEX - 80g/t	55 % Passing DM	C1	2	115,51	263,34	115,51				3,78	436,93	3,78	91,01			15,56	1796,94	15,56	87,21			10,30	1189,72	10,30	92,14		
	MIBC - 25g/t		C2	6	38,83	270,81	154,34				0,69	26,69	3,00	96,56			3,12	121,05	12,43	93,09			1,27	49,39	8,03	95,96		
	Senkol 700 - 10g/t		C3	12	24,22	241,69	178,56				0,15	3,70	2,62	97,34			1,21	29,37	10,91	94,51			0,29	7,09	6,98	96,51		
	Copper sulfate - 160g/t		C4	20	16,78	254,20	195,34				0,13	2,13	2,40	97,78			1,05	17,63	10,06	95,37			0,24	3,99	6,40	96,82		
			F		1318,68						0,47	618,82					1,86	2450,60					1,20	1583,02				
			T		1079,97																							
			T2		23,22						0,01	0,23					0,09	2,02					0,04	0,87				
			T3		20,15						0,01	0,19					0,08	1,67					0,04	0,72				
			Cc+Tt									0,364						1,563						0,979				
			Accountability																									
			Mass Pull		14,81%																							

A-5: 60 % passing 75 µm (RD and RW)

Table A-5: 60 % passing 75 µm (RD and RW)

Run no.	Reagents	Label	Sample	Time, min	Mass Pull, g	Water Rec, g	Cum Mass, g	Cum m. pull (%)	Ave cum Mass, g	Ave cum w Rec, g	Copper %	Copper Mass	Copper Grade %	Copper Rec %	Ave Cu Grade	Ave Copper rec %	Lead %	Lead Mass	Lead Grade %	Lead Rec %	Ave Lead Grade	Ave Lead rec %	Zinc %	Zinc Mass	Zinc Grade %	Zinc Recovery %	Average Zinc Grade	Average Zinc recovery %
				0				0,00	0,00	0,00						0,00						0,00						0,00
13	SEX - 80g/t	60 % Passing WM	C1	2	80,55	149,47	80,55	6,10	80,12	193,47	5,85	470,91	5,85	78,08	5,71	77,97	24,09	1940,13	24,09	79,15	23,48	78,92	17,64	1420,90	17,64	88,56	16,95	88,41
	MIBC - 25g/t		C2	6	35,18	252,86	115,73	8,81	115,71	453,77	2,53	89,05	4,84	92,84	4,69	92,52	7,72	271,56	19,11	90,23	18,52	89,93	3,10	109,08	13,22	95,36	12,64	95,18
	Senkol 700 - 10g/t		C3	12	29,13	260,97	144,86	11,02	144,69	709,13	0,79	23,04	4,02	96,66	3,91	96,52	2,73	79,43	15,82	93,47	15,37	93,28	0,70	20,44	10,70	96,63	10,25	96,51
	Copper sulfate - 160g/t		C4	20	21,21	348,59	166,07	12,62	165,78	1020,23	0,34	7,13	3,55	97,85	3,46	97,78	1,57	33,40	14,00	94,83	13,61	94,69	0,35	7,35	9,38	97,09	8,99	96,99
			F		1317,60						0,44	582,92					1,77	2328,49					1,13	1494,29				
			T		1112,72																							
			T2		17,29						0,01	0,20					0,11	1,90					0,04	0,69				
			T3		21,52						0,01	0,24					0,11	2,37					0,04	0,88				
			Cc+Tt									0,458						1,860						1,218				
			Accountability																									
			Mass Pull		12,60%																							
14	SEX - 80g/t	60 % Passing WM	C1	2	79,68	237,47	79,68				5,57	443,78	5,57	77,87			22,87	1822,20	22,87	78,69			16,27	1296,26	16,27	88,26		
	MIBC - 25g/t		C2	6	36,01	267,74	115,69				2,27	81,63	4,54	92,19			7,03	253,18	17,94	89,63			2,75	98,93	12,06	95,00		
	Senkol 700 - 10g/t		C3	12	28,82	249,75	144,51				0,83	23,80	3,80	96,37			2,79	80,38	14,92	93,10			0,71	20,32	9,80	96,38		
	Copper sulfate - 160g/t		C4	20	20,98	273,60	165,49				0,37	7,68	3,37	97,72			1,60	33,47	13,23	94,54			0,35	7,25	8,60	96,88		
			F		1308,99						0,47	611,36					1,81	2372,20					1,18	1540,90				
			T		1106,15																							
			T2		18,92						0,01	0,22					0,11	2,11					0,04	0,77				
			T3		18,43						0,01	0,21					0,11	2,01					0,04	0,72				
			Cc+Tt									0,435						1,769						1,122				
			Accountability																									
			Mass Pull		12,64%																							
				0				0,00	0,00	0,00						0,00						0,00						0,00
19	SEX - 80g/t	60 % Passing DM	C1	2	137,09	376,99	137,09	10,26	134,21	377,39	4,26	584,41	4,26	90,84	4,02	90,96	16,87	2312,41	16,87	87,87	16,21	87,57	11,41	1564,33	11,41	92,77	10,86	92,65
	MIBC - 25g/t		C2	6	48,76	271,56	185,85	13,72	179,50	647,46	0,84	41,01	3,37	97,21	3,20	96,78	3,51	171,16	13,36	94,38	12,96	93,60	1,44	69,97	8,79	96,92	8,46	96,55
	Senkol 700 - 10g/t		C3	12	22,43	210,19	208,28	15,73	205,85	876,37	0,21	4,77	3,03	97,95	2,82	97,58	1,44	32,30	12,08	95,60	11,47	95,00	0,34	7,70	7,88	97,38	7,42	97,08
	Copper sulfate - 160g/t		C4	20	13,38	181,58	221,66	16,81	219,96	1058,68	0,14	1,86	2,85	98,24	2,64	97,89	1,09	14,55	11,42	96,16	10,81	95,61	0,24	3,28	7,42	97,58	6,96	97,30
			F		1309,93						0,46	602,26					1,80	2357,59					1,17	1528,07				
			T		1049,74																							
			T2		19,53						0,01	0,21					0,09	1,83					0,04	0,72				
			T3		19,00						0,01	0,19					0,09	1,75					0,04	0,72				
			Cc+Tt									0,491						2,009						1,287				
			Accountability																									
			Mass Pull		16,92%																							
20	SEX - 80g/t	60 % Passing DM	C1	2	131,32	377,79	131,32				3,78	496,74	3,78	91,08			15,56	2042,89	15,56	87,26			10,30	1352,56	10,30	92,53		
	MIBC - 25g/t		C2	6	41,82	268,58	173,14				0,69	28,74	3,04	96,35			3,12	130,37	12,55	92,83			1,27	53,20	8,12	96,17		
	Senkol 700 - 10g/t		C3	12	30,28	247,63	203,42				0,15	4,63	2,61	97,20			1,21	36,72	10,86	94,40			0,29	8,86	6,95	96,78		
	Copper sulfate - 160g/t		C4	20	14,83	183,04	218,25				0,13	1,88	2,44	97,54			1,05	15,58	10,20	95,07			0,24	3,53	6,50	97,02		
			F		1307,01						0,44	581,56					1,85	2424,38					1,14	1489,85				
			T		1042,97																							
			T2		24,44						0,01	0,30					0,11	2,61					0,04	0,98				
			T3		21,35						0,01	0,26					0,11	2,25					0,04	0,85				
			Cc+Tt									0,417						1,791						1,118				
			Accountability																									
			Mass Pull		16,70%																							

A-6: 70 % passing 75 µm (RD and RW)

Table A-6: 70 % passing 75 µm (RD and RW)

Run no.	Reagents	Label	Sample	Time, min	Mass Pull, g	Water Rec, g	Cum Mass, g	Cum m. pull (%)	Ave cum Mass, g	Ave cum w Rec, g	Copper %	Copper Mass	Copper Grade %	Copper Rec %	Ave Cu Grade	Ave Copper rec %	Lead %	Lead Mass	Lead Grade %	Lead Rec %	Ave Lead Grade	Ave Lead rec %	Zinc %	Zinc Mass	Zinc Grade %	Zinc Recovery %	Average Zinc Grade	Average Zinc recovery %
				0				0,00	0,00	0,00						0,00						0,00						0,00
15	SEX - 80g/t	70 % Passing WM	C1	2	84,10	192,90	84,10	6,29	82,31	169,80	5,26	442,22	5,26	77,40	5,54	77,77	21,69	1824,22	21,69	78,18	22,95	78,68	15,74	1323,37	15,74	88,06	16,57	88,42
	MIBC - 25g/t		C2	6	35,21	226,84	119,31	9,03	118,31	402,64	2,53	88,98	4,45	92,97	4,61	93,13	7,93	279,06	17,63	90,14	18,31	90,32	3,12	109,82	12,01	95,36	12,43	95,41
	Senkol 700 - 10g/t		C3	12	28,92	365,32	148,23	11,24	147,17	728,46	0,75	21,70	3,73	96,77	3,86	96,85	2,60	75,09	14,70	93,35	15,23	93,46	0,64	18,46	9,79	96,59	10,12	96,61
	Copper sulfate - 160g/t		C4	20	17,83	334,31	166,06	12,65	165,67	1047,32	0,37	6,65	3,37	97,93	3,46	97,94	1,75	31,13	13,31	94,69	13,71	94,72	0,48	8,62	8,79	97,17	9,03	97,14
			F		1310,56						0,45	584,23					1,77	2322,64					1,14	1497,67				
			T		1108,82																							
			T2		19,13						0,01	0,20					0,11	2,17					0,04	0,73				
			T3		16,55						0,01	0,17					0,10	1,71					0,04	0,60				
			Cc+Tt									0,436						1,780						1,147				
			Accountability																									
			Mass Pull		12,67%																							
16	SEX - 80g/t	70 % Passing WM	C1	2	80,52	146,70	80,52				5,83	469,21	5,83	78,14			24,21	1949,47	24,21	79,19			17,41	1401,46	17,41	88,78		
	MIBC - 25g/t		C2	6	36,78	238,84	117,30				2,48	91,05	4,78	93,30			7,57	278,39	18,99	90,50			2,87	105,43	12,85	95,46		
	Senkol 700 - 10g/t		C3	12	28,81	286,32	146,11				0,76	21,85	3,98	96,94			2,62	75,58	15,77	93,57			0,64	18,54	10,44	96,63		
	Copper sulfate - 160g/t		C4	20	19,17	303,40	165,28				0,32	6,12	3,56	97,96			1,53	29,31	14,11	94,76			0,40	7,68	9,28	97,12		
			F		1308,54						0,45	592,42					1,79	2339,39					1,14	1490,43				
			T		1103,59																							
			T2		21,11						0,01	0,23					0,11	2,42					0,04	0,84				
			T3		18,56						0,01	0,20					0,11	2,07					0,04	0,74				
			Cc+Tt									0,459						1,881						1,206				
			Accountability																									
			Mass Pull		12,63%																							
				0				0,00	0,00	0,00						0,00						0,00						0,00
21	SEX - 80g/t	70 % Passing DM	C1	2	129,14	338,95	129,14	9,82	129,06	330,71	4,43	571,81	4,43	86,13	4,35	85,76	17,18	2218,53	17,18	83,40	16,76	82,77	11,86	1531,55	11,86	90,58	11,55	90,07
	MIBC - 25g/t		C2	6	51,04	330,88	180,18	13,73	180,48	659,07	1,18	60,09	3,51	95,18	3,45	95,08	4,33	221,08	13,54	91,71	13,23	91,37	1,79	91,29	9,01	95,97	8,78	95,74
	Senkol 700 - 10g/t		C3	12	30,97	269,42	211,15	16,00	210,32	905,13	0,37	11,57	3,05	96,92	3,01	96,77	2,02	62,47	11,85	94,06	11,63	93,66	0,47	14,56	7,75	96,84	7,60	96,59
	Copper sulfate - 160g/t		C4	20	20,08	241,72	231,23	17,64	231,87	1146,47	0,23	4,60	2,80	97,61	2,75	97,56	1,47	29,47	10,95	95,16	10,69	94,90	0,31	6,24	7,11	97,20	6,92	97,00
			F		1316,40						0,43	569,89					1,67	2204,25					1,11	1462,84				
			T		1045,46																							
			T2		21,49						0,01	0,31					0,12	2,56					0,04	0,89				
			T3		18,22						0,01	0,27					0,12	2,15					0,05	0,83				
			Cc+Tt									0,504						2,021						1,284				
			Accountability																									
			Mass Pull		17,57%																							
22	SEX - 80g/t	70 % Passing DM	C1	2	128,97	322,47	128,97				4,26	549,93	4,26	85,39			16,33	2106,50	16,33	82,13			11,24	1449,25	11,24	89,56		
	MIBC - 25g/t		C2	6	51,80	325,83	180,77				1,19	61,77	3,38	94,98			4,41	228,24	12,92	91,03			1,86	96,09	8,55	95,50		
	Senkol 700 - 10g/t		C3	12	28,72	222,71	209,49				0,37	10,53	2,97	96,62			1,99	57,12	11,42	93,26			0,47	13,53	7,44	96,34		
	Copper sulfate - 160g/t		C4	20	23,02	240,96	232,51				0,25	5,68	2,70	97,50			1,54	35,41	10,44	94,64			0,33	7,52	6,74	96,80		
			F		1313,06						0,47	616,18					1,86	2440,15					1,20	1576,28				
			T		1043,39																							
			T2		18,76						0,02	0,29					0,13	2,46					0,05	0,96				
			T3		18,40						0,01	0,27					0,12	2,27					0,04	0,82				
			Cc+Tt									0,490						1,953						1,232				
			Accountability																									
			Mass Pull		17,71%																							

A-7: 75 % passing 75 µm (RD and RW)

Table A-7: 75 % passing 75 µm (RD and RW)

Run no.	Reagents	Label	Sample	Time, min	Mass Pull, g	Water Rec, g	Cum Mass, g	Cum m. pull (%)	Ave cum Mass, g	Ave cum w Rec, g	Copper %	Copper Mass	Copper Grade %	Copper Rec %	Ave Cu Grade	Ave Copper rec %	Lead %	Lead Mass	Lead Grade %	Lead Rec %	Ave Lead Grade	Ave Lead rec %	Zinc %	Zinc Mass	Zinc Grade %	Zinc Recovery %	Average Zinc Grade	Average Zinc recovery %
				0				0,00	0,00	0,00						0,00						0,00						0,00
17	SEX - 80g/t	75 % Passing WM	C1	2	81,66	188,50	81,66	6,25	82,01	200,89	5,52	450,95	5,52	76,81	5,44	77,65	22,60	1845,17	22,60	77,85	22,26	78,42	16,74	1366,68	16,74	88,23	16,33	88,46
	MIBC - 25g/t		C2	6	43,34	266,40	125,00	9,58	125,67	462,13	2,19	95,09	4,37	93,01	4,26	93,14	6,75	292,60	17,10	90,19	16,71	90,22	2,55	110,61	11,82	95,37	11,48	95,26
	Senkol 700 - 10g/t		C3	12	26,83	278,08	151,83	11,53	151,22	729,82	0,75	20,01	3,73	96,42	3,66	96,45	2,52	67,65	14,53	93,05	14,32	93,06	0,63	16,92	9,84	96,47	9,65	96,45
	Copper sulfate - 160g/t		C4	20	17,24	252,67	169,07	12,96	169,90	997,58	0,42	7,28	3,39	97,66	3,30	97,65	1,70	29,23	13,22	94,28	12,92	94,30	0,47	8,04	8,89	96,99	8,64	96,93
			F		1312,33						0,46	601,29					1,78	2338,92					1,18	1542,85				
			T		1106,76																							
			T2		19,21						0,01	0,23					0,12	2,27					0,04	0,77				
			T3		17,29						0,01	0,21					0,12	2,05					0,04	0,72				
			Cc+Tt									0,447						1,806						1,180				
			Accountability																									
			Mass Pull		12,88%																							
18	SEX - 80g/t	75 % Passing WM	C1	2	82,35	213,27	82,35				5,36	441,20	5,36	78,48			21,92	1804,89	21,92	78,99			15,92	1311,09	15,92	88,69		
	MIBC - 25g/t		C2	6	43,98	256,09	126,33				1,89	83,11	4,15	93,26			5,84	257,01	16,32	90,24			2,17	95,45	11,13	95,14		
	Senkol 700 - 10g/t		C3	12	24,27	257,29	150,60				0,74	18,05	3,60	96,47			2,66	64,66	14,12	93,07			0,78	19,04	9,47	96,43		
	Copper sulfate - 160g/t		C4	20	20,13	282,86	170,73				0,32	6,53	3,22	97,64			1,41	28,45	12,62	94,32			0,32	6,52	8,39	96,87		
			F		1310,22						0,47	615,44					1,80	2357,83					1,18	1545,78				
			T		1103,54																							
			T2		17,45						0,01	0,20					0,11	1,98					0,04	0,71				
			T3		18,50						0,01	0,22					0,11	2,12					0,04	0,75				
			Cc+Tt									0,429						1,744						1,128				
			Accountability																									
			Mass Pull		13,03%																							
				0				0,00	0,00	0,00						0,00						0,00						0,00
23	SEX - 80g/t	75 % Passing DM	C1	2	137,83	385,09	137,83	10,74	139,85	400,88	4,03	555,53	4,03	88,99	4,04	88,88	15,87	2187,46	15,87	86,01	15,77	85,69	10,63	1465,22	10,63	91,13	10,62	91,14
	MIBC - 25g/t		C2	6	49,12	304,48	186,95	14,42	187,79	694,54	0,90	44,33	3,21	96,09	3,25	96,09	3,66	179,65	12,66	93,08	12,71	92,79	1,53	75,33	8,24	95,82	8,33	95,95
	Senkol 700 - 10g/t		C3	12	33,00	308,27	219,95	16,86	219,58	1007,84	0,28	9,10	2,77	97,55	2,82	97,44	1,69	55,69	11,02	95,27	11,11	94,82	0,41	13,37	7,06	96,65	7,18	96,71
	Copper sulfate - 160g/t		C4	20	18,15	243,77	238,10	18,19	236,93	1254,24	0,19	3,51	2,57	98,11	2,63	97,96	1,38	25,11	10,28	96,25	10,40	95,75	0,30	5,49	6,55	96,99	6,67	97,04
			F		1304,22						0,43	563,49					1,85	2412,09					1,12	1466,36				
			T		1030,19																							
			T2		19,88						0,01	0,18					0,06	1,29					0,05	0,90				
			T3		16,05						0,01	0,21					0,11	1,83					0,05	0,73				
			Cc+Tt									0,479						1,950						1,233				
			Accountability																									
			Mass Pull		18,26%																							
24	SEX - 80g/t	75 % Passing DM	C1	2	141,87	416,66	141,87				4,05	574,13	4,05	88,77			15,66	2221,66	15,66	85,36			10,61	1505,18	10,61	91,15		
	MIBC - 25g/t		C2	6	46,75	282,84	188,62				1,01	47,32	3,29	96,08			3,98	186,06	12,76	92,51			1,74	81,38	8,41	96,08		
	Senkol 700 - 10g/t		C3	12	30,59	318,33	219,21				0,26	8,06	2,87	97,33			1,59	48,67	11,21	94,38			0,38	11,58	7,29	96,78		
	Copper sulfate - 160g/t		C4	20	16,54	249,03	235,75				0,19	3,15	2,68	97,82			1,36	22,46	10,51	95,24			0,31	5,06	6,80	97,09		
			F		1300,20						0,46	602,50					1,88	2439,61					1,18	1540,68				
			T		1027,10																							
			T2		17,56						0,01	0,23					0,12	2,05					0,05	0,81				
			T3		19,79						0,01	0,26					0,12	2,30					0,04	0,88				
			Cc+Tt									0,497						2,002						1,270				
			Accountability																									
			Mass Pull		18,13%																							

A-8: Recovery by Size

Table A-8: Recovery by Size

Run no.	Reagents	Label	Sample	Time, min	Mass Pull, g	Water Rec, g	Cum Mass, g	Cum Water, g	Ave cum Mass, g	Ave cum w Rec, g	Copper %	Copper Grade %	Copper Rec %	Ave Copper grade %	Ave Copper rec %	Lead %	Lead Grade %	Lead Rec %	Ave Lead grade %	Ave Lead rec %	Zinc %	Zinc Grade %	Zinc Recovery %	Average Zinc grade %	Average Zinc recovery %
				0					0,00	0,00					0,00					0,00					0,00
1	SEX - 80g/t	Recovery by size	C1	1	95,57	361,83	95,57	361,83	96,70	374,46	4,04	4,04	66,16	4,04	65,80	21,85	21,85	75,72	21,85	75,53	13,48	13,48	82,66	13,48	82,44
	MIBC - 25g/t	RD	C2	5	52,16	397,24	147,73	759,07	150,75	792,13	2,88	3,63	91,94	3,63	92,06	7,69	16,85	90,27	16,78	90,39	3,86	10,09	95,59	10,03	95,64
	Senkol 700 - 10g/t	65% Passing 75µm	F		1291,25						0,44					2,12					1,14				
	Copper sulfate - 160g/t		T		1143,52																				
			T1		0,00						0,04					0,23					0,06				
			T2		0,00						0,04					0,24					0,06				
			Ce+Tt																						
			Accountability																						
			Mass Pull		11,44%																				
2	SEX - 80g/t	Recovery by size	C1	1	96,45	376,30	96,45	376,30			4,04	4,04	65,00			21,85	21,85	75,03			13,48	13,48	81,94		
	MIBC - 25g/t	RD	C2	5	56,50	445,06	152,95	821,36			2,88	3,61	92,20			7,69	16,62	90,50			3,86	9,93	95,69		
	Senkol 700 - 10g/t	65% Passing 75µm	F		1290,03						0,44					2,12					1,14				
	Copper sulfate - 160g/t		T		1137,08																				
			T1		0,00						0,04					0,23					0,06				
			T2		0,00						0,04					0,24					0,06				
			Ce+Tt																						
			Accountability																						
			Mass Pull		11,86%																				
				0																					
3	SEX - 80g/t	Recovery by size	C1	1	98,70	395,71	98,70	395,71			4,04	4,04	66,56			21,85	21,85	76,14			13,48	13,48	82,93		
	MIBC - 25g/t	RD	C2	5	53,27	411,64	151,97	807,35			2,88	3,63	92,21			7,69	16,89	90,60			3,86	10,11	95,75		
	Senkol 700 - 10g/t	65% Passing 75µm	F		1286,64						0,44					2,12					1,14				
	Copper sulfate - 160g/t		T		1134,67																				
			T1		0,00						0,04					0,23					0,06				
			T2		0,00						0,04					0,24					0,06				
			Ce+Tt																						
			Accountability																						
			Mass Pull		11,81%																				
4	SEX - 80g/t	Recovery by size	C1	1	96,09	363,98	96,09	363,98			4,04	4,04	65,50			21,85	21,85	75,25			13,48	13,48	82,25		
	MIBC - 25g/t	RD	C2	5	54,27	416,74	150,36	780,72			2,88	3,62	91,91			7,69	16,74	90,20			3,86	10,01	95,55		
	Senkol 700 - 10g/t	65% Passing 75µm	F		1315,13						0,44					2,12					1,14				
	Copper sulfate - 160g/t		T		1164,77																				
			T1		0,00						0,04					0,23					0,06				
			T2		0,00						0,04					0,24					0,06				
			Ce+Tt																						
			Accountability																						
			Mass Pull		11,43%																				

Recovery by size screen analysis

Table A-9: Recovery by Size Screen Analysis

	Conc			Tails			Calc_Feed	
Screen size (mm)	Mass retained (g)	Mass retained (%)	Cum. %. Passing	Mass retained (g)	Mass retained (%)	Cum. %. Passing	Mass retained (%)	Cum. %. Passing
212			100,0			100,0		100,0
150	0,51	0,09	99,9	25,43	3,14	96,9	2,79	97,2
106	3,33	0,61	99,3	96,61	11,93	84,9	10,61	86,6
75	33,89	6,19	93,1	182,71	22,57	62,4	20,66	65,9
53	36,27	6,63	86,5	180,49	22,29	40,1	20,47	45,5
38	38,09	6,96	79,5	84,49	10,44	29,6	10,03	35,4
25	27,04	4,94	74,6	70,55	8,71	20,9	8,27	27,2
0	408,23	74,58		169,37	20,92		27,16	
	547,36			809,65				
Starting mass	549,14			812,64				
Losses	0,32%			0,37%				

Feed		
Mass retained (g)	Mass retained (%)	Cum. %. Passing
		100,0
21,53	2,66	97,3
81,43	10,07	87,3
174,59	21,59	65,7
148,48	18,36	47,3
88,08	10,89	36,4
67,72	8,38	28,0
226,74	28,04	
808,57		
812,38		
0,47%		

Recovery by size (elemental recovery by size)

Table A-10: Recovery by size (elemental recovery by size)

Grades - Cu	**Cu**				
Screen size (µm)	Avg size	Conc	Tails	Feeds	Rec (%)
212					
150	178	1,97	0,03	0,04	22,0
106	126	5,66	0,06	0,09	39,2
75	89	6,71	0,07	0,22	77,7
53	63	7,21	0,04	0,31	87,7
38	45	6,31	0,02	0,40	96,5
25	31	5,21	0,02	0,46	95,6
10	16	2,87	0,04	0,88	97,2
Grades - Pb	**Pb**				
Screen size (µm)	Avg size	Conc	Tails	Feeds	Rec (%)
212					
150	178	4,54	0,15	0,22	10,5
106	126	15,96	0,15	0,27	41,7
75	89	22,18	0,16	0,79	83,3
53	63	24,58	0,16	1,40	85,8
38	45	24,66	0,17	1,90	92,8
25	31	23,66	0,19	2,27	90,4
10	16	14,22	0,48	5,06	93,3
Grades - Zn	**Zn**				
Screen size (µm)	Avg size	Conc	Tails	Feeds	Rec (%)
212					
150	178	5,04	0,05	0,09	29,2
106	126	16,92	0,05	0,18	69,2
75	89	19,03	0,05	0,49	93,1
53	63	19,38	0,05	0,85	93,8
38	45	17,10	0,04	1,12	97,2
25	31	14,53	0,05	1,30	95,7
10	16	7,01	0,10	2,28	96,9

A-9: VRM Batch Flotation Data

Table A-11: VRM Batch Flotation Data

Run no.	Reagents	Label	Sample	Time, min	Mass Pull, g	Water Rec, g	Cum Mass, g	Cum Water, g	Ave cum Mass, g	Ave cum w Rec, g	Copper %	Copper Grade %	Copper Rec %	Ave Cu Grade	Ave Copper rec %	Lead %	Lead Grade %	Lead Rec %	Ave Pb Grade	Ave Lead rec %	Zinc %	Zinc Grade %	Zinc Recovery %	Ave Zn Grade	Average Zinc recovery %
				0					0,00	0,00					0,00					0,00					0,00
1	SEX - 80g/t	9818 -12	C1	2	100,74	138,06	100,74	138,06	97,57	181,82	6,72	6,72	80,34	6,67	81,34	28,60	28,60	82,98	28,19	83,24	17,31	17,31	88,98	16,55	87,68
	MIBC - 25g/t	65% Passing 75µm	C2	6	23,00	117,83	123,74	255,89	120,05	304,45	4,17	6,24	91,74	6,14	92,05	8,76	24,91	88,79	24,56	89,24	5,12	15,04	94,99	14,51	94,66
	Senkol 700 - 10g/t	800 kN/m2	C3	12	15,43	144,59	139,17	400,48	135,63	448,47	1,81	5,75	95,05	5,63	95,33	4,85	22,69	90,95	22,28	91,45	1,28	13,52	96,01	13,04	96,08
	Copper sulfate - 160g/t		C4	20	12,49	161,08	151,66	561,56	147,87	612,65	0,94	5,36	96,45	5,23	96,64	3,82	21,13	92,32	20,72	92,74	0,69	12,46	96,45	12,02	96,54
			F		1328,95						0,46					1,98					1,12				
			T		1130,60																				
			T2		24,75						0,03					0,23					0,06				
			T3		21,94						0,02					0,22					0,06				
			Cc+Tt																						
			Accountability																						
			Mass Pull		11,41%																				
2	SEX - 80g/t	9818 -12	C1	2	94,40	225,58	94,40	225,58			6,63	6,63	82,35			27,79	27,79	83,50			15,78	15,78	86,39		
	MIBC - 25g/t	65% Passing 75µm	C2	6	21,96	127,42	116,36	353,00			3,46	6,03	92,36			8,85	24,21	89,69			6,24	13,98	94,32		
	Senkol 700 - 10g/t	800 kN/m2	C3	12	15,72	143,46	132,08	496,46			1,57	5,50	95,61			4,53	21,87	91,96			2,00	12,56	96,15		
	Copper sulfate - 160g/t		C4	20	12,00	167,28	144,08	663,74			0,78	5,11	96,84			3,14	20,31	93,16			0,71	11,57	96,64		
			F		1305,02						0,47					2,03					1,10				
			T		1115,17																				
			T2		23,20						0,02					0,18					0,05				
			T3		22,57						0,02					0,19					0,05				
			Cc+Tt																						
			Accountability																						
			Mass Pull		11,04%																				
				0					0,00	0,00					0,00					0,00					0,00
3	SEX - 80g/t	9818 -13	C1	2	101,53	260,05	101,53	260,05	100,95	220,16	5,41	5,41	84,34	5,56	86,50	24,21	24,21	83,21	24,33	84,57	15,09	15,09	91,29	15,25	91,90
	MIBC - 25g/t	65% Passing 75µm	C2	6	18,54	141,65	120,07	401,70	123,51	356,25	2,78	5,01	92,24	4,92	93,68	8,44	21,77	88,50	21,23	90,21	3,44	13,29	95,09	12,95	95,41
	Senkol 700 - 10g/t	1000 kN/m2	C3	12	11,14	138,65	131,21	540,35	139,10	508,52	1,54	4,71	94,87	4,48	95,77	5,53	20,39	90,59	19,30	92,14	1,15	12,26	95,85	11,61	96,12
	Copper sulfate - 160g/t		C4	20	11,32	178,59	142,53	718,94	149,45	657,27	0,91	4,41	96,46	4,22	96,88	4,16	19,10	92,18	18,18	93,30	0,69	11,34	96,31	10,84	96,50
			F		1304,55						0,48					2,27					1,28				
			T		1116,44																				
			T2		28,68						0,02					0,21					0,05				
			T3		16,90						0,02					0,19					0,05				
			Cc+Tt																						
			Accountability																						
			Mass Pull		10,93%																				
				0					0,00	0,00															
4	SEX - 80g/t	9818 -13	C1	2	100,37	180,26	100,37	180,26			5,71	5,71	88,67			24,46	24,46	85,92			15,42	15,42	92,52		
	MIBC - 25g/t	65% Passing 75µm	C2	6	26,57	130,54	126,94	310,80			1,57	4,84	95,12			6,45	20,69	91,93			2,02	12,61	95,72		
	Senkol 700 - 10g/t	1000 kN/m2	C3	12	20,05	165,88	146,99	476,68			0,50	4,25	96,67			2,52	18,21	93,69			0,56	10,97	96,40		
	Copper sulfate - 160g/t		C4	20	9,37	118,91	156,36	595,59			0,44	4,02	97,31			2,22	17,25	94,42			0,52	10,34	96,69		
			F		1294,20						0,48					2,27					1,30				
			T		1091,56																				
			T2		25,58						0,02					0,14					0,05				
			T3		20,70						0,02					0,14					0,05				
			Cc+Tt																						
			Accountability																						
			Mass Pull		12,08%																				

Run no.	Reagents	Label	Sample	Time, min	Mass Pull, g	Water Rec, g	Cum Mass, g	Cum Water, g	Ave cum Mass, g	Ave cum w Rec, g	Copper %	Copper Grade %	Copper Rec %	Ave Cu Grade	Ave Copper rec %	Lead %	Lead Grade %	Lead Rec %	Ave Pb Grade	Ave Lead rec %	Zinc %	Zinc Grade %	Zinc Recovery %	Ave Zn Grade	Average Zinc recovery %
				0					0,00	0,00					0,00					0,00					0,00
5	SEX - 80g/t	9818 -08	C1	2	81,90	169,81	81,90	169,81	83,09	190,92	5,75	5,75	64,86	5,75	65,27	29,24	29,24	77,93	29,72	76,20	16,31	16,31	75,56	14,57	66,17
	MIBC - 25g/t	55% Passing 75µm	C2	6	18,85	108,36	100,75	278,17	102,11	322,22	4,40	5,49	76,29	5,50	76,71	9,50	25,55	83,76	26,40	83,14	9,52	15,04	85,71	13,86	77,26
	Senkol 700 - 10g/t	600 kN/m2	C3	12	15,22	135,23	115,97	413,40	117,15	466,67	2,73	5,13	82,02	5,14	82,32	5,74	22,95	86,60	24,01	86,72	3,45	13,51	88,68	13,24	84,58
	Copper sulfate - 160g/t		C4	20	14,98	158,91	130,95	572,31	131,31	629,84	1,32	4,70	84,74	4,73	84,88	4,07	20,79	88,58	22,04	89,17	1,08	12,09	89,59	12,59	89,98
			F		1292,66						0,53					2,41					1,39				
			T		1118,06																				
			T2		20,71						0,09					0,31					0,16				
			T3		22,94						0,10					0,30					0,16				
			Cc+Tt																						
			Accountability																						
			Mass Pull		10,13%																				
				0					0,00	0,00															
6	SEX - 80g/t	9818 -08	C1	2	84,27	212,03	84,27	212,03			5,75	5,75	65,68			30,19	30,19	74,47			12,84	12,84	56,79		
	MIBC - 25g/t	55% Passing 75µm	C2	6	19,19	154,24	103,46	366,27			4,40	5,50	77,13			14,34	27,25	82,53			11,94	12,67	68,81		
	Senkol 700 - 10g/t	600 kN/m2	C3	12	14,87	153,67	118,33	519,94			2,73	5,15	82,63			9,92	25,07	86,85			14,97	12,96	80,49		
	Copper sulfate - 160g/t		C4	20	13,33	167,43	131,66	687,37			1,32	4,76	85,02			7,45	23,29	89,75			14,12	13,08	90,37		
			F		1290,69						0,53					2,36					1,33				
			T		1117,33																				
			T2		22,90						0,09					0,31					0,16				
			T3		18,80						0,10					0,30					0,16				
			Cc+Tt																						
			Accountability																						
			Mass Pull		10,20%																				
				0					0,00	0,00															
7	SEX - 80g/t	9818 -01	C1	2	69,82	207,04	69,82	207,04	68,88	190,96	6,74	6,74	73,13	6,78	70,79	30,99	30,99	75,14	32,33	74,82	12,89	12,89	54,37	12,98	53,00
	MIBC - 25g/t	75% Passing 75µm	C2	6	16,48	140,65	86,30	347,69	85,87	332,19	3,41	6,11	81,85	6,17	80,26	12,26	27,41	82,15	28,55	82,37	15,05	13,30	69,34	13,54	68,91
	Senkol 700 - 10g/t	600 kN/m2	C3	12	10,57	162,85	96,87	510,54	96,69	499,06	2,16	5,67	85,40	5,73	83,95	7,33	25,22	84,85	26,18	85,08	13,01	13,27	77,64	13,48	77,26
	Copper sulfate - 160g/t		C4	20	7,66	144,83	104,53	655,37	105,77	671,43	2,19	5,42	88,00	5,43	87,08	6,88	23,88	86,68	24,51	87,13	12,59	13,22	83,47	13,35	83,68
			F		1296,51						0,46					2,18					1,27				
			T		1147,88																				
			T2		21,36						0,06					0,32					0,23				
			T3		22,74						0,07					0,32					0,23				
			Cc+Tt											0,53					2,43					1,38	
			Accountability											10,17					10,07					9,70	
			Mass Pull		8,06%																				
8	SEX - 80g/t	9818 -01	C1	2	67,93	174,87	67,93	174,87			6,81	6,81	68,45			33,68	33,68	74,50			13,06	13,06	51,64		
	MIBC - 25g/t	75% Passing 75µm	C2	6	17,50	141,82	85,43	316,69			3,95	6,23	78,67			14,17	29,68	82,58			16,55	13,78	68,49		
	Senkol 700 - 10g/t	600 kN/m2	C3	12	11,07	170,89	96,50	487,58			2,34	5,78	82,51			7,60	27,15	85,32			13,01	13,69	76,87		
	Copper sulfate - 160g/t		C4	20	10,50	199,90	107,00	687,48			2,35	5,44	86,15			6,65	25,14	87,59			11,49	13,47	83,89		
			F		1295,01						0,44					2,15					1,20				
			T		1138,63																				
			T2		22,27						0,08					0,33					0,24				
			T3		27,11						0,08					0,31					0,22				
			Cc+Tt																						
			Accountability																						
			Mass Pull		8,26%																				

Run no.	Reagents	Label	Sample	Time, min	Mass Pull, g	Water Rec, g	Cum Mass, g	Cum Water, g	Ave cum Mass, g	Ave cum w Rec, g	Copper %	Copper Grade %	Copper Rec %	Ave Cu Grade	Ave Copper rec %	Lead %	Lead Grade %	Lead Rec %	Ave Pb Grade	Ave Lead rec %	Zinc %	Zinc Grade %	Zinc Recovery %	Ave Zn Grade	Average Zinc recovery %
				0					0,00	0,00															
9	SEX - 80g/t	9818 -05	C1	2	84,67	204,07	84,67	204,07	85,31	220,60	6,43	6,43	81,14	6,25	82,74	27,77	27,77	77,87	26,62	78,32	14,86	14,86	72,89	14,69	75,64
	MIBC - 25g/t	70% Passing 75µm	C2	6	23,23	177,39	107,90	381,46	106,49	388,49	3,04	5,70	91,68	5,56	91,90	10,57	24,07	86,01	23,20	85,22	11,39	14,12	88,20	13,83	88,77
	Senkol 700 - 10g/t	600 kN/m2	C3	12	15,24	222,84	123,14	604,30	120,74	566,12	1,33	5,16	94,71	5,05	94,61	5,31	21,75	88,69	21,10	87,88	5,11	13,00	92,71	12,77	92,95
	Copper sulfate - 160g/t		C4	20	11,16	184,52	134,30	788,82	130,90	728,02	0,82	4,80	96,08	4,73	95,94	4,91	20,35	90,50	19,83	89,57	3,71	12,23	95,11	12,07	95,27
			F		1275,74						0,47					2,24					1,28				
			T		1098,96																				
			T2		20,90						0,02					0,25					0,07				
			T3		21,58						0,02					0,25					0,08				
			Cc+Tt											0,52					2,37					1,34	
			Accountability											9,02					8,37					9,01	
			Mass Pull		10,53%																				
10	SEX - 80g/t	9818 -05	C1	2	85,95	237,12	85,95	237,12			6,08	6,08	84,33			25,47	25,47	78,78			14,52	14,52	78,40		
	MIBC - 25g/t	70% Passing 75µm	C2	6	19,13	158,39	105,08	395,51			2,52	5,43	92,12			8,22	22,33	84,44			9,11	13,54	89,34		
	Senkol 700 - 10g/t	600 kN/m2	C3	12	13,26	132,42	118,34	527,93			1,12	4,95	94,51			5,52	20,45	87,07			4,62	12,54	93,19		
	Copper sulfate - 160g/t		C4	20	9,16	139,28	127,50	667,21			0,88	4,66	95,81			4,74	19,32	88,63			3,90	11,92	95,44		
			F		1291,98						0,47					2,29					1,32				
			T		1120,47																				
			T2		20,92						0,02					0,27					0,06				
			T3		23,09						0,02					0,28					0,06				
			Cc+Tt																						
			Accountability																						
			Mass Pull		9,87%																				
				0					0,00	0,00															
11	SEX - 80g/t	9818 -07	C1	2	77,64	191,92	77,64	191,92	77,06	165,59	6,32	6,32	74,68	6,45	74,54	28,23	28,23	78,17	28,55	77,91	15,80	15,80	75,26	15,96	74,93
	MIBC - 25g/t	60% Passing 75µm	C2	6	25,43	174,55	103,07	366,47	101,61	339,11	3,62	5,66	88,69	5,79	88,30	8,29	23,31	85,69	23,72	85,35	9,68	14,29	90,38	14,55	90,03
	Senkol 700 - 10g/t	600 kN/m2	C3	12	16,25	160,36	119,32	526,83	116,27	495,52	1,89	5,15	93,37	5,30	92,51	5,41	20,87	88,82	21,44	88,24	4,51	12,96	94,88	13,31	94,22
	Copper sulfate - 160g/t		C4	20	11,65	178,22	130,97	705,05	129,98	647,52	1,17	4,79	95,44	4,88	95,12	4,82	19,45	90,83	19,71	90,71	1,77	11,96	96,14	12,13	96,02
			F		1284,01						0,45					2,08					1,16				
			T		1105,59																				
			T2		24,69						0,03					0,22					0,05				
			T3		22,76						0,02					0,22					0,05				
			Cc+Tt											0,50					2,17					1,25	
			Accountability																						
			Mass Pull		10,20%																				
12	SEX - 80g/t	9818 -07	C1	2	76,48	139,26	76,48	139,26			6,57	6,57	74,41			28,86	28,86	77,64			16,13	16,13	74,60		
	MIBC - 25g/t	60% Passing 75µm	C2	6	23,67	172,49	100,15	311,75			3,85	5,92	87,91			8,86	24,13	85,02			10,54	14,81	89,68		
	Senkol 700 - 10g/t	600 kN/m2	C3	12	13,07	152,45	113,22	464,20			1,94	5,46	91,66			5,75	22,01	87,66			4,91	13,67	93,57		
	Copper sulfate - 160g/t		C4	20	15,77	125,78	128,99	589,98			1,34	4,96	94,79			5,28	19,97	90,59			2,45	12,30	95,90		
			F		1301,60						0,47					2,33					1,25				
			T		1124,17																				
			T2		22,77						0,03					0,23					0,06				
			T3		25,67						0,03					0,23					0,06				
			Cc+Tt																						
			Accountability																						
			Mass Pull		9,91%																				

Run no.	Reagents	Label	Sample	Time, min	Mass Pull, g	Water Rec, g	Cum Mass, g	Cum Water, g	Ave cum Mass, g	Ave cum w Rec, g	Copper %	Copper Grade %	Copper Rec %	Ave Cu Grade	Ave Copper rec %	Lead %	Lead Grade %	Lead Rec %	Ave Pb Grade	Ave Lead rec %	Zinc %	Zinc Grade %	Zinc Recovery %	Ave Zn Grade	Average Zinc recovery %
				0					0,00	0,00															
13	SEX - 80g/t	9818 -15	C1	2	97,22	172,92	97,22	172,92	98,02	172,50	5,47	5,47	86,25	5,47	87,06	24,96	24,96	84,13	25,15	84,17	15,43	15,43	91,37	15,49	91,62
	MIBC - 25g/t	65% Passing 75µm	C2	6	23,74	130,66	120,96	303,58	121,46	298,39	1,97	4,78	93,83	4,78	94,27	7,73	21,57	90,50	21,79	90,37	2,77	12,94	95,38	13,03	95,49
	Senkol 700 - 10g/t	600 kN/m2	C3	12	16,93	156,28	137,89	459,86	137,39	448,43	0,83	4,29	96,12	4,32	96,26	3,77	19,39	92,71	19,72	92,50	0,78	11,45	96,19	11,61	96,24
	Copper sulfate - 160g/t	Try mimic rod mill	C4	20	10,33	147,63	148,22	607,49	147,04	585,93	0,53	4,03	97,01	4,07	97,07	2,98	18,25	93,78	18,64	93,60	0,58	10,69	96,55	10,89	96,58
			F		1305,33						0,47					2,36					1,33				
			T		1110,39																				
			T2		24,81						0,02					0,16					0,05				
			T3		21,91						0,02					0,15					0,05				
			Cc+Tt											0,50					2,20					1,26	
			Accountability																						
			Mass Pull		11,35%																				
14	SEX - 80g/t	9818 -15	C1	2	98,82	172,07	98,82	172,07			5,48	5,48	87,88			25,34	25,34	84,21			15,55	15,55	91,87		
	MIBC - 25g/t	65% Passing 75µm	C2	6	23,14	121,13	121,96	293,20			1,82	4,78	94,71			7,76	22,00	90,25			2,70	13,11	95,60		
	Senkol 700 - 10g/t	600 kN/m2	C3	12	14,93	143,80	136,89	437,00			0,70	4,34	96,41			4,07	20,05	92,29			0,77	11,77	96,29		
	Copper sulfate - 160g/t	Try mimic rod mill	C4	20	8,96	127,36	145,85	564,36			0,50	4,10	97,13			3,75	19,04	93,42			0,60	11,08	96,61		
			F		1304,31						0,45					2,29					1,34				
			T		1112,16																				
			T2		23,29						0,02					0,17					0,05				
			T3		23,01						0,02					0,17					0,05				
			Cc+Tt																						
			Accountability																						
			Mass Pull		11,18%																				
				0				0,00	0,00	0,00					0,00					0,00					0,00
15	SEX - 80g/t	9818 -11	C1	2	96,56	192,92	96,56	192,92	95,06	178,37	5,46	5,46	84,43	5,56	84,80	25,16	25,16	85,55	25,80	85,75	15,08	15,08	90,61	15,47	90,86
	MIBC - 25g/t	65% Passing 75µm	C2	6	22,75	140,85	119,31	333,77	118,36	317,05	2,38	4,87	93,09	4,91	93,18	7,43	21,78	91,50	22,15	91,69	3,33	12,84	95,33	13,05	95,44
	Senkol 700 - 10g/t	600 kN/m2	C3	12	13,60	131,47	132,91	465,24	133,12	461,20	1,09	4,48	95,47	4,47	95,61	3,39	19,89	93,13	20,05	93,38	0,87	11,62	96,07	11,69	96,21
	Copper sulfate - 160g/t		C4	20	12,26	159,52	145,17	624,76	143,94	609,26	0,66	4,16	96,76	4,19	96,74	2,40	18,42	94,16	18,73	94,29	0,58	10,68	96,51	10,86	96,61
			F		1296,55						0,47					2,36					1,31				
			T		1104,52																				
			T2		21,76						0,02					0,15					0,05				
			T3		25,10						0,02					0,14					0,05				
			Cc+Tt											0,48					2,23					1,26	
			Accountability																						
			Mass Pull		11,20%																				
16	SEX - 80g/t	9818 -11	C1	2	93,56	163,82	93,56	163,82			5,66	5,66	85,18			26,44	26,44	85,95			15,86	15,86	91,11		
	MIBC - 25g/t	65% Passing 75µm	C2	6	23,84	136,51	117,40	300,33			2,11	4,94	93,28			7,16	22,53	91,88			3,03	13,25	95,54		
	Senkol 700 - 10g/t	600 kN/m2	C3	12	15,93	156,82	133,33	457,15			0,96	4,46	95,75			3,16	20,21	93,63			0,84	11,77	96,36		
	Copper sulfate - 160g/t		C4	20	9,38	136,61	142,71	593,76			0,64	4,21	96,72			2,41	19,04	94,41			0,58	11,03	96,70		
			F		1279,56						0,46					2,26					1,29				
			T		1093,06																				
			T2		19,90						0,02					0,15					0,05				
			T3		23,89						0,02					0,14					0,05				
			Cc+Tt																						
			Accountability																						
			Mass Pull		11,15%																				

Run no.	Reagents	Label	Sample	Time, min	Mass Pull, g	Water Rec, g	Cum Mass, g	Cum Water, g	Ave cum Mass, g	Ave cum w Rec, g	Copper %	Copper Grade %	Copper Rec %	Ave Cu Grade	Ave Copper rec %	Lead %	Lead Grade %	Lead Rec %	Ave Pb Grade	Ave Lead rec %	Zinc %	Zinc Grade %	Zinc Recovery %	Ave Zn Grade	Average Zinc recovery %
				0					0,00	0,00															
17	SEX - 80g/t	9818 -16	C1	2	108,36	204,15	108,36	204,15	108,77	201,03	5,08	5,08	90,15	5,09	90,23	20,20	20,20	84,48	20,07	84,31	12,06	12,06	92,45	12,23	92,38
	MIBC - 25g/t	65% Passing 75µm	C2	6	31,64	130,91	140,00	335,06	143,76	348,13	1,01	4,16	95,36	4,09	95,64	4,80	16,72	90,35	16,31	90,50	1,48	9,67	95,76	9,59	95,76
	Senkol 700 - 10g/t	600 kN/m2	C3	12	23,14	170,47	163,14	505,53	166,99	527,22	0,40	3,63	96,88	3,57	97,08	2,64	14,72	92,71	14,40	92,81	0,44	8,36	96,49	8,32	96,45
	Copper sulfate - 160g/t	Air temp: 363 K	C4	20	12,50	157,70	175,64	663,23	178,05	669,44	0,30	3,39	97,48	3,37	97,61	2,13	13,83	93,74	13,64	93,78	0,38	7,79	96,82	7,83	96,76
			F		1286,79						0,46					2,16					1,22				
			T		1068,47																				
			T2		22,39						0,01					0,15					0,04				
			T3		20,29						0,01					0,15					0,04				
			Cc+Tt											0,48					2,13					1,19	
			Accountability																						
			Mass Pull		13,65%																				
18	SEX - 80g/t	9818 -16	C1	2	109,18	197,91	109,18	197,91			5,10	5,10	90,32			19,94	19,94	84,13			12,40	12,40	92,30		
	MIBC - 25g/t	65% Passing 75µm	C2	6	38,34	163,29	147,52	361,20			0,90	4,01	95,91			4,40	15,90	90,65			1,32	9,52	95,75		
	Senkol 700 - 10g/t	600 kN/m2	C3	12	23,32	187,71	170,84	548,91			0,36	3,51	97,28			2,52	14,07	92,92			0,42	8,28	96,42		
	Copper sulfate - 160g/t	Air temp: 363 K	C4	20	9,62	126,73	180,46	675,64			0,30	3,34	97,74			2,41	13,45	93,81			0,43	7,86	96,70		
			F		1291,65						0,48					2,20					1,20				
			T		1069,29																				
			T2		21,56						0,01					0,14					0,04				
			T3		20,34						0,01					0,15					0,04				
			Cc+Tt																						
			Accountability																						
			Mass Pull		13,97%																				

VRM Summary Results

Table A-12: VRM Summary Results

Test Code	Grind (%)	Grin. Pres (kN/m2)	Clas. Rotor. Speed (1/min)	Load Factor	Mass Pull (%)	Cu Rec (%)	Cu Grade (%)	Pb Rec (%)	Pb Grade (%)	Zn Rec (%)	Zn Grade (%)
9818 -01	73,2	600	272	0,54	8,16	87,08	5,43	87,13	24,51	83,68	13,35
9818 -05	70,4	600	245	0,68	10,20	95,94	4,73	89,57	19,83	95,27	12,07
9818 -07	61,1	600	200	0,83	10,12	95,12	4,88	90,71	19,71	96,02	12,13
9818 -08	55,4	600	175	0,95	10,17	84,88	4,73	89,17	22,04	89,98	12,59
9818 -11	64,7	600	223	0,75	11,21	96,74	4,19	94,29	18,73	96,61	10,86
9818 -12	65,2	800	210	0,93	11,23	96,64	5,23	92,74	20,72	96,54	12,02
9818 -13	64,7	1000	197	1,09	11,50	96,88	4,22	93,30	18,18	96,50	10,84
9818 -15	64	600	205		11,45	97,07	4,07	93,60	18,64	96,58	10,89
9818 -16	64,3	600	220	0,73	13,87	97,61	3,37	93,78	13,64	96,76	7,83

A-10: Recovery Kinetics Modelling

Table A-13: Recovery Kinetics Modelling (Klimpel First Order Kinetics)

Cu

Time	RD_Rec	RD_mod	(rec-mod)^2	RW	RW_mod	(rec-mod)^2	VRM	VRM_mod	(rec-mod)^2
0	0,00	0	0	0,00	0	0	0,00	0	0
2	77,44	77,49	0,00	81,33	81,36	0,00	84,80	84,73	0,01
6	91,56	91,33	0,05	92,87	92,74	0,02	93,18	93,45	0,07
12	94,63	94,85	0,05	95,53	95,60	0,00	95,61	95,64	0,00
20	96,28	96,25	0,00	96,70	96,74	0,00	96,74	96,51	0,05
		SS	0,10		SS	0,03		SS	0,13
		RMSS	0,32		RMSS	0,16		RMSS	0,36

Pb

Time	RD_Rec	RD_mod	(rec-mod)^2	RW	RW_mod	(rec-mod)^2	VRM	VRM_mod	(rec-mod)^2
0	0,00	0	0	0,00	0	0	0,00	0	0
2	85,37	85,44	0,00	82,26	82,29	0,00	85,75	85,69	0,00
6	92,37	92,07	0,09	90,35	90,19	0,02	91,69	91,90	0,04
12	93,57	93,72	0,02	92,08	92,17	0,01	93,38	93,45	0,01
20	94,30	94,38	0,01	92,93	92,96	0,00	94,29	94,07	0,05
		SS	0,13		SS	0,03		SS	0,10
		RMSS	0,36		RMSS	0,18		RMSS	0,31

Zn

Time	RD_Rec	RD_mod	(rec-mod)²	RW	RW_mod	(rec-mod)²	VRM	VRM_mod	(rec-mod)²
0	0,00	0	0	0,00	0	0	0,00	0	0
2	92,44	92,53	0,01	93,34	93,38	0,00	90,86	90,91	0,00
6	96,62	96,26	0,13	96,60	96,42	0,03	95,44	95,21	0,05
12	97,10	97,19	0,01	97,13	97,18	0,00	96,21	96,28	0,00
20	97,38	97,56	0,03	97,38	97,48	0,01	96,61	96,71	0,01
		SS	0,18		SS	0,05		SS	0,07
		RMSS	0,43		RMSS	0,21		RMSS	0,27

Klimpel Kinetic First Order Constants

$$R(t) = R_{max}\left[1 - \frac{1}{kt}(1 - e^{-kt})\right]$$

Table A-14: Klimpel Kinetic First Order Constants

	Klimpel Model	RD	RW	VRM
Chalcopyrite	R_max	98,4	98,5	97,8
	k	2,3	2,9	3,7
Galena	R_max	95,4	94,1	95,0
	k	4,8	4,0	5,1
Sphalerite	R_max	98,1	97,9	97,4
	k	8,8	10,8	7,6

B. APPENDIX B: MILLING DATA

B-1: Milling curves

Wet Rod Milling

Table B-1: Grind time vs. achieved grind (% passing 75 µm) for wet rod milling

Wet Grinding				
Grind Time (min)	% passing 75 µm sieve	Mass (g)	Tray (g)	Tray+Dry (g)
12	54,9	268,56	328,48	449,58
15	62,5	258,15	256,55	353,38
18	71,1	221,55	330,8	394,87

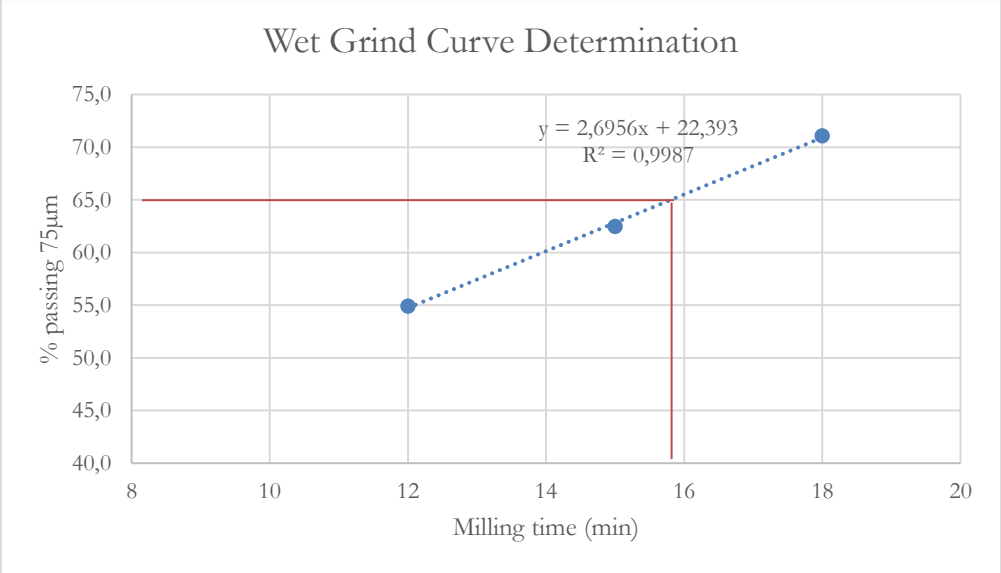

Figure B-1: Wet Rod Milling Calibration Curve

Dry Rod Milling

Table B-2: Grind time vs. achieved grind (% passing 75 µm) for dry rod milling

Dry Grinding			
Grind Time (min)	% passing 75 µm sieve	Starting mass (g)	Retained 75 µm (g)
15	63,0	264,16	97,66
18,25	69,9	265,06	79,76
12	52,4	267,69	127,43
9	45,1	261,21	143,31
16,5	66,0	264,56	89,89

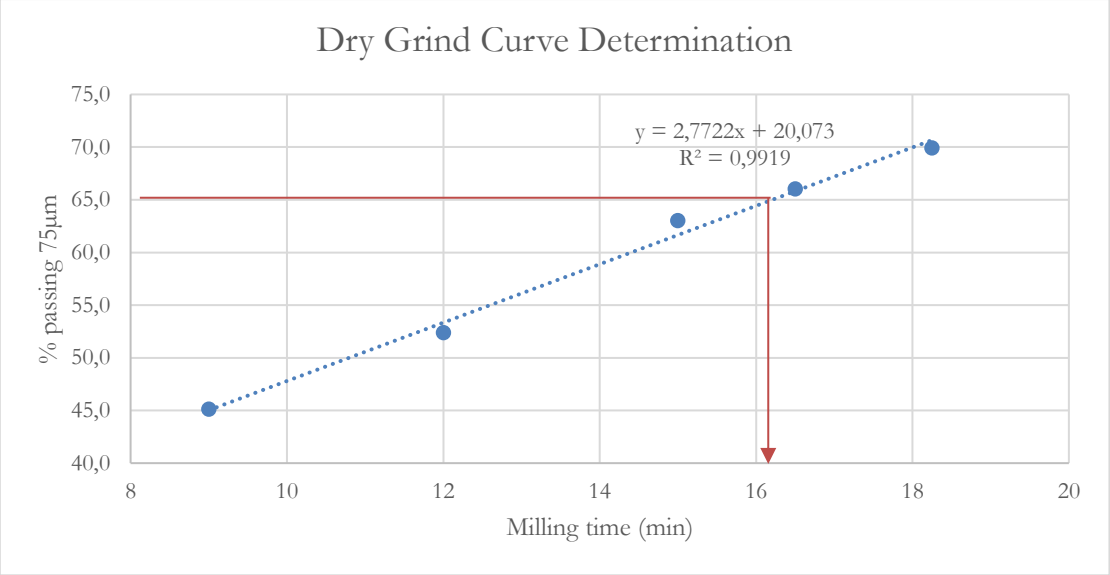

Figure B-2: Dry Rod Milling Calibration Curve

Calculated Milling Time

Table B-3: Required milling time to achieve target grind

Grind (% passing 75um)	RW (min)	RD (min)
55	12,0	12,6
60	14,0	14,4
65	15,8	16,2
70	17,7	18,0
75	19,5	19,8

B-2: Rod Milling and VRM PSDs per Grind Tested

55 % Passing 75 µm

Table B-4: PSD summary (55 % passing 75 µm)

Size (mm)	RD_55% Mass retained (g)	RD_55% Mass retained (%)	RD_55% Cum. %. Passing	RW_55% Mass retained (g)	RW_55% Mass retained (%)	RW_55% Cum. %. Passing	55-600 Size (mm)	55-600 Cum. %. Passing
0,600	0,00		100,0	0,00		100,0	0,600	100
0,425	0,00	0,00	100,0	0,00	0,00	100,0	0,400	100
0,300	0,00	0,00	100,0	0,33	0,12	99,9	0,355	99,7
0,212	1,58	0,53	99,5	1,22	0,46	99,4	0,212	96,4
0,150	22,26	7,51	92,0	20,69	7,82	91,6	0,160	89,9
0,106	36,19	12,20	79,8	27,39	10,35	81,2	0,106	73,3
0,075	72,16	24,33	55,4	69,15	26,13	55,1	0,090	65
0,053	47,13	15,89	39,5	42,61	16,10	39,0	0,075	55,4
0,038	28,55	9,63	29,9	25,64	9,69	29,3	0,063	49,4
0,025	25,39	8,56	21,4	18,98	7,17	22,2	0,040	33
0,000	63,33	21,35		58,66	22,16		0,032	27,2
Total	296,59			264,67			0,025	21,5
Starting mass	298,02			266,01				
% loss	0,48%			0,50%				

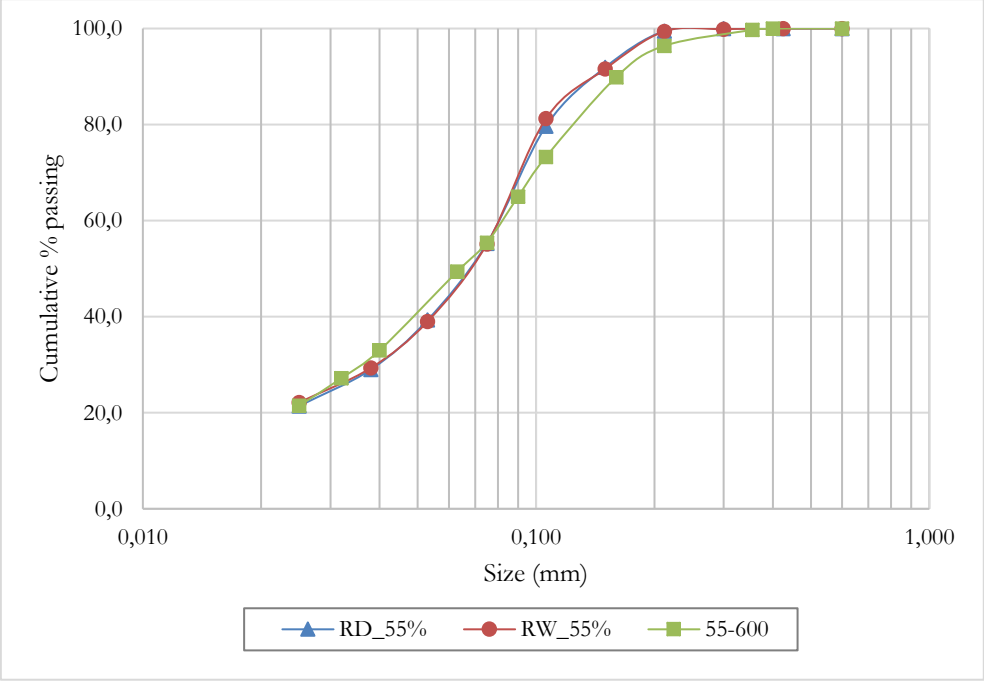

Figure B-3: The progeny PSDs from comminution using 3 grinding mechanisms (55 % passing 75 µm)

60 % Passing 75 µm

Table B-5: PSD summary (60 % passing 75 µm)

Size (mm)	RD_60% Mass retained (g)	RD_60% Mass retained (%)	RD_60% Cum. %. Passing	RW_60% Mass retained (g)	RW_60% Mass retained (%)	RW_60% Cum. %. Passing
0,600	0,00		100,0	0,00		100,0
0,425	0,00	0,00	100,0	0,00	0,00	100,0
0,300	0,00	0,00	100,0	0,22	0,07	99,9
0,212	1,02	0,31	99,7	1,15	0,37	99,6
0,150	19,66	5,90	93,8	21,40	6,88	92,7
0,106	39,12	11,73	82,1	32,60	10,48	82,2
0,075	72,29	21,68	60,4	68,45	22,00	60,2
0,053	55,32	16,59	43,8	52,77	16,96	43,2
0,038	36,72	11,01	32,8	32,89	10,57	32,7
0,025	33,74	10,12	22,7	31,69	10,18	22,5
0,000	75,56	22,66		69,98	22,49	
Total	333,43			311,15		
Starting mass	334,02			313,15		
% loss	0,18%			0,64%		

60-600 Size (mm)	60-600 Cum. %. Passing
0,600	100
0,400	100
0,355	99,9
0,212	98
0,160	93,2
0,106	78,4
0,090	70,3
0,075	61,1
0,063	53
0,040	35,2
0,032	29
0,025	22,6

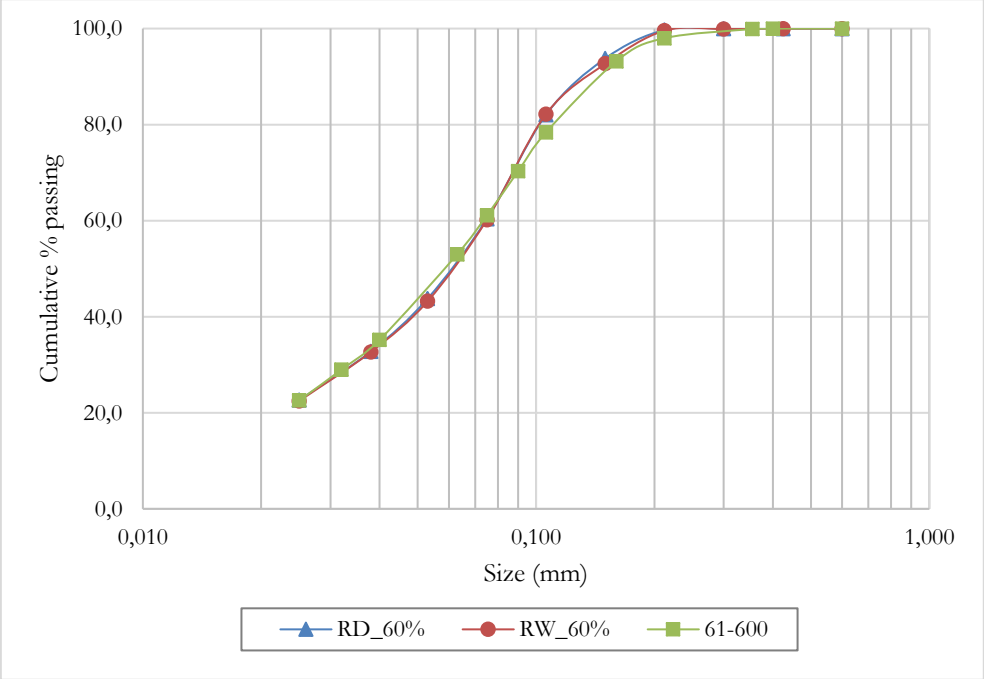

Figure B-4: The PSDs from comminution using 3 grinding mechanisms (60 % passing 75 µm)

65 % Passing 75 µm

Table B-6: PSD summary (65 % passing 75 µm)

Size (mm)	RD_65% Mass retained (g)	RD_65% Mass retained (%)	RD_65% Cum. %. Passing	RW_65% Mass retained (g)	RW_65% Mass retained (%)	RW_65% Cum. %. Passing
0,600	0,00		100,0	0,00		100,0
0,425	0,00	0,00	100,0	0,00	0,00	100,0
0,300	0,00	0,00	100,0	0,00	0,00	100,0
0,212	0,58	0,17	99,8	3,52	0,93	99,1
0,150	6,04	1,75	98,1	7,05	1,86	97,2
0,106	29,28	8,48	89,6	38,75	10,25	87,0
0,075	82,45	23,88	65,7	83,02	21,96	65,0
0,053	62,36	18,06	47,7	70,77	18,72	46,3
0,038	35,42	10,26	37,4	37,98	10,05	36,2
0,025	31,44	9,11	28,3	33,35	8,82	27,4
0,000	97,69	28,29		103,62	27,41	
Total	345,26			378,06		
Starting mass	348,02			382,87		
% loss	0,79%			1,26%		

65-600 Size (mm)	65-600 Cum. %. Passing
0,600	100
0,400	100
0,355	99,8
0,212	98,7
0,160	95,5
0,106	82,6
0,090	75,2
0,075	64,7
0,063	57,1
0,040	38
0,032	31,7
0,025	24,8

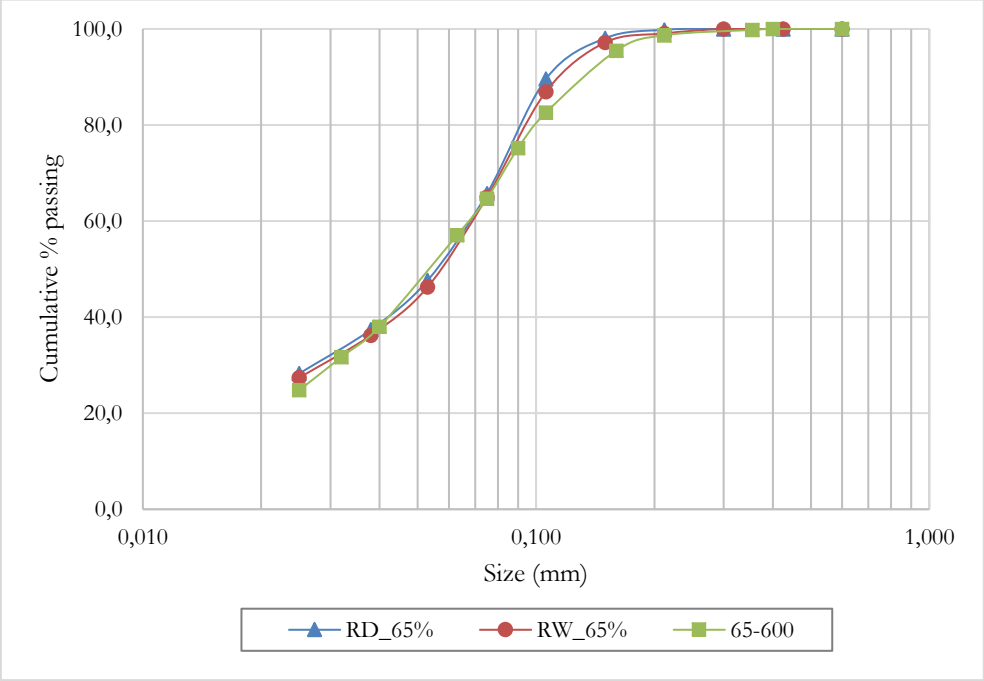

Figure B-5: The progeny PSDs from comminution using 3 grinding mechanisms (65 % passing 75 µm)

70 % Passing 75 µm

Table B-7: PSD summary (70 % passing 75 µm)

Size (mm)	RD_70% Mass retained (g)	RD_70% Mass retained (%)	RD_70% Cum. %. Passing	RW_70% Mass retained (g)	RW_70% Mass retained (%)	RW_70% Cum. %. Passing
0,600	0,00		100,0	0,00		100,0
0,425	0,00	0,00	100,0	0,00	0,00	100,0
0,300	0,00	0,00	100,0	0,00	0,00	100,0
0,212	0,26	0,09	99,9	2,29	0,89	99,1
0,150	6,78	2,35	97,6	8,04	3,12	96,0
0,106	23,15	8,01	89,6	18,59	7,21	88,8
0,075	55,57	19,22	70,3	49,55	19,21	69,6
0,053	51,83	17,93	52,4	44,97	17,43	52,2
0,038	41,76	14,45	38,0	37,85	14,67	37,5
0,025	30,45	10,53	27,4	26,83	10,40	27,1
0,000	79,26	27,42		69,88	27,09	
Total	289,06			258,00		
Starting mass	289,62			260,31		
% loss	0,19%			0,89%		

70-600 Size (mm)	70-600 Cum. %. Passing
0,600	100
0,400	100
0,355	99,9
0,212	99,3
0,160	97,3
0,106	87
0,090	80,5
0,075	70,4
0,063	61,8
0,040	42
0,032	35,1
0,025	27,4

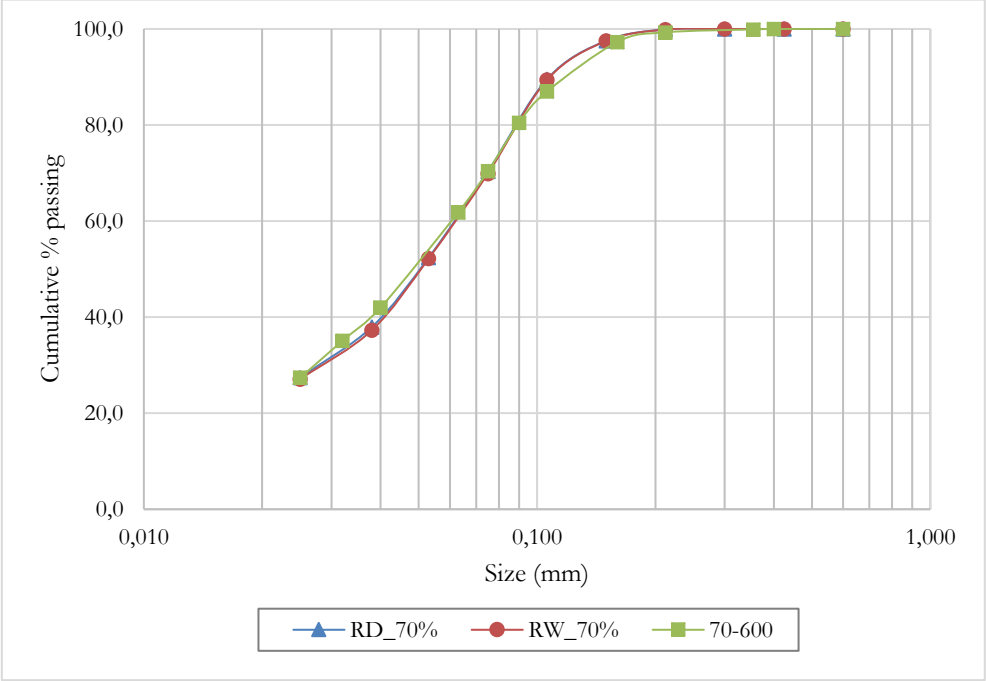

Figure B-6: The progeny PSDs from comminution using 3 grinding mechanisms (70 % passing 75 µm)

75 % Passing 75 µm

Table B-8: PSD summary (75 % passing 75 µm)

Size (mm)	RD_75% Mass retained (g)	RD_75% Mass retained (%)	RD_75% Cum. %. Passing	RW_75% Mass retained (g)	RW_75% Mass retained (%)	RW_75% Cum. %. Passing
0,600	0,00		100,0	0,00		100,0
0,425	0,00	0,00	100,0	0,00	0,00	100,0
0,300	0,00	0,00	100,0	0,00	0,00	100,0
0,212	0,66	0,24	99,8	0,90	0,35	99,7
0,150	4,78	1,73	98,0	3,78	1,46	98,2
0,106	19,20	6,96	91,1	18,20	7,02	91,2
0,075	43,63	15,82	75,2	42,00	16,21	75,0
0,053	50,69	18,38	56,9	47,98	18,52	56,4
0,038	45,44	16,48	40,4	43,68	16,86	39,6
0,025	35,36	12,82	27,6	31,66	12,22	27,4
0,000	76,01	27,56		70,89	27,36	
Total	275,77			259,09		
Starting mass	277,07			260,53		
% loss	0,47%			0,55%		

73-600 Size (mm)	73-600 Cum. %. Passing
0,600	100
0,400	100
0,355	100
0,212	99,7
0,160	98,3
0,106	90,4
0,090	83,8
0,075	73,2
0,063	63,9
0,040	41,6
0,032	34,3
0,025	26,6

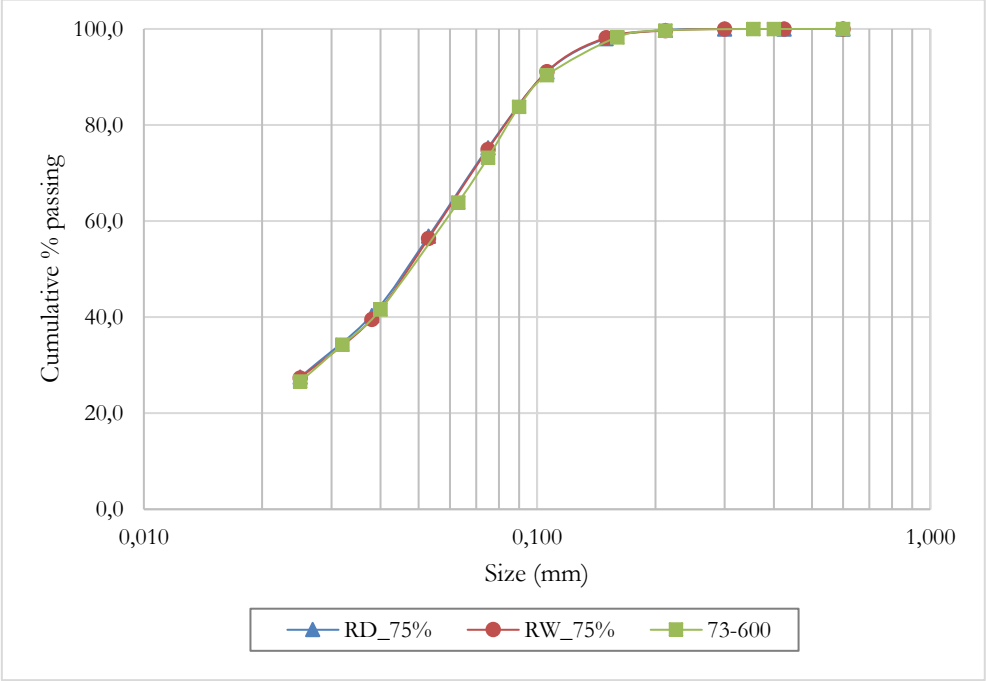

Figure B-7: The progeny PSDs from comminution using 3 grinding mechanisms (75 % passing 75 µm)

B-3: VRM PSDs

Table B-9: PSD summary for all VRM tests conducted

Size (mm)	73-600	70-600	61-600	55-600	VRM	65-800	65-1000	64_RM-c	64_363K
0,6	100	100	100	100	100	100	100	100	100
0,4	100	100	100	100	100	100	99,9	100	99,9
0,355	100	99,9	99,9	99,7	99,8	99,8	99,8	99,8	99,7
0,212	99,7	99,3	98	96,4	98,7	98,8	97,5	98,9	98,7
0,16	98,3	97,3	93,2	89,9	95,5	95	93,9	96,4	96
0,106	90,4	87	78,4	73,3	82,6	82,9	80,9	83,3	82,7
0,09	83,8	80,5	70,3	65	75,2	74,9	73,9	75,4	74,9
0,075	73,2	70,4	61,1	55,4	64,7	65,2	64,7	64	64,3
0,063	63,9	61,8	53	49,4	57,1	56,9	57,1	56,5	51,7
0,04	41,6	42	35,2	33	38	37,9	39,6	38,9	32,5
0,032	34,3	35,1	29	27,2	31,7	31,6	33	31,8	25,6
0,025	26,6	27,4	22,6	21,5	24,8	24,4	26,7	25,4	19,3

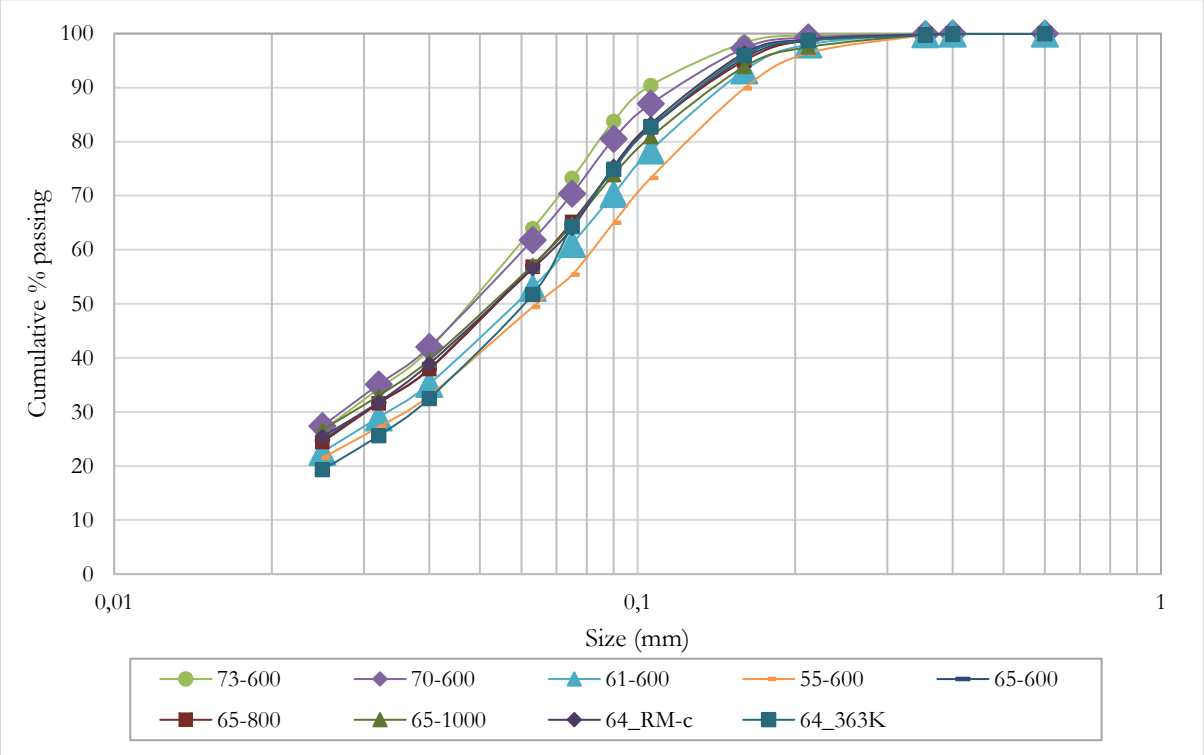

Figure B-8: The progeny PSDs from comminution using the VRM (all tests)

B-4: UCT/ BMM Ore Blending PSD results (Mintek)

Table B-10: Blending validation PSD data

	Subsample 1			Subsample 2			Subsample 3		
Sieve(μm)	mass(kg)	Mass%	cumulative % passing	mass(kg)	Mass%	cumulative % passing	mass(kg)	Mass%	cumulative % passing
16	0,0	0,0	100,0	0,0	0,0	100,0	0,0	0,0	100,0
13,2	10,0	1,1	98,9	4,6	0,5	99,5	0,0	0,0	100,0
9,5	151,1	16,2	82,7	150,5	15,8	83,7	198,4	17,2	82,8
7	201,0	21,6	61,1	192,9	20,3	63,4	233,0	20,2	62,5
5	104,4	11,2	49,9	110,0	11,6	51,8	135,2	11,7	50,8
3	58,4	6,3	43,7	62,6	6,6	45,2	77,1	6,7	44,1
2	44,6	4,8	38,9	47,4	5,0	40,2	58,6	5,1	39,0
2	27,3	2,9	36,0	30,7	3,2	37,0	32,7	2,8	36,2
1	31,1	3,3	32,6	33,3	3,5	33,5	39,9	3,5	32,7
0,85	29,4	3,2	29,5	28,7	3,0	30,4	36,1	3,1	29,6
0,6	35,6	3,8	25,7	38,6	4,1	26,4	44,5	3,9	25,7
0,425	31,9	3,4	22,2	33,8	3,6	22,8	39,1	3,4	22,3
0,3	43,7	4,7	17,5	46,7	4,9	17,9	53,9	4,7	17,6
0,212	33,1	3,6	14,0	34,5	3,6	14,3	41,9	3,6	14,0
0,15	33,4	3,6	10,4	34,7	3,7	10,6	41,1	3,6	10,4
0,106	25,0	2,7	7,7	26,2	2,8	7,8	30,5	2,6	7,8
0,075	20,8	2,2	5,5	21,6	2,3	5,6	25,9	2,2	5,5
0,053	13,3	1,4	4,1	13,5	1,4	4,1	16,5	1,4	4,1
0,038	9,9	1,1	3,0	10,2	1,1	3,1	13,7	1,2	2,9
0,025	5,0	0,5	2,5	5,3	0,6	2,5	6,2	0,5	2,4
0	23,0	2,5		23,9	2,5		27,4	2,4	
Total	932,0	100,0		949,7	100,0		1151,7	100,0	

C. APPENDIX C: MINERAL LIBERATION DATA

C-1: Dry Rod Mill

Table C-1: Feed Liberation Data (Dry Rod Mill: 65 % passing 75µm)

	% in Fraction		Liberation of Chalcopyrite											
			0%	<= 10%	<= 20%	<= 30%	<= 40%	<= 50%	<= 60%	<= 70%	<= 80%	<= 90%	< 100%	100%
Feed	Fraction	-300/+75	0,00	8,03	3,44	3,29	2,03	3,59	2,76	2,72	6,38	4,90	44,78	18,08
		-75/+38	0,00	2,29	2,05	2,92	2,85	1,33	1,70	2,19	1,91	6,17	76,03	0,56
		-38/+10	0,00	1,91	0,94	0,63	0,74	1,03	1,27	1,33	2,78	7,91	56,19	25,27
		-10/+0	0,00	4,32	4,00	2,04	2,49	2,44	2,29	3,31	6,04	10,15	13,79	49,11
		Combined	**0,00**	**3,56**	**2,45**	**1,94**	**1,92**	**1,87**	**1,88**	**2,31**	**4,04**	**7,76**	**46,63**	**25,64**
	% in Fraction		Liberation of Galena											
			0%	<= 10%	<= 20%	<= 30%	<= 40%	<= 50%	<= 60%	<= 70%	<= 80%	<= 90%	< 100%	100%
	Fraction	-300/+75	0,00	15,94	6,26	5,15	2,25	0,84	0,00	3,20	1,20	3,48	61,68	0,00
		-75/+38	0,00	6,51	2,86	1,36	0,33	1,58	1,51	1,05	0,89	3,43	80,47	0,00
		-38/+10	0,00	1,62	0,96	0,64	0,68	0,66	0,58	1,37	4,25	20,92	61,85	6,49
		-10/+0	0,00	3,05	3,63	2,75	2,80	3,61	3,42	4,84	9,79	15,37	15,74	34,99
		Combined	**0,00**	**4,29**	**2,69**	**1,88**	**1,45**	**1,85**	**1,67**	**2,63**	**5,18**	**14,10**	**50,04**	**14,23**
	% in Fraction		Liberation of Sphalerite											
			0%	<= 10%	<= 20%	<= 30%	<= 40%	<= 50%	<= 60%	<= 70%	<= 80%	<= 90%	< 100%	100%
	Fraction	-300/+75	0,00	3,08	1,46	1,04	0,52	0,93	1,11	0,00	1,95	13,88	76,03	0,00
		-75/+38	0,00	1,18	0,15	0,30	0,59	0,14	0,67	0,92	0,00	7,56	88,48	0,00
		-38/+10	0,00	0,34	0,26	0,36	0,22	0,22	0,50	0,87	2,16	13,83	73,42	7,82
		-10/+0	0,00	0,64	1,26	1,30	1,55	2,04	2,07	3,32	6,91	14,86	22,66	43,39
		Combined	**0,00**	**0,94**	**0,67**	**0,70**	**0,74**	**0,83**	**1,08**	**1,52**	**3,05**	**12,64**	**62,04**	**15,78**

Table C-2: Tailings Liberation Data (Dry Rod Mill: 65 % passing 75µm)

% in Fraction		Liberation of Chalcopyrite											
		0%	<= 10%	<= 20%	<= 30%	<= 40%	<= 50%	<= 60%	<= 70%	<= 80%	<= 90%	< 100%	100%
Fraction	-300/+75	0,00	42,15	11,06	9,84	8,84	12,30	2,89	1,50	0,00	5,62	5,80	0,00
	-75/+38	0,00	33,18	10,81	7,38	9,56	4,55	11,88	0,00	0,31	0,51	14,63	7,20
	-38/+10	0,00	28,42	11,73	7,26	3,31	2,92	1,01	1,84	1,58	3,97	12,83	25,13
	-10/+0	0,00	9,13	6,10	2,86	2,81	2,38	3,29	3,19	13,07	15,39	10,37	31,43
	Combined	**0,00**	**30,46**	**9,86**	**7,28**	**6,89**	**7,05**	**4,80**	**1,62**	**3,46**	**6,68**	**9,71**	**12,19**
% in Fraction		Liberation of Galena											
		0%	<= 10%	<= 20%	<= 30%	<= 40%	<= 50%	<= 60%	<= 70%	<= 80%	<= 90%	< 100%	100%
Fraction	-300/+75	0,00	63,62	11,21	3,89	5,69	0,00	0,00	0,00	0,00	0,00	15,59	0,00
	-75/+38	0,00	41,98	13,86	3,87	0,08	3,19	0,00	0,00	1,20	7,46	28,12	0,24
	-38/+10	0,00	14,19	4,55	5,77	2,41	0,75	0,15	2,70	2,84	11,34	53,04	2,26
	-10/+0	0,00	4,19	3,05	2,24	3,65	3,44	4,58	6,94	9,61	11,94	20,68	29,68
	Combined	**0,00**	**33,93**	**8,79**	**3,95**	**2,91**	**1,82**	**1,00**	**2,06**	**3,00**	**7,18**	**28,52**	**6,84**
% in Fraction		Liberation of Sphalerite											
		0%	<= 10%	<= 20%	<= 30%	<= 40%	<= 50%	<= 60%	<= 70%	<= 80%	<= 90%	< 100%	100%
Fraction	-300/+75	0,00	58,41	12,29	11,47	1,47	0,00	1,15	0,00	0,00	7,45	7,35	0,41
	-75/+38	0,00	34,61	7,59	1,74	4,00	0,71	0,00	0,75	0,00	0,50	45,96	4,14
	-38/+10	0,00	9,31	7,09	1,74	1,59	0,20	1,07	0,43	0,51	3,62	49,37	25,06
	-10/+0	0,00	2,41	1,88	1,36	2,23	0,96	1,97	1,84	5,70	12,23	20,33	49,08
	Combined	**0,00**	**32,03**	**8,07**	**5,17**	**2,28**	**0,41**	**1,00**	**0,63**	**1,21**	**5,89**	**27,72**	**15,59**

C-2: Wet Rod Mill

Table C-3: Feed Liberation Data (Wet Rod Mill: 65 % passing 75µm)

Feed	% in Fraction		Liberation of Chalcopyrite											
			0%	<= 10%	<= 20%	<= 30%	<= 40%	<= 50%	<= 60%	<= 70%	<= 80%	<= 90%	< 100%	100%
	Fraction	-300/+75	0,00	8,53	4,23	1,81	3,37	2,00	2,46	2,64	3,74	13,66	34,94	22,61
		-75/+38	0,00	2,92	2,31	1,69	1,51	1,54	1,31	1,73	3,55	4,78	29,05	49,60
		-38/+10	0,00	1,93	1,06	0,93	0,63	0,58	0,69	1,37	1,80	3,52	19,96	67,54
		-10/+0	0,00	4,29	4,33	3,02	3,05	3,81	2,78	4,11	7,10	10,42	12,43	44,67
		Combined	**0,00**	**3,81**	**2,72**	**1,81**	**1,91**	**1,90**	**1,68**	**2,40**	**3,95**	**7,24**	**22,27**	**50,34**
	% in Fraction		Liberation of Galena											
			0%	<= 10%	<= 20%	<= 30%	<= 40%	<= 50%	<= 60%	<= 70%	<= 80%	<= 90%	< 100%	100%
	Fraction	-300/+75	0,00	26,65	12,63	4,54	2,04	0,72	1,49	0,73	0,64	1,02	34,80	14,74
		-75/+38	0,00	3,24	1,62	1,11	1,76	0,97	0,88	0,56	1,11	3,08	51,46	34,22
		-38/+10	0,00	1,39	0,93	0,51	0,95	0,74	0,68	1,53	2,79	8,28	40,86	41,34
		-10/+0	0,00	2,60	3,62	3,25	3,28	5,80	3,56	5,90	11,03	14,93	12,92	33,10
		Combined	**0,00**	**3,94**	**2,78**	**1,82**	**1,96**	**2,45**	**1,73**	**2,72**	**5,02**	**8,92**	**33,35**	**35,32**
	% in Fraction		Liberation of Sphalerite											
			0%	<= 10%	<= 20%	<= 30%	<= 40%	<= 50%	<= 60%	<= 70%	<= 80%	<= 90%	< 100%	100%
	Fraction	-300/+75	0,00	3,54	1,57	0,88	0,92	0,74	0,25	0,83	1,30	7,78	80,34	1,86
		-75/+38	0,00	0,99	0,56	0,27	0,36	0,42	0,64	0,87	1,31	6,00	82,26	6,32
		-38/+10	0,00	0,46	0,38	0,33	0,25	0,30	0,35	0,91	2,12	6,97	55,51	32,43
		-10/+0	0,00	0,60	1,37	1,67	2,11	3,35	2,80	4,06	8,31	15,73	18,68	41,32
		Combined	**0,00**	**1,11**	**0,85**	**0,72**	**0,82**	**1,12**	**0,99**	**1,63**	**3,25**	**8,93**	**57,43**	**23,14**

Table C-4: Tailings Liberation Data (Wet Rod Mill: 65 % passing 75µm)

% in Fraction		Liberation of Chalcopyrite											
		0%	<= 10%	<= 20%	<= 30%	<= 40%	<= 50%	<= 60%	<= 70%	<= 80%	<= 90%	< 100%	100%
Fraction	-300/+75	0,00	34,50	13,62	8,72	3,46	2,06	2,48	2,53	10,79	4,73	11,74	5,38
	-75/+38	0,00	34,45	18,72	10,87	11,31	6,22	0,80	1,57	0,44	1,71	8,98	4,93
	-38/+10	0,00	24,88	8,19	6,59	3,56	6,34	1,18	5,53	8,18	13,81	20,31	1,45
	-10/+0	0,00	28,92	10,62	5,38	5,95	4,70	6,46	6,53	8,68	5,00	4,49	13,27
	Combined	**0,00**	**32,28**	**13,39**	**8,33**	**5,37**	**3,87**	**2,57**	**3,37**	**8,09**	**5,47**	**11,33**	**5,92**
% in Fraction		Liberation of Galena											
		0%	<= 10%	<= 20%	<= 30%	<= 40%	<= 50%	<= 60%	<= 70%	<= 80%	<= 90%	< 100%	100%
Fraction	-300/+75	0,00	58,01	16,46	4,68	6,13	3,15	3,33	0,00	0,00	0,00	8,24	0,00
	-75/+38	0,00	26,08	7,33	4,20	4,40	0,97	0,47	0,40	0,24	15,44	40,46	0,00
	-38/+10	0,00	13,53	6,47	1,24	1,35	0,87	0,92	1,60	3,65	17,25	50,63	2,48
	-10/+0	0,00	6,27	5,49	3,76	5,83	6,36	9,93	11,28	16,53	20,34	11,18	3,04
	Combined	**0,00**	**26,74**	**9,18**	**3,48**	**4,48**	**2,93**	**3,80**	**3,38**	**5,20**	**12,85**	**26,55**	**1,40**
% in Fraction		Liberation of Sphalerite											
		0%	<= 10%	<= 20%	<= 30%	<= 40%	<= 50%	<= 60%	<= 70%	<= 80%	<= 90%	< 100%	100%
Fraction	-300/+75	0,00	49,03	15,63	14,94	4,17	0,55	0,00	0,00	0,00	0,00	15,68	0,00
	-75/+38	0,00	36,94	13,02	3,94	4,54	0,82	0,00	0,95	0,00	3,99	33,10	2,69
	-38/+10	0,00	12,44	5,80	2,07	1,41	0,73	0,51	0,70	5,04	17,57	42,88	10,85
	-10/+0	0,00	2,77	3,19	2,61	2,61	3,28	2,94	6,97	14,79	29,58	21,51	9,75
	Combined	**0,00**	**29,41**	**10,49**	**7,41**	**3,36**	**1,20**	**0,71**	**1,77**	**4,06**	**10,54**	**26,23**	**4,82**

C-3: VRM

Table C-5: Feed Liberation Data (VRM: 65 % passing 75µm, 600 kN/m^2 grinding pressure)

Feed	**% in Fraction**		**Liberation of Chalcopyrite**											
			0%	**<= 10%**	**<= 20%**	**<= 30%**	**<= 40%**	**<= 50%**	**<= 60%**	**<= 70%**	**<= 80%**	**<= 90%**	**< 100%**	**100%**
	Fraction	**-300/+75**	0,00	9,12	5,17	3,70	2,68	2,09	3,20	3,36	1,80	4,58	45,81	18,49
		-75/+38	0,00	2,65	1,63	1,17	1,50	2,19	1,29	1,68	2,31	4,71	35,37	45,51
		-38/+10	0,00	1,30	0,88	0,77	0,96	0,89	0,81	1,39	2,11	3,33	23,13	64,43
		-10/+0	0,00	2,87	2,32	1,36	1,42	1,61	1,82	2,50	4,48	9,14	15,53	56,95
		Combined	**0,00**	**3,22**	**2,07**	**1,46**	**1,48**	**1,62**	**1,54**	**2,03**	**2,70**	**5,33**	**28,19**	**50,35**
	% in Fraction		**Liberation of Galena**											
			0%	**<= 10%**	**<= 20%**	**<= 30%**	**<= 40%**	**<= 50%**	**<= 60%**	**<= 70%**	**<= 80%**	**<= 90%**	**< 100%**	**100%**
	Fraction	**-300/+75**	0,00	20,54	9,80	4,72	0,00	2,66	7,35	2,40	0,00	4,25	35,69	12,60
		-75/+38	0,00	2,98	1,71	1,19	0,56	1,19	0,84	1,56	1,48	4,29	52,96	31,23
		-38/+10	0,00	1,17	0,89	0,69	0,71	0,64	0,75	0,82	1,79	5,57	47,83	39,14
		-10/+0	0,00	1,69	2,07	1,89	2,02	2,32	2,56	3,96	7,81	15,42	20,22	40,04
		Combined	**0,00**	**3,38**	**2,16**	**1,48**	**0,97**	**1,41**	**1,80**	**2,00**	**3,19**	**7,77**	**40,82**	**35,02**
	% in Fraction		**Liberation of Sphalerite**											
			0%	**<= 10%**	**<= 20%**	**<= 30%**	**<= 40%**	**<= 50%**	**<= 60%**	**<= 70%**	**<= 80%**	**<= 90%**	**< 100%**	**100%**
	Fraction	**-300/+75**	0,00	6,88	2,26	2,19	0,90	0,77	2,38	0,86	0,00	42,10	41,66	0,00
		-75/+38	0,00	0,89	0,40	0,67	0,66	0,52	0,31	0,46	1,04	5,55	83,61	5,89
		-38/+10	0,00	0,28	0,29	0,35	0,52	0,33	0,69	0,75	2,13	7,30	72,07	15,28
		-10/+0	0,00	0,43	0,80	0,71	1,06	1,47	2,13	3,75	8,69	18,50	29,15	33,31
		Combined	**0,00**	**1,59**	**0,76**	**0,83**	**0,74**	**0,70**	**1,15**	**1,31**	**2,83**	**14,87**	**61,57**	**13,64**

Table C-6: Tailings Liberation Data (VRM: 65 % passing 75µm, 600 kN/m^2 grinding pressure)

% in Fraction		**Liberation of Chalcopyrite**											
		0%	**<= 10%**	**<= 20%**	**<= 30%**	**<= 40%**	**<= 50%**	**<= 60%**	**<= 70%**	**<= 80%**	**<= 90%**	**< 100%**	**100%**
Fraction	**-300/+75**	0,00	40,89	14,08	6,27	11,30	1,08	0,00	0,00	1,89	0,00	10,55	13,94
	-75/+38	0,00	37,70	16,23	11,73	1,64	0,00	0,00	6,92	0,00	0,00	6,30	19,48
	-38/+10	0,00	7,95	3,47	0,85	3,04	1,17	0,00	10,41	2,61	4,64	16,70	49,15
	-10/+0	0,00	18,42	9,06	3,32	2,71	1,99	1,64	1,29	2,64	4,60	9,54	44,82
	Combined	**0,00**	**32,36**	**12,40**	**6,28**	**6,74**	**1,02**	**0,29**	**2,92**	**1,70**	**1,36**	**10,18**	**24,73**
% in Fraction		**Liberation of Galena**											
		0%	**<= 10%**	**<= 20%**	**<= 30%**	**<= 40%**	**<= 50%**	**<= 60%**	**<= 70%**	**<= 80%**	**<= 90%**	**< 100%**	**100%**
Fraction	**-300/+75**	0,00	27,34	6,28	2,00	2,97	0,00	0,00	4,34	1,64	0,00	24,57	30,87
	-75/+38	0,00	5,60	2,40	0,79	3,41	0,57	0,75	1,01	2,46	3,78	54,26	24,98
	-38/+10	0,00	1,88	1,78	1,30	1,87	0,98	2,81	3,64	9,15	12,83	28,14	35,62
	-10/+0	0,00	2,59	3,14	3,00	3,17	3,92	4,73	6,24	9,48	14,04	14,66	35,04
	Combined	**0,00**	**9,34**	**3,33**	**1,68**	**2,79**	**1,21**	**1,97**	**3,67**	**5,65**	**7,57**	**31,17**	**31,63**
% in Fraction		**Liberation of Sphalerite**											
		0%	**<= 10%**	**<= 20%**	**<= 30%**	**<= 40%**	**<= 50%**	**<= 60%**	**<= 70%**	**<= 80%**	**<= 90%**	**< 100%**	**100%**
Fraction	**-300/+75**	0,00	62,30	2,85	3,02	0,00	0,00	0,00	0,00	0,00	0,00	31,84	0,00
	-75/+38	0,00	22,72	8,46	0,00	4,82	1,30	0,00	4,30	0,00	10,61	47,79	0,00
	-38/+10	0,00	4,43	3,29	1,00	2,57	0,14	4,00	4,57	27,14	30,71	17,29	4,86
	-10/+0	0,00	1,46	1,49	1,11	1,05	0,35	2,51	2,73	3,90	13,70	34,22	37,49
	Combined	**0,00**	**31,52**	**4,18**	**1,55**	**1,91**	**0,42**	**1,15**	**2,41**	**5,76**	**10,73**	**33,61**	**6,77**

C-4: Summary of Liberation Data and Grain Size Distributions

Table C-7: Summary of feed liberation data

	Chalcopyrite			Galena			Sphalerite		
	RD	RW	VRM	RD	RW	VRM	RD	RW	VRM
Liberated	80	80	84	78	78	84	90	90	90
HG Middlings	8	8	6	9	9	7	6	6	5
MG Middlings	4	4	3	3	4	2	2	2	1
Locked	8	8	7	9	9	7	2	3	3
Total	100	100	100	100	100	100	100	100	100
Liberated+HGMiddlings	88	88	90	88	87	91	96	95	95

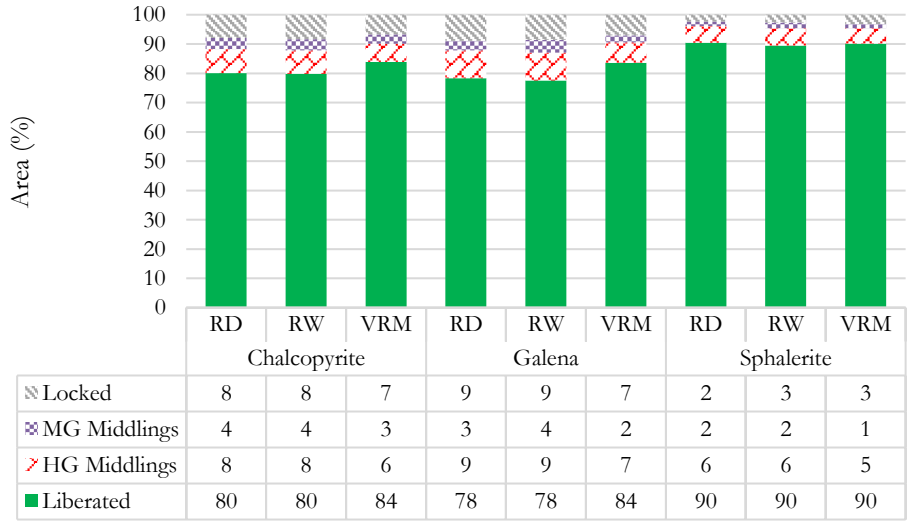

Figure C-1: Summary of feed liberation for VRM, RD and RW (65 % passing 75 µm)

Table C-8: Summary of tailings liberation data

	Chalcopyrite			Galena			Sphalerite		
	RD	RW	VRM	RD	RW	VRM	RD	RW	VRM
Liberated	29	23	36	43	41	70	49	42	51
HG Middlings	10	14	5	6	12	11	3	7	9
MG Middlings	14	9	8	5	7	4	3	5	2
Locked	48	54	51	47	39	14	45	47	37
Total	100	100	100	100	100	100	100	100	100
Liberated+HGMiddlings	38	37	41	49	53	82	52	48	60

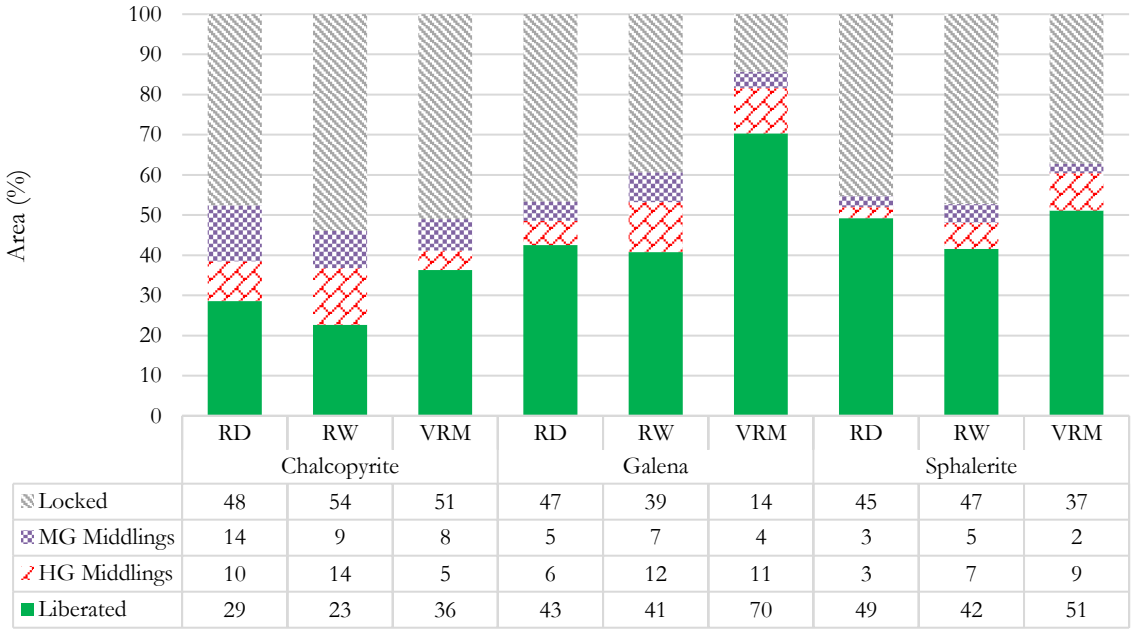

Figure C-2: Summary of tailings liberation for VRM, RD and RW (65 % passing 75 µm)

Table C-9: Benchmarking grind comminution products grain size distribution (chalcopyrite)

		Grain size																										
		<10	<15	<20	<25	<30	<35	<40	<45	<50	<55	<60	<65	<70	<75	<80	<85	<90	<95	<100	<110	<120	<130	<140	<150	<200	<250	<300
RD	Mass Chalcopyrite	0,37	0,24	0,13	0,11	0,09	0,09	0,08	0,06	0,04	0,05	0,05	0,05	0,04	0,02	0,03	0,03	0,02	0,02	0,02	0,04	0,01	0,01	0,01	0,00	0,00	0,00	0,00
		23,35	14,83	8,49	6,78	5,45	5,45	4,81	4,06	2,22	3,08	3,19	3,43	2,57	0,99	1,66	1,64	1,02	1,55	1,54	2,50	0,50	0,47	0,33	0,02	0,06	0,01	0,00
	Size (% passing)	10	15	20	25	30	35	40	45	50	55	60	65	70	75	80	85	90	95	100	110	120	130	140	150	200	250	300
	Cum. % Passing	23,35	38,19	46,68	53,46	58,91	64,36	69,17	73,23	75,45	78,53	81,72	85,15	87,73	88,71	90,37	92,01	93,02	94,57	96,11	98,62	99,12	99,58	99,91	99,93	99,99	100,00	100,00
		Grain size																										
		<10	<15	<20	<25	<30	<35	<40	<45	<50	<55	<60	<65	<70	<75	<80	<85	<90	<95	<100	<110	<120	<130	<140	<150	<200	<250	<300
RW	Mass Chalcopyrite	0,46	0,24	0,12	0,11	0,09	0,07	0,07	0,07	0,06	0,05	0,05	0,06	0,06	0,04	0,03	0,03	0,03	0,04	0,02	0,02	0,03	0,01	0,00	0,01	0,02	0,00	0,00
		26,08	13,70	7,00	6,26	5,21	3,72	3,74	3,69	3,43	2,91	2,67	3,27	3,13	1,99	1,64	1,65	1,59	2,21	1,21	1,34	1,67	0,44	0,15	0,41	0,86	0,01	0,03
	Size (% passing)	10	15	20	25	30	35	40	45	50	55	60	65	70	75	80	85	90	95	100	110	120	130	140	150	200	250	300
	Cum. % Passing	26,08	39,78	46,78	53,04	58,25	61,97	65,71	69,40	72,83	75,74	78,40	81,67	84,80	86,79	88,43	90,08	91,67	93,88	95,10	96,44	98,11	98,55	98,70	99,11	99,96	99,97	100,00
		Grain size																										
		<10	<15	<20	<25	<30	<35	<40	<45	<50	<55	<60	<65	<70	<75	<80	<85	<90	<95	<100	<110	<120	<130	<140	<150	<200	<250	<300
VRM	Mass Chalcopyrite	0,39	0,26	0,16	0,14	0,13	0,11	0,07	0,07	0,09	0,07	0,06	0,06	0,05	0,02	0,03	0,03	0,04	0,03	0,02	0,02	0,02	0,01	0,02	0,03	0,02	0,00	0,00
		20,29	13,63	8,20	7,32	6,64	5,62	3,79	3,57	4,41	3,41	2,86	3,09	2,52	1,28	1,61	1,39	1,97	1,44	1,10	0,87	0,83	0,66	1,25	1,36	0,88	0,02	0,01
	Size (% passing)	10	15	20	25	30	35	40	45	50	55	60	65	70	75	80	85	90	95	100	110	120	130	140	150	200	250	300
	Cum. % Passing	20,29	33,91	42,11	49,43	56,07	61,69	65,48	69,05	73,46	76,87	79,73	82,82	85,35	86,62	88,23	89,62	91,59	93,03	94,13	95,00	95,83	96,49	97,74	99,10	99,98	99,99	100,00

Table C-10: Benchmarking grind comminution products grain size distribution (galena)

		Grain size																										
		<10	<15	<20	<25	<30	<35	<40	<45	<50	<55	<60	<65	<70	<75	<80	<85	<90	<95	<100	<110	<120	<130	<140	<150	<200	<250	<300
RD	Mass Galena	0,96	0,55	0,29	0,21	0,18	0,14	0,17	0,08	0,09	0,07	0,04	0,02	0,02	0,02	0,01	0,04	0,03	0,05	0,02	0,01	0,01	0,00	0,00	0,00	0,00	0,00	0,00
		31,61	18,18	9,39	6,84	5,84	4,70	5,75	2,57	3,05	2,25	1,37	0,78	0,77	0,73	0,49	1,47	0,95	1,69	0,62	0,47	0,21	0,04	0,06	0,03	0,14	0,00	0,00
	Size (% passing)	10	15	20	25	30	35	40	45	50	55	60	65	70	75	80	85	90	95	100	110	120	130	140	150	200	250	300
	Cum. % Passing	31,61	49,79	59,18	66,03	71,87	76,57	82,31	84,88	87,93	90,18	91,55	92,33	93,10	93,82	94,31	95,78	96,73	98,42	99,04	99,51	99,72	99,76	99,83	99,86	100,00	100,00	100,00
		Grain size																										
		<10	<15	<20	<25	<30	<35	<40	<45	<50	<55	<60	<65	<70	<75	<80	<85	<90	<95	<100	<110	<120	<130	<140	<150	<200	<250	<300
RW	Mass Galena	1,24	0,60	0,31	0,26	0,15	0,17	0,14	0,08	0,11	0,08	0,06	0,09	0,06	0,05	0,06	0,01	0,03	0,01	0,01	0,02	0,02	0,01	0,00	0,00	0,02	0,00	0,00
		34,44	16,83	8,51	7,20	4,30	4,83	3,98	2,34	3,07	2,32	1,61	2,49	1,73	1,27	1,58	0,33	0,81	0,25	0,22	0,48	0,46	0,16	0,09	0,07	0,53	0,04	0,06
	Size (% passing)	10	15	20	25	30	35	40	45	50	55	60	65	70	75	80	85	90	95	100	110	120	130	140	150	200	250	300
	Cum. % Passing	34,44	51,27	59,78	66,98	71,27	76,11	80,09	82,42	85,50	87,82	89,42	91,91	93,64	94,91	96,49	96,82	97,64	97,89	98,11	98,59	99,05	99,22	99,31	99,37	99,91	99,94	100,00
		Grain size																										
		<10	<15	<20	<25	<30	<35	<40	<45	<50	<55	<60	<65	<70	<75	<80	<85	<90	<95	<100	<110	<120	<130	<140	<150	<200	<250	<300
VRM		0,76	0,56	0,31	0,28	0,22	0,22	0,18	0,14	0,13	0,10	0,11	0,07	0,05	0,06	0,05	0,04	0,04	0,03	0,02	0,01	0,01	0,01	0,02	0,01	0,02	0,00	0,00
		21,78	16,16	8,87	7,95	6,48	6,38	5,26	4,09	3,86	2,91	3,26	2,16	1,31	1,79	1,58	1,09	1,18	0,82	0,55	0,24	0,41	0,15	0,62	0,22	0,67	0,09	0,12
	Size (% passing)	10	15	20	25	30	35	40	45	50	55	60	65	70	75	80	85	90	95	100	110	120	130	140	150	200	250	300
	Cum. % Passing	21,78	37,94	46,81	54,76	61,23	67,61	72,87	76,96	80,83	83,73	86,99	89,15	90,46	92,25	93,83	94,92	96,10	96,92	97,47	97,71	98,12	98,28	98,90	99,12	99,79	99,88	100,00

Table C-11: Benchmarking grind comminution products grain size distribution (sphalerite)

		Grain size																										
		<10	<15	<20	<25	<30	<35	<40	<45	<50	<55	<60	<65	<70	<75	<80	<85	<90	<95	<100	<110	<120	<130	<140	<150	<200	<250	<300
RD	Mass Sphalerite	0,58	0,37	0,22	0,15	0,15	0,15	0,12	0,10	0,07	0,12	0,05	0,06	0,06	0,05	0,05	0,02	0,02	0,02	0,02	0,02	0,05	0,01	0,01	0,00	0,00	0,00	0,00
		23,31	15,12	9,09	6,24	6,10	5,96	5,00	4,24	2,96	4,66	2,16	2,50	2,39	1,86	1,97	0,70	0,96	1,00	0,70	0,77	1,83	0,21	0,27	0,00	0,00	0,00	0,00
	Size (% passing)	10	15	20	25	30	35	40	45	50	55	60	65	70	75	80	85	90	95	100	110	120	130	140	150	200	250	300
	Cum. % Passing	23,31	38,43	47,53	53,77	59,87	65,83	70,83	75,07	78,03	82,69	84,85	87,35	89,74	91,60	93,57	94,26	95,23	96,22	96,92	97,69	99,51	99,73	100,00	100,00	100,00	100,00	100,00
		Grain size																										
		<10	<15	<20	<25	<30	<35	<40	<45	<50	<55	<60	<65	<70	<75	<80	<85	<90	<95	<100	<110	<120	<130	<140	<150	<200	<250	<300
RW	Mass Sphalerite	0,68	0,35	0,20	0,16	0,13	0,11	0,11	0,10	0,09	0,10	0,10	0,08	0,05	0,05	0,05	0,04	0,05	0,04	0,02	0,04	0,02	0,02	0,01	0,00	0,01	0,00	0,00
		25,95	13,39	7,50	6,24	5,00	4,09	4,36	3,66	3,49	3,92	3,65	3,21	1,79	1,89	1,98	1,60	2,04	1,47	0,81	1,50	0,90	0,80	0,21	0,11	0,44	0,00	0,02
	Size (% passing)	10	15	20	25	30	35	40	45	50	55	60	65	70	75	80	85	90	95	100	110	120	130	140	150	200	250	300
	Cum. % Passing	25,95	39,34	46,84	53,07	58,07	62,17	66,53	70,18	73,67	77,58	81,23	84,44	86,23	88,12	90,10	91,69	93,74	95,21	96,02	97,52	98,41	99,21	99,42	99,53	99,98	99,98	100,00
		Grain size																										
		<10	<15	<20	<25	<30	<35	<40	<45	<50	<55	<60	<65	<70	<75	<80	<85	<90	<95	<100	<110	<120	<130	<140	<150	<200	<250	<300
VRM	Mass Sphalerite	0,43	0,33	0,20	0,20	0,17	0,15	0,12	0,12	0,10	0,10	0,10	0,09	0,05	0,08	0,03	0,02	0,03	0,02	0,01	0,01	0,01	0,00	0,00	0,00	0,01	0,00	0,00
		18,26	13,86	8,35	8,37	7,34	6,19	5,11	5,11	4,03	4,21	4,15	3,67	2,11	3,33	1,38	0,70	1,36	0,82	0,48	0,43	0,28	0,09	0,04	0,03	0,23	0,08	0,00
	Size (% passing)	10	15	20	25	30	35	40	45	50	55	60	65	70	75	80	85	90	95	100	110	120	130	140	150	200	250	300
	Cum. % Passing	18,26	32,11	40,46	48,84	56,18	62,37	67,48	72,59	76,62	80,82	84,97	88,64	90,75	94,09	95,47	96,17	97,53	98,34	98,83	99,26	99,53	99,62	99,66	99,69	99,92	100,00	100,00

The End